Epigenetic Regulation of Immune Tolerance in Intestinal Epithelial Cells

Ashley J. Thorpe

A Thesis Submitted to the University of London in Partial Fulfilment of the Requirements of the Degree of Doctor of Philosophy

July 2015

Centre for Digestive Diseases, Blizard Institute of Cell and Molecular Science,

Barts and The London Medical School, Queen Mary, University of London

I, Ashley Thorpe, confirm that the research included within this thesis is my own work or that where it has been carried out in collaboration with, or supported by others, that this is duly acknowledged below and my contribution indicated. Previously published material is also acknowledged below.

I attest that I have exercised reasonable care to ensure that the work is original, and does not to the best of my knowledge break any UK law, infringe any third party's copyright or other Intellectual Property Right, or contain any confidential material.

I accept that the College has the right to use plagiarism detection software to check the electronic version of the thesis.

I confirm that this thesis has not been previously submitted for the award of a degree by this or any other university.

Signature: 

Date: 14 July 2015

Acknowledgements

Firstly, I would like to express my sincere appreciation and gratitude to my supervisor Professor Ian Sanderson for the continuous support of my PhD study, for his patience, guidance, and immense expertise. His encouragement, assistance and advice, enabling my growth as a researcher, have been invaluable. In addition, I would like to thank Professor Vardhman Rakyan, Dr Tom Vulliamy and Professor Ping Wang for their insightful comments and knowledge, but also for the difficult questions and review comments that facilitated the further development of my research. This work was made possible through funding from the Medical Research Council, grant number: MR/J500409/1, and The Barts Charity, grant number: 723/1625.

My heartfelt thanks also go to Dr Jenny Waters, Dr Tania Marchbank and Dr William Ogunkolade, who taught me the necessary research techniques and assisted me when it came to solving problems. Thanks also to Nici Kingston for her help and organisational skills. Without all their help and expertise I would not have accomplished nearly as much.

I thank the fellow members of the lab, in particular Dr Jean-Marie Delalande, Dr Protima Amon and Dr Farah Barakat, for the stimulating discussions, the scientific support and for all the fun we have had, both in and out of the laboratory.

Last but not least, I would like to thank my family and friends, especially my partner Robert Foster, for their unconditional support and encouragement throughout my PhD and when writing this thesis.

Abstract

Objectives:

Tolerance is a hyporesponsive state caused by repeated exposure to a stimulus. In the intestine, dysregulation of tolerance to luminal stimuli may lead to chronic and deleterious inflammation, such as characterizes Inflammatory Bowel Disease. The role of T-cells in immune tolerance is well known, but that of the epithelium requires investigation. Epithelial tolerance is gene-specific and differentially regulated, but the role of and involvement of epigenetics in tolerance regulation is unknown. We hypothesized that prior stimulation may cause epithelial cells to become hyporesponsive (tolerized) and that modification of histone methylation may alter the response to pro-inflammatory stimulation. The aim of this work was to examine if known inhibitors of histone methylation modifying enzymes affected the expression of CXCL8 in response to IL-1β.

Methods:

CXCL8 production of intestinal epithelial cells was measured by ELISA after stimulation with the pro-inflammatory stimuli P3CK and IL-1β and small molecule epigenetic inhibitors. The CXCL8 production of cells stimulated with a pro-inflammatory stimulus was compared to pre-stimulated cells after a second stimulus. CXCL8 production of IL-1β-pre-stimulated cells was also compared to CXCL8 production when these cells were incubated with epigenetic inhibitors. The effects of these inhibitors on histone methylation levels were examined by Western blotting for the global effect and by ChIP-qPCR for specific effects at the CXCL8 locus.

Results:

Intestinal epithelial cells stimulated with pro-inflammatory stimuli produced a large CXCL8 response. Pre-stimulation significantly decreased CXCL8 production after a second stimulus. The time-coiurse of CXCL8 expression was measured to ensure that CXCL8 expression due to pre-

stimulation was over before the second IL-1β-stimulation. In the presence of specific epigenetic inhibitors, pre-stimulation by IL-1β did not reduce CXCL8 production after a second IL-1β-stimulation. The specific effect of these inhibitors on the epigenetic signature at the CXCL8 locus was confirmed by ChIP. Thus, histone methylation modification disrupted tolerization of intestinal epithelial cells to a pro-inflammatory stimulus.

Conclusion:

The inflammatory response of the intestinal epithelium can be tolerized by prior stimulation with pro-inflammatory cytokines. Tolerization is lost after incubation with inhibitors known to modify histone methylation status, indicating for the first time, the involvement of histone methylation in this phenomenon.

Table of Contents

Table of Contents – Figures

Table of Contents – Tables

Abbreviations

2,4-PDCA	2,4-pyridinedicarboxylic acid
A20/TNFAIP3	Tumour necrosis factor, alpha induced protein 3
ACTB	β-Actin
ANOVA	Analysis of variance
AP-1	Activator protein 1
ATP	Adenosine-triphosphate
BCA	Bicinchoninic acid
BSA	Bovin Serum Albumin
CBCC	Crypt base columnar cells
ChIP	Chromatin Immunoprecipitation
CINCA	Chronic infantile neurological cutaneous and articular syndrome
CLR	C-type Lectin Receptor
COX2	type-2-Cyclooxygenase
CXCL8	Interleukin-8
DAMP	Danger-associated molecular pattern
DAP	Diaminopimelic acid
DC	Dendritic Cell
DMEM	Dulbecco's modified Eagle medium
DNA	Deoxyribonucleic acid
DNase	Deoxyribonuclease
DNMT	DNA Methyltransferase
dNTP	deoxynucleoside triphosphate
EDTA	Ethylenediaminetetraacetic acid

ELISA	Enzyme Linked Immunosorbent Assay
ETP	Epidithio-diketopiperazine
FACS	Fluorescence Activated Cell Sorting
FAD	Flavin Adenine Dinucleotide
FCAS	Familial cold autoinflammatory sundrome
FCS	Fetal calf serum
GLP2	Glucagon-like peptide-2
HAT	Histone Acetyltransferase
HCG	Human chorionic gonadotropin
HDAC	Histone Deacetylase
HDM/KDM	Histone/Lysine Demethylase
HKG	House-keeping Gene
HMT/KMT	Histone/Lysine Methyltransferase
HRP	Horseradish peroxidase
IBD	Inflammatory bowel disease
IFN	Interferon
IKKα/β/ε	Inhibitor of nuclear factor kappa-B kinase subunit alpha/beta/epsilon
IL-10	Interleukin-10
IL-12	Interleukin-12
IL-15	Interleukin-15
IL-17	Interleukin-17
IL-1R	Interleukin-1 receptor
IL-1Ra	Interleukin-1 receptor antagonist
IL-1β	Interleukin-1 beta
IL-5	Interleukin-5

IL-6	Interleukin-6
IL8RB	Interleukin-8 receptor beta
IRAK1/2/4	Interleukin-1 receptor associated kinase 1/2/4
IRF	Interferon regulatory factor
ITS	Insulin, transferrin, selenium
IκB	Inhibitor of NF-κB
JNK	c-JUN N-terminal kinase
LPS	Lipopolysaccharide
LSD1	Lysine Specific Demethylase 1
MAPK	Mitogen-activated protein kinase
MBL	Mannose-binding lectin
MD2	Lymphocyte antigen 96
MDP	Muramyl dipeptide
MFI	Median fluorescence intensity
MWS	Muckle Wells Syndrome
MyD88	Myeloid differentiation primary response gene 88
NALP/NLRP	NACHT, LRR and PYD domain
NEAA	Non-Essential Amino Acids
NEC	Necrotizing entereocolitis
NEMO	NF-kappa-B essential modulator
NF-κB	Nuclear Factor kappa-light-chain-enhancer of activated B cells
NLR	NOD-like receptor
NLRP3	NLR family, pyrin domaining containing 3
NLS	Nuclear localisation signal
NOD	Nucelotide-binding oligomerization domain

P3CK	Pam_3CysK_4
PAMP	Pathogen-associated molecular pattern
PBS	Phosphate Buffered Saline
PCR	Polymerase Chain Reaction
PE	Phycoerythrin
PGE_2	Prostaglandin E2
PMSF	Phenylmethylsulfonyl fluoride
PRR	Pattern Recognition Receptor
PTM	Post-Translational Modification
PVDF	Polyvinylidene difluoride
qPCR	quantitative Polymerase Chain Reaction
RNA	Ribonucleic acid
RNase	Ribonuclease
RPMI	Roswell Park Memorial Institute
RT	Room temperature
RT-PCR	Reverse Transcriptase – Polymerase Chain Reaction
SA	Streptavidin
SAH	*S*-adenosyl-L-homocysteine
SAM	*S*-adenosyl-methionine
SDS-PAGE	Sodium dodecyl sulphate polyacrylamide gel electrophoresis
SEM	Standard error of the mean
SIGIRR	Single Ig IL-1-Related Receptor
SLE	Systemic lupus erythematosus
SNP	Single Nucleotide Polymorphism
SUV39H1	Suppressor of Variegation 3-9 Homolog 1

TAB1/2	Transforming growth factor β activated kinase 1 binding protein 1/2
TACE/ADAM17	TNF alpha converting enzyme
TAK1	Transforming growth factor β activated kinase 1
TBK1	TANK-binding kinase 1
TBS	Tris-buffered saline
TBST	Tris-buffered saline TWEEN
TEB	Triton Extraction Buffer
TGF	Transforming growth factor
Th1/2	T helper type 1/2 cells
TIR	Toll-like/Interleukin-1 receptor homology
TIRAP	Toll-interleukin 1 receptor (TIR) domain containing adaptor protein
TLR	Toll-like receptor
TMB	Tetramethylbenzidine
TNF	Tumour necrosis factor alpha
TRAF	TNF receptor associated factor
TRAM	TRIF-related adaptor molecule
T_{reg}	T regulatory cells
TRIF	TIR-domain-containing adapter-inducing interferon-β
UC	Ulcerative Colitis
UTR	Untranslated region

1 Introduction

1.1 Inflammation

1.1.1 Inflammation and its Clinical Consequences

Inflammation is a complex protective response to infection and trauma (1). Acute or temporary inflammation is essential to combat infection by killing the pathogens and any infected host cells. It also prevents further microbial invasion and heals the ensued tissue damage from both the infection itself and the immune response. However, dysregulated or chronic inflammation is deleterious, causing persistent tissue damage (2) and a wide range of diseases including Rheumatoid arthritis, cancer, Inflammatory Bowel Disease (IBD), coeliac disease, atherosclerosis, systemic lupus erythematosus (SLE), asthma and sepsis, among many others (1). It is essential that the inflammatory response is strictly controlled in order to combat infection, but not result in adverse consequences.

The critical importance of inflammation is highlighted by the increased probability of fatal infections in people with a genetic mutation in one or more of the genes encoding a component of the inflammatory pathway. For example, mutations causing a deficiency in mannose-binding lectin (MBL) predisposes people to infections (3), including meningococcal disease (4) and > 90% of those with a rare genetic deficiency of C1q develop SLE (5). There are several mutations to NLRP3 (NLR family, pyrin domain containing 3) that are associated with an increase in the production of IL-1β (interleukin-1 beta) and three autosomal dominant diseases characterised by

chronic inflammation: Muckle-Wells syndrome (MWS), chronic infantile neurological cutaneous and articular syndrome (CINCA) and familial cold autoinflammatory syndrome (FCAS) (6).

30 000 cases of severe sepsis occur every year in the UK (7); 2.9 million people are living with diabetes (8); 580 000 people suffer from rheumatoid arthritis (9) and over 150 000 people are affected by IBD (10). It is difficult to determine exactly how many people are living with diseases caused by dysregulated inflammation; but it is easy to see how wide-ranging the effects are on the body in the large number of diseases and how debilitating they can be on the patient's quality of life. In addition, they are a significant burden on clinical services.

An inflammatory response is induced upon detection of infection. Vasodilation, an increase in respiration and increased permeability of the blood vessels, causes the characteristic redness, heat and swelling (due to exudation of plasma proteins and fluid into the tissue) (11). The extravasation of neutrophils from the blood vessels to the site of infection is the next step to phagocytose the infectious organism (11). Other cytokines and chemokines are released to activate the complement system thereby promoting opsonisation, chemotaxis, coagulation, fibrinolysis and tissue damage repair (11). Once the inflammatory stimulus is removed, acute phase inflammation ceases due to the short half lives of the inflammatory mediators (12), and the initiation of anti-inflammatory pathways (such as resolvins).

Systemic inflammation occurs when the infectious organism cannot be confined to the local area and the organism can access the lymphatic or circulatory systems. If the infection is still not confined, it is possible for inflammation to surmount the host and a systemic inflammatory response syndrome develops, which progresses to sepsis ultimately leading to multiple organ failure, septic shock and death (13). Other systemic effects of inflammation are an alteration in

leukocyte number, both leucocytosis (an increase of, usually, neutrophils) and leukopenia (a decrease in white blood cells, often as a result of neutrophilia, seen in certain diseases e.g. viral) (14).

However, not all cases of inflammation have infectious origins (2). Many inflammatory diseases show no evidence of infection and are idiopathic in origin. For example, obesity is significantly associated with a low level of chronic inflammation (as seen by an increase in IL-6, CXCL8, TNF and insulin etc levels affecting the endothelium), which then presents its own complications including an increased risk of type II diabetes, heart disease, renal and hepatic failure etc (15). Persistent inflammation in coeliac disease results in villous atrophy and consequent malabsorption (16). Loss of the epithelium due to continual inflammation, as seen in IBD, can require surgical removal of the affected area, if anti-inflammatory drugs are not effective.

1.1.2 Inflammation and the Innate Immune System

The innate immune system is the body's first line of defence against pathogenic invasion. It recognises "danger" signals or PAMPs (pathogen-associated molecular patterns) that are common to microorganisms but are not found in the human body e.g. lipopolysaccharide (LPS) (a major component of Gram negative bacterial cell walls), bacterial lipoproteins (present in bacterial cell membranes), flagellin (protein component of the bacterial flagellum), double-stranded RNA (forms some viral genomes) etc. Pattern recognition receptors (PRRs) recognise and bind to PAMPs and DAMPs (damage-associated molecular patterns). DAMPS are cellular components released upon damage e.g. stress. The signal cascade that is initiated upon interaction of the PRR and its ligand activates the inflammatory responses.

PRRs include Toll-like receptors (TLRs), NOD-like receptors (NLRs and NALP/NLRPs) and C-type lectin Receptors (CRPs). There are thirteen classes of TLRs, each with a specific ligand, as shown in Figure 1-1. TLR1 and TLR6 recognise triacyl and diacyl lipopeptides, respectively; TLR2's ligand is lipoteichoic acid and other lipoproteins; TLR3 recognises double-stranded RNA whilst TLR7 and TLR8 recognise single-stranded RNA and small synthetic compounds (TLR8 only); TLR4 binds to lipopolysaccharide; TLR5 recognises flagellin; TLR9's ligand is unmethylated CpG oligonucleotides; and TLRs 10 – 13 are only found in certain cell types so are not as ubiquitous as the first 9. NLR ligands include peptidoglycans (NOD1 binds to meso-DAP (meso-diaminopimelic acid) whereas NOD2 binds to muramyl dipeptide (MDP), both of which are peptidoglycan components of the bacterial cell wall (17)); other NLR ligands include nucleoside triphosphates, bacterial DNA, toxins, double-stranded RNA, ATP and uric acid crystals (18).

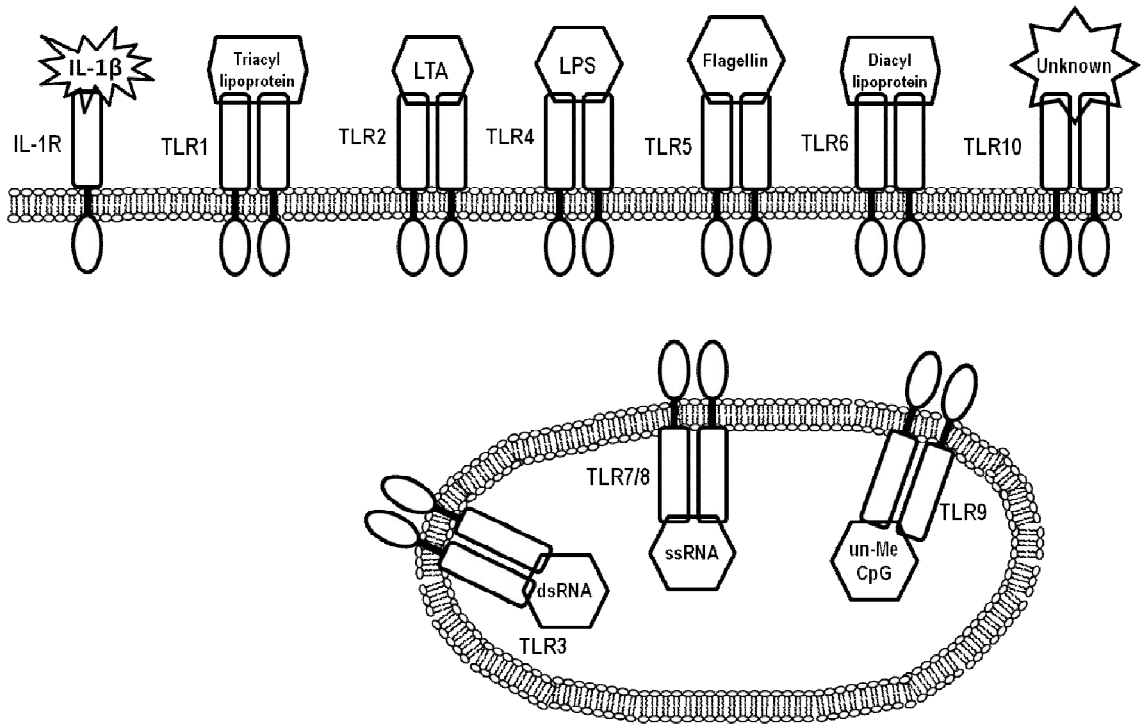

Figure 1-1 TLRs and IL-1 Receptor Agonists

TLRs and IL-1R are PRRs located at both the cellular membrane and at intracellular compartments. The association between individual TLRs/IL-1R and their specific ligand is depicted in the above figure. After receptor and agonist bind, a signalling pathway resulting in activation of NF-κB and induction of pro-inflammatory cytokine expression is initiated.

Once the ligand (PAMP) has bound to the receptor (PRR), the TLR dimerises and adaptor molecules are recruited (Figure 1-2) via the association of the TIR (Toll/Interleukin-1 receptor homology) domains located in both the receptor and the adaptor molecules. The majority of TLRs form homodimers however a selection of TLRs in specific circumstances for heterodimers. TLR2 forms heterodimers with TLR1, TLR6 (19) and TLR10 (20). Both TLR4 and TLR5 usually form homodimers, but they can also form heterodimers, which causes an increase in this activity. Conversely, heterodimers between TLR4 and TLR1 appear to inhibit TLR activity (21). TLR4 also requires an extracellular co-factor, MD2, for optimal ligand-receptor binding (22). After TLR dimerization, adaptor molecules are recruited and the signalling pathways initiated for expression of pro-inflammatory and anti-microbial genes. The same pathways are also activated via binding of IL-1β to interleukin-1 receptor (IL-1R).

All TLRs, except TLR3 and including IL-1R, recruit MyD88 whereas TLR3 (and TLR4) recruit TRIF. The sorting adaptors TRAM and TIRAP determine whether MyD88 or TRIF, respectively, is recruited to the receptor and which subsequent pathway is activated. Whilst both pathways result in the activation of NF-κB (p50-p65 complex), the TRIF-dependent pathway also activates TRAF3 which activates the kinases TBK1 and IKKε, which phosphorylate and activate IRF3 (Interferon regulatory factor 3). IRF3 induces transcription of type I interferon (interferon-β) and interferon-inducible genes. One of those genes is IRF7, which interacts with IRF3, leading to transcription of NF-κB and interferon-α and the subsequent expression of pro-inflammatory cytokines and the transcription factor TNF (tumour necrosis factor α) (18).

NF-κB is activated via both MyD88- and TRIF-dependent signalling pathways following TLR and IL-1R activation (Figure 1-2). MyD88 recruits IRAK4, IRAK1, IRAK2 and TRAF6 via a phosphorylation cascade. TRAF6 transduces the signal amplified by the phosphorylation cascade

and activates the kinase TAK1 in complex with TAB1 and TAB2. This activates the IKK complex (consisting of the two kinase subunits IKKα and IKKβ and the regulatory subunit NEMO) which phosphorylates the inhibitory IκB protein (23). Phosphorylated-IκB dissociates from the p50-p65 complex, thus revealing the nuclear localisation signal (NLS) and allowing activated NF-κB to translocate to the nucleus and induce expression of pro-inflammatory cytokines (24). NF-κB is activated via MyD88-dependent TRAF6 signalling, but also via TRIF-dependent activation of TRAF6. The subsequent TAK1-TAB1-TAB2 complex propagates the TLR or IL-1β signal via two routes: activation of NF-κB via the IKK kinase complex and initiation of the MAPK (mitogen-activated protein kinase) pathway. TAK1 activates the kinases p38 and JNK, which phosphorylate and activate the transcription factor AP1 (25). AP1, like NF-κB, translocates to the nucleus where it induces expression of pro-inflammatory cytokines.

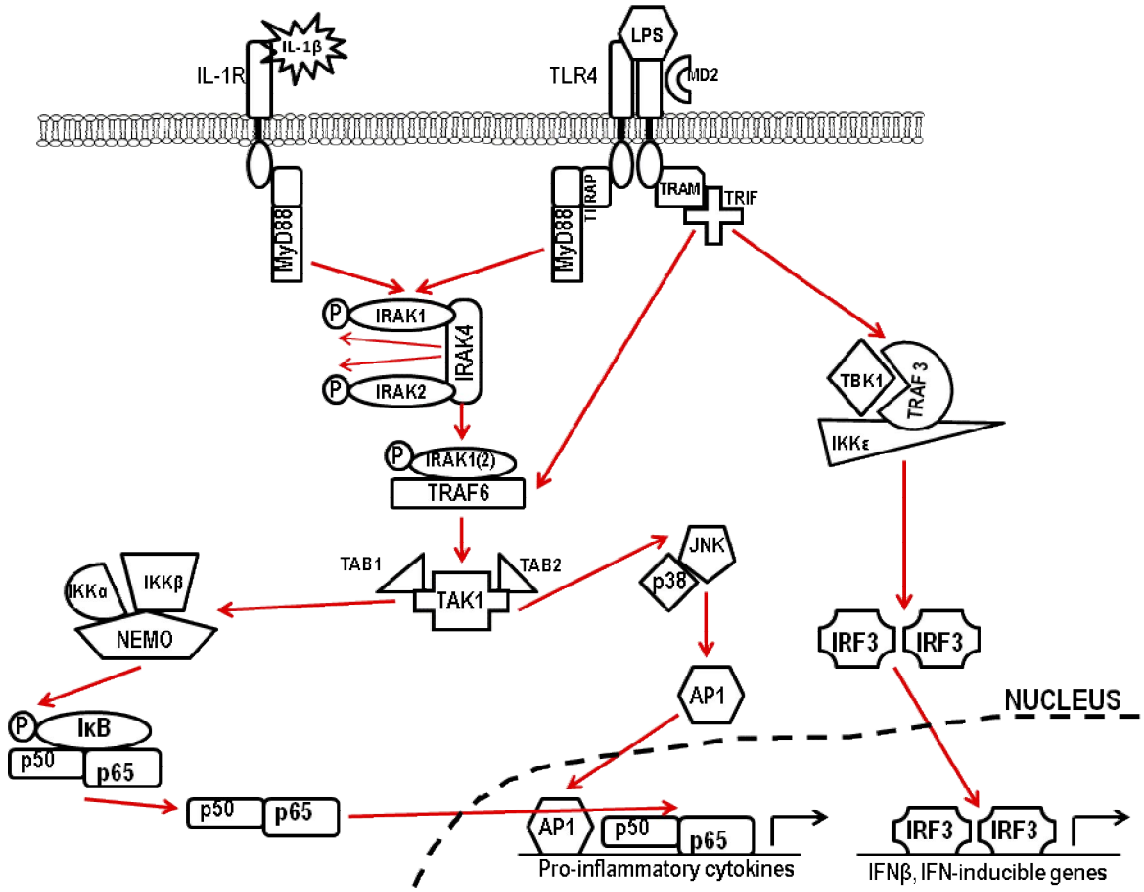

Figure 1-2 TLR- and IL-1R-Signalling Pathways

TLR- and IL-1R-mediated responses use the same signalling pathway mediated by MyD88. All TLRs are dependent on MyD88, except TLR3 which uses the TRIF-dependent pathway along with TLR4. TRAM and TIRAP are sorting adaptors used to determine whether MyD88 or TRIF is recruited. MyD88 recruits IRAK4, IRAK1, IRAK2 and TRAF6 via a phosphorylation cascade. TRAF6 activates TAK1 in complex with TAB1 and TAB2 and activates the IKK complex (consisting of NEMO, IKKα and IKKβ) which phosphorylates the IκB protein thereby releasing NF-κB (p50-p65 complex). NF-κB translocates to the nucleus and induces the expression of pro-inflammatory cytokines. The TAK1-TAB1-TAB2 complex also activates the MAPK pathway resulting in phosphorylation and activation of AP1. AP1 translocates to the nucleus and induces expression of pro-inflammatory cytokines. The alternative TRIF-dependent pathway activates TRAF6, NF-κB and AP1 as described in the MyD88-dependent pathway, as well as TRAF3 which activates the kinases TBK1 and IKKε, which phosphorylate and activate IRF3. IRF3 induces expression of type I interferon (IFNβ).

1.1.3 Inflammatory Mediators

Inflammation is induced by expression of interleukin-1β (IL-1β), interleukin-6 (IL-6), interleukin-8 (CXCL8 – neutrophil chemotactic factor) and TNF, among other cytokines. TNF is a 17 kDa protein whose gene is located on chromosome 6 which is released from its membrane-bound state by proteolytic cleavage by TNF alpha converting enzyme (TACE or ADAM17) into soluble TNF which trimerizes to form the active 51 kDa homotrimer (26). Its main function is a systemic inflammatory cytokine involved in the acute phase reaction. It induces fever, apoptosis, sepsis, inflammation and inhibits tumourigenesis and viral replication (27). TNF binds to its receptor resulting in activation of NF-κB and JNK (via the MAPK pathway) which induces pro-inflammatory gene expression, including CXCL8 (28); and apoptosis via activation of the caspase pathway. Varying levels of TNF are thought to play a role in IBD (29), though this role is controversial. The effective use of anti-TNF therapeutics in the treatment of both UC and CD implies that TNF is functional in intestinal inflammation. Reducing the amount of TNF present through the use of specific antibodies alleviates inflammation and promotes disease remission (30, 31). This does not prove whether or not TNF is causal in the development of IBD, just that it is an important inflammatory mediator.

IL-1β is a 15kDa protein whose gene is located on chromosome 2, which is converted into its active form by cleavage of the IL-1β precursor by caspase-1 (previously known as IL-1β converting enzyme) (32). Its receptor shares a similar cytoplasmic domain and the same signalling pathway adaptors as the TLR-signalling pathway, thus amplifying the signalling cascade through increasing the activation of NF-κB. IL-1β increases expression of pro-inflammatory cytokines and chemokines e.g. IL-6, CXCL8, type-2-cyclooxygenase (COX2) and nitric oxide synthase etc, whilst modulating the surface expression of IL-1R and TNF receptors (33).

IL-1R and TLRs share a number of similarities in their structure and signalling pathway components (34). This is mainly due to the conservation of the TIR domain between TLRs and IL-1R and their adaptor molecules. The structure of each receptor is highly conserved across species with similarities between shared domains e.g. TIR. The differences in structure create a range of receptors with specificity to a range of different ligands. Therefore, whilst the cytosolic domains provide the specificity for each ligand, the shared TIR domains in the receptors and adaptor molecules activate the same signalling pathways. Activation of NF-κB, AP1 and IRF3 and the subsequent induction of gene expression is shared between the different receptors, but the exact profile of genes that are expressed is specific to the individual receptor. TLRs and IL-1R are also linked through NLRP3, a receptor which regulates caspase-1, which in turn maturates IL-1β (35).

Both of the IL-6 and CXCL8 promoters contain NF-κB transcription factor binding sites; hence expression of these cytokines depends on NF-κB activation via either TLR- or IL-1R-mediated signalling. IL-6 is a 21 kDa pro-inflammatory cytokine located on chromosome 7. It is responsible for inducing fever by crossing the blood brain barrier and stimulating expression of PGE_2 in the hypothalamus (36). IL-6 also increases respiration to increase body temperature; B cell maturation and neutrophil production in the bone marrow. Though IL-6 is expressed in large amounts by leukocytes, it is also expressed in lesser amounts by intestinal epithelial cells (37, 38). In particular, IL-1β stimulates less IL-6 than CXCL8 in intestinal epithelial cells.

CXCL8 is an 8.5 kDa chemokine located between 74,606,223 and 74,609,433 of the forward strand of chromosome 4. Its main function is as a granulocyte chemoattractant (primarily neutrophils, but also macrophages and mast cells) in order to cause neutrophils to migrate to the

site of inflammation (39). Once they have arrived, CXCL8 induces phagocytosis. CXCL8 also increases vascular permeability, necessary for neutrophil migration, through down-regulation of tight junction proteins (40). N-terminal processing of the CXCL8 protein results in a number of cleavage isoforms, whose activity or affinity relative to the complete protein is altered (41-43). Post-translational modification of residue Arg-27 with citrulline alters the activity of CXCL8 by reducing tissue inflammation and increasing leukocytosis due to the increased mobilization of neutrophils into the blood (44, 45). It is also a potent angiogenesis factor and a biomarker of senescence, particularly of oncogene-induced senescence in colon adenomas (46). CXCL8 is potently expressed by intestinal epithelial cells, making it an ideal indicator of inflammatory induction, via activation of NF-κB, by IL-1β- and P3CK-stimulated Caco-2 cells (47, 48).

There are three splice variants of CXCL8, though only two produce a functional protein (Figure 1-3) due to the third variant retaining an intron with a premature stop codon.

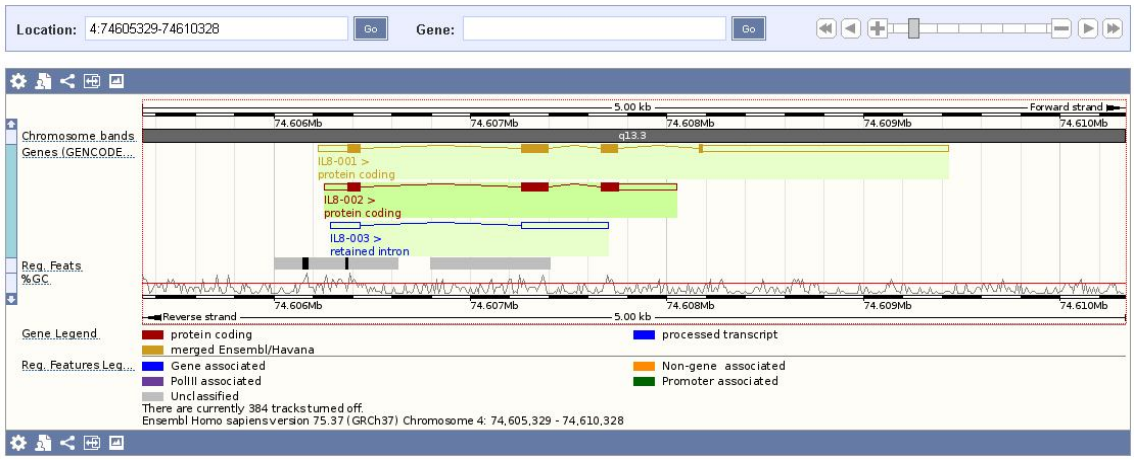

Figure 1-3 CXCL8 Transcripts

Screen shot from Ensembl showing the genomic loci and intron and exon locations of the three CXCL8 splice variants on chromosome 4. The transcripts are displayed graphically with introns as connecting lines between the exonic rectangles. Protein coding exons are distinguished from non-protein coding exons by filled rectangles.

There is very little known about the conditions that determine which splice variant is transcribed. The first splice variant is the reference gene. It is the longest transcript of 1705 bp from all 4 exons producing a protein of 99 amino acids. In comparison, the alternative variant only has 3 exons, the first two of which are identical to the reference transcript and the third is a slightly longer version using an alternative splice site, as shown in Figure 1-4. As the majority of both CXCL8 splice variants share the same sequence, experimental methods that detect epitopes in the transcribed protein, should detect all CXCL8 variants produced.

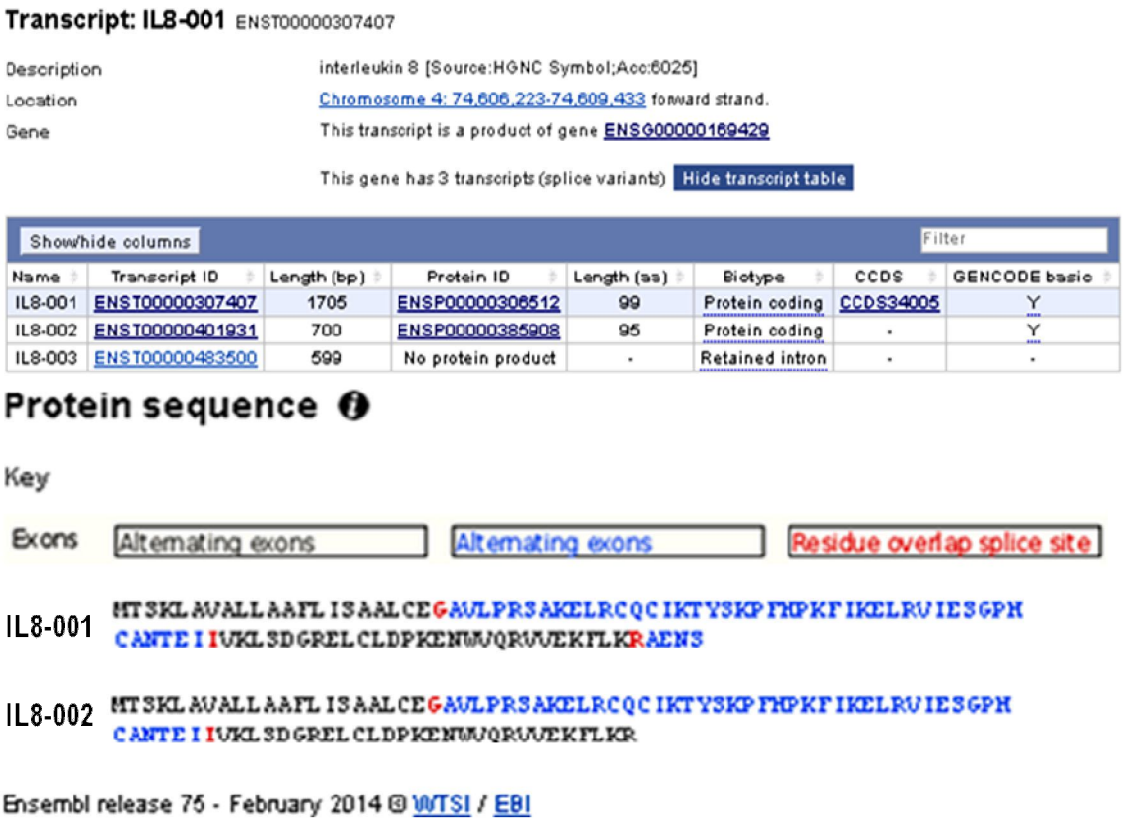

Figure 1-4 CXCL8 Splice Variants

Screen shot from Ensembl illustrating the genomic loci, primary protein sequences and exon locations as well as transcript and protein IDs of the two functional CXCL8 transcripts. There are three splice variants of CXCL8: IL8-001, IL8-002 and IL8-003. IL8-001 produces the reference protein and IL8-002 is the alternative variant. The primary protein sequences of these two proteins are listed with the different exons indicated by colour, black and blue, and the overlapping residues highlighted in red.

1.2 Intestine

1.2.1 Structure and Function of the Intestine

The intestine is the segment of the alimentary canal extending from the stomach to the anus. In mammals it consists of two sections, the small intestine and the large intestine, or colon. The main function of the small intestine is to digest and absorb nutrients from food. In light of this, the structure of the small intestine is designed to maximise surface area thus increasing the efficiency of absorption. The epithelium is a highly folded inner surface creating villi and microvilli that expand the surface area 30-60-fold. Three highly specialised and differentiated cell types are present in the epithelium (49), in addition to the columnar cells required for absorption (Figure 1-5). Goblet cells are simple columnar cells that have differentiated further into mucin-secreting cells. Therefore, goblet cells play a role in innate immunity by producing mucus to maintain the gastrointestinal barrier against infectious microorganisms. Paneth cells in the small intestine are also involved in innate immunity by secreting antimicrobial products such as defensins, lysozyme and TNF. Due to their location in the base of the crypt next to the stem cell, it is possible that the function of Paneth cells is involved with the protection of stem cells that proliferate and regenerate the crypt. The third cell type, enteroendocrine cells, secretes hormones in response to various stimuli. They act as sensors for the contents of the intestine with possible roles in mucosal immunity including secretion of preproglucagon splice product, GLP-2, which improves TGF-γβ-dependent intestinal wound healing (50).

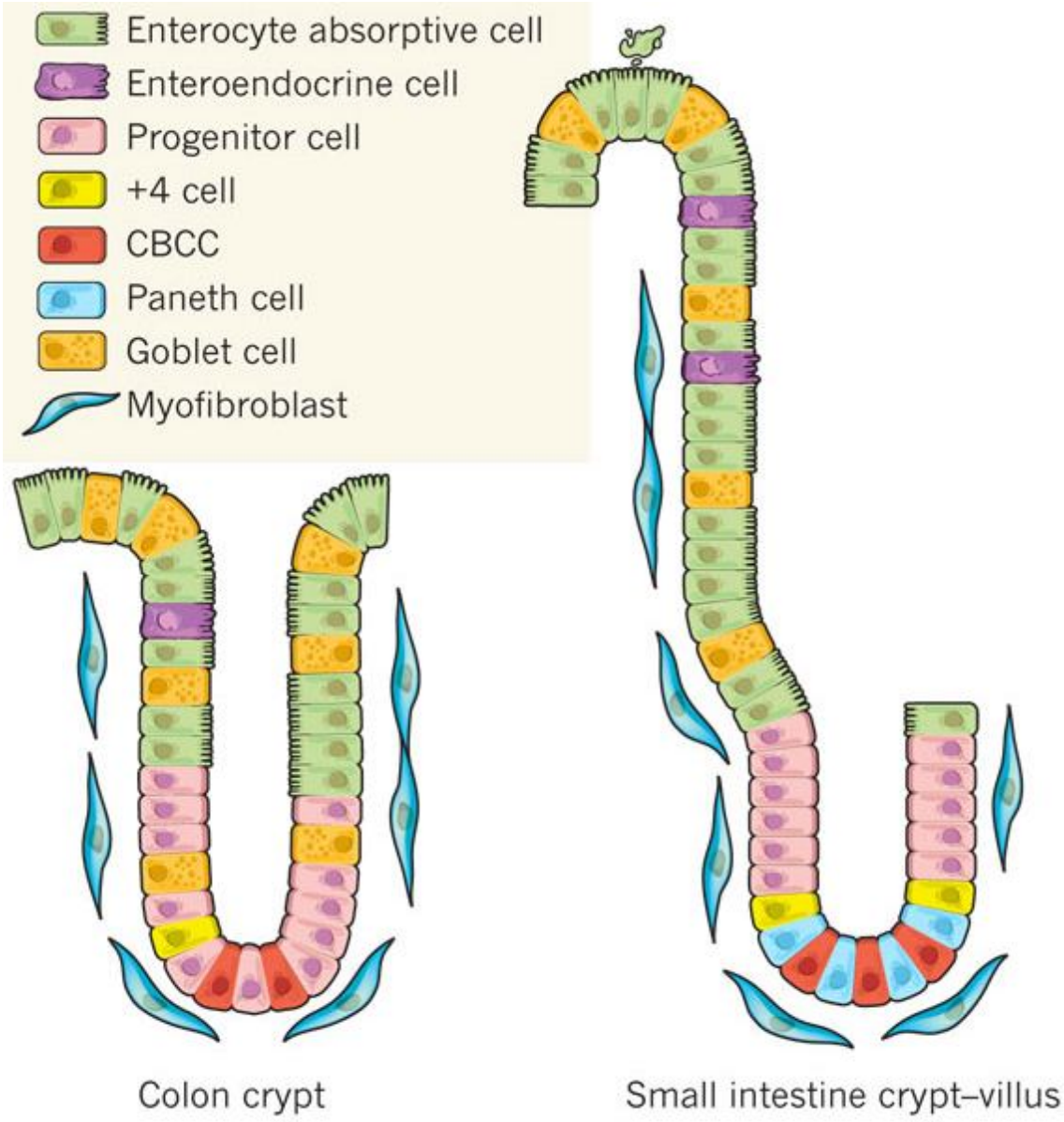

Figure 1-5 Organization of the Colon Crypt and the Small Intestinal Crypt–Villus

Both the colon crypt (left) and the small intestinal crypt (right) contain a stem-cell compartment at the crypt base. CBCCs (crypt base columnar cells) and the +4 stem cell have been indicated to be present between and just above the Paneth cells, respectively. Of note, Paneth cells are not detected in the colon, yet a Paneth-like cell has been suggested to be present at the crypt base. All four lineages (three in the colon) — enterocytes, Paneth cells, goblet cells and enteroendocrine cells — appear in different, but set ratios. Paneth cells move down to the base and are long-lived, whereas other lineages move up and are shed (a few days later) into the lumen while undergoing apoptosis. Rare cell types reported to exist in crypts, such as tuft cells, are not shown. Reprinted by permission from Macmillan Publishers Ltd: Nature (51), copyright 2011.

The lamina propria is located directly beneath the epithelium. It is a loose connective tissue supporting the epithelium and containing many lymphatic cells, which together with the epithelium forms the mucosa (52). Peyer's patches are lymphoid nodules located in the lamina propria of the small intestine that are enriched with immune cells (53). A large number of T-lymphocytes, dendritic cells (DCs) and macrophages are located in the intestinal lamina propria functioning as part of the innate and adaptive immune systems to protect the host from bacteria, whether microbiota or a potential pathogen (54, 55). Though T-lymphocytes are exposed to antigens from the microbiota, as well as pathogens, they do not constantly activate the immune system. This reduction in activity is achieved through reduced signal transduction through the T cell receptor to antigens and an increased sensitivity to the co-stimulatory molecule CD2, which results in increased production of IL-10 (56). During the pathogenesis of Crohn's disease, the lamina propria is infiltrated by T-lymphocytes, which have been shown to express increased levels of the cytokines IL-5, IL-12 and IL-15 (57). These cytokines activate the adaptive immune system and contribute to the dysregulation of the immune system observed in IBD. Lymphocytes also migrate from the lamina propria to the epithelium when barrier integrity is compromised thus exposing the large population of lamina propria lymphocytes to luminal bacteria and the subsequent initiation of inflammation (58).

The structure of the large intestine has much in common with that of the small intestine, but without the villi and Paneth cells. Instead its lumen is larger, goblet cells are more abundant and intestinal glands or invaginations of the epithelium are present. The main function of the colon is to absorb water from the fecal matter and vitamins such as vitamin K, vitamin B12, thiamine and riboflavin that are produced by the resident bacteria (59). It is also the location of many species of

bacteria that constitute the microbiota, whose functions in disease are the centre of intense investigation (see below).

Because the function of the intestine is to absorb molecules, it is an ideal site for infectious microorganisms to target e.g. *Salmonella enterica, Campylobacter jejuni, Escherichia coli, Salmonella typhi* (typhoid fever), *Vibrio cholera, Clostridium difficile,* norovirus/rotavirus etc (60). The lumen of the intestine is topologically external to the body and it is important that the immune system functions appropriately. The first line of defence for organisms that have survived the low pH of the stomach is the layer of mucus produced by goblet cells. The increased proportion of goblet cells in the colon as compared with the small intestine reflects the fact that few bacteria are present in the small intestine, unlike the ~10^{14} bacteria resident in the colon (61). The colonic epithelium is under constant stimulation by bacteria; however the colon is not constantly inflamed, as one would expect the epithelium of other tissues in the body to be when interacting with bacteria. Therefore, the epithelium is capable of being de-sensitized or tolerized to repeated inflammatory stimuli.

Inflammation in the intestine has several effects on the epithelium. The epithelium is the first cell-type to come into contact with bacteria (62) and as such epithelial cells express many innate immune system receptors (TLRs, NLRs, NLRPs). It forms a protective barrier between sites for potential pathogens e.g. intestinal lumen and the rest of the organism. Barrier integrity is therefore a vital property and is composed of intestinal epithelial homeostasis and integrity, mucus production and excellent innate immune system responses. The loss of any of these functions can lead to inflammation and IBD pathogenesis (63). An indicator of active IBD is altered intestinal epithelial homeostasis with increased apoptosis, reduced differentiation and differences in proliferation (64). As described above, the interaction between the microbiota and

the intestinal epithelium is an important factor in altering the epithelial transcriptome to achieve the necessary functional physiological response, including the induction of inflammation. Therefore, investigating how healthy epithelial cells regulate their inflammatory response will provide insights into dysregulated conditions, such as IBD.

1.2.2 Microbiota

The human body contains over 100 trillion (10^{14}) bacteria (65), ten times as many as the number of eukaryotic cells in the human body (3.72×10^{13} eukaryotic cells (66)), the majority of which are resident in the colon (65). Despite the abundance of bacteria, species diversity is relatively low with only 8 of the 55 known bacterial divisions present. Using rRNA sequence comparison, ~800 different species are identified with > 7 000 unique strains (67). The commensal bacteria provide a range of benefits to the host, particularly in aiding digestion of nutrients. This is represented by the large and diverse microbiotal gemone, which contains 100-fold more unique genes than the human genome (61). They are also necessary to maintain the lack of immune and inflammatory response to the presence of the large bacterial load in the colon (68) as mice reared in a germ-free environment show an increased susceptibility to infection and an impaired immune system. Human foetuses show a similar naivety to bacteria. This changes after a rapid commensal colonization at birth (69). Full maturation of the immune system and induction of tolerance to the microbiota requires the presence of the microbiota itself (70, 71).

Recent studies have shown a causal link between the intestinal microbiota composition and improvement of symptoms in IBD (72) (73) (74) (75). Transplantation of fecal microbiota has shown a small amount of success in a small number of patients with severe inflammatory disease, resulting in improved symptoms, resolution of histological inflammation and cessation of

treatment (steroids, antibiotics, anti-TNF) (76). A meta-analysis performed by Colman and Rubin on 18 fecal microbiota transplantation as therapy for IBD studies showed that some patients did achieve clinical remission but the effect is variable (77). There are many inconsistencies between studies including the timing and frequency of transplantation, donor selection, transplantation delivery system and method of microbiota analysis. Further work is required to standardise fecal microbiota transplantation as a consistent and effective therapeutic treatment. However, it is a successful method for treating *C. difficile* (78). A recent discovery by Gerding *et al* found that recurrent *C. difficile* infections can be cured by using spores of nontoxigenic *C. difficile* to colonise the space occupied by the toxic *C. difficile*. A major benefit of this method is that it avoids the stool donating associated with fecal transplantation (79).

1.3 Tolerance

Immune tolerance is a hyporesponsive state where the cell or organism becomes transiently unresponsive to repeated or prolonged stimulation (80). This effect is seen when macrophages are repeatedly stimulated with LPS (81). However, although tolerance functions as a protective mechanism against the potentially damaging effects of chronic inflammation, the antimicrobial functions of innate immunity must be retained or the host would become immunocompromised. The majority of existing research into tolerance has been conducted on macrophages to LPS (82). Prior stimulation of macrophages and monocytes with LPS results in a tolerized phenotype with altered IL-1 and IL-6 production and impaired NF-κB activation (82). Evidence from Savidge *et al.* suggests that CXCL8 tolerance can be induced independently of the TLR4 signalling cascade (83). Considering that Caco-2 cells, which will be used for the majority of this research, do not express TLR4, this published research is an example of tolerance in a specific set of circumstances. This phenotype is also seen in patients with sepsis, which demonstrates that inflammation in immune cells is a self-regulating process (84). Tolerance is not only a phenomenon of intestinal immune cells acquired postnatally (85), but also of peripheral leukocytes (86).

Foster *et al*. describe how the two classes of genes, "tolerizable" (genes not inducible in tolerant macrophages) and "non-tolerizable" (genes inducible in tolerant macrophages) are differentially regulated (87). Expression of both gene classes is similarly induced by the stimulus LPS, showing that neither class of genes is inherently more sensitive to stimulation nor is either class dependent on positive feedback of IFN-α/β or any other secreted factor. Therefore, the differential regulation must be gene-specific and they demonstrated that it was epigenetic in nature. Foster *et al* describe how only the histones (see 1.4.2 Histone Modifications) in non-tolerizable gene

promoters were re-acetylated in tolerized macrophages, though both classes of promoter were acetylated in naive cells. Whilst both classes of genes showed an increase in histone H3 lysine 4 tri-methylation (H3K4me3) levels upon initial LPS stimulation, the tolerizable gene promoters lost the histone H3K4me3 mark and the non-tolerizable gene promoters retained it. The presence of histone H4 acetylation and histone H3K4me3 in non-tolerizable gene classes correlates with continued expression of this gene class (87). H3K9me2 has also been shown to be increased in tolerized immune cells (88).

1.3.1 Regulation of Tolerance

As previously described, down-regulation of inflammation is essential to prevent further injury. The mechanisms can be classified into three functional groups: the clearance of immune complexes and apoptotic cells (complement system); the orchestrated progression of leukocytes and lymphocytes through activation, amplification and apoptosis (cytokine and chemokine signalling pathways); and the avoidance of injury by oxidation (restrictions placed on respiration and removal of haem) (1). Paradoxically, many proteins that contribute to the down-regulation of inflammation are also instrumental in inducing inflammation e.g. NF-κB. NF-κB regulates its own activation via a negative feedback loop (e.g. NF-κB induces expression of IκB, its own inhibitor (89), thereby limiting the amount of activated NF-κB).

A major regulator of IL-1β is IL-1Ra (IL-1 receptor antagonist). IL-1Ra has similar binding affinities to IL-1R as IL-1α and IL-1β do, but it does not initiate a signalling cascade when it binds to the receptor (90). Its expression is induced by LPS and TNF, themselves inducing inflammation, as a naturally occurring inhibitor of IL-1 limiting the degree of inflammation (91).

Another cytokine whose expression is induced by pro-inflammatory mediators, e.g. AP1 via TLR2 signalling, is interleukin-10 (IL-10). It downregulates the expression of pro-inflammatory cytokines such as IFN-γ, interleukins 2 and 3 and TNF; it enhances B cell survival and antibody production; it blocks NF-κB activity; and regulates the JAK-STAT signalling pathway (92). IL-10 is particularly important in establishment of tolerance in the intestine as mice deficient in IL-10 spontaneously develop chronic intestinal inflammation (enterocolitis) (93). However, this can be reduced to just local inflammation of the proximal colon by housing the mice in a specific pathogen-free environment. This highlights the involvement of microbiota in the development of tolerance in a healthy individual and the opposing contribution to disease development in an immunocompromised host. Indeed, a phase I trial which treated Crohn's Disease patients with recombinant IL-10-producing bacteria showed a marked decrease in the Crohn's Disease Activity Index during the treatment period i.e. when IL-10 was present (94).

TGF-β (transforming growth factor – β) is another essential immune regulation cytokine. It inhibits the differentiation of T helper type 1 (Th1) and Th2 cells and regulates tolerance via T regulatory (T_{reg}) cells (95). Mice deficient in TGF-β show an increased susceptibility to colitis, as do IL-10-deficient mice. Also, as shown by IL-10 deficiency, a decrease in TGF-β signalling increases the susceptibility to IBD (96) and maintains the persistence of inflammation seen in these patients (97). The induction of tolerance is not dependent upon the expression of the anti-inflammatory genes mentioned above (e.g. TGF-β, IL-10) (98).

1.3.2 Inflammatory Bowel Disease

While the pathology of IBD can be considered in several ways, it can be regarded as an example of disrupted inflammatory tolerance in the intestine. The main forms are Ulcerative Colitis (UC)

and Crohn's Disease. Both are characterized by flares of acute inflammation amongst a long term chronic inflammatory state. Crohn's Disease can affect the entire gastrointestinal tract, whilst UC only affects the colon. However, they both have an aberrant inflammatory response, possibly due to loss of a hyporesponsive state (99).

UC is defined as idiopathic, diffuse, continuous and superficial inflammation in the large intestine, which relapses and remits over time. The patient is also likely to experience diarrhoea, rectal bleeding and inflammation in other organs with an increased long-term risk of colorectal cancer. UC pathogenesis is complicated and incompletely understood, but is thought to be caused by inappropriate immune responses. Genetically mutated genes integral to preservation of the epithelial barrier have also been implicated by genome-wide association studies (100). Disruption of the epithelial barrier allows commensal bacteria access to the underlying immune cells leading to a dysregulated T cell driven inflammatory response.

The highest incidence rates are in the developed world for young adults with rates ranging from 0.6 to 24.3 cases per 100 000 person-years in Europe and North America compared with 0.1 to 6.3 cases per 100 000 person-years in Asia and Middle East (101). Approximately 500 people per 100 000 live with UC worldwide. It can severely impact a patient's quality of life as 67-83% will experience relapsing and remitting courses over the first 10 years post diagnosis (102). Treatments aim to heal the mucosa thereby reducing the risk of relapse or the need for a colectomy. 5-aminosalicylates are effective treatments for mild to moderate conditions and for preventing disease relapse (103). More severe cases may require glucocorticosteroids, thiopurines, ciclosporin and/or anti-TNF antibodies and eventually surgery (104).

Crohn's Disease is similar to UC in that it is an idiopathic inflammatory disease of the gastrointestinal tract, but there are several distinct differences. In Crohn's Disease, inflammation

can affect any part of the gastrointestinal tract, though it is most common in the ileum (final section of the small intestine) and colon. Symptoms include diarrhoea, fatigue, weight loss, narrowing of the colon over time and the added complications of bowel obstructions, fistulae and abcesses, as well as an increased risk of cancer and malnutrition. Crohn's Disease is a chronic inflammatory condition that is associated with several reported susceptibility genes (105). Other factors implicated include variations in the microbiota composition, specific food elements or infections and a strong correlation between smoking and worsening disease activity (106). Regardless of what the initiating factor is, excessive transmural inflammation (inflammation that spans the entire depth of the intestinal wall) is induced by T cells and further amplified and maintained by pro-inflammatory cytokines and other cell types (107).

The incidence of Crohn's Disease is higher in the Western world (108) with a highest annual incidence rate of 12.7 -20.2 cases per 100 000 person-years in Europe and North America compared with 5 cases per 100 000 person-years in Asia and the Middle East (101). Crohn's Disease is rarer than UC in adults as shown by the worldwide prevalence of 300 – 400 per 100 000. Disease development tends to peak in early adulthood (15 – 30 years old) and again in the elderly. Treatment, as for UC, involves 5-aminosalicylates, glucocorticosteroids, anti-TNF antibodies, thiopurines, cessation of smoking and surgery (109). Crohn's Disease can relapse, even after surgery. Unlike UC, an enteral liquid diet for 6 – 8 weeks is prescribed for patients with Crohn's Disease, which has similar efficacy to corticosteroids (107), though its usefulness as a treatment is limited by its cost and the difficulty that patients have in adhering solely to this diet (109).

As described above, IBD is characterised by chronic inflammation. It is therefore important to understand how both tolerance and the dysregulation of tolerance occurs; and how tolerance can be re-established with the aim of identifying novel therapeutic targets.

1.4 Epigenetics

1.4.1 Chromatin

Chromatin is composed of DNA wrapped around highly conserved histone proteins to assemble nucleosomes. Each nucleosome is composed of a histone octamer (2 copies each of the core histones H2A, H2B, H3 and H4) with 146 bp of DNA wrapped around the octamer in 1.67 left-handed superhelical turns (110). Between each core nucleosome is 10 – 80 bp DNA and a histone H1 or linker histone protein (111). Many other histone variants exist and compromise a proportion of the core octamer nucleosomes. Under specific conditions they play a functional role, e.g. H2AX is phosphorylated in response to DNA double-strand breaks (112).

Chromatin can be visualised with an electron microscope where the nucleosomes look like "beads on a string" with the string representing the rest of the DNA not wrapped around the histone octamer (113). Due to the linker DNA length being adjustable, chromatin is not in a fixed state. Relaxed, or open, chromatin, with the nucleosomes spaced apart, is called euchromatin. This exposes the DNA to proteins in the transcriptional machinery, including RNA polymerases, TFs and other DNA binding proteins. Heterochromatin is the repressed or closed state of chromatin where the nucleosomes are closely associated and the DNA is not easily accessed (114). A change from heterochromatin to euchromatin is required for gene transcription to be induced.

Histones are positively charged proteins due to their high proportion of lysine and arginine residues. However, post-translational modifications (PTMs) to residues in the histone, particularly in the histone tail, neutralise the positive charge thus altering the histone-DNA interaction and

allowing the transcriptional machinery access to the DNA. Histone acetylation and methylation of specific residues e.g. H3K4me3 allow this to happen (115).

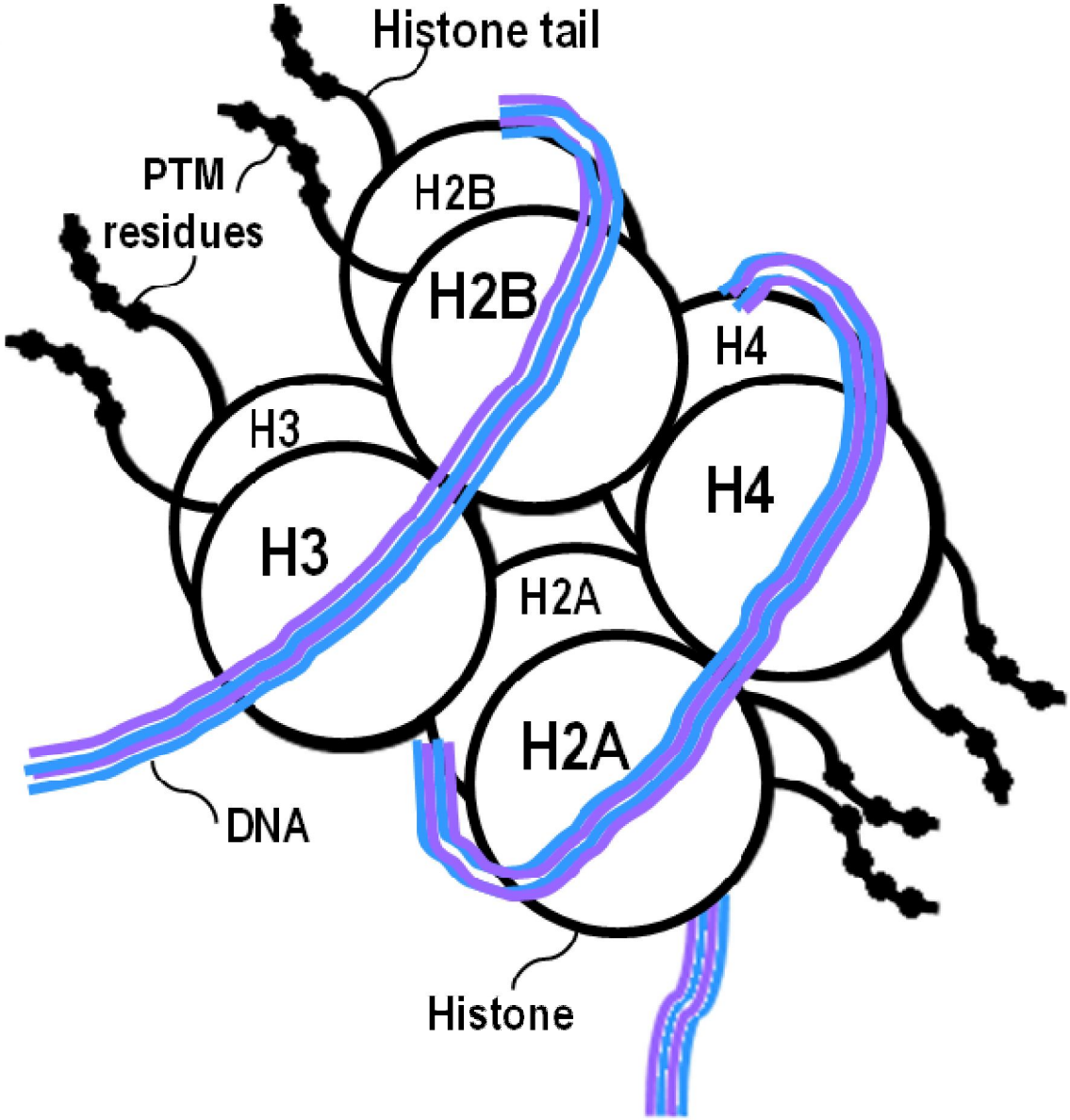

Figure 1-6 Structure of the Nucleosome

The nucleosome is an octamer of histone proteins around which is wrapped 146 bp DNA in 1.67 left-handed superhelical turns. Two copies each of four different histone proteins (H2A, H2B, H3 and H4) compose the histone octamer. The tail of each histone protein is enriched with residues that can be post-translationally modified. Figure adapted from (116).

1.4.2 Histone Modifications

Epigenetics are defined as the heritable changes in gene expression or cellular phenotype due to changes above the DNA sequence hence epi- (Greek: above) genetics (study of heredity and the variation of inherited characteristics). There are three main types of epigenetic transcriptional regulation: DNA methylation, histone acetylation and histone methylation. DNA methylation in the gene promoter region causes gene silencing e.g. of transcription factors during embryonic stem cell differentiation (117), as well as X chromosome inactivation (118) and is an indicator of mitotic age (119); whilst histone acetylation is necessary for transcriptional activation (120, 121). Methylation of, in particular, lysine residues is a common PTM associated with a change in gene transcripition. Activated transcription is associated with e.g. H3K4me3, whilst repression of gene transcription is associated with e.g. H3K9me3 or H3K27me3 (122). Methylation of H3K4 has different roles depending on the amount of methylation. Tri-methylation of H3K4 is associated with active gene transcription, but mono-methylation (H3K4me1) is found to be enriched at enhancer regions (123). Histone methylation also maintains the boundary between transcribed and non-transcribed genes (124).

In addition to the histone PTMs associated with gene transcriptional status, there are a variety of other modifications with a range of purposes. Histone phosphorylation is required for release of the transcriptional elongation complex (125) and activation of the DNA damage response (126); ubiquitination is a pre-requisite for H3K4 and H3K79 methylation (127); sumoylation mediates gene silencing (128); and biotinylation is involved in cell proliferation and the DNA damage response (129). Table 1-1 describes the range of PTMs available for the different residues in the histone tails, the enzymes (if known) that catalyse the histone PTM and the function of the epigenetic mark. PTM of residues in the body of histones also occur (Table 1-1), but are rarer

than PTMs to residues in the histone tail (130). These modifications are mainly believed to alter the strength of nucleosome binding to DNA.

Chronic inflammation involves epigenetic changes to pro-inflammatory cytokines resulting in constitutively high gene expression. An reduction in histone acetylation at tolerizable gene promoters is associated with reduced gene transcription (87) and differences in DNA methylation is seen at multiple IBD susceptibility genes, including the IL8 receptor beta (IL8RB), between healthy controls and patients with IBD (131). Modification of the chromatin regulatory enzymes can inhibit the progression of inflammatory-diseases and small molecule inhibitors of these enzymes show great potential as novel therapeutics.

Histone	Modification	Site^	Enzyme	Function
H1	Methylation	K26	Ezh2	Transcriptional silencing
	Phosphorylation	S27	Unknown	Transcriptional activation, chromatin decondensation
H2A	Acetylation	K5	Tip60, p300/CBP	Transcriptional activation
		K36^	Unknown	Unknown
		K119^	Unknown	Unknown
	Methylation	K74^	Unknown	Unknown
		K75^	Unknown	DNA binding
		R77	Unknown	Inserts into minor groove
		K99	Unknown	Unknown
	Phosphorylation	S1	Unknown	Mitosis & Chromatin assembly
		S1	MSK1	Transcriptional repression
		S139 (H2A.X)	ATR, ATM, DNA-PK	DNA repair, biomarker of DNA double-strand breaks
	Ubiquitylation	K119	Ring2	Spermatogenesis
	Biotinylation	K9	Biotinidase	Unknown
		K13	Biotinidase	Unknown
		K129	Biotinidase	Unknown
H2B	Acetylation	K5	ATF2	Transcriptional activation
		K12	ATF2, p300/CBP	Transcriptional activation
		K15	ATF2, p300/CBP	Transcriptional activation
		K20	p300	Transcriptional activation
		K82^	Unknown	Charge neutralization of negative helix dipole
		K105^	Unknown	Unknown
		K113^	Unknown	Unknown
	Methylation	K31^	Unknown	Unknown
		K40^	Unknown	Indirect DNA binding
		R76^	Unknown	Unknown
		R83^	Unknown	DNA binding
		R89^	Unknown	Unknown

		R96^	Unknown	Unknown
	Phosphorylation	S14	Mst1, Unknown	Apoptosis and DNA repair, respectively
		S33^	TAF1	DNA binding, transcriptional activation (132)
	Ubiquitylation	K120	UbcH6	Meiosis
		K123^	Rad6	Required for methylation of H3K4 and H3K79 (133)
H3	Acetylation	K9	Unknown	Histone deposition
			Gcn5, SRC-1	Transcriptional activation
		K14	Unknown	Histone deposition
			Gcn5, PCAF, SRC-1, Esal, Tip60, p300	Transcriptional activation
			Esal, Tip60	DNA repair
			Elp3, Sas3	Transcriptional elongation
			Hpa2	Unknown
			TAF1	RNA polymerase II transcription
			hTFIIIC90	RNA polymerase III transcription
			Sas2	Euchromatin
		K18	Gcn5, p300/CBP	Transcriptional activation
			Gcn5	DNA repair
			p300/CBP	DNA replication
		K23	Unknown	Histone deposition
			Gcn5, p300/CBP	Transcriptional activation
			Gcn5, Sas3	DNA repair
		K27	Gcn5	Transcriptional activation
		K115^	Unknown	Indirect DNA binding
		K122^	Unknown	Indirect DNA binding
	Methylation	K4	Set7/9	Transcriptional activation (tri-Me)
			MLL, ALL-1	Transcriptional activation
		R8	PRMT5	Transcriptional repression
		K9	Suv39h, Clr4	Transcriptional silencing (tri-Me)
			G9a	Transcriptional repression, genomic imprinting
			SETDB1	Transcriptional repression (tri-Me)
		R17	CARM1	Transcriptional activation

		K27	Ezh2	Transcriptional silencing, X inactivation (tri-Me)
			G9a	Transcriptional silencing
		K36	Set2	Transcriptional activation (elongation)
		R52^	Unknown	Indirect DNA binding (H_2O-mediated)
		R53	Unknown	Unknown
		K56^	Unknown	Indirect DNA binding
		K79	Dot1	Euchromatin, Transcriptional activation (elongation), checkpoint response
		K122^	Unknown	Indirect DNA binding
	Phosphorylation	T3	Haspin/Gsg2	Mitosis
		S10	Aurora-B kinase	Mitosis, meiosis
			MSK1, MSK2	Immediate-early gene activation
			IKK-α, Snf1	Transcriptional activation
		T11	Slk/Zip	Mitosis
		S28	Aurora-B kinase	Mitosis
			MSk1, MSK2	Immediate-early gene activation
		T118^	Unknown	DNA binding with H4R46
	Biotinylation	K4	Biotinidase	Gene expression
		K9	Biotinidase	Gene expression
		K18	Biotinidase	Gene expression
H4	Acetylation	K5	Hat1	Histone deposition
			Esa1, Tip60, ATF2, p300	Transcriptional activation
			Esa1, Tip60	DNA repair
			Hpa2	Unknown
		K8	Gcn5, PCAF, Esa1, Tip60, ATF2, p300	Transcriptional activation
			Esa1, Tip60	DNA repair
			Elp3	Transcriptional elongation
		K12	Hat1	Histone deposition, telomeric silencing
			Esa1, Tip60, p300	Transcriptional activation
			Esa1, Tip60	DNA repair
			Hpa2	Unknown

		K16	Gcn5, Esa1, Tip60, ATF2 Esa1, Tip60 Sas2	Transcriptional activation
				DNA repair
				Euchromatin
		K31^	Unknown	Indirect DNA binding
		K77^	Unknown	Indirect DNA binding
		K91^	Unknown	Forms salt bridges with H2BE63
	Biotinylation	K8	Biotinidase	DNA damage response
		K12	Biotinidase	DNA damage response
	Methylation	R3	PRMT1	Transcriptional activation
			PRMT5	Transcriptional repression
		K20	PR-Set7	Transcriptional silencing (mono-methylation)
			Suv4-20h	Heterochromatin (tri-Me)
		K59	Unknown	Forms salt bridge with H4E63, transcriptional silencing
		K79^	DOT1	DNA binding
		R92^	Unknown	Unknown
	Phosphorylation	S1	Unknown	Mitosis, chromatin assembly
			CK2	DNA repair
		S47^	Unknown	Indirect DNA binding

Table 1-1 Histone Modifications, Enzymes and Functions in Humans

The table lists the different post-translational modifications possible at residues in the five different histone proteins (H1, H2A, H2B, H3 and H4), as well as the enzymes responsible for the modification and the physiological function. ^ denotes a residue present in the globular histone protein rather than the histone tail. Adapted from (134) (135) (136).

1.4.3 Histone Modifications and Gene Transcription

As previously described, gene transcriptional status is associated with specific chromatin modifications, usually in the gene promoter region, but also throughout the gene (H3K36me3 is present on the exons of the actively transcribed gene and is a marker of transcriptional elongation (123)). Acetylation of various lysine residues on histones H3 and H4 are associated with gene transcription, though the specific lysine residue is dependent upon the affinity of the histone

acetyltransferases (HATs) (137) (Table 1-1). Histone methylation produces a variety of effects: as a general rule, histone H3K4me3 is associated with activation of gene transcription whilst histone H3K9me3 and histone H3K27me3 are associated with transcriptional repression (122) (Table 1-1). Not all genes require histone acetylation for transcriptional activation. Histone H3S10 phosphorylation is sufficient, in the absence of histone acetylation, for IL-10 expression in macrophages, for examples (92). Therefore, regulation of H3S10 phosphorylation may play a role in downregulating inflammation.

Individual lysine residues in a histone tail can be methylated up to three times thus changing its functional role accordingly (Table 1-2). However, many genes have multiple histone modifications, often ones that have opposing effects (Table 1-2). Depending on the combination of modifications present, different proteins are able to bind to the chromatin and specifically target certain genes for either activation or repression of gene transcription. For example, transcribed inflammatory gene promoters are marked with histone H3K4me3. Under non-transcribed conditions the gene promoters are marked with the repressive histone H3K9me3 mark. However, some gene promoters have both H3K4me3 and H3K9me3 marks. These marks correlate with the genes that have slower gene expression kinetics than the genes that only have H3K4me3 marks (138). The combinatorial nature of the histone code means that genes can be poised between activated and repressed (H3K4me2 and H3K9me2) until a stimulus causes further modification in one direction or the other (loss of H3K9me2 and an increase in H3K4me3 or *vice versa*) (139). Though much research has been conducted into histone modification and the subsequent effect on gene transcription, it is fair to say that histone methylation's relationship with gene transcription has not been fully characterised and the complete epigenetic code for each gene in every circumstance has not been determined. Therefore, we cannot accurately state which changes to the epigenetic code are required to induce or repress transcription.

Modification	Histone Site					
	H3K4	H3K9	H3K27	H3K36	H3K79	H4K20
Mono-methylation	Activation	Activation	Activation	---	Activation	---
Di-methylation	---	Repression	Repression	---	Activation	---
Tri-methylation	Activation	Repression	Repression	Activation	Activation, Repression	Repression

Table 1-2 Histone Methylation Modifications and their Effect on Transcription

Table 1-2 summarises the published associations between different histone methylation modifications and gene transcription (adapted from Table 1-1).

Different cell types exhibit differences in how histone methylation modulates gene expression. For example, bivalent histone modifications are commonly found in stem cells. Developmental genes often contain both H3K4me3 and H3K27me3 before one or the other mark is removed and the cell fate is determined (140). Very little is understood about genes displaying opposing epigenetic signatures. Though bivalent modifications may be found in one cell type under certain experimental conditions, it does not necessarily hold true that these relationships exist in all cell types in all environmental conditions.

1.4.4 Regulation of Histone Modifications

The post-translational modification of histones is catalyzed by a variety of enzymes with different affinities and specificities (141). These include histone acetyltransferases (HATs), histone deacetylases (HDACs), DNA methyltransferases (DNMTs), histone/lysine methyltransferases (HMTs/KMTs), histone/lysine demethylases (HDM/KDM) as well as the histone phosphorylases required for activation of the transcriptional initiation complex. Modifying the degree of acetylation

through use of butyrate, a known histone deacetylase inhibitor, thereby increases the amount of histone acetylation present and exacerbates the inflammatory response to IL-1β and LPS (121).

Until the discovery of histone demethylases in 2004, histone methylation was thought to be a permanent modification (142). A variety of small molecule inhibitors of histone deacetylases, methyltransferases and demethylases have been developed as novel therapeutic agents. The majority have an application in cancer (143) (144), though trials for inflammatory diseases are also underway (145). One example in particular that shows promise in inflammatory disorders is Lysine specific demethylase 1 (LSD1). LSD1 only demethylates H3K4me2 and H3K9me2, the latter when in complex with the androgen receptor (146), thus modulating the transcriptional state of the gene. Janzer *et al*. describes how LSD1 alters the methylation state of several pro-inflammatory cytokine promoters including IL-1β and CXCL8 (139).

1.4.5 Epigenetics and Inflammatory Bowel Disease

Epigenetics is a relatively new area of research so the understanding of epigenetics in IBD is limited. However, many complex diseases, including IBD, are beginning to be researched for the epigenetic mechanisms underlying a proportion of the disease. Genetic loci discovered to promote susceptibility to IBD pathogenesis only account for a small proportion of the disease variance, 13.6% for Crohn's Disease and 7.5% for UC (147). Environmental factors, including smoking, account for much of the remaining disease variance. These factors cause an alteration in gene expression and lead to development of IBD. As gene expression is also known to be regulated by epigenetics, it is logical to assume that a small percentage of the disease variance is due to epigenetics. Further evidence is provided by the mechanism of action of some of the known drugs used to treat patients with IBD (148).

Glucocorticoids are steroid hormones which are used in IBD to suppress the immune response. Expression of anti-inflammatory genes is increased due to increased histone acetylation. However, glucocorticoids can also suppress gene expression via specific histone deacetylation of pro-inflammatory cytokines (149). Methotrexate, an immunosuppressant, is used to maintain remission of Crohn's disease. It has the effect of reducing the amount of folic acid by inhibiting dihydrofolate reductase. Folic acid is known to be involved in the DNA methylation pathway. A reduction in folic acid by methotrexate has been associated with an increase in DNA methylation levels in patients suffering from arthritis (150), though the before and after effects of methotrexate in patients with IBD has not yet been investigated.

Analysis of the differences in intestinal microbiotal composition between healthy controls and patients with IBD indicate an underrepresentation of butyrate-producing bacterial species (151). Butyrate and other short chain fatty acids have been implicated in the regulation of gene transcription via inhibition of histone deacteylase activity (121). Therefore, the use of butyrate as a treatment for IBD should increase the level of histone acetylation and promote gene transcription. This is associated with an alleviation of symptoms and a statistically significant decrease in endoscopic and histological inflammation (152). Therefore, there is strong evidence for an epigenetic component to regulation of inflammation and IBD pathogenesis.

Other evidence for the involvement of epigenetics in the development of IBD comes from parent-of-origin studies. Analysis of IBD inheritance from parent to child showed that disease transmission from mother to child was statistically far more likely than from father to child ($P=0.00001$) (153) and that this is likely due to genomic imprinting. Genomic imprinting is the heritable DNA methylation of a particular gene to prevent its transcription. Therefore, the

conditions required for the development of IBD in the parent can be programmed epigenetically for inheritance in the child. Evidence for the involvement of epigenetics in IBD pathogenesis is described by the relatively low concordance rate for IBD in monozygotic twins (148), indicating that the environment plays a large role. Epigenetics can be considered to be at the boundary between the environment and the DNA. Epigenetic permutations between genetically identical twins are an interpretation of the environmental effect on the DNA and gene expression and can be very different between two individuals with the same genetic background.

Petronis describes the association between epigenetics and differences in the DNA sequence of candidate susceptibility genes (148). SNPs (single nucleotide polymorphisms) are variations at the same position in the DNA that occur in at least 1% of the population. Some SNPs e.g. G(-308)A in the AP2 TF binding site, are sensitive to DNA methylation and can thus control whether the gene can be epigenetically modified leading to a change in gene transcription. The C(-511)T SNP in the IL-1β promoter, depending on the study, has shown a conflicting association with IBD (148).

Diet is another environmental factor, along with smoking, whose effect on gene expression can be seen epigenetically. As previously mentioned, butyrate and other short chain fatty acids have an effect on both gene transcription and IBD. Diets rich in methyl-donor metabolites, such as choline, methionine and folate can increase the amount of DNA methylation and the presence of dietary pholyphenols, such as curcumin and catechins found in tea, inhibit DNMTs and HATs (154, 155). It has previously been shown that diet has a clinical benefit in IBD e.g. an elemental diet for children suffering from Crohn's disease is as effective as high dose steroids (156) and curcumin, a component of tumeric, enhances anti-inflammatory gene expression in patients with IBD (157). However, much more research is required before we fully understand the effects of

diet in epigenetics and disease and before diet can become a therapeutic tool in the treatment of IBD, based on epigenetic predictions.

In conclusion, there is an increasing amount of evidence for the role of epigenetics in IBD pathogenesis. Epigenetics acts as a central mediator for several IBD susceptibility and risk factors (158). The effects of diet, environment, microbiota and susceptibility genes on the immune system and gene transcription are mediated through epigenetics and as such, modifying the epigenetic signature may, in time, allow us to develop treatments that will reverse IBD pathogenesis.

2 Aims and Hypotheses

The aims of this research project are:

- To establish the induction of tolerance in intestinal epithelial cells to pro-inflammatory agents. Intestinal epithelial cell-lines Caco-2 and NCM460 will be first stimulated with P3CK and/or IL-1β to produce an inflammatory response then tolerized by pre-stimulating the cells followed by another pro-inflammatory stimulation.
- To study the epigenetic mechanisms involved in the regulation of tolerance. This will be achieved by the use of a range of small molecule epigenetic inhibitors to alter the methylation level of particular histone H3 lysine residues associated with a role in gene transcription. These inhibitors will then be incubated with tolerized cells and the effect on inflammatory gene expression measured.

I hypothesise that the inflammatory gene expression profile of intestinal epithelial cells is tolerized to pro-inflammatory agents following pre-stimulation with said agents. I also hypothesise that modifying the epigenetic signature of intestinal epithelial cells, via modification of the relative levels of histone methylation, will alter the expression level of inflammatory genes.

3 Materials and Methods

3.1 Cell Culture

Reagent	Supplier	Address
Caco-2 cell line	ECACC	Salisbury, UK
HT29 cell line	ECACC	Salisbury, UK
NCM460 cell line	INCELL Corporation LCC	San Antonio, USA
THP-1 cell line	ECACC	Salisbury, UK
Dulbecco's modified Eagle medium (DMEM)	Invitrogen	Paisley, UK
M3 base medium	INCELL Corporation LCC	San Antonio, USA
Fetal Calf Serum (FCS)	Gibco	Paisley, UK
Non-Essential Amino Acids (NEAA)	Gibco	Paisley, UK
Hepes Buffer	Gibco	Paisley, UK
Penicillin/Streptomycin (Pen/Strep)	Gibco	Paisley, UK
Dulbecco's Phosphate-Buffered Saline (PBS)	Invitrogen	Paisley, UK
Insulin-Transferrin-Selenium (ITS)	Invitrogen	Paisley, UK
Interleukin-1β (IL-1β)	Gibco	Paisley, UK
N-Palmitoyl-S-[2,3-bis(palmitoyloxy)-(2*RS*)-propyl]-(*R*)-cysteinyl-(*S*)-seryl-(*S*)-lysyl-(*S*)-lysyl-(*S*)-lysyl-(*S*)-lysine Pam_3CysK_4 (P3CK)	EMC	Tuebingen, Germany
Roswell Park Memorial Institute (RPMI) medium	Invitrogen	Paisley, UK

Table 3-1 Reagents used in Tissue Culture

3.1.1 Caco-2 and HT29 Cell Lines

All experiments were performed on the human cell lines Caco-2 and HT29, as relevant to the study of inflammatory bowel disease and its potential treatment in humans. Both Caco-2 and HT29 cells have been used extensively to model intestinal epithelial function *in vitro* for over 25 years as they are derived from human colorectal adenocarcinomas. Whilst the two cell lines have

similar phenotypes, there are some critical differences. Both cell lines are immortalised and differentiate spontaneously in long-term culture to form a monolayer. However, Caco-2 cells dedifferentiate and acquire some characteristics of mature small intestinal enterocytes including apical microvilli and intercellular tight junctions. They also express small intestinal hydrolases including sucrose-isomaltase and lactase which are transiently expressed in the human foetal colon but not the adult colon. HT29 cells do not acquire enterocytic characteristics and remain as exclusive colonocytes.

As the number of passages increases, the function, metabolism and rate of differentiation of Caco-2 cells changes, as shown by the increasing expression of enterocyte differentiation markers such as the glucose transporter (GLUT)-5 (159) (160). We address this potentially confounding factor by performing all experiments on Caco-2 cells between passages 47 and 60 (supplied from ECACC at passage 45). We were able to achieve reproducibility of results using cell lines of relative uniformity and ready availability and minimised other influencing factors such as seeding density, culture conditions and media composition by strictly standardising them to achieve robust reproducibility of results.

Whilst Caco-2 and HT29 cell lines are derived from adenocarcinomas and therefore contain multiple mutations that are not present in the normal, non-malignant colon, they are still a suitable model. Cancer cells have already become immortalised escaping cellular senescence and thus able to proliferate indefinitely. This is necessary for a cell line as it ensures that there is a continuous supply of genetically identical cells. However, in order to confirm that the results are not due to cancerous mutations, we performed repeat experiments in a non-malignant cell line. Caco-2 and HT29 cell lines also grow and proliferate much more quickly than normal cell lines, making them an appropriate research model.

Caco-2 and HT29 cells (both human colon epithelial cell lines) were grown in DMEM supplemented with 10% heat inactivated-FCS (HI-FCS), 1% NEAA, 10 mM Hepes Buffer, 10000 U/ml / 10000 µg/ml Pen/Strep (+FCS media) at 37 °C and 5% CO2. When the cells reached 80-95% confluency, they were seeded at 0.5 x 10^4 cells per ml (Caco-2) or 2.5 x 10^4 cells per ml (HT29) into either 6-well or 12-well plates, or if not required for an experiment subcultured at ~1:10. 6-well plates were used originally whilst optimising the experimental conditions of IL-1β stimulation. 12-well plates were used for the majority of experiments as they require smaller volumes of media than 6-well plates and as such are more economical.

After seeding, the cells were grown for a total of 7 days before sample collection. The cells were pre-stimulated 48 hours prior to sample collection, stimulated again (for the tolerized cells or stimulated for the first time for the stimulated cells) 24 hours prior to sample collection and the samples were collected ater 7 days. 24 hours prior to the first stimulation with P3CK or IL-1β or the first epigenetic inhibitor incubation, the +FCS media is discarded, the cells washed with PBS and the media replaced with +ITS media (DMEM supplemented with 1% NEAA, 10mM Hepes Buffer, 10000 U/ml / 10000 µg/ml Pen/Strep and 1000 mg/L Insulin, 550 mg/L Transferrin and 0.67 mg/L sodium selenite). Cells in the control condition had their +FCS media replaced by +ITS media 48 hours before sample collection. In the tolerization experiments, the cells in the control and stimulation conditions, as well as the cells that received the tolerizing pre-stimulation of P3CK or IL-1β were all given fresh media 48 hours prior to sample collection. The control cells also received fresh media 24 hours prior to sample collection when the other cells were stimulated for the first (stimulated) and second (tolerized) time. Therefore, substances secreted by the cells into the media only accumulated for 24 hours before the cells were washed with PBS and the media replaced.

When using media free from FCS, as described in 4.1.3 and Figure 4-14 onwards, DMEM was supplemented with insulin, transferrin and selenium as these are obligatory nutrients for optimal performance in the absece of FCS. Whilst serum contains the required growth factors, transport proteins, minerals, trace elements, lipids, extracellular matrix components, protease inhibitors and detoxifying factors necessary for cell proliferation and growth, it is possible to replace FCS with just insulin, transferrin and selenium. This reduces the inherent variability in the amount of endotoxin, haemoglobin, microbial contaminants and other adverse factors present in serum (161).

3.1.2 NCM460 Cell Line

NCM460 cells are a non-malignant epithelial cell line derived from the colon mucosa of a 68-year old Hispanic male Moyer et al., 1996. This cell line has been used in a number of studies investigating the function of normal colonic epithelial cells in infectious disease, cell signalling, cytokine production, gene regulation, protein expression and phosphorylation in multiple growth regulatory pathways. Like Caco-2 and HT29 cell lines, NCM460 cells form a mixed monolayer/suspension culture and express colonic epithelial cell associated antigens, such as cytokeratins and villin. Some cells are also positive for mucin synthesis. Though the cells show normal growth characteristics and are not tumourigenic, they have acquired some transformation-associated properties due to being in culture for a long time.

NCM460 cells were cultured in M3 medium supplemented with 10% HI-FCS (+FCS), or 1000 mg/L Insulin, 550 mg/L Transferrin and 0.67 mg/L sodium selenite (+ITS), and 10000 U/ml / 10000 µg/ml Pen/Strep at 37 °C and 5% CO_2. When the cells reached 80-95% confluency, they were seeded at 8 x 10^4 cells per ml into 12-well plates, or if not required for an experiment

subcultured at ~1:10. As for Caco-2 cells, after seeding the NCM460 cells were grown for a total of 7 days before sample collection. The cells were pre-stimulated 48 hours prior to sample collection, stimulated again (for the tolerized cells or stimulated for the first time for the stimulated cells (Figure 3-2)) 24 hours prior to sample collection and the samples were collected ater 7 days. +FCS medium was replaced by +ITS medium 24 hours prior to the first stimulation with P3CK or IL-1β or 48 hours before sample collection for the control cells. In the tolerization experiments, the cells in the control and stimulation conditions as well as the cells that received the tolerizing pre-stimulation of P3CK were all given fresh media 48 hours prior to sample collection. The control cells also received fresh media 24 hours prior to sample collection when the other cells were stimulated for the first (stimulated) and second (tolerized) time. Therefore, substances secreted by the cells into the media only accumulated for 24 hours before the cells were washed with PBS and the media replaced.

In this project, the NCM460 cell line was therefore used to show that IL-1β-induced tolerance is not just a consequence of malignancy in the Caco-2 and HT29 cell lines and is instead a property of epithelial cells.

3.1.3 THP-1 Cell Line

THP-1 cells are a peripheral blood monocyte cell line derived from a one-year old male with acute monocytic leukemia. After stimulation with phorbol esters THP-1 monocytes differentiate into macrophages closely mimicking native monocyte-derived macrophages (162). This cell line has a substantially different transcriptome to the previously described intestinal epithelial cell lines. However, as the THP-1 cell line was only used an IL-1 receptor positive control to ensure that the IL-1β was active *in vivo*, the difference in transcriptomes was not relevant.

THP-1 cells were cultured in RPMI-1640 medium supplemented with 10% HI-FCS, 2 mM $_L$-Glutamine and 10000 U/ml / 10000 µg/ml Pen/Strep at 37 °C and 5% CO_2.

3.1.4 Experimental Protocols

The optimum concentration of stimulant was determined by producing a dose-response curve. Caco-2 and NCM460 cell-lines were stimulated with a range of concentrations of Interleukin-1β (IL-1β) or Pam_3CysK_4 (P3CK) for 24 hours (Figure 3-1) before the conditioned media is collected and the cells harvested with CelLytic™ M solution.

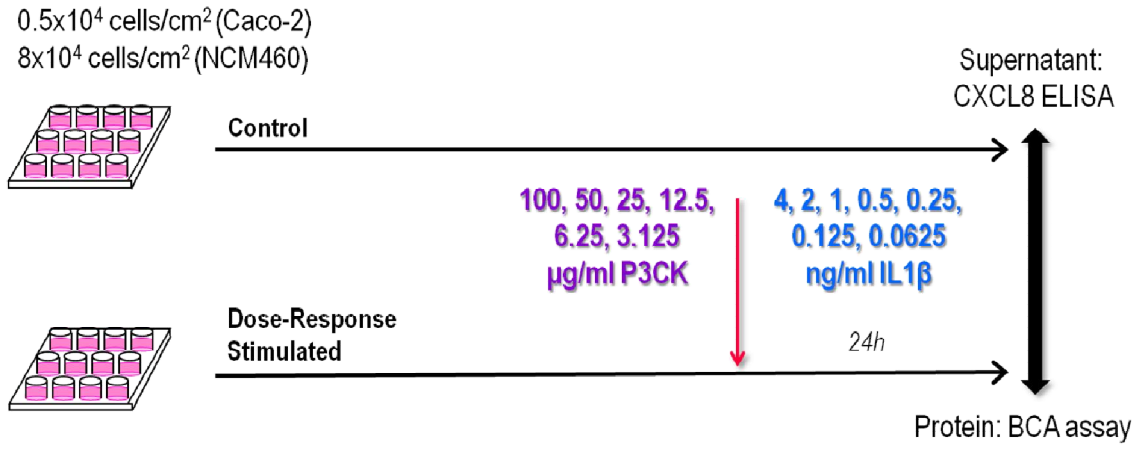

Figure 3-1 Experimental Protocol for the P3CK and IL-1β Dose-Response Curves

Dose-Response curve experimental protocols are described diagramatically. +FCS media was replaced with +ITS media 48 hours before sample collection. Caco-2 and NCM460 cell lines were stimulated with a two-fold serial dilution of P3CK (100 – 3.125 µg/ml) or IL-1β (4 – 0.0625 ng/ml) for 24 hours. CXCL8 was measured by ELISA and normalized to cellular protein content (measured by BCA protein assay).

Tolerance of CXCL8 protein levels was induced by stimulating Caco-2 and NCM460 (P3CK only) cells twice with either 1 ng/ml IL-1β or 25 μg/ml P3CK for 24 hours each (Figure 3-2). Cross-tolerization, the induction of a hyporesponsive state of gene expression following repeated stimulations of different pro-inflammatory stimuli, was induced by pre-stimulating Caco-2 cells with 25 μg/ml P3CK for 24 hours followed by stimulation with 1 ng/ml IL-1β for 24 hours. In between the two stimulations, the media was discarded, the cells washed with PBS and the next stimulation added prepared in fresh +ITS media. Samples of conditioned media were collected for measurement of CXCL8 (or IL-6) production by ELISA and the cells harvested with CelLytic™ M solution. Total cellular protein content was measured by BCA protein assay. CXCL8 (or IL-6) production was normalized to total cellular protein content (pg/mg protein). Multiple experiments were combined by converting each CXCL8 production value to a percentage of the mean production by the stimulated samples.

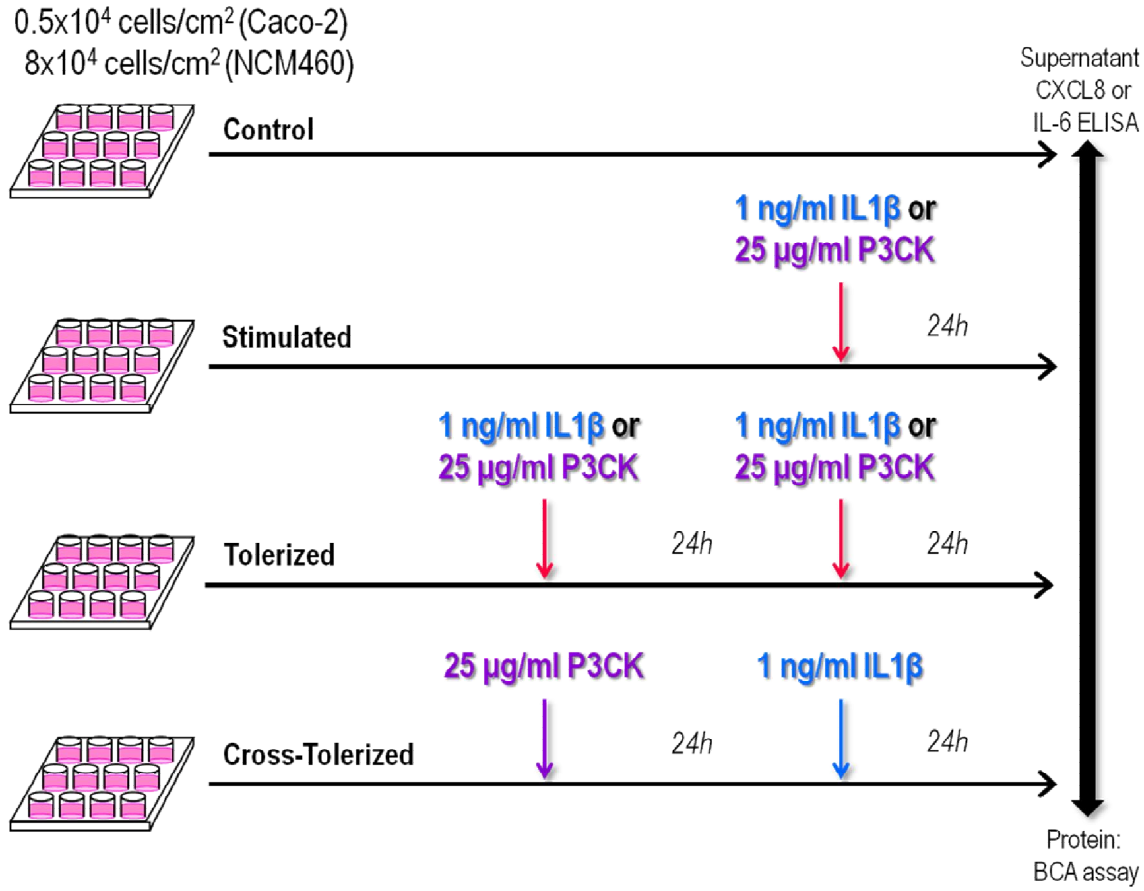

Figure 3-2 Experimental Protocol for Inducing Tolerance

Tolerance and cross-tolerance experimental protocols are described diagramatically. +FCS media was replaced with +ITS media 72 hours before sample collection. Caco-2 and NCM460 (P3CK only) cells were stimulated with either 1 ng/ml IL-1β or 25 µg/ml P3CK for 24 hours and tolerized by a prior stimulation of either 1 ng/ml IL-1β or 25 µg/ml P3CK 24 hours earlier. Caco-2 cells were cross-tolerized by pre-stimulating the cells with 25 µg/ml P3CK for 24 hours followed by stimulation with 1 ng/ml IL-1β for 24 hours. Conditioned media was discarded and the cells washed with PBS between the two stimulations for tolerized and cross-tolerized cells. IL-6 and CXCL8 were measured by ELISA and normalized to cellular protein content (measured by BCA protein assay).

In order to address the concern that the reduced levels of CXCL8 in "tolerized" cells was due to the tail-off in expression from the pre-stimulation and not from the re-induction of the second stimulation, an additional control condition was incorporated into the experimental protocol shown in Figure 3-2. CXCL8 expression in tolerized Caco-2 cells was compared to stimulated and pre-stimulated cells (Figure 3-3). Caco-2 cells were stimulated with 1 ng/ml IL-1β for 24 hours, pre-stimulated with 1 ng/ml IL-1β for 24 hours followed by 24 hours incubation with unconditioned media, and tolerization induced by pre-stimulation with 1 ng/ml IL-1β for 24 hours followed by stimulation with 1 ng/ml IL-1β for another 24 hours. After the first stimulation for 24 hours, the media was discarded, the cells washed with PBS and the next stimulation added prepared in fresh +ITS media. Samples of conditioned media were collected for measurement of CXCL8 production by ELISA and the cells harvested with CelLytic™ M solution. Total cellular protein content was measured by BCA protein assay. CXCL8 production was normalized to total cellular protein content (pg/mg protein). Multiple experiments were combined by converting each CXCL8 production value to a percentage of the mean production by the stimulated samples.

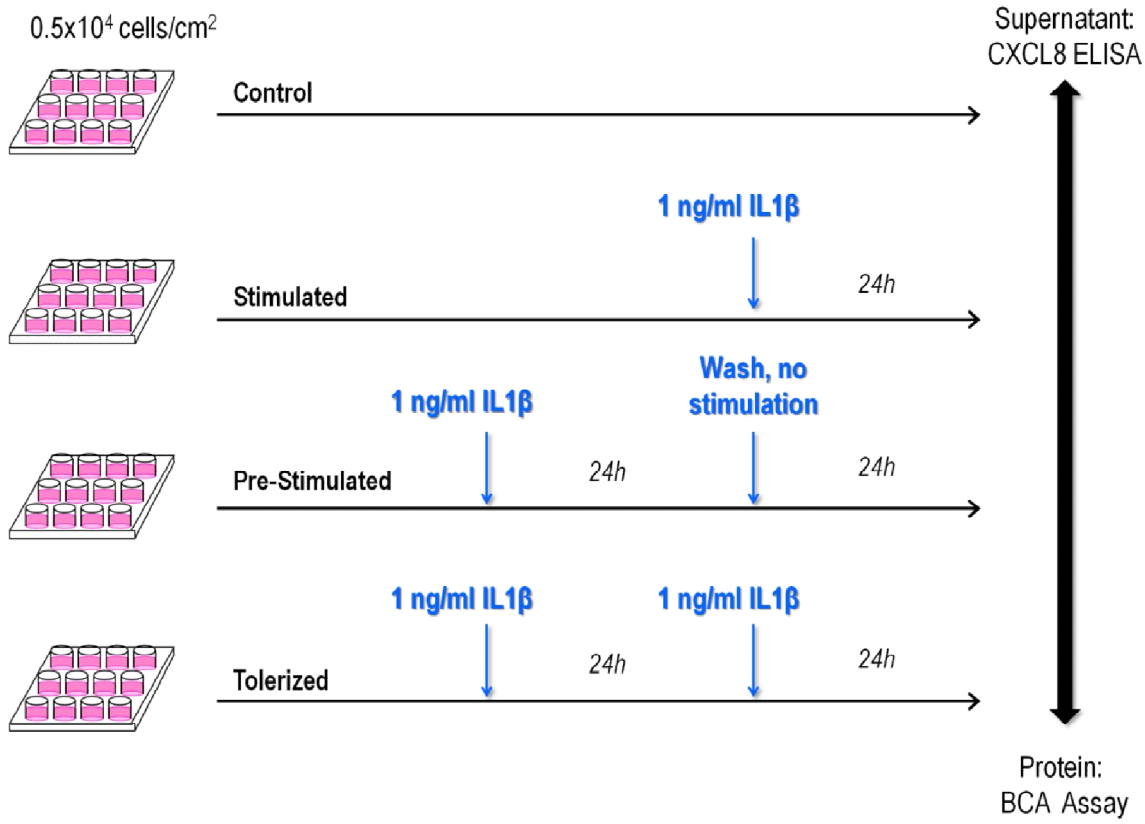

Figure 3-3 Experimental Protocol for Inducing Tolerance in Comparison to Pre-Stimulation

Tolerance experimental protocols are described diagramatically. +FCS media was replaced with +ITS media 72 hours before sample collection. Caco-2 cells were stimulated with 1 ng/ml IL-1β for 24 hours, pre-stimulated with 1 ng/ml IL-1β for 24 hours followed by 24 hours incubation with unconditioned medium and tolerized by a prior stimulation of either 1 ng/ml IL-1β 24 hours followed by an additional stimulation of 1 ng/ml IL-1β for 24 hours. Conditioned media was discarded and the cells washed with PBS after each 24 hour incubation period. CXCL8 was measured by ELISA and normalized to cellular protein content (measured by BCA protein assay).

The optimum stimulation length for mRNA analysis was determined by stimulating the cells with 1 ng/ml IL-1β for 0 – 4 hours before harvesting with TRIzol® (Figure 3-4). Total RNA was extracted from the cells using TRIzol®, as described below in 3.2.1. The amount of RNA extracted was quantified using a NanoDrop spectrophotometer, which calculates the amount of nucleic acid present according to the level of UV absorbance. Equal amounts of RNA were used in cDNA synthesis. CXCL8 mRNA transcribed by Caco-2 cells in response to IL-1β stimulation was measured by RT-PCR and normalized to the amount of β-Actin.

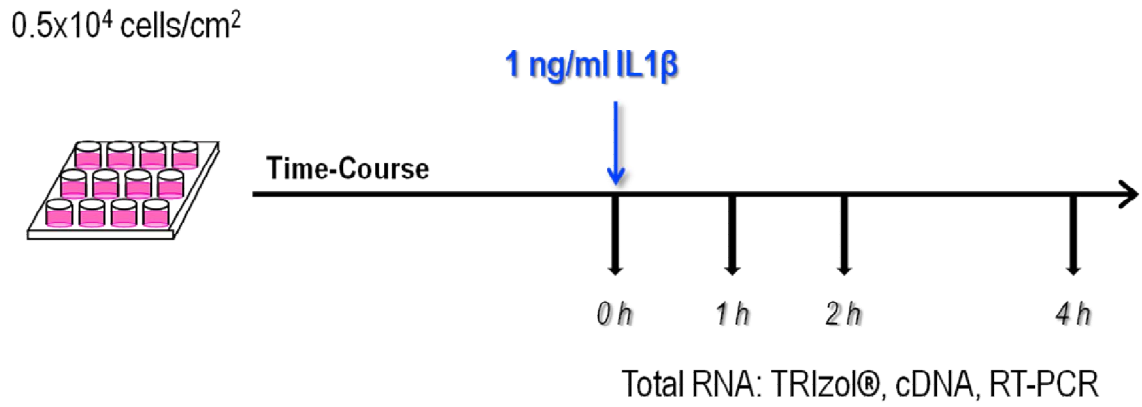

Figure 3-4 Experimental Protocol for the Time-Course of IL-1β-Stimulated Caco-2 Cells

Experimental protocol for obtaining RNA from IL-1β-stimulated Caco-2 cells is described diagramatically. +FCS media was replaced with +ITS media 24 hours before stimulation with 1 ng/ml IL-1β. All Caco-2 cells were stimulated with 1 ng/ml IL-1β at time point 0h. Samples were collected using TRIzol® 0, 1, 2 and 4 hours after stimulation with IL-1β. Conditioned media was discarded and the cells collected with TRIzol®. Total RNA was extracted from the TRIzol® samples, converted to cDNA and the amount of CXCL8 measured by RT-PCR and normalized to the amount of β-Actin.

Tolerance experiments were performed by pre-stimulating the Caco-2 cells with 1 ng/ml IL-1β for 24 hours followed by stimulation for 2 hours (Figure 3-5). The +FCS media was replaced with +ITS media 24 hours prior to pre-stimulation by IL-1β. Total RNA was extracted from the cells using TRIzol®. The amount of RNA extracted was measured by nanodrop and equal amounts of RNA were used in cDNA synthesis. CXCL8 mRNA transcribed by Caco-2 cells in response to IL-1β stimulation was measured by RT-PCR and normalized to the amount of β-Actin. CXCL8 mRNA transcribed by stimulated cells was compared to the CXCL8 mRNA produced by tolerized cells and analysed using ImageJ software (see 3.10 Statistics).

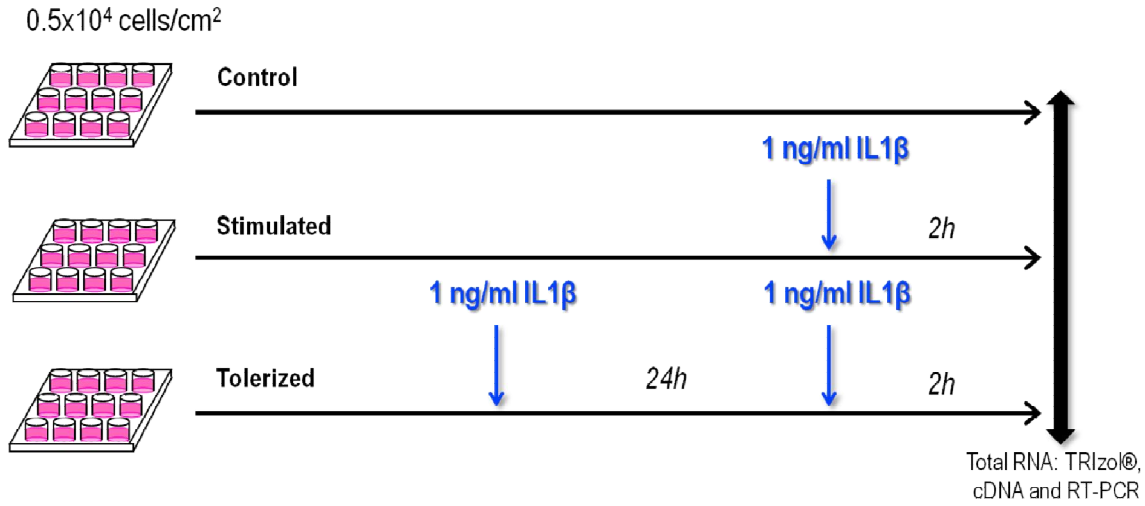

Figure 3-5 Experimental Protocol for the Induction of Tolerance as Measured by Transcription

Experimental protocol for inducing tolerance as measured by transcription in Caco-2 cells is described diagramatically. +FCS media was replaced with +ITS media 50 hours before sample collection. Tolerance in Caco-2 cells was induced by a prior stimulation of 1 ng/ml IL-1β for 24 hours followed by stimulation with 1 ng/ml IL-1β for 2 hours. Between the two stimulation of IL-1β, the conditioned media is discarded and the cells washed with PBS. Stimulated cells were stimulated with 1 ng/ml IL-1β for 2 hours only. Conditioned media was discarded and the cells collected with TRIzol®. Total RNA was extracted from the TRIzol® samples, converted to cDNA and the amount of CXCL8 measured by RT-PCR and normalized to the amount of β-Actin).

To support the data collected in Figure 3-3, mRNA expression was measured over 48 hours of IL-1β-stimulation. Caco-2 cells were pre-stimulated with 1 ng/ml IL-1β for 24 hours followed by another stimulation with 1 ng/ml IL-1β stimulation for a further 24 hours. Samples were collected at the time points illustrated in Figure 3-3. Samples collected during the first 24 hours (0, 1, 2, 4, 8 and 24 hours) after IL-1β-stimulation are from stimulated Caco-2 cells, whilst the samples collected from the second 24 hours (24, 25, 26, 28, 32 and 48 hours) are from tolerized cells. Total RNA was extracted from the cells using TRIzol®. The amount of RNA extracted was measured by nanodrop and equal amounts of RNA were used in cDNA synthesis. The amount of

cDNA present was measured by qPCR. A number of genes were measured (IL-6, CXCL8, IL-10, CCL2, BD-2, TNF) and normalized to the amount of β-Actin.

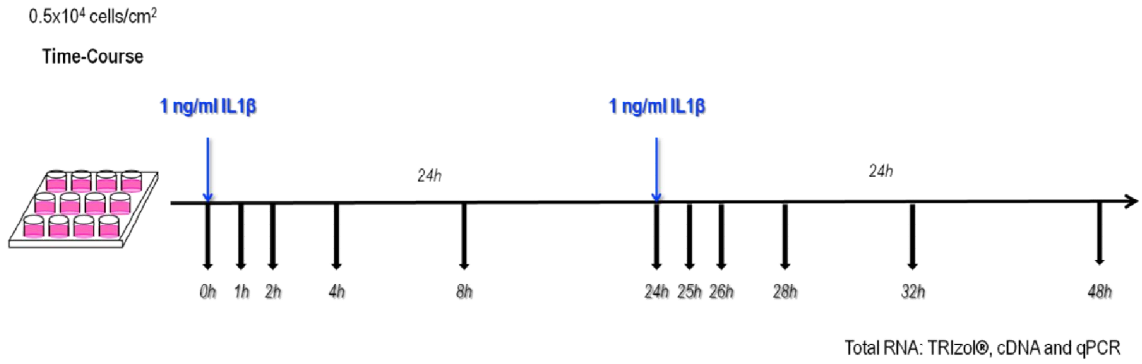

Figure 3-6 Experimental Protocol for the Expression of Tolerizable and Non-Tolerizable Genes Over 48 Hours in IL-1β-Stimulated Caco-2 Cells

Experimental protocol for measuring the expression of tolerizable and non-tolerizable genes over 48 hours in IL-1β-stimulated Caco-2 cells. +FCS media was replaced with +ITS media 24 hours before the first sample collection. Caco-2 cells were stimulated with 1 ng/ml IL-1β for 24 hours, the conditioned media was discarded and the cells washed with PBS, followed by a further stimulation with 1 ng/ml IL-1β for another 24 hours. At each time point (0, 1, 2, 4, 8, 24, 25, 26, 28, 32 and 48 hours) conditioned media was discarded and the cells collected with TRIzol®. Total RNA was extracted from the TRIzol® samples, converted to cDNA and the amount of IL6, CXCL8, IL-10, CCL2, BD-2, TNF and ACTB measured by qPCR. The expression of each gene was normalized to the amount of β-Actin).

The involvement of epigenetics in the regulation of tolerance was investigated by incubating small molecule epigenetic inhibitors with tolerized cells and measuring the production of CXCL8. If the production of CXCL8 increases by a statistically significant level above that of tolerized only cells, tolerance is said to be broken. The experimental protocol for breaking tolerance with epigenetic inhibitors is pictured in Figure 3-7. Both SAH and 2,4-PDCA are incubated with tolerized Caco-2 cells for a total of 72 hours. 24 hours prior to pre-stimulation with 1 ng/ml IL-1β 100 μM SAH or 5

mM 2,4-PDCA is incubated with the cells. IL-1β is diluted in fresh preparations of 100 μM SAH or 5 mM 2,4-PDCA to 1 ng/ml for the pre-stimulation and stimulation stages, 24 hours apart.

Chaetocin and pargyline were incubated with the tolerized cells in two separate treatments. Based on a comparable experiment on macrophages by Foster *et al.* (87), pargyline and Chaetocin are incubated with the tolerized cells for 1 hour prior to the second stimulation with IL-1β. This was found to not be a sufficient length of time to break tolerance (see Figure 5-26) and a number of other incubation lengths were investigated, as described in Figure 5-24. Therefore, 3 mM pargyline hydrochloride was incubated with tolerized Caco-2 cells for 1 hour prior to the second stimulation with IL-1β and again for 18 hours prior to sample collection i.e. added to the IL-1β-conditioned media 6 hours after the second stimulation. Chaetocin was incubated with tolerized Caco-2 cells in a similar manner to the pargyline incubation. However, two different time periods for the second Chaetocin incubation were used, 8 hours and 18 hours (Figure 3-7). The conditioned media is only discarded and the cells washed with PBS before the first and second stimulations with IL-1β, not when Chaetocin and pargyline are added to the cells. The conditioned media samples were collected and the cells harvested with CelLytic™ M solution (as described below in 3.2.2). The production of CXCL8 is measured by ELISA and normalised to the total cellular protein content (as measured by BCA assay). Multiple experiments were combined by converting each CXCL8 production value to a percentage of the mean CXCL8 expression produced by the stimulated samples.

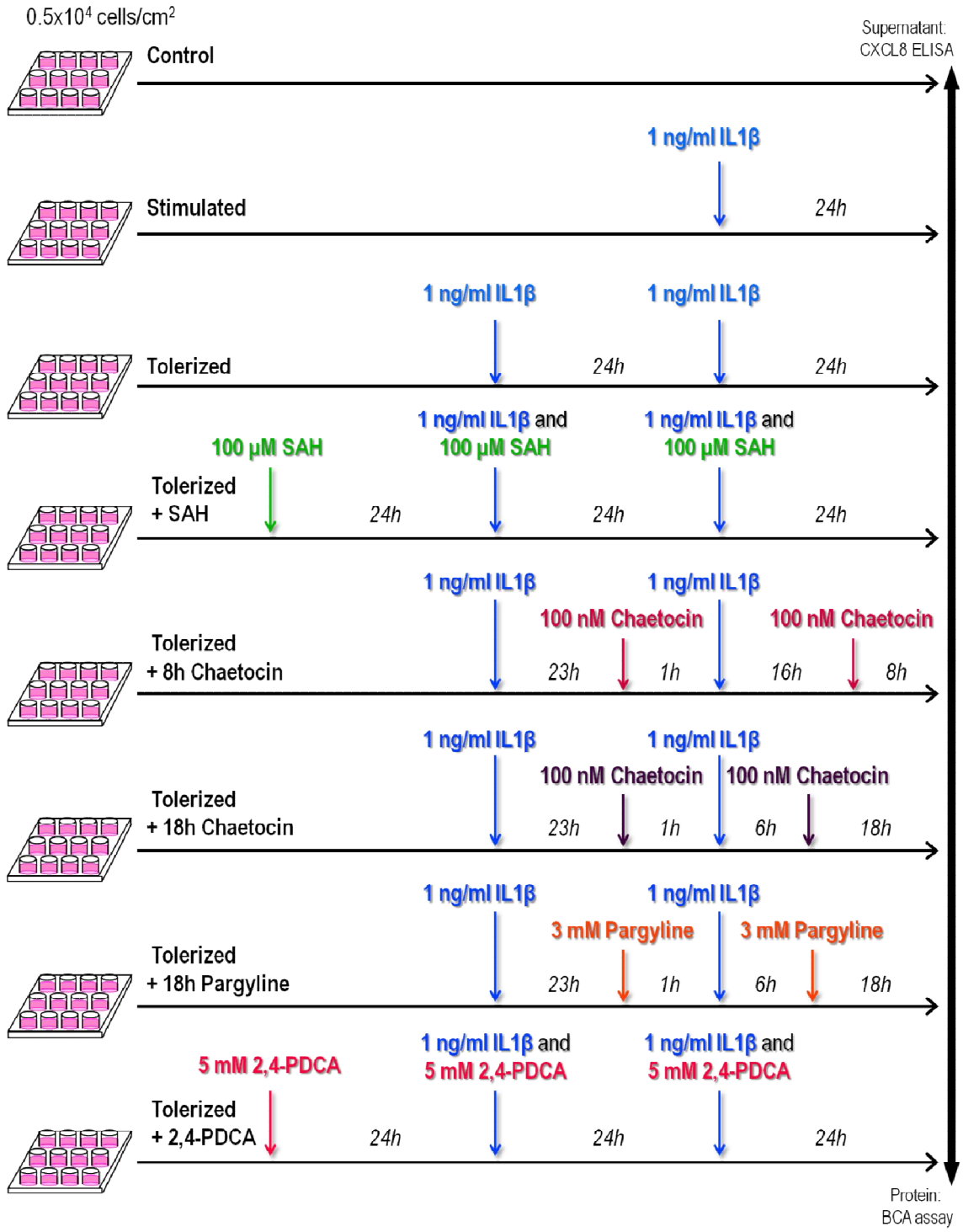

Figure 3-7 Experimental Protocol for Breaking Tolerance with Epigenetic Inhibitors

Experimental protocols for breaking tolerance through the use of epigenetic inhibitors are described diagramatically. +FCS media was replaced with +ITS media 72 hours before sample collection (96 hours before sample collection for Tolerized + SAH and Tolerized + 2,4-PDCA). Caco-2 cells were stimulated with 1 ng/ml IL-1β for 24 hours and tolerized by a prior stimulation of 1 ng/ml IL-1β 24 hours earlier. Conditioned media was discarded and the cells washed with PBD between the two IL-1β stimulations. Tolerized cells were incubated with a variety of small molecule epigenetic inhibitors: SAH, Chaetocin, pargyline and 2,4-PDCA. 100 µM SAH and 5 mM 2,4-PDCA were incubated with the tolerized cells for a total of 72 hours (24 hours prior to stimulation with IL-1β). 100 nM Chaetocin and 3 mM pargyline were incubated with the tolerized cells for an hour at the end of the pre-stimulation with IL-1β and again for the final 8 (Chaetocin) or 18 (Chaetocin and pargyline) hours before sample collection. CXCL8 production was measured by ELISA and normalized to cellular protein content (measured by BCA protein assay.

3.2 Cell Harvesting Methods

Reagent	Supplier	Address
CelLytic™ M	Sigma-Aldrich	Gillingham, UK
TRIzol® and TRI Reagent®	Invitrogen	Paisley, UK
Chloroform	Sigma-Aldrich	Gillingham, UK
Isopropanol	Sigma-Aldrich	Gillingham, UK
Ethanol	VWR	Lutterworth, UK
RNase-free H_2O	Qiagen	Manchester, UK
Trypsin-EDTA	PAA	Yeovil, UK
Triton™ X-100	Sigma-Aldrich	Gillingham, UK
Phenylmethylsulfonyl fluoride (PMSF)	Sigma-Aldrich	Gillingham, UK
Sodium Azide (NaN_3)	Sigma-Aldrich	Gillingham, UK
Hydrochloric Acid (HCl)	Sigma-Aldrich	Gillingham, UK
Sodium Hydroxide (NaOH)	Sigma-Aldrich	Gillingham, UK

Table 3-2 Reagents used to Harvest Cells

3.2.1 RNA

Growth medium was aspirated and discarded. After washing the cells with PBS, 1 ml TRIzol® was added to each well and the cells lysed from the plate by pipetting up and down. This solution was stored at -70 °C until ready to extract the RNA. All samples were brought to room temperature and incubated for a further 5 minutes before adding 200 µl chloroform per 1 ml TRIzol® and inverting vigorously for 15 seconds. The samples were incubated at room temperature for 2-3 minutes and centrifuged at 12 000 rpm for 15 minutes at 4 °C. The aqueous layer was carefully aspirated and placed in a new tube, ensuring that none of the interphase or organic layers was disturbed. RNA is always lost at this step as some of the aqueous layer must remain behind in order that it is not contaminated by the organic layer. 500 µl ice-cold 100% isopropanol was added to each sample and incubated on ice for 10 minutes before centrifuging at

12 000 rpm for 12 minutes at 4 °C. The supernatant was carefully aspirated and discarded leaving ~50 µl behind so as not to disturb the pellet. The pellet was washed with 1 ml ice-cold 75% ethanol, vortexed briefly and centrifuged at 8 000 rpm for 8 minutes at 4 °C. The supernatant was carefully aspirated and discarded, ensuring that the pellet remained undisturbed, and was left to air-dry for ~20 minutes. It is important not to over-dry the pellet or it will degrade, as shown by an $A_{260/280}$ ratio of <1.6. The air-dried pellet was resuspended in 40 µl RNase-free H_2O and incubated at 58 °C for 10 minutes so that any remaining alcohol could evaporate.

Although RNA extraction using TRIzol® is prone to DNA and protein contamination, the RNA is protected by the reagent during the extraction procedure (and should be performed on ice to limit degradation) and is cheaper than using spin columns. Spin columns also have a lower maximum yield and do not collect very small RNAs (<200 nt), unlike TRIzol®.

RNA is inherently less stable than DNA and more difficult to work with than either DNA or protein. RNA, unlike DNA, is a single strand molecule and contains ribose not deoxyribose. Because of this difference there is an additional hydroxyl group present at the 2' position of the sugar ring moiety making RNA more susceptible to alkaline hydrolysis than DNA and therefore less stable (163). It is essential that RNA work is always carried out on a surface that has been treated with an RNase inhibitor e.g. RNaseZap® (Invitrogen), on ice and stored at -70 °C to minimise degradation.

3.2.2 Protein

Growth medium was removed from the Caco-2 and HT29 cells and stored at -20 °C for further analysis. After washing the cells with PBS, 200 µl CelLytic™ M reagent was added and incubated

for 15 minutes at 37 °C. Cells were collected, assisted by scraping, and centrifuged for 15 minutes at 4 °C at 18 000 *x g* to pellet the cellular debris. The supernatant was removed into a pre-chilled tube and stored at -20 °C or -70 °C for long-term storage. When harvesting the THP-1 cells, which grow in suspension, the cells must first be centrifuged to pellet the cells and the supernatant stored at -20 °C. After resuspending the cell pellet in PBS and centrifuging again, the new cell pellet was resuspended in 200 µl CelLytic™ M reagent and preceded as above.

CelLytic™ M reagent is a rapid, non-denaturing method of lysing cultured mammalian cells and is up to 50% more efficient than other products and methods of cell lysis e.g. sonication. It does not interfere with many downstream processes, such as Western blotting and BCA protein assay, which make it particularly suitable for this procedure (164).

3.2.3 Histones

Cells for histone analysis by Western Blotting or Histone H3 PTM Multiplex assay were grown in T75 flasks at a seeding density of 1.2 - 1.7 x10^4. Histone modifying enzyme inhibitors were diluted to the appropriate concentrations to produce a dose-response curve and added to the cells in fresh medium for the time required. An aliquot of growth medium was removed and stored at -20 °C for future analysis whilst the rest was discarded. After washing the cells twice with ice-cold PBS, cells were scraped into Triton Extraction Buffer (TEB: PBS containing 0.5% Triton X-100 (v/v), 2 mM PMSF, 0.02% (w/v) NaN_3) at a cell density of approximately 10^7 cells per ml. Scraping the cells directly into the extraction buffer preserves the histone post-translational modifications and interactions with DNA, as using trypsin to lyse the cells from the flask can digest the histone tails. PMSF, a protease inhibitor, prevents histone degradation by proteases in the cells.

The cells were left to lyse on ice for 10 minutes with regular inversion to gently mix then centrifuged at 2 000 rpm for 10 minutes at 4 °C. The supernatant was discarded and the pellet resuspended in half the volume of TEB and centrifuged as before. The supernatant was discarded and the pellet resuspended in 0.2 N HCl at a cell density of approximately 4 x 10^7 cells per ml. The histones were acid extracted overnight at 4 °C and centrifuged at 2 000 rpm for 10 minutes at 4 °C. The supernatant was aspirated and the pH neutralized by addition of 1/5^{th} volume 1 M NaOH. The extracted and pH-neutralized histones were stored at -20 °C and the protein concentration determined by BCA protein assay.

It is critical that the pH of the extracted histones is neutralized or the histones will degrade, even whilst frozen and the epitopes to be detected by antibody-binding and Western blot will be destroyed.

3.3 Reverse Transcriptase – Polymerase Chain Reaction (RT-PCR)

Reagent	Supplier	Address
RQ1 RNase-free DNase	Promega	Southampton, UK
High Capacity cDNA Reverse Transcription Kit	Invitrogen	Paisley, UK
GoTaq® Flexi DNA Polymerase	Promega	Southampton, UK
PCR Tubes	StarLab	Milton Keynes, UK
dNTP mix	Bioline	London, UK
Primers	Sigma-Aldrich	Gillingham, UK
GelRed™ Nucleic Acid Gel Stain	VWR	Lutterworth, UK

Table 3-3 Reagents used in RT-PCR

PCR is a technique used to specifically amplify DNA. The discovery of thermostable DNA polymerases enabled the reaction to proceed efficiently at high temperatures without destruction of neither the polymerase nor the requirement for additional enzymes such as DNA helicase. The double-stranded DNA helix is denatured by heating it to 95 °C. This separates the two strands so that the DNA polymerase can access the DNA. The temperature is lowered to ~60 °C so that primers, short oligonucleotides ~20 nt long whose sequence is complementary to the 3' ends of the DNA to be amplified, anneal to the single-stranded DNA. DNA polymerase can only bind to double-stranded DNA, hence the requirement for primers. This annealing temperature varies depending on the primers used. It is typically ~5 °C lower than the Tm of the primers (temperature at which half of the primers will be denatured). As the annealing temperature increases, primers that contain mismatches to the desired sequence will dissociate thus resulting in a more specific product. As the annealing temperature decreases, the primers are able to bind to sequences that are not 100% complementary to their sequence and incorrect products will be formed. Therefore, the annealing temperature must be a compromise between being low enough to allow the primers to bind securely to the DNA, but high enough to get specific binding. The

temperature is then increased to 72 °C for the elongation phase. 72 °C is the optimum temperature for the DNA polymerase isolated from the bacterium *Thermus aquaticus*, though it is stable at the higher temperatures required to denature the double-stranded DNA. As in semi-conservative replication that occurs in every cell, the DNA polymerase synthesizes a new complementary strand of DNA thus creating two identical double-stranded DNA molecules identical to the original molecule. Each new molecule contains one strand of the original molecule and one new strand. The whole process is then repeated with the newly synthesized molecules being denatured, the primers annealing and DNA polymerase synthesizing a new DNA strand, except that this time there are twice as many single strands of DNA. The steps are repeated 30-40 times resulting in an exponential increase in the number of identical DNA molecules.

PCR is a very sensitive and accurate technique, with widespread applications. A single DNA molecule can be specifically amplified millions of times to create a genetic fingerprint used in forensic science, as well as uses in DNA cloning for sequencing, phylogeny, functional gene analysis, medical diagnoses and paternity testing.

The discovery of reverse transcriptase in bacteria revolutionised RNA analysis as it allowed amplification using PCR and development of quantitative PCR (qPCR), which is much more sensitive, efficient and precise than Northern Blotting. It also extended the range of applications of PCR to gene expression analysis; forensic detection of RNA not just DNA; identification of introns, exons and transcriptional start sites; disease diagnosis; and more precise genetic engineering e.g. insertion of the gene after the introns have been spliced out into bacteria for recombinant protein production.

Total RNA was extracted with TRIzol® as described in 3.2.1 and quantified using a NanoDrop Spectrophotometer. Equal concentrations of RNA were DNase-treated to remove any contaminating DNA. Though TRIzol® extraction includes a separation of DNA and RNA stage; it is easy to accidentally aspirate part of the DNA-containing interphase layer when aspirating the RNA-containing aqueous layer from the centrifuged tube. The DNase-treated RNA is used to synthesize complementary DNA (cDNA) using reverse transcriptase (RT) enzyme. It is important to dilute the DNase-treated RNA before cDNA synthesis as the inhibitors of the DNase interfere with the subsequent PCR. Also, a –RT reaction should be included, where no reverse transcriptase enzyme is added, as a control in the subsequent PCR for genomic DNA (gDNA). Only if there is DNA contamination in the RNA sample will there be a product formed in the PCR in the – RT as no cDNA synthesis has occurred. A negative control (-ve), water instead of cDNA, should be included in the PCR to determine whether there was any contamination present setting up the PCR as no product can be formed unless there is DNA present.

The PCR is performed using primers specific to the gene of interest and a constitutively expressed gene or house-keeping gene (HKG). As the expression of the HKG is constant, it acts as a loading control to ensure that the same quantity of cDNA is added to each reaction. We used *ACTB* as the HKG, as it has been shown to be a good normalizing gene in Caco-2 cells (165) and is highly expressed thus acting as a positive control for the PCR. CXCL8 primers were designed using Primer-BLAST and specified to span an exon-exon junction, thereby reducing the possibility that any contaminating gDNA present will be amplified. The β-Actin primer sequences were taken from (166) (Table 3-4). The optimum primer annealing temperature was determined by performing a temperature gradient reaction with 58 °C resulting in the cleanest and highest yielding product. The PCR reactions were performed using the conditions as described in Table

3-5. The PCR products were separated by gel electrophoresis in a 2% agarose gel stained with GelRed (1:10 000 v/v) and visualised with a UV transilluminator.

		Gene	
		ACTB	**CXCL8**
Accession Number		NM_001101	NM_000584
Primer Sequences	**Forward**	CTGGAACGGTGAAGGTGACA	CTCTGTGTGAAGGTGCAGTT
	Reverse	AAGGGACTTCCTGTAACAACGCA	ACTTCTCCACAACCCTCTGC
Product Size (bp)		140	222

Table 3-4 Primer Sequences

Table illustrating the primer sequences and product sizes of the genes analysed by RT-PCR.

Step	Temperature (°C)	Time (mins)	Reason
1	95	5	Initial denaturation
2	95	1	Denaturation
3	58	1	Annealing
4	72	1	Extension
5	Repeat steps 2 – 4 x35		
6	72	5	Final extension
7	4	∞	Prevent degradation

Table 3-5 RT-PCR Reaction Conditions

Table illustrating the temperatures and incubation lengths of the RT-PCR reaction.

3.4 Quantitative Polymerase Chain Reaction (qPCR)

Reagent	Supplier	Address
High Capacity cDNA Reverse Transcription Kit	Invitrogen	Paisley, UK
Power SYBR® Green PCR Master Mix	Thermo Fisher Scientific	Paisley, UK
MicroAmp® Optical 96-well Reaction Plate	Thermo Fisher Scientific	Paisley, UK
MicroAmp® Optical Adhesive Film	Thermo Fisher Scientific	Paisley, UK
Primers	Thermo Fisher Scientific	Paisley, UK

Table 3-6 Reagents used in qPCR

Quantitative or real-time PCR (qPCR) is a variation of PCR that measures the amplification of DNA in real time, unlike conventional PCR which only measures the relative amount at the end of the reaction. qPCR is quantitative thereby allowing statistical analysis of the data. DNA amplification is measured in one of two ways, non-specific DNA-intercalating fluorescent dyes or sequence-specific probes labelled with a fluorescent reporter which enables detection after hybridzation with its complementary sequence.

Fluorescent dyes such as SYBR Green, intercalate with double-stranded (ds) DNA thus as the amount of dsDNA increases with each PCR cycle, so does the fluorescence intensity. Theoretically, the fluorescence intensity is directly proportional to the amount of dsDNA present. However, as SYBR Green is a non-specific dye and binds to all DNA regardless of the sequence, the fluorescence intensity can be misleading as it includes all PCR product as well as primer dimers and PCR products from non-specific binding. The advantages of this method include the relatively cheap cost and only requiring one pair of primers per target. Unfortunately, multiplex reactions are not possible as the detection method is not sequence specific.

Sequence-specific probes with attached fluorescence reporters, known as Taqman probes, only fluoresce when bound to the complementary DNA sequence. The probe, which has sequence-specificity complementary to the target, has reporter and quencher molecules attached at either end. When the probe is bound to the target, the close proximity of the reporter and quencher prevents fluorescence. However, as the DNA is amplified, the probe is destroyed by the exonuclease activity of the Taq polymerase, thus enabling fluorescence detection proportional to the amount of target DNA. This method greatly increases the specificity of the qPCR technique as other dsDNA e.g. non-specific PCR products do not affect the fluorescent intensity. Primer dimers, however, can reduce the amplification of the desired target. Also, by using different fluorescent reporters for different target probes, it is possible to multiplex several targets into one reaction. A limitation is the increased difficulty of designing both primers and a probe that meet the specificity requirements.

Analysis of qPCR data, whether it is obtained from the fluorescent dye or sequence-specific probe method, is dependent upon the cycle threshold or C_T value. It is a relative value taken from the exponential part of the amplification curve. Amplification curves plot the amount of fluorescence against the PCR cycle number. A threshold level is chosen for the fluorescence level of all samples is being produced in the exponential phase, though it may be at different points in the PCR reaction. Conversely, the higher the C_T value, the smaller the amount of the target present in the sample as it takes more PCR cycles for it to reach the same fluorescence level as targets present in greater amounts.

The Power SYBR Green master mix from Invitrogen was used with primers designed using Primer-BLAST (for sequences of each gene see Table 3-7). In order to accurately measure the amount of cDNA present, the target is referenced to an internal control or HKG. As in RT-PCR,

ACTB was used as the HKG in qPCR. The comparative C_T or $2^{-\Delta\Delta C_T}$ method was used to analyse the qPCR results (167). The first comparison or ΔC_T is the subtraction of the HKG C_T from the C_T of the target gene. The second comparison or $\Delta\Delta C_T$ is the subtraction of an internal control from the target ΔC_T. Two raised to the negative power of the second comparison, or $2^{-\Delta\Delta C_T}$, gives the fold change in expression of the target gene. The mean of the fold changes for each condition was calculated and plotted.

Gene	Accession Number	Forward	Reverse	Product size (bp)
IL-6	NM_000600	GGCACTGGCAGAAAACAACC	GCTCTGGCTTGTTCCTCACT	177
CXCL8	NM_000584	CTCTGTGTGAAGGTGCAGTT	ACTTCTCCACAACCCTCTGC	222
IL-10	NM_000572	TACGGCGCTGTCATCGATTT	TAGAGTCGCCACCCTGATGT	191
DEFB4A	NM_004942	CTCGTTCCTCTTCATATTCCTGA	CTAGGGCAAAAGACTGGATGAC	111
CCL2	NM_002982	GATCTCAGTGCAGAGGCTCG	TTTGCTTGTCCAGGTGGTCC	155
TNF	NM_000594	AGCCCATGTTGTAGCAAACC	TGAGGTACAGGCCCTCTGAT	134
ACTB	NM_001101	CTGGAACGGTGAAGGTGACA	AAGGGACTTCCTGTAACAACGCA	140

Table 3-7 qPCR primer sequences

Table illustrating the primer sequences and product sizes of the genes analysed by qPCR.

3.5 Protein Concentration Determination – BCA Assay

Reagent	Supplier	Address
Bovine serum albumin (BSA) Standard	Sigma-Aldrich	Gillingham, UK
Bicinchoninic Acid (BCA)	Sigma-Aldrich	Gillingham, UK
Copper Sulphate	Sigma-Aldrich	Gillingham, UK
96-well plate	VWR	Southampton, UK

Table 3-8 Reagents used for Determination of Protein Concentration

The protein concentration of the CelLytic™ M extractions was calculated by BCA protein assay. Each sample was tested in duplicate and the concentration calculated by comparison to a BSA protein standard curve. Results were analysed and presented using Microsoft Excel software.

The CelLytic™ M protein extractions were thawed on ice and diluted 1:5 and 1:10 in PBS. A 6-point standard curve starting at 1 mg/ml was prepared by serially diluting BSA in PBS by a factor of two. 5 µl standard/sample was added per well in duplicate to a 96-well plate. 200 µl BCA solution (50:1 ratio of BCA to $CuSO_4$) was added per well. The plate was sealed and incubated for 30 minutes at 37 °C. The optical density of each well was determined using a microplate reader set to 570 nm and used to calculate the protein concentration.

It is important that the BSA and the samples use the same diluent in order to achieve an accurate standard curve and that the samples are sufficiently diluted so that their optical density reading lies within the linear part of the standard curve. Errors are usually caused by pipetting error hence the need for duplicates of each sample. Any samples where the optical densities are greater than ±10% from the mean should be repeated.

3.6 Enzyme-Linked Immunosorbent Assay (ELISA)

Reagent	Supplier	Address
Human CXCL8/IL-8 DuoSet	R&D Systems	Abingdon, UK
Human IL-6 DuoSet	R&D Systems	Abingdon, UK
BSA (≥96%)	Sigma-Aldrich	Gillingham, UK
TWEEN® 20	Sigma-Aldrich	Gillingham, UK
Trizma base	Sigma-Aldrich	Gillingham, UK
Sodium Chloride (NaCl)	Sigma-Aldrich	Gillingham, UK
TMB Substrate Solution	R&D Systems	Abingdon, UK
TMB Substrate Solution	Cambridge Bioscience	Cambridge, UK
TMB Substrate Solution	Biolegend	London, UK
Sulphuric Acid (H_2SO_4)	Sigma-Aldrich	Gillingham, UK
Human IL-8 ELISA MAX™ Standard	Biolegend	London, UK
CXCL8 Recombinant Protein	R&D Systems	Abingdon, UK

Table 3-9 Reagents used in ELISA

The immunological response of Caco-2 and HT29 cells to stimulation by IL-1β and P3CK was determined by measuring the quantity of CXCL8 and IL-6 secreted into the growth media. Each sample was tested in duplicate and the concentration calculated by comparison to the appropriate standard curve. Results were analysed and presented and statistical tests performed using Microsoft Excel and GraphPad Prism software.

ELISA is a quantifiable immunological technique used to detect the amount of antigen in a sample. This type of ELISA, where two antibodies are used to bind and detect the antigen, is known as a sandwich ELISA. Therefore, the measured antigen or protein must be multivalent with at least two antigenic sites, one each for the capture and the detection antibodies. As it is an antibody-based technique, it is highly specific and can detect very low concentrations of the antigen, even when the sample is not pure, as long as the antibody does not have cross-

reactivity. It has found many applications ranging from diagnostics (e.g. measurement of HCG in pregnancy tests), toxicology (drug screening) and the food industry for seeking traces of potential allergens.

Two different manufacturers of ELISA antibody kits, R&D Systems and Biolegend, were used to measure the production of CXCL8. The protocols are similar, with a couple of differences in the compositions of the blocking and reagent diluents and the recommended use of a plate shaker by Biolegend. However, despite the Biolegend kit being significantly cheaper than R&D Systems, I would recommend the use of the R&D Systems DuoSet as its CXCL8 protein produces a more reliable standard curve compared to the one from Biolegend, which is not supplied at its stated concentration and increases its absorbance readings for the same concentration in successive experiments.

The capture antibody is diluted to the specified concentration (using PBS: R&D Systems; carbonate-bicarbonate buffer: Biolegend) and left to coat the 96-well plate overnight. The excess is then washed off using PBST (PBS + 0.05% Tween-20) a minimum of 3 times (preferably 5 times) and the plate blotted against clean paper towels each time. The washing steps are critical to ensure low background levels and reproducibility of results. The antigen-binding sites in the capture antibody are then blocked with BSA (1% BSA in PBS with 0.05% NaN_3: R&D Systems CXCL8; 1% BSA in PBS: R&D Systems IL-6 and Biolegend CXCL8) for a minimum of 1 hour to reduce non-specific binding to the antibody. The plate is washed, as described above, and the sample solutions and standards are applied in duplicate. These should both be diluted in the reagent diluent (0.1% BSA, 0.05% Tween-20 in Tris-buffered Saline (20mM Trizma base, 150 mM NaCl) pH 7.2-7.4, 0.2 µm filtered: R&D Systems CXCL8; 1% BSA in PBS: R&D Systems IL-6 and Biolegend) so that the standard curve is as accurate as possible.

It is important to perform duplicate measurements to minimise pipetting errors. After sufficient time has been left to allow the antibody-antigen complex to form, the diluted (in reagent diluent) detection antibody is added. This antibody is conjugated to biotin, which binds specifically to streptavidin in the streptavidin-conjugated horseradish peroxidise (HRP) enzyme applied in the next step. A substrate solution of equal parts H_2O_2 and tetramethylbenzidine (TMB) is added and left to develop in the dark. The HRP enzyme uses hydrogen peroxide to oxidize TMB into the blue oxidation product and the reaction is stopped using 0.2 N H_2SO_4, which produces the yellow diimine product (168). A schematic of the ELISA reaction is shown in Figure 3-8. The intensity of the yellow coloured product, as read by a microplate reader at 450 nm wavelength, is directly correlated with the amount of antigen present. The optical density is converted into a concentration through comparison with the known standard curve generated in the same experiment. It is important to read the colour intensity promptly so that the signal does not degrade. The microplate reader is set to dual wavelength (450 nm - 570 nm) in order to correct for any signal originating from the plate itself at 570 nm. If the values calculated from the duplicates had a variation greater than ±10%, the experiment was repeated.

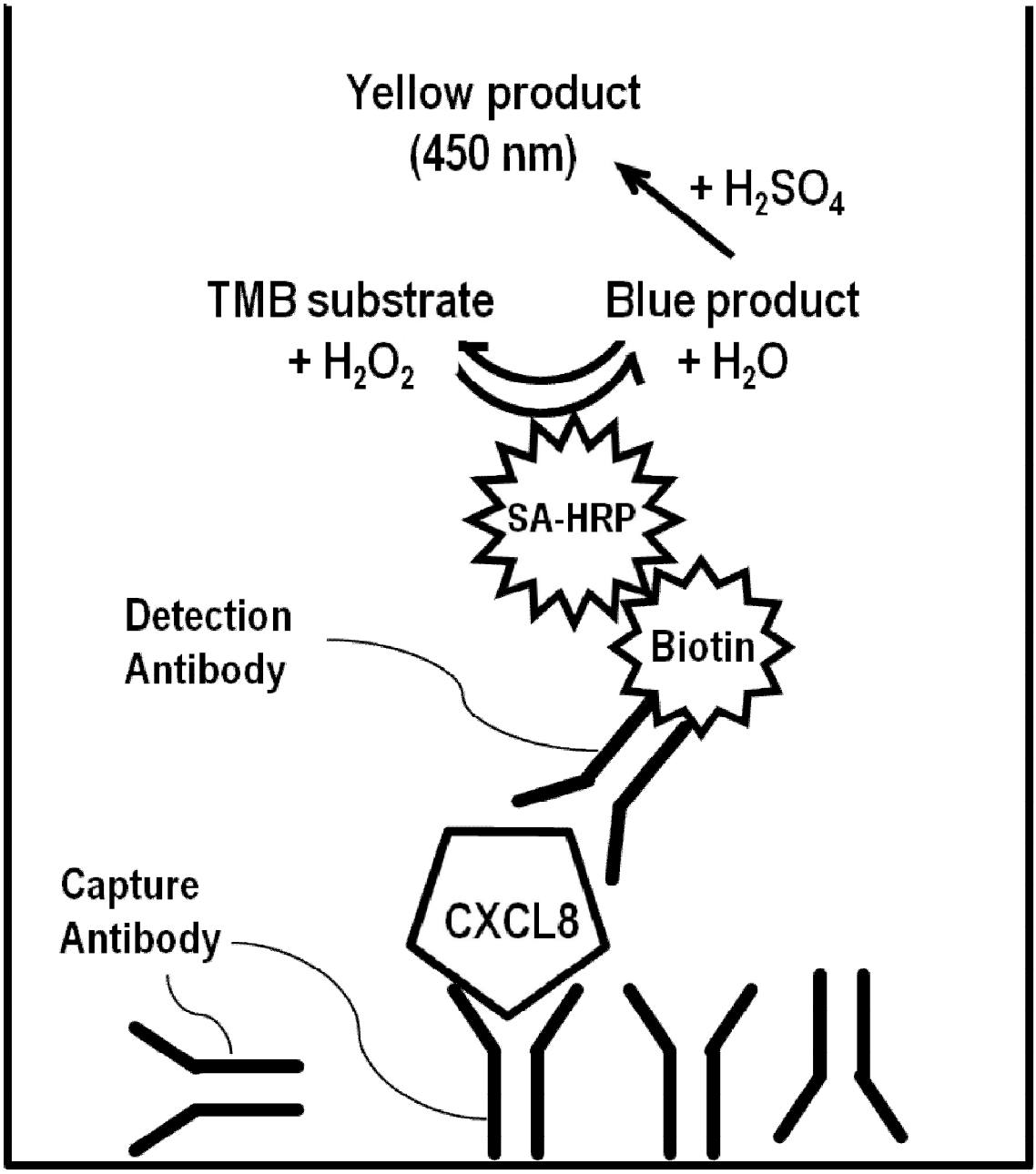

Figure 3-8 Schematic of the CXCL8 ELISA Reaction

A diagram representing the CXCL8 ELISA reaction from both R&D Systems and Biolegend. The capture antibody adheres to the 96-well reaction plate (one well illustrated here) in all orientations. CXCL8 binds to the capture antibody and the biotinylated detection antibody binds to the CXCL8 to form a sandwich complex. Streptavidin conjugated horseradish peroxidase (SA-HRP) binds to the biotinylated complex and catalyses the oxidation of TMB substrate with hydrogen peroxide (H_2O_2) to the blue diimine product. The reaction is stopped by addition of sulphuric acid (H_2SO_4) which causes the reaction product to turn yellow. This has a maximum absorbance at 450 nm and can be measured with a microplate reader. The colour intensity is proportional to the amount of CXCL8-antibody sandwich complex.

3.7 Protein Immunoblot (Western Blot)

Reagent	Supplier	Address
SDS	Sigma-Aldrich	Gillingham, UK
Glycerol	Sigma-Aldrich	Gillingham, UK
Bromophenol blue	Sigma-Aldrich	Gillingham, UK
NuPAGE® Novex® 4-12% Bis-Tris Gel 1.0 mm, 15 well	Invitrogen	Paisley, UK
NuPAGE® Novex® 12% Bis-Tris Gel 1.0 mm, 15 well	Invitrogen	Paisley, UK
NuPAGE® MOPS SDS Running Buffer	Invitrogen	Paisley, UK
NuPAGE® Transfer Buffer	Invitrogen	Paisley, UK
Methanol	VWR	Lutterworth, UK
PVDF Membranes	Invitrogen	Paisley, UK
Non-Fat Dry Milk	Supermarket	London, UK
Anti-Histone H3 Antibody (ab1791)	Abcam	Cambridge, UK
Anti-Histone H3 (tri-methyl K4) Antibody (ab12209)	Abcam	Cambridge, UK
Anti-Histone H3 (tri-methyl K9) Antibody (ab8898)	Abcam	Cambridge, UK
Goat anti-Rabbit (HRP) Secondary Antibody (ab97051)	Abcam	Cambridge, UK
Anti-Histone H3 tri-methyl Lysine4 Antibody	Merck Millipore	Watford, UK
Anti-Histone H3 tri-methyl Lysine9 Antibody	Merck Millipore	Watford, UK
Anti-Histone H3 tri-methyl Lysine27 Antibody	Merck Millipore	Watford, UK
ECL Detection Reagent	Promega	Southampton, UK
Amersham ECL Detection Reagent	GE Healthcare Life Sciences	Little Chalfont, UK
Amersham Hyperfilm ECL		

Table 3-10 Reagents used in Western Blotting

Histones were extracted as described in 3.2.3 and the protein concentration determined by BCA assay as described in 3.4. Samples were normalized to the sample with the lowest protein concentration then loaded onto 4-12% or 12% gels before being resolved by sodium dodecyl sulphate polyacrylamide gel electrophoresis (SDS-PAGE) run in MOPS buffer. They were transferred onto PVDF (Polyvinylidene difluoride) membranes, blocked with 5% milk/BSA in 0.1% TBST and probed overnight with primary antibodies to Anti-Histone H3 loading control (molecular weight 17 kDa), histone H3 (tri-methyl K4) (molecular weight 17 kDa), histone H3 (tri-methyl K9)

(molecular weight 17 kDa) and histone H3 (tri-methyl K27) (molecular weight 17 kDa) (all diluted in 5% milk/BSA in 0.1% TBST). Membranes were washed in 0.1% TBST for 1 hour, changing the wash buffer every 10 minutes. The membranes were re-probed with HRP-conjugated rabbit anti-mouse/ goat anti-rabbit secondary antibodies (raised against the primary antibody host) and the wash step repeated. It is essential that the membranes are thoroughly washed to reduce non-specific binding and background luminescence. A chemiluminescent substrate is applied and the western blot visualised by hyperfilm development.

Western blotting is a highly specific though only semi-quantitative, technique. It can detect the protein of interest amongst a complex mixture of other biological components. Therefore, evaluation of the primary antibody specificity to the target protein is essential to ensure that it is not binding non-specifically to another protein and producing false negative results. Accurate determination of sample concentration is important to ensure that the samples are loaded equally and that any differences in signal intensity are truly due to differences in the protein expression. A control antibody should always be included against a protein whose expression does not vary in the experimental conditions used. We were measuring the difference in histone H3 methyl signatures so histone H3 is a good control as it has to be present in order to measure the methyl signature.

Proteins migrate through a polyacrylamide gel at a rate proportional to their size. The higher the polyacrylamide percentage is, the smaller the pore size in the gel is and the smaller the size of protein that can fit through. It is essential that the protein samples are properly denatured by heating to 95 °C in a reducing buffer to break any disulphide bonds as protein tertiary structure retards the rate of migration. SDS is also added to the reducing buffer in order to help denature the proteins and give them a uniformly negative charge so that they migrate towards the positive

anode. A ladder consisting of proteins of known molecular weight is always run alongside the samples of interest so that the target proteins can be identified by their size. The membrane is able to bind any and all proteins so must be blocked before the primary antibody is applied.

The secondary antibody is conjugated to the enzyme HRP so that the protein-antibody complex can be visualised. A chemiluminescent substrate is used, instead of TMB like in an ELISA, which produces light. This can be captured on film and developed photographically. The intensity of the signal correlates with the abundance of the antigen. This can be measured quantitatively if using fluorescent antibodies, but chemiluminescence will only indicate whether one sample is more or less than another rather than giving a numerical value.

We chose this technique as we needed to verify that the histone methyltransferase inhibitor/histone demethylase inhibitor was having an effect on the cells, but quantification of the effect was not required. It requires careful optimisation as it contains multiple critical steps, each of which can affect the final outcome. Troubleshooting was systematic and comprehensive, as well as challenging and gave experience in correlating specific sub-optimal results with likely problems and causes.

3.7.1 Antibody Stripping for Restaining of Protein Immunoblots

Stripping and restaining western blots is a cost-effective and efficient method of probing for multiple primary antibodies from the same sample. This is particularly useful when the two or more proteins of interest cannot be sufficiently resolved by SDS-PAGE or when looking at different modifications of the same protein e.g. Histone H3 and H3K4me3. PVDF membranes are recommended for blots that are to be reprobed as they bind protein with a higher capacity than

nitrocellulose membranes and are also more resistant to mechanical and chemical damage. Chemiluminescent developing substrates are also recommended as colourimetric/chromogenic substrates can stick to the membrane and interfere with subsequent antibody binding. An acidic buffer (200 mM Glycine, 3.5 mM SDS, 1% TWEEN® 20 in H_2O, pH 2.2), is used to denature the antibody-protein complex so that the antibody can be washed away whilst the protein sample remains bound to the membrane. The blot is incubated with enough stripping buffer to cover the membrane at RT for 5-10 mins and repeated with fresh buffer. It is then washed with PBS for 10 mins twice and with 0.1% TBST for 5 mins twice. Thorough washing is required to ensure that the stripping buffer is completely removed from the blot otherwise it can prevent the antibody from binding. The blot is then ready for blocking with 5% milk in 0.1% TBST and incubation with the second primary antibody. Blocking the blot again is not always necessary, depending on the quality of the primary antibody used for restaining, but it can help to keep the background level low, as this tends to rise as the membrane is repeatedly stripped.

A small amount of protein is lost from the sample with each round of stripping and restaining so ideally, quantitative comparisons should not be made before and after stripping. However, by comparing the signal intensity patterns using the same primary antibody before and after stripping blots assuming that they are similar means that it can be used for quantitative analysis.

3.8 Histone H3 PTM (Post-Translational Modifications) Multiplex Assay

Reagent	Supplier	Address
Histone H3 PTM Multiplex Assay	Active Motif	La Hulpe, Belgium
Histone H3 Total Antibody-conjugated Beads	Active Motif	La Hulpe, Belgium
Histone H3K4me3 Antibody-conjugated Beads	Active Motif	La Hulpe, Belgium
Histone H3K9me3 Antibody-conjugated Beads	Active Motif	La Hulpe, Belgium
Histone H3K27me3 Antibody-conjugated Beads	Active Motif	La Hulpe, Belgium
MAGPIX™	Luminex	's-Hertogenbosch, The Netherlands

Table 3-11 Reagents used in Histone H3 PTM Multiplex Assay

The histone H3 post-translational modifications multiplex assay is a novel antibody-based bead method that can simultaneously measure the levels of multiple modifications at once using Luminex technology. It is a high-throughput ELISA technique producing quantitative results as an alternative to qualitative Western Blotting results. The sample binds to the histone H3 post-translationally modified (PTM) antibody conjugated to magnetic Luminex beads. The secondary biotinylated Histone H3 antibody then binds to the sample and provides the internal control for normalization across multiple samples. Streptavidin-phycoerythrin binds to the biotinylated histone H3 antibody and produces fluorescence proportional to the amount of modified histone H3 present. The median fluorescence intensity (MFI) is measured with a MAGPIX™ instrument and xPONENT software. These steps are illustrated in Figure 3-9.

The Active Motif Histone H3 PTM Multiplex assay is based upon Luminex technology. Luminex technology involves the production of supramagnetic beads containing a range of dye ratios that produce distinctive fluorescent signals capable of identifying the bead. Active Motif developed the Luminex technology for use with histone H3 PTM antibodies. Each PTM antibody is associated

with a unique fluorescent signal thereby allowing later identification of each bead in the multiplexed system. As the beads pass through the MAGPIX™ instrument, the beads are excited by two wavelengths; the first to excite the fluorescent dye in the bead and identify the PTM antibody, and the second to measure the magnitude of the streptavidin-phycoerythrin signal. The streptavidin-phycoerythrin signal is directly proportional to the amount of sample bound to that particular PTM antibody-conjugated bead. A major advantage of this assay over Western blotting is that multiple PTMs can be interrogated in the same sample, a smaller sample size is required than for immunoblotting and the results area quantitative and subject to statistical analysis.

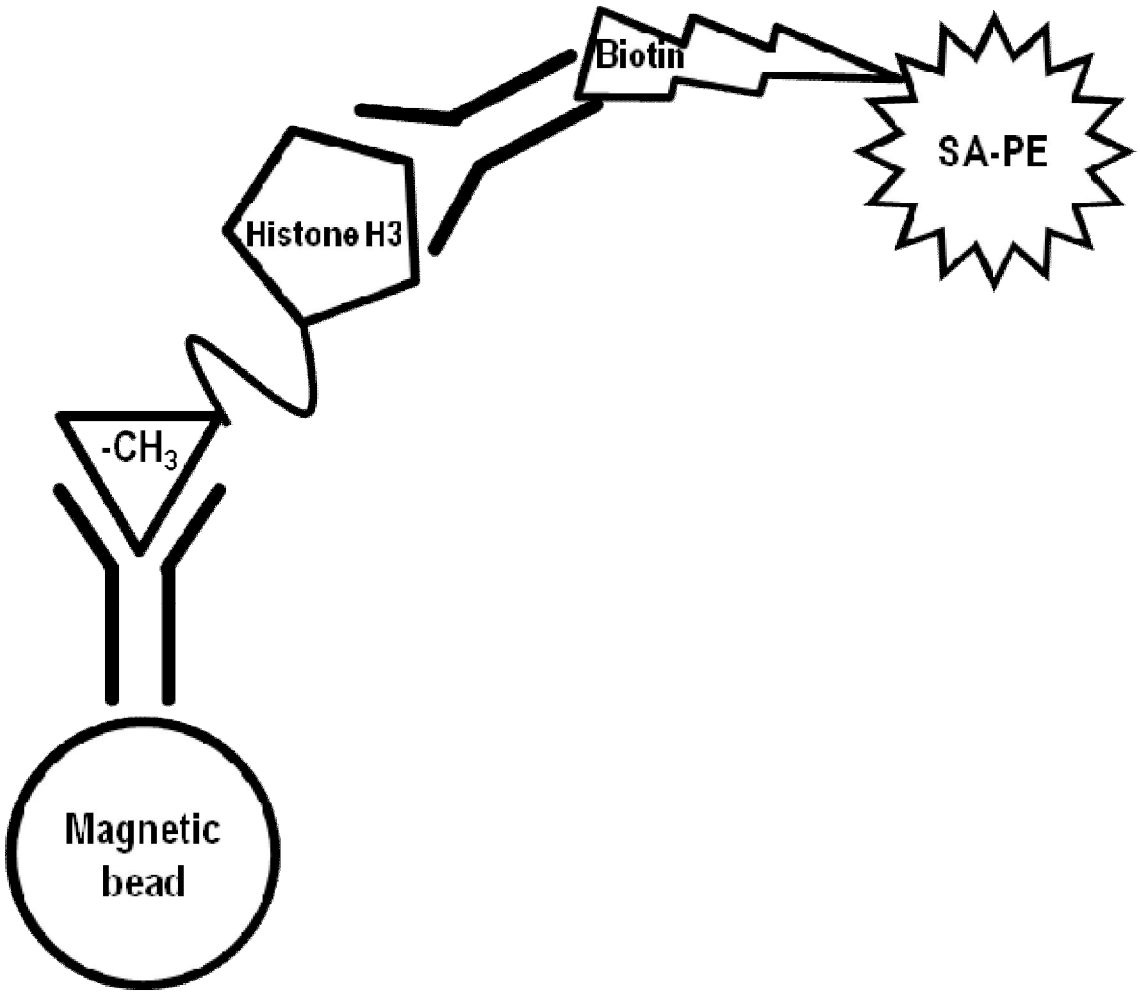

Figure 3-9 Schematic of the Histone H3 PTM Multiplex Bead-based Sandwich Assay

A diagram representing the Active Motif Histone H3 PTM Multiplex Assay: circle – PTM antibody-conjugated magnetic bead; triangle – PTM methyl group; pentagon – histone H3 protein sample; lightning bolt – biotinylated histone H3 antibody; star – streptavidin-phycoerythrin (SA-PE). The histone sample (pentagon with attached triangle modification) binds to the PTM antibody-conjugated magnetic bead. This forms a sandwich complex with a biotinylated Histone H3 antibody. SA-PE bindsto the histone-antibody sandwich complex and fluoresces in proportion to the amount of histone H3 sample bound to the PTM antibody. The fluorescence is measured using MAGPIX™ and xPONENT software.

3.9 Chromatin Immunoprecipitation (ChIP)

Reagent	Supplier	Address
37% Formaldehyde	Sigma-Aldrich	Gillingham, UK
Glycine	Sigma-Aldrich	Gillingham, UK
IGEPAL® CA-630	Sigma-Aldrich	Gillingham, UK
Triton-X 100	Sigma-Aldrich	Gillingham, UK
NaCl	Sigma-Aldrich	Gillingham, UK
EDTA	Sigma-Aldrich	Gillingham, UK
EGTA	Sigma-Aldrich	Gillingham, UK
PMSF	Sigma-Aldrich	Gillingham, UK
SDS	Sigma-Aldrich	Gillingham, UK
Tris-HCl, pH 8.0	Sigma-Aldrich	Gillingham, UK
cOmplete, EDTA-free Protease Inhibitor Cocktail	Roche	Burgess Hill, UK
Magna ChIP™ Protein A/G Magnetic Beads	Merck Millipore	Watford, UK
Anti-Histone H3 Antibody	Abcam	Cambridge, UK
Anti-trimethyl-Histone H3 (Lys4) Antibody	Merck Millipore	Watford, UK
Anti-trimethyl-Histone H3 (Lys9) Antibody	Merck Millipore	Watford, UK
Anti-trimethyl-Histone H3 (Lys27) Antibody	Merck Millipore	Watford, UK
Primers	Sigma-Aldrich	Gillingham, UK

Table 3-12 Reagents used in ChIP

Chromatin immunoprecipitation (ChIP) is a method used to determine the nature of protein-DNA interactions. It can be used to profile the binding pattern of transcription factors and proteins that interact with DNA, as well as determining the positions that histone modifications are associated with. DNA is fixed to the proteins that are bound to it using formaldehyde and sheared into small pieces by sonication or micrococcal nuclease. Antibodies against the protein of interest precipitate the specific protein-DNA immune complex thereby isolating the specific regions of DNA that are boiund to the protein. Degradation of the protein with proteinase K is followed by purification of the DNA which is analysed by PCR. The precipitated DNA is analysed either by

sequencing (ChIP-seq) to identifiy the specific regions, or primers against specific areas are used in qPCR to measure the fold change difference at certain specific loci.

There are a number of limitations to consider when performing ChIP. The main limitation is that ChIP is an antibody-based technique, which is inherently inefficient. Non-specific binding is a major issue and although some antibodies work perfectly well for other techniques e.g. ELISA and Western blotting, they do not work well in ChIP. It is recommended to use a ChIP-validated antibody and empirically determine the optimum concentration and incubation time for maximum binidng.

Fragmentation is another limitation. There are two methods of fragmentation, sonication and micrococcal nuclease digestion. Sonication uses sound waves to agitate particles, or as in this situation, break chromatin into small pieces. The samples need to be sonicated enough to produce fragment sizes of 200 – 1000 bp, which is small enough to easily analyse but large enough to include at least one whole nucleosome and not just the linker DNA (Figure 1-6). Sonication produces a range of fragment sizes but by using a Bioruptor® (sonication device using a water bath), the fragmentation is more reproducible. A further complication is that sonication causes an increase in temperature which can degrade the chromatin, reverse fixation and cause the SDS in the buffer to precipitate. Therefore, it is necessary to keep the samples cool and, if possible, on ice. An alternative method of fragmentation is enzymatic digestion using micrococcal nuclease (MNase). MNase is an endo-exonuclease that cleaves DNA. As formaldehyde crosslinks prevent MNase access to the DNA, this technique is restricted to native ChIP and the analysis of proteins that are naturally bound to DNA (169).

SDS is a detergent which is used in several of the ChIP buffers to facilitate lysis and increase sonication efficiency. However, it can interfere with antibody-antigen binding by preventing the antibody associating with its epitope. Therefore, although it is required for efficient sonication, it needs to be diluted out after fragmentation in order to maximise antibody binding (170).

.

Chromatin was extracted for histone methylation analysis by ChIP. Intestinal epithelial (Caco-2) cells were grown in T75 flasks at a seeding density of 1.2 – 1.7 x 10^4 cells/ml and were incubated with IL-1β and epigenetic inhibitors as described in Figure 3-7. An aliquot of growth medium was removed for analysis by ELISA, in order to confirm both tolerance and the breaking of tolerance by the epigenetic inhibitor. The chromatin was fixed by adding formaldehyde to the cells to a final concentration of 1%. The flasks were gently agitated for 10 mins to ensure thorough fixation, followed by 5 mins incubation with 125 mM glycine to quench the reaction. The cells were washed twice with ice-cold PBS, placed on ice and scraped into cold lysis buffer with added protease inhibitor cocktail (PIC). After 10 mins incubation on ice with gentle agitation, the samples were centrifuged at 500 x *g* for 5 mins at 4 °C. The supernatant was discarded and the pellet resuspended in cold post-lysis buffer with added PIC. After 10 mins incubation with gentle agitation, the samples were centrifuged at 500 x *g* for 5 mins at 4 °C. The supernatant was discarded and the pellet resuspended in 1.8 ml sonication buffer with added PIC. Each sample was aliquoted into 6 volumes of 300 ml. The chromatin was sheared by sonication using a Bioruptor for 15 mins in 30 sec pulses in ice-cold water. The samples were centrifuged at 12 000 x *g* for 10 mins at 4 °C to pellet any debris. The resulting supernatant containing the sheared chromatin was then stored at -70 °C until ready for ChIP analysis.

Using the EZ-Magna ChIP A/G kit from Merck Millipore, protease inhibitor cocktail was added to dilution buffer, which was used to dilute the ChIP samples in half. (The kit recommends a 1 in 10

dilution, but to maximise the amount of chromatin available to the antibody, a 1 in 2 dilution was used.) 5 µl of the diluted sample was removed as the "input" and stored at 4 °C until the elution step. 20 µl of fully resuspended protein A/G magnetic beads with the appropriate antibody of interest or control IgG antibody, at the amount listed in Table 3-13, were added to each sample and incubated overnight with rotation at 4 °C. Although the antinobdy incubation time can be reduced to as little as 1 hour, overnight incubation was used to maximise antibody binding and precipitate the maximal amount of chromatin.

Antibody	**Amount (µg)**
Anti-Histone H3	2
Anti-trimethyl-Histone H3 (Lys4)	1
Anti-trimethyl-Histone H3 (Lys9)	4
Anti-trimethyl-Histone H3 (Lys27)	4

Table 3-13 Table Describing the Amount of Each Antibody used in ChIP

The immunoprecipitated chromatin binds to the magnetic beads. A magnetic rack is used to separate the beads from the buffer and the supernatant is discarded. A series of wash buffers including low salt, high salt, LiCl and TE are used to wash the immunoprecipitated chromatin. After the final wash, the chromatin is resuspended in ChIP elution buffer and incubated with Proteinase K for 2 hours with shaking at 65 °C. The reaction is stopped by incubation at 95 °C for 10 mins. Proteinase K degrades any protein fixed to the DNA, leaving just the sheared DNA pieces, which are cooled down to room temperature before being purified for PCR analysis. Purification is necessary to remove salts and degraded proteins which may interfere with or inhibit PCR. This is achieved by using spin columns and centrifuging with a succession of buffers, the first of which is a wash buffer, followed by a binding buffer which binds the DNA to the spin column. Finally, the DNA is eluted and is analysed immediately by qPCR or stored at -20 °C for future analysis using the primer pairs in Table 3-14.

CXCL8 Primers	Forward	Reverse	Product size (bp)
5'	GGTGCTAGTCTCTGCTCATCAA	AGAGCAAAGTGGGGTACAAAGT	172
Promoter	AACTGAGGTCAAGGGCTAGGAG	TCTTTAGCACTCCTTGGCAAAAC	188
Gene Body	AGGAAGTGTGATGACTCAGG	GTCCTAGAAGCTTGTGTGCT	189

Table 3-14 CXCL8 qPCR Primers used in ChIP Analysis

3.10 Statistics

CXCL8 production was normalized to the amount of protein per well, as as measured by BCA assay (pg/mg protein) and different experiments standardized to each other by expressing the CXCL8 pg/mg protein values as a percentage of the mean singly stimulated CXCL8 production values (performed in Microsoft Excel 2007).

The pooled data from each experiment was tested for Gaussian distribution i.e. that the scatter of multiple data points around the mean resembles a bell-shaped curve with a continuous probability distribution approaching zero on either side. This was tested for using the D'Agostino and Pearson omnibus normality test, which tests the null hypothesis that the data has Gaussian distribution. Therefore it tests how closely the data resembles the Gaussian ideal, but does not say what distribution the data is if it is not Gaussian. As it is almost impossible to actually have a data set with ideal Gaussian distribution, many statistical tests work well with data sets that closely resemble normal distribution.

Data was plotted as mean ± SEM (standard error of the mean), using SEM to show how precise the mean is. As the data set increases in size the SEM tends to decrease as the data values tend not to vary far from the mean thus reinforcing the authenticity of the mean. The student's *t*-test and the Mann-Whitney *U* test were used to test the null hypothesis that the mean of the two data sets is equal. The student's *t* test was used for data sets that conformed to Gaussian distribution whereas the non-parametric Mann-Whitney *U* test was used for non-Gaussian distributed data. Both of these statistical tests test the quality of the mean between two groups whereas ANOVA tests the equality between three or more data sets. As the Mann-Whitney *U* test compares the sum of ranks, it is less likely than the student's *t* test to produce an incorrect significant result,

especially for non-normally distributed data containing outliers. ANOVA, or analysis of variance, is particularly appropriate for testing the equality of means in three or more groups as it avoids producing a false positive result and rejecting the null hypothesis when it should not be, as often occurs when performing multiple two-group statistical tests. Two-tailed P values were calculated as they are more stringent than one-tailed tests and account for deviation from the null hypothesis in either direction happening by chance. Results were considered significant where $P<0.05$ (according to convention). Data were analysed and presented after normalization and standardization using GraphPad Prism 5 statistical and graphical software.

4 Immune Tolerance in Intestinal Epithelial Cells

4.1 Establishment of Immune Tolerance in Intestinal Epithelial Cells to Bacterial Lipoprotein

4.1.1 Optimization of Bacterial Lipoprotein-Stimulation

Bacterial lipoprotein is found naturally in the small intestine and colon where, being a component of bacteria, it is shed by the microbiota. It is a highly recognisable PAMP common to many bacteria and as such activates the innate immune system. Bacterial lipoprotein is an agonist of TLR2 and causes expression of pro-inflammatory cytokines e.g. CXCL8. Although there is a large range of different natural bacterial lipoproteins, a synthetic bacterial lipoprotein has been developed, Pam_3CysK_4 (P3CK), which is regularly used as a TLR2 agonist (Figure 4-1). CXCL8 is expressed in low amounts in the healthy intestine, but in large amounts in patients with UC, correlating with disease severity (171). Epithelial cell chemokine expression results in extensive neutrophil recruitment (172) in to the lamina propria. As epithelial cells respond to TLR stimulation, we compared the effect on CXCL8 production of repeatedly stimulating intestinal epithelial cells to cells with a single stimulation.

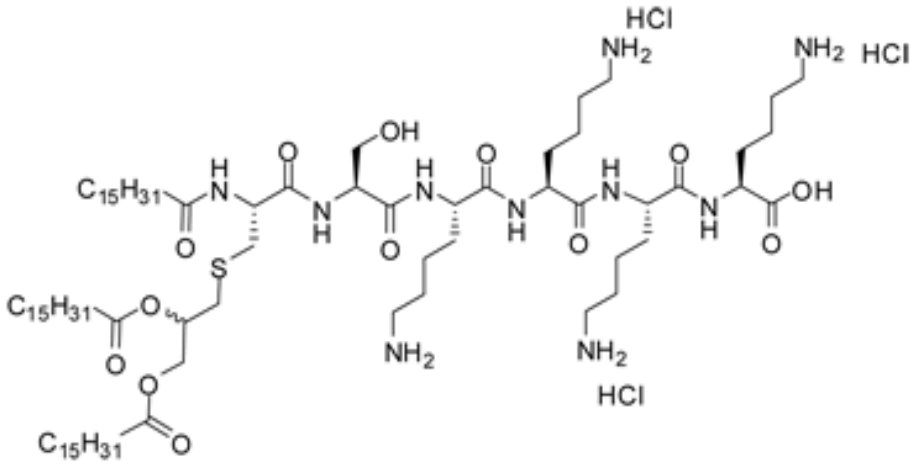

Figure 4-1 Structure of P3CK

The chemical structure of P3CK, taken as a screenshot from (173).

The optimum concentration of P3CK required to both stimulate the intestinal epithelial cell lines was determined by establishing a dose-response curve. As described in Figure 3-1, Caco-2 cells were stimulated by serial dilutions of P3CK (0 – 100 µg/ml) for 24 hours. The conditioned media samples were collected for analysis by CXCL8 ELISA and the cells harvested and measured for total protein content. As can be seen in Figure 4-2, the production of CXCL8 increased as the concentration of P3CK increased, with statistically significant production of CXCL8 as compared to unstimulated cells. Caco-2 cells stimulated with 6.25 µg/ml P3CK produced a statistically significant greater expression of CXCL8 than cells stimulated with 3.125 µg/ml P3CK ($P<0.001$). Cells stimulated with 12.5 µg/ml P3CK also produced a statistically significant greater secretion of CXCL8 than the preceding concentration (6.25 µg/ml) ($P<0.05$). Each further concentration of P3CK (25, 50 and 100 µg/ml) produced a greater, though non-significant, quantity of CXCL8. However, as it was not economical to use 100 µg/ml P3CK for subsequent tolerization experiments, 25 µg/ml was chosen as it induces a large and statistically significant CXCL8 response.

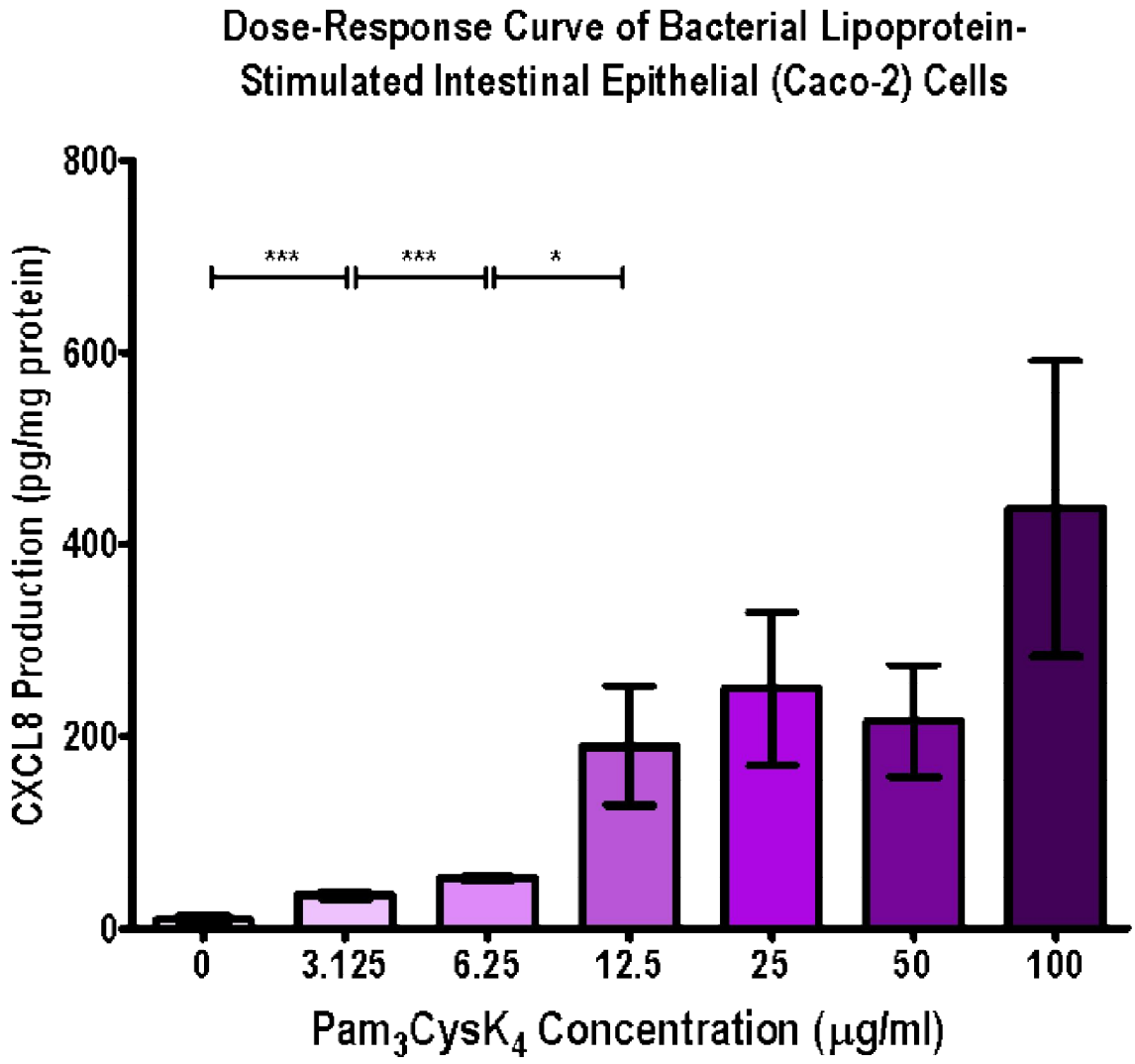

Figure 4-2 Dose-Response Curve of Bacterial Lipoprotein-Stimulated Intestinal Epithelial (Caco-2) Cells

P3CK was serially diluted by a factor of two (0-100 μg/ml) and used to stimulate Caco-2 cells for 24 hours, as described in Figure 3-1. CXCL8 production was measured by ELISA and normalized to cellular protein content (measured by BCA protein assay). Bars represent mean ± SEM, n = 2. Statistical analysis was performed using the Student's *t*-test (for normally distributed data) or the Mann-Whitney *U* test (for non-normally distributed data). * and *** signify $P<0.05$ and <0.001.

P3CK stimulation of NCM460 cells, non-malignant intestinal epithelial cells, also showed a dose-dependent increase in CXCL8 production. Two-fold serial dilutions of P3CK (0-100 μg/ml) were used to stimulate NCM460 cells. As was seen in Caco-2 cells, the optimum P3CK concentration for NCM460 cell CXCL8 production was 25 μg/ml, as higher P3CK concentrations did not produce a statistically significantly greater production of CXCL8 (Figure 4-3). Both cell types produce a similar dose-response curve and although the optimum concentration is the same for both Caco-2 and NCM460 cells, NCM460 cells stimulated by 25 μg/ml P3CK produced more CXCL8 than Caco-2 cells when expressed as cytokine per cell weight (533.2 pg/mg protein vs. 249.4 pg/mg protein, $p<0.05$). Therefore, both types of intestinal epithelial cell express TLR2. It can be deduced and is logical to assume that both cell types initiate signalling cascades that result in similar levels of CXCL8 expression.

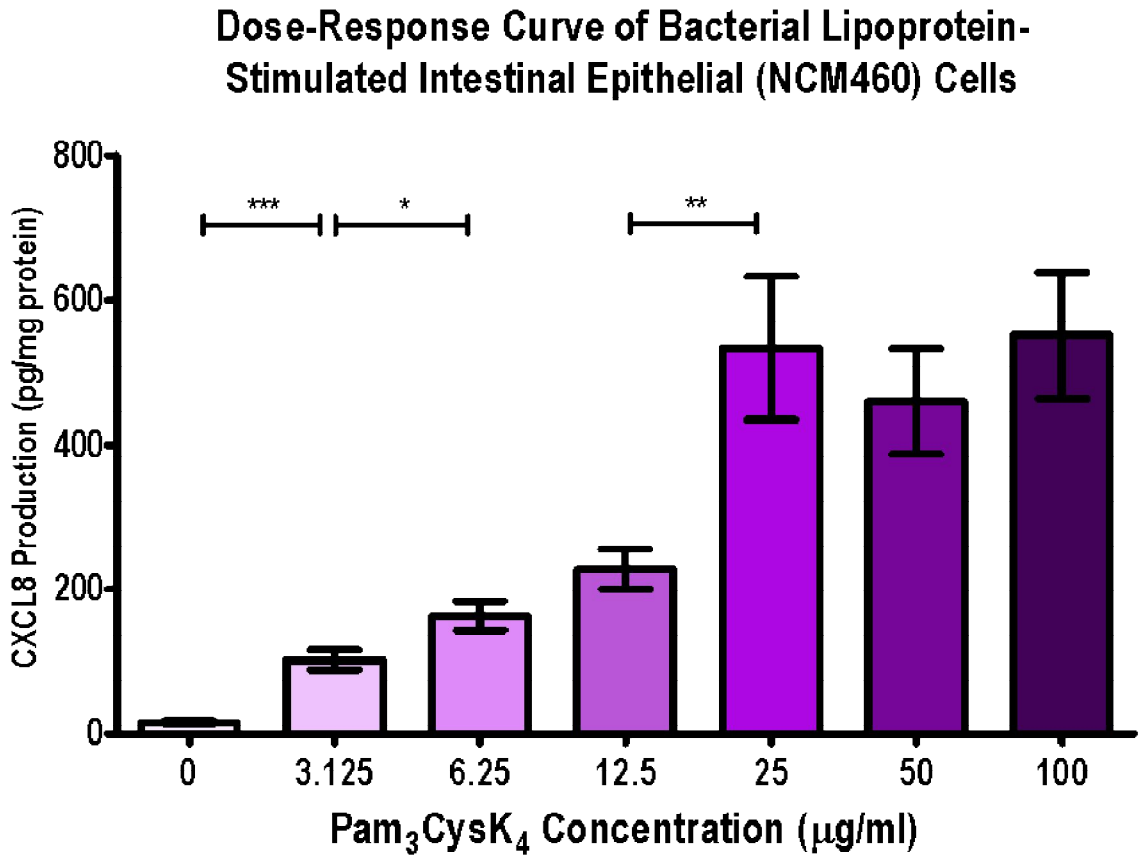

Figure 4-3 Dose-Response Curve of Bacterial Lipoprotein-Stimulated Intestinal Epithelial (NCM460) Cells

P3CK was serially diluted by a factor of two (0-100 μg/ml) and used to stimulate NCM460 cells for 24 hours, as described in Figure 3-1. CXCL8 production was measured by ELISA and normalized to cellular protein content (measured by BCA protein assay). Bars represent mean ± SEM, n = 4. Statistical analysis was performed using the Student's *t*-test (for normally distributed data) or the Mann-Whitney *U* test (for non-normally distributed data). *, ** and *** signify P<0.05, <0.01 and <0.001, respectively.

4.1.2 Tolerance to Bacterial Lipoprotein

We were interested in determining whether cells with a prior stimulation of P3CK could become hyporesponsive (tolerized) following further P3CK stimulation, because this represents a natural bacterial product present in the intestinal lumen. This was established by comparing the CXCL8 production of cells that were stimulated with 25 µg/ml P3CK for 24 hours with similarly stimulated cells that had been stimulated with 25 µg/ml P3CK 24 hours previously (as described in Figure 3-2). Conditioned media samples were collected and CXCL8 expression measured by ELISA and normalized to the cellular protein content, as measured by BCA protein assay. These experimental conditions reflect the physiological situation of the intestinal epithelium which is responding to the presence of the gut microbiota. Constant stimulation by the millions of bacteria found in the gut would result in a massive, chronic, deleterious inflammatory response, if cytokine expression were left unchecked and not tightly controlled. A reduced ability to induce CXCL8 by small concentrations of lipoprotein could help to prevent excessive inflammatory cascade initiating a lower response (tolerance).

As shown in Figure 4-4, the production of CXCL8 was greatest in the cells that have only been stimulated once with P3CK and was decreased, but still greater than the unstimulated control cells, in the cells that were stimulated 24 hours earlier. This was a statistically significant reduction ($P<0.001$), as calculated by Student's *t* test and was 37.3% of the stimulated production.

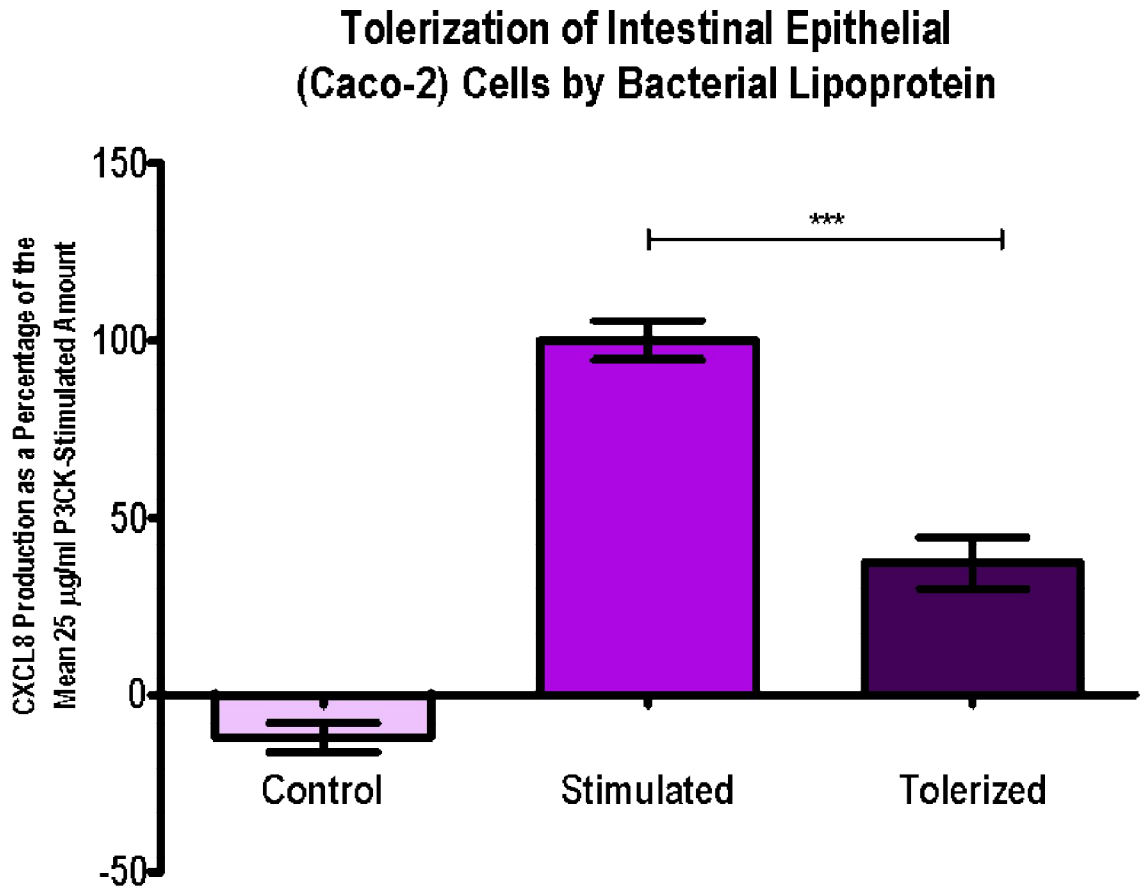

Figure 4-4 Tolerization of Intestinal Epithelial (Caco-2) Cells by Bacterial Lipoprotein

Caco-2 cells were stimulated with 25 µg/ml P3CK for 24 hours and tolerized by a prior stimulation of 25 µg/ml P3CK 24 hours earlier, as described in Figure 3-2. CXCL8 production was measured by ELISA, normalized to cellular protein content (measured by BCA protein assay) and represented as a percentage of the mean stimulated amount. Bars represent mean ± SEM, n = 4 Statistical analysis was performed using the Student's *t*-test. *** signifies $P<0.001$.

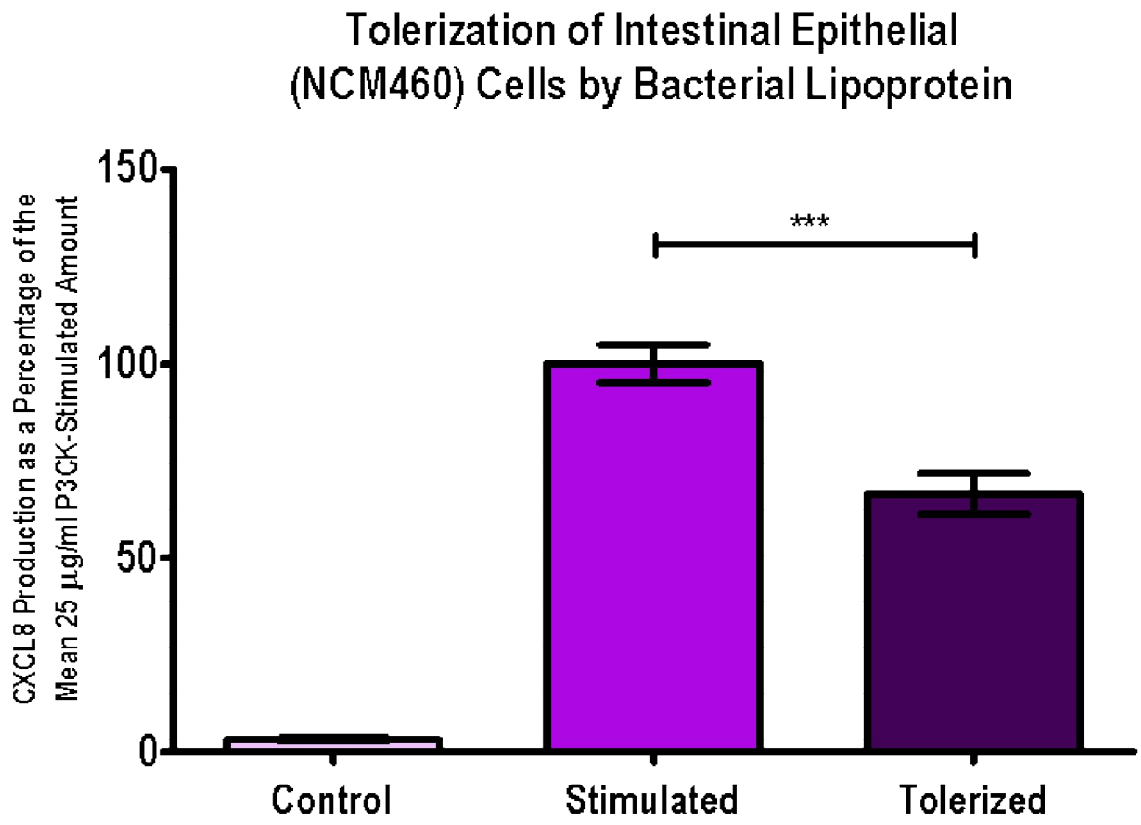

Figure 4-5 Tolerization of Intestinal Epithelial (NCM460) Cells by Bacterial Lipoprotein

NCM460 cells were stimulated with 25 µg/ml P3CK for 24 hours and tolerized by a prior stimulation of 25 µg/ml P3CK 24 hours earlier, as described in Figure 3-2. CXCL8 production was measured by ELISA, normalized to cellular protein content (measured by BCA protein assay) and represented as a percentage of the mean stimulated amount Bars represent mean ± SEM, n = 4 . Statistical analysis was performed using the Student's *t*-test. *** signifies $P<0.001$.

Tolerance was also established in NCM460 cells, as described in Figure 3-2. Tolerized cells were stimulated twice with 25 µg/ml P3CK for 24 hours each and CXCL8 expression was compared to CXCL8 expression by NCM460 cells that had only been stimulated once with P3CK (Figure 4-5). As seen with Caco-2 cells in Figure 4-4, the reduction in CXCL8 production by tolerized NCM460 cells compared to stimulated NCM460 cells is statistically significant ($P<0.001$) (Figure 4-5).

In summary, tolerance, a hyporesponsive state, was established in both Caco-2 and NCM460 cells, as measured by the decrease in CXCL8 expression following TLR pre-stimulation thereby demonstrating that tolerance is a phenomenon in epithelial cell lines. Furthermore, it is not one that is confined to malignant cell lines.

4.1.3 Optimization of IL-1β Stimulation

As demonstrated above, P3CK produces a tolerized immune response in intestinal epithelial cells. P3CK represents the presence of microbiota in the intestine and their effect on the inflammatory immune response of epithelial cells. The effect of IL-1β on intestinal epithelial cells was also investigated, as IL-1β is a major inflammatory mediator, particularly in IBD (174). IL-1β represents the effect of active inflammation on the intestinal epithelium, regardless of whether the inflammation is a result of an infection, stress or a disease. Therefore, the effect of IL-1β on intestinal epithelial cells was investigated.

The optimum concentration of IL-1β required to stimulate the Caco-2 cells was determined by production of a dose-response curve. As described in Figure 3-1, Caco-2 cells were stimulated by a two-fold serial dilution of IL-1β (4 – 0 ng/ml) for 24 hours. The conditioned media samples were collected for analysis by CXCL8 ELISA and the cells harvested and measured for protein content. As can be seen in Figure 4-6 a significant increase in the expression of CXCL8 was seen each time the IL-1β concentration doubled (except between 0.0625 ng/ml and 0.125 ng/ml) up to 1 ng/ml. Although both 2 ng/ml and 4 ng/ml IL-1β stimulated a greater production of CXCL8 than the amount produced by 1 ng/ml IL-1β, it is not a statistically significant increase. 1 ng/ml IL-1β was, therefore, the most efficient stimulant and therefore the optimum concentration for CXCL8 stimulation.

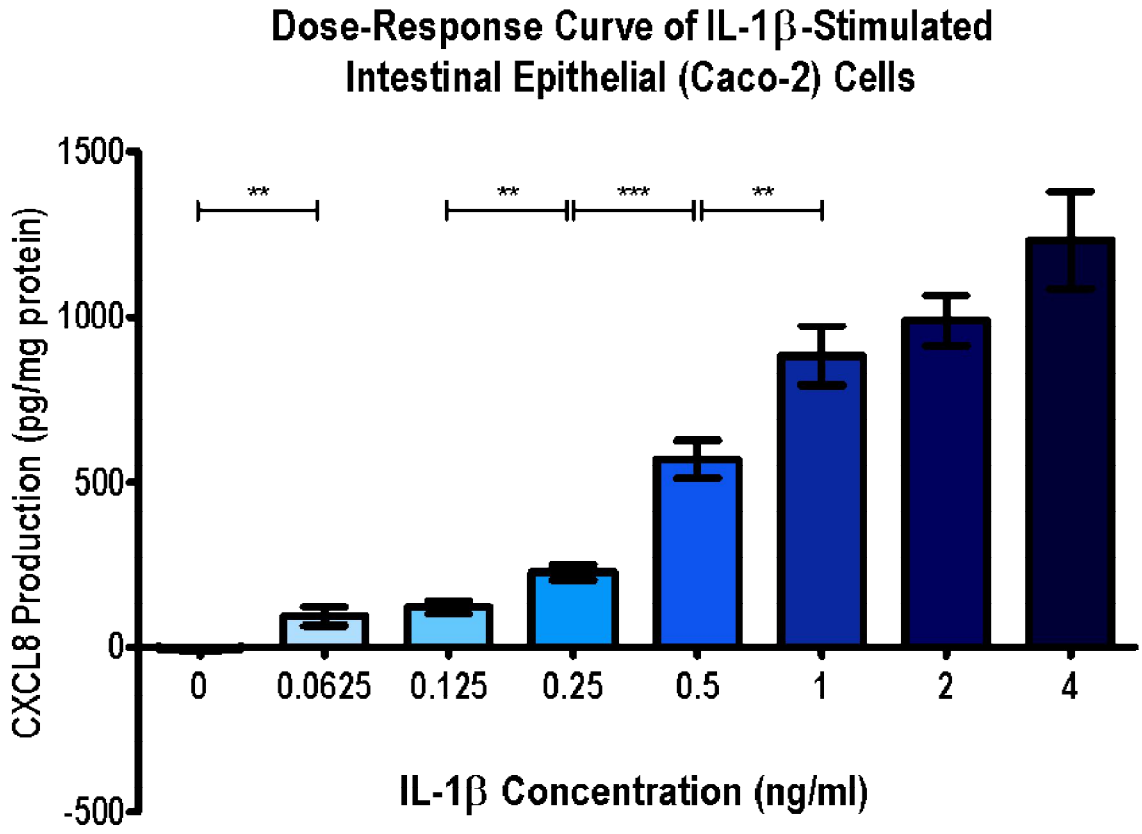

Figure 4-6 Dose-Response Curve of IL-1β-Stimulated Intestinal Epithelial (Caco-2) Cells

IL-1β was serially diluted by a factor of two (0-4 ng/ml) and used to stimulate Caco-2 cells for 24 hours, as described in Figure 3-1. CXCL8 production was measured by ELISA and normalized to cellular protein content (measured by BCA protein assay). Bars represent mean ± SEM, n = 4. Statistical analysis was performed using the Student's *t*-test or the Mann-Whitney *U* test. ** and *** signify P<0.01 and <0.001.

The effect of IL-1β on NCM460 cells was different from that observed on Caco-2 cells. NCM460 cells stimulated with a two-fold serial dilution (4 – 0 ng/ml) of IL-1β did not produce a statistically significant increase in CXCL8 secretion (Figure 4-7). NCM460 cells stimulated with 1 ng/ml IL-1β, the standard IL-1β concentration used to stimulate Caco-2 cells, produced similar levels of CXCL8 as unstimulated cells (Figure 4-7). A small, but statistically significant ($P<0.05$), increase in CXCL8 production by NCM460 cells resulted from stimulation with 10 ng/ml IL-1β (Figure 4-7). However, this production of CXCL8 (41.8 pg/mg protein vs. 25.3 pg/mg protein, $P<0.05$), was not even a two-fold increase above background production levels. Though 10 mg/ml IL-1β stimulated a statistically greater production of CXCL8 than 1 ng/ml IL-1β did ($P<0.05$, Figure 4-7), 10 ng/ml is a disproportionate concentration that produces an insufficient production of CXCL8. Background levels of CXCL8 production were higher in NCM460 cells than Caco-2 cells, making a statistically significant induction of CXCL8 expression harder to achieve in the NCM460 cell-line. IL-1β was not a potent enough stimulant in NCM460 cells, as insufficient CXCL8 was produced to observe a statistically significant difference in CXCL8 expression between control, unstimulated and tolerized cells. We concluded that this cell line did not express CXCL8 in response to IL-1β. Therefore, further experiments investigating the effect of tolerance to IL-1β in intestinal epithelial cells were conducted only on Caco-2 cells.

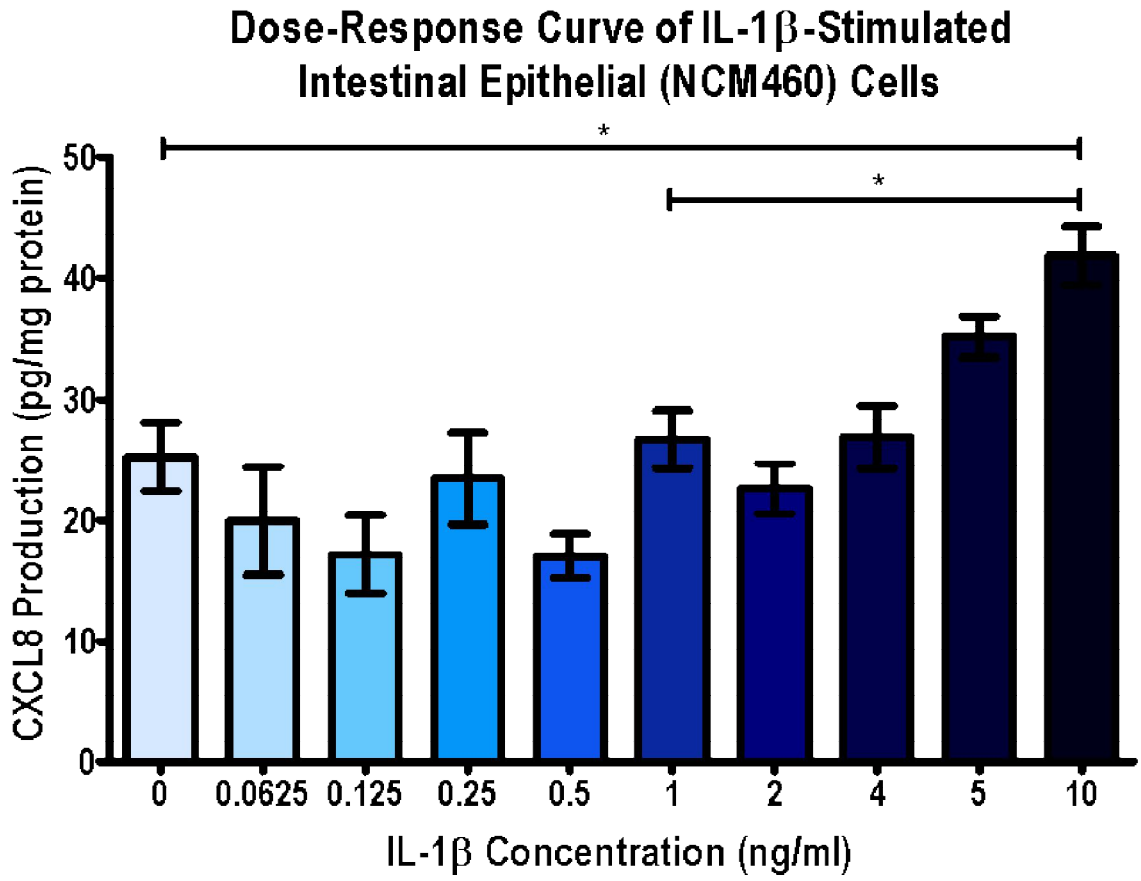

Figure 4-7 Dose-Response Curve of IL-1β-Stimulated Intestinal Epithelial (NCM460) Cells

IL-1β was serially diluted by a factor of two (0-4, 5, 10 ng/ml) and used to stimulate NCM460 cells for 24 hours, as described in Figure 3-1. CXCL8 production was measured by ELISA and normalized to cellular protein content (measured by BCA protein assay). Bars represent mean ± SEM, n = 5. Statistical analysis was performed using the Student's *t*-test. * signifies P<0.05.

4.1.4 Technical Difficulties in Establishing Tolerance to IL-1β

Technical difficulties had to be overcome during the course of the investigation when attempting to induce tolerance. There was a period in which the Caco-2 cells stopped responding to IL-1β stimulation and could not be either stimulated or tolerized. HT29 cells at this time, in comparison, produced large, but not non-significant, differences in the production of CXCL8, regardless of whether or not the cells were stimulated with IL-1β. Before describing the successful results, I will outline the difficulties encountered.

Tolerance was induced as described in Figure 3-2. Caco-2 cells were stimulated with 1 ng/ml IL-1β for 24 hours. Tolerized cells were pre-stimulated with 1 ng/ml IL-1β for 24 hours followed by another 24 hour stimulation of 1 ng/ml IL-1β. However, the production of CXCL8 was not significantly different between the control, stimulated and tolerized cells (Figure 4-8), as measured by ANOVA (P=0.4504).

After repeating the initial stimulation experiment a number of times with a consistent failure of stimulation, the protocol was tested on HT29 cells, in case the Caco-2 cells, through multiple passages, had lost the ability to produce CXCL8. I hypothesized that this may have been due to a number of reasons such as epigenetic silencing, expulsion of chromosome 4, presence of small molecule inhibitors e.g. in FCS etc. However, whilst the Caco-2 cells did not produce CXCL8, both the control and the stimulated HT29 cells produced large amounts of CXCL8 with a non-significant difference (Figure 4-9). Our suspicions that problems had occurred, in these particular experiments, were confirmed as the stimulated Caco-2 cells produced a lower expression of CXCL8 than the control. Therefore, neither intestinal epithelial cell line responded to IL-1β.

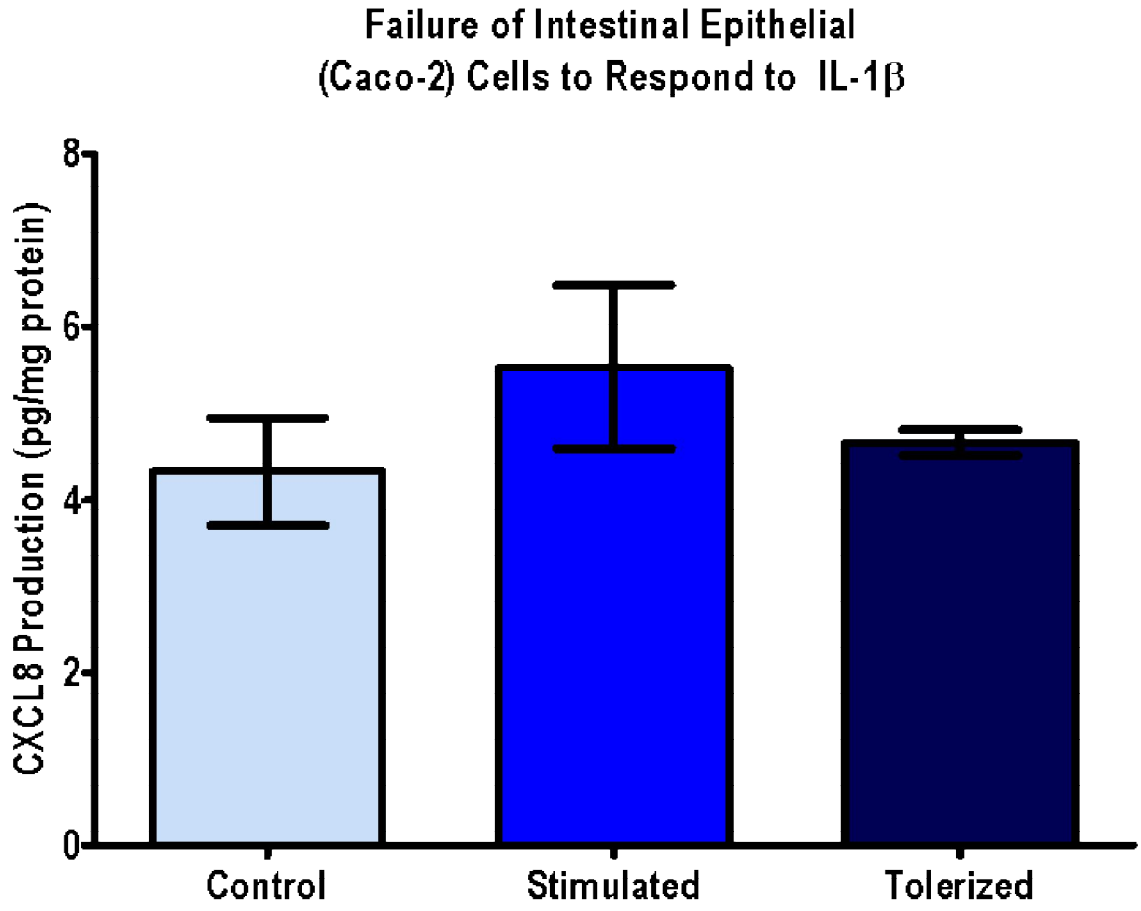

Figure 4-8 Failure of Intestinal Epithelial (Caco-2) Cells to Respond to IL-1β

Caco-2 cells were stimulated with 1 ng/ml IL-1β for 24 hours and tolerized by a prior stimulation of 1 ng/ml IL-1β 24 hours earlier, as described in Figure 3-2. CXCL8 production was measured by ELISA and normalized to cellular protein content (measured by BCA protein assay). Bars represent mean ± SEM, n = 1. ANOVA P=0.4504

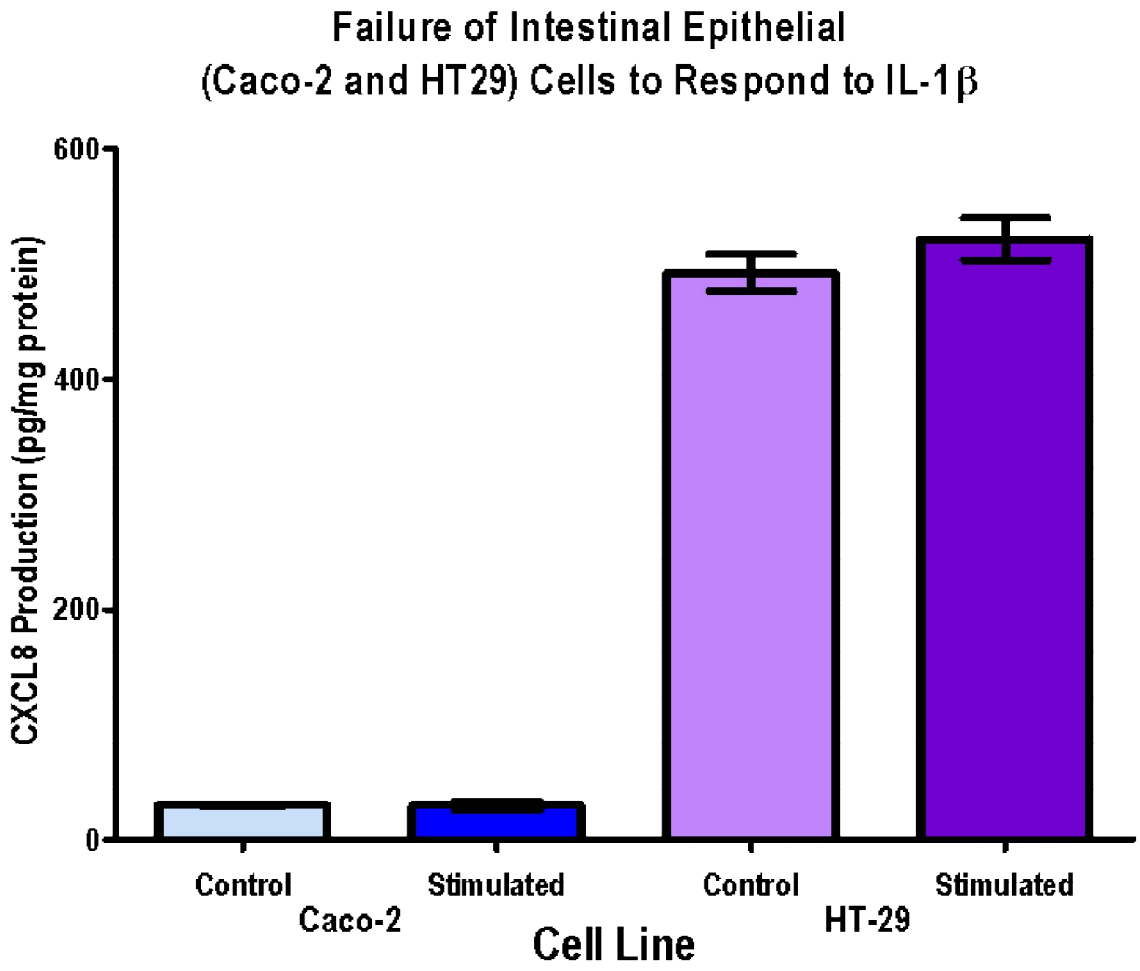

Figure 4-9 Failure of Intestinal Epithelial (Caco-2 and HT29) Cells to Respond to IL-1β

Caco-2 and HT29 cells were stimulated with 1 ng/ml IL-1β for 24 hours. CXCL8 production was measured by ELISA and normalized to cellular protein content (measured by BCA protein assay). Bars represent mean ± SEM, n = 2.

Interleukin-6 (IL-6) is another pro-inflammatory cytokine that is produced by intestinal epithelial cells in response to IL-1β stimulation (37). This has been shown to be an indicator of tolerance in macrophages (87), as CXCL8 was shown to be in response to tolerization by P3CK in Caco-2 and NCM460 cells (Figure 4-4 and Figure 4-5, respectively). We investigated whether expression of IL-6 was differentially regulated in epithelial cells as well as in macrophages. This would also show if the lack of CXCL8 response (sometimes seen in response to IL-1β stimulation) was in the IL-1β receptor and signal transduction, or in CXCL8 activation. Foster *et al* used LPS to induce tolerance as measured by IL-6. However as Caco-2 cells are hyporesponsive to LPS (175) due to an absence of TLR4, IL-1β was used to investigate the effect on IL-6 expression (as described in Figure 3-2).

Caco-2 cells were not successfully stimulated or tolerized with IL-1β according to the expression of IL-6 produced per mg protein (Figure 4-10 a)). However, when IL-6 production was represented as a percentage of the mean stimulated amount, the reduction in IL-6 expression by tolerized cells became statistically significant ($P<0.001$) (Figure 4-10 b)). Figure 4-10 highlights the importance of not just relying on one method of results presentation. Epithelial cells have been shown to produce less IL-6 than CXCL8 in response to IL-1β (38). Epithelial cells in these experiments, unlike leukocytes in (87), did not produce a sufficient expression of IL-6 (mean production of 4 pg/mg protein by stimulated cells), as shown in Figure 4-10 a). IL-6 was therefore not a suitable alternative to CXCL8 for measuring the induction of tolerance, as the effect of IL-1β-stimulation was not readily observable.

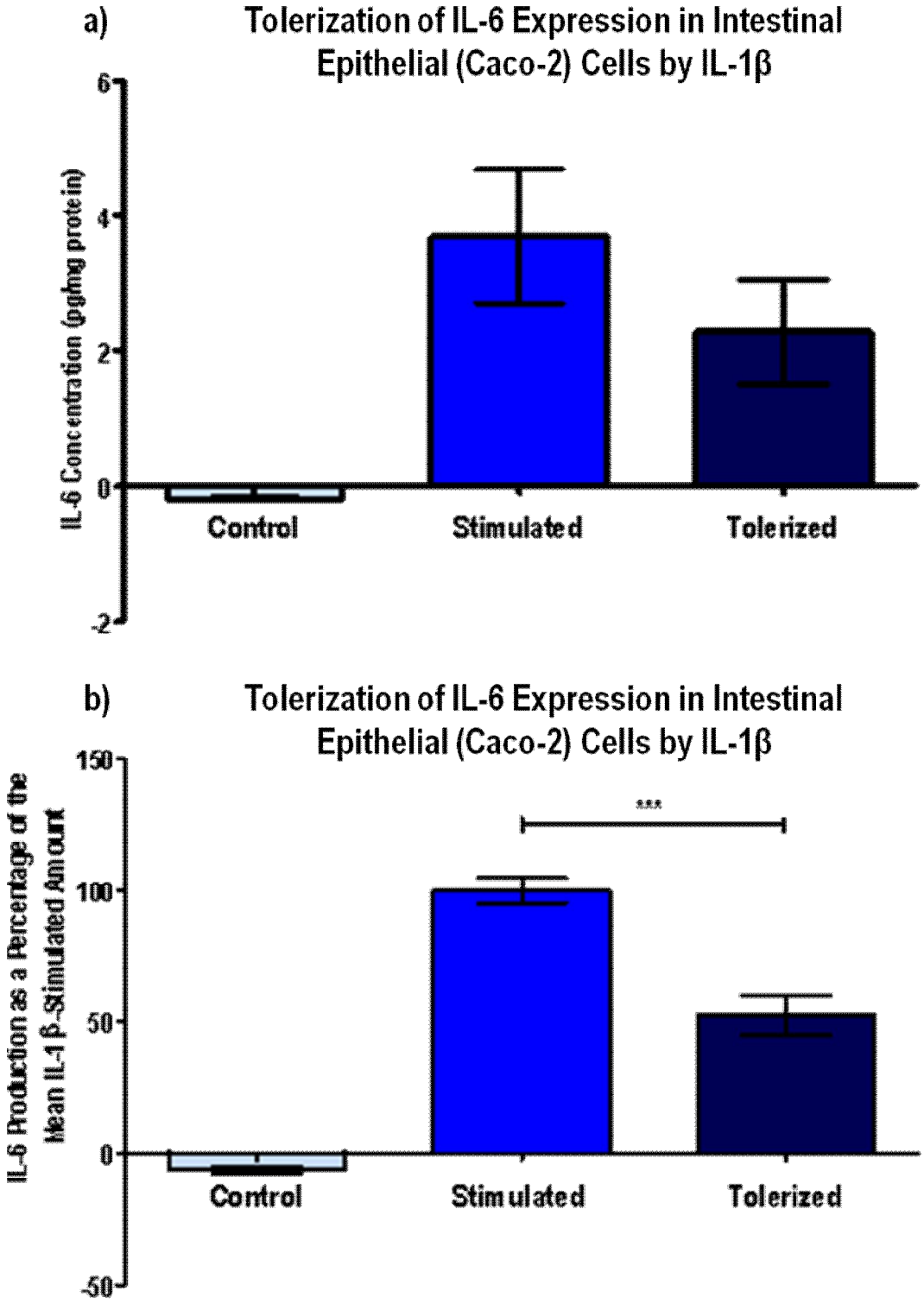

Figure 4-10 Tolerization of IL-6 Expression in Intestinal Epithelial (Caco-2) Cells by IL-1β

Caco-2 cells were stimulated with 1 ng/ml IL-1β for 24 hours and tolerized by a prior stimulation of 1 ng/ml IL-1β 24 hours earlier, as described in Figure 3-2. IL-6 production was measured by ELISA and normalized to cellular protein content (measured by BCA protein assay) (**a**). Multiple experiments were combined by calculating IL-6 production as a percentage of the mean IL-6 production per single stimulation of IL-1β (**b**). Bars represent mean ± SEM, n = 2. Statistical analysis was performed using the Student's *t*-test. *** signifies P<0.001.

Following the failure of IL-1β to induce significant quantities of IL-6 (4 pg/mg protein) or CXCL8 proteins, silencing of transcription was tested for. Silencing of transcription would result in a lack of mRNA translation e.g. by epigenetic silencing via DNA methylation of the CXCL8 gene. Caco-2 cells were stimulated with IL-1β and the total RNA extracted for analysis of CXCL8 production. The optimum concentration of IL-1β required to stimulate CXCL8 mRNA production was therefore determined by production of a dose-response curve similar to the protocol described in Figure 3-1. However, the Caco-2 cells were stimulated with IL-1β for 2 hours not 24 hours. Caco-2 cells were stimulated by serial dilutions of IL-1β (4 – 0 ng/ml) for 2 hours. CXCL8 and β-Actin mRNA production was measured by RT-PCR, as shown in Figure 4-11. Increasing concentrations of IL-1β resulted in increasing amounts of CXCL8 mRNA produced. CXCL8 production plateaued at 1 – 4 ng/ml IL-1β so 1 ng/ml IL-1β, the same concentration as required for optimum CXCL8 protein production, was used for subsequent experiments.

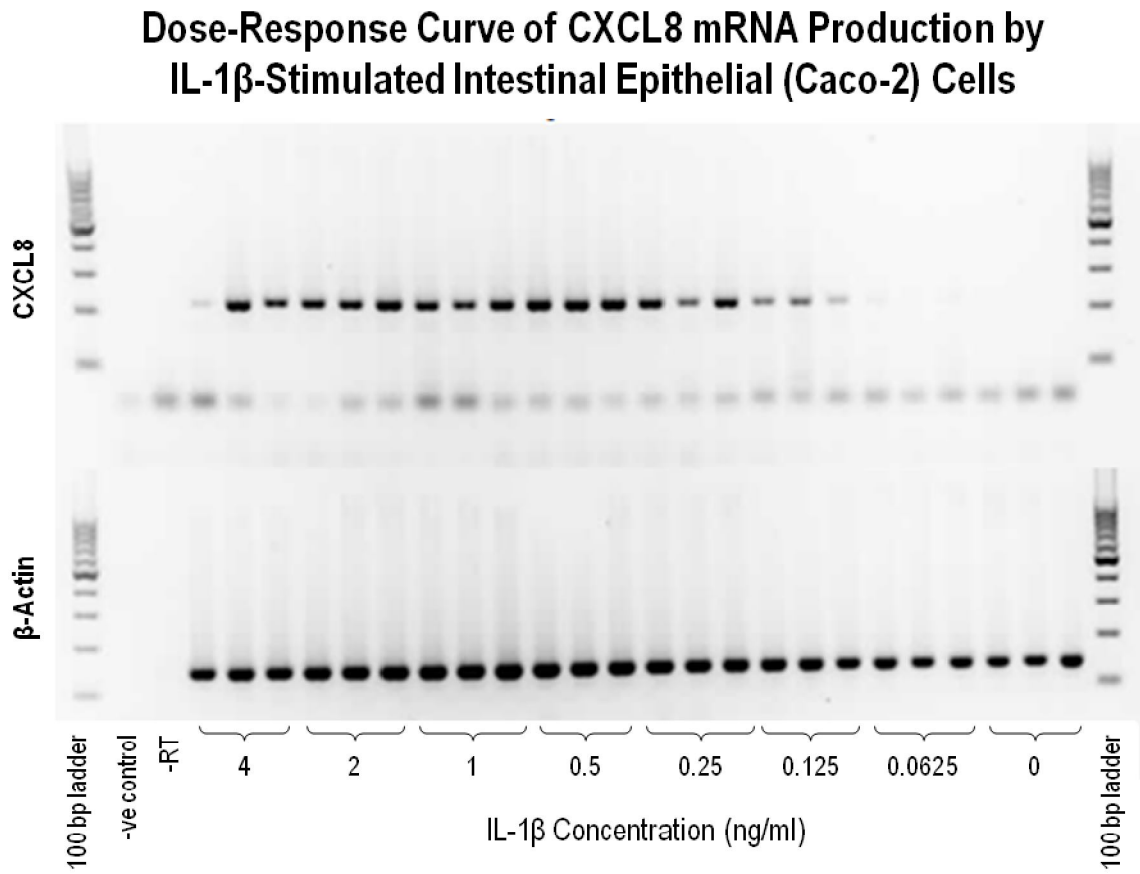

Figure 4-11 Dose-Response Curve of CXCL8 mRNA Production by IL-1β-Stimulated Intestinal Epithelial (Caco-2) Cells

IL-1β was serially diluted by a factor of two (0-4 ng/ml) and used to stimulate Caco-2 cells for 2 hours. CXCL8 mRNA production was measured using RT-PCR with β-Actin as a loading control. –ve and –RT signify negative and "no Reverse Transcriptase" controls, respectively.

By measuring the production of CXCL8 over time (0 – 4 hours), as described in Figure 3-4, 2 hours was determined as the optimum stimulation time for maximum CXCL8 production (Figure 4-12).

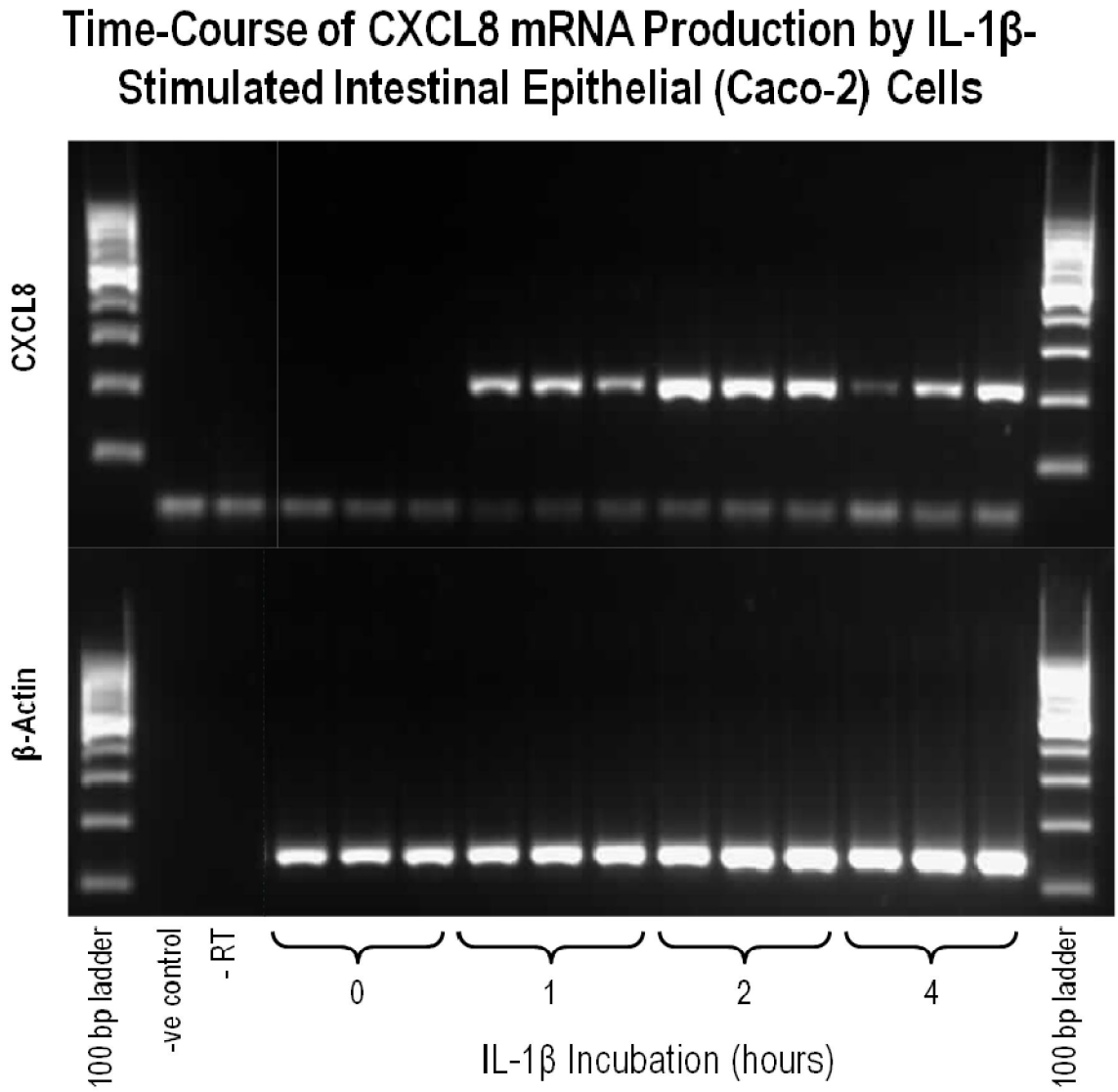

Figure 4-12 Time-Course of CXCL8 mRNA Production by IL-1β-Stimulated Intestinal Epithelial (Caco-2) Cells

Caco-2 cells were stimulated with 1 ng/ml IL-1β for 0 – 4 hours, as described in Figure 3-4. CXCL8 mRNA production was measured by RT-PCR with β-Actin as the loading control. –ve and –RT signify negative and "no Reverse Transcriptase" controls, respectively.

As previously shown in Figure 4-11 and Figure 4-12, IL-1β was capable of stimulating production of CXCL8 mRNA, even if no CXCL8 protein was produced at that time. Therefore, a positive control to examine IL-1β activity was required. The THP1 cell-line is a monocytic cell-line derived from an acute monocytic leukemia. THP1 responds to inflammatory stimulation and produces inflammatory cytokines, such as CXCL8. This cell-line was used as a good model for CXCL8 expression.

We also decided to investigate whether the preparation and storage of IL-1β affected its activity. According to the Gibco manual supplied with recombinant human IL-1β (176), freeze-thaw cycles should be kept to a minimum. However, the advice supplied by Abcam with their human IL1 beta product (ab9617) is to avoid repeated freeze-thaw cycles (177). Therefore, we decided to compare the ability of repeatedly freeze-thawed IL-1β and freshly prepared (no freeze-thaw cycles) IL-1β to stimulate the production of CXCL8 in the THP1 cell-line. As shown in Figure 4-13, repeatedly freeze-thawed IL-1β was unable to stimulate THP1 cells to produce CXCL8, whereas the freshly prepared IL-1β stimulated a statistically significant production of CXCL8. Therefore, all subsequent preparations of IL-1β were aliquoted into small working volumes, frozen only once and any excess discarded.

CXCL8 mRNA was produced, as demonstrated in Figure 4-11 and Figure 4-12 due to an inadvertant fresh preparation of IL-1β

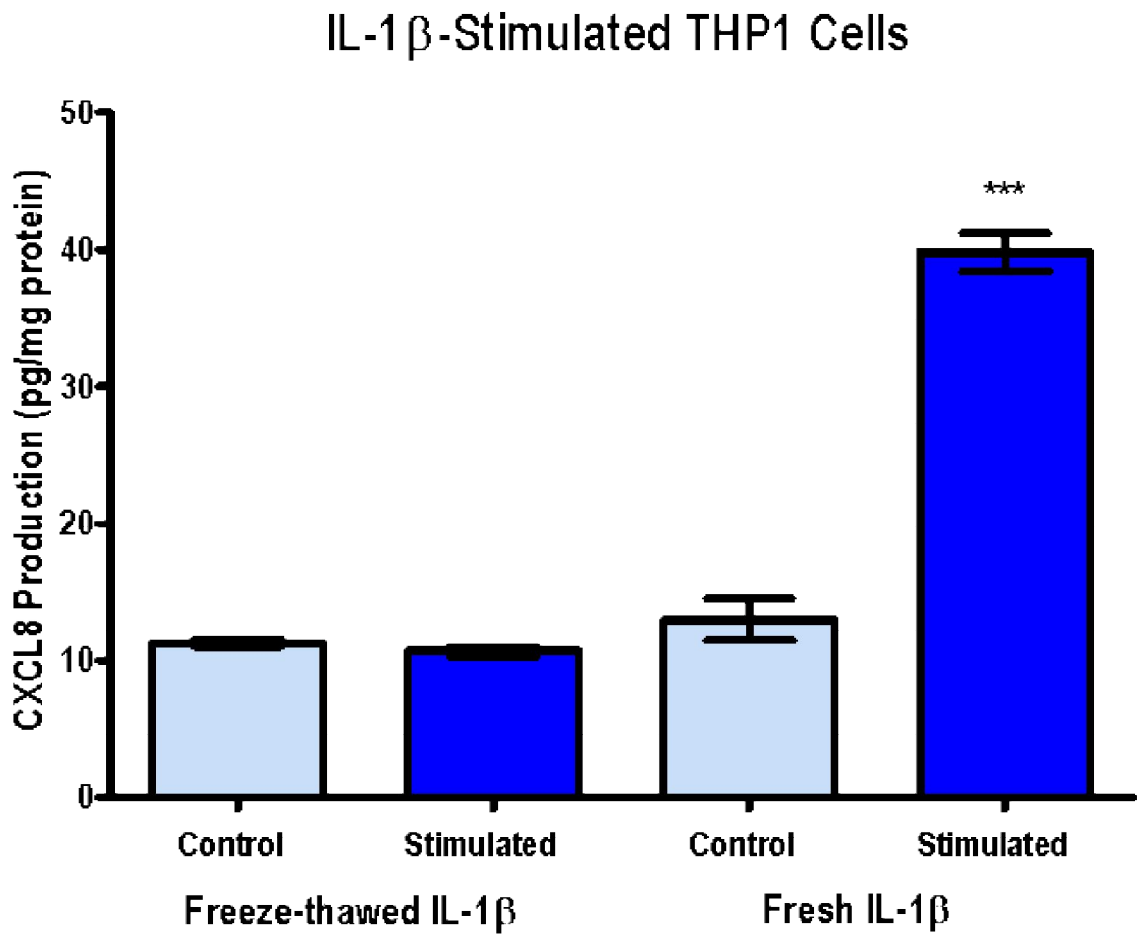

Figure 4-13 IL-1β-Stimulated THP1 Cells

Thp1 cells were stimulated with 1 ng/ml IL-1β for 24 hours prepared from two different sources, one that had been repeatedly freeze-thawed (freeze-thawed IL-1β) and one that had been freshly prepared with no freeze-thaw cycles (fresh IL-1β). CXCL8 production was measured by ELISA and normalized to cellular protein content (measured by BCA protein assay). Bars represent mean ± SEM, n = 2.

4.1.5 Induction of Tolerance to IL-1β

Once the effect of thawing had been identified (Figure 4-13), a fresh IL-1β preparation in each experiment was used to stimulate Caco-2 cells and compared against the absence of stimulation with freeze-thawed stimulant. As shown in Figure 4-14, the use of a fresh IL-1β preparation resulted in a statistically significant increase in the production of CXCL8 ($P<0.001$).

CXCL8 production was also analysed when using different growth medium supplements (178), as described in 3.1.4 and Figure 3-2. Though the CXCL8 production amounts are greater when using +FCS media (medium supplemented with fetal calf serum), the variation in CXCL8 results was less when using the +ITS media (medium supplemented with insulin, transferrin and selenium), thereby giving the statistical significance calculations more confidence.

Upon repetition of the stimulation experiment in both Caco-2 and HT29 cells, the same level of statistical significance was found as before, but the individual values varied between different preparations (Figure 4-14 and Figure 4-15). Therefore, it was decided that the CXCL8 production amount should be standardized between similar experiments by converting each CXCL8 production value into a percentage of the mean IL-1β-stimulated production (Figure 4-16).

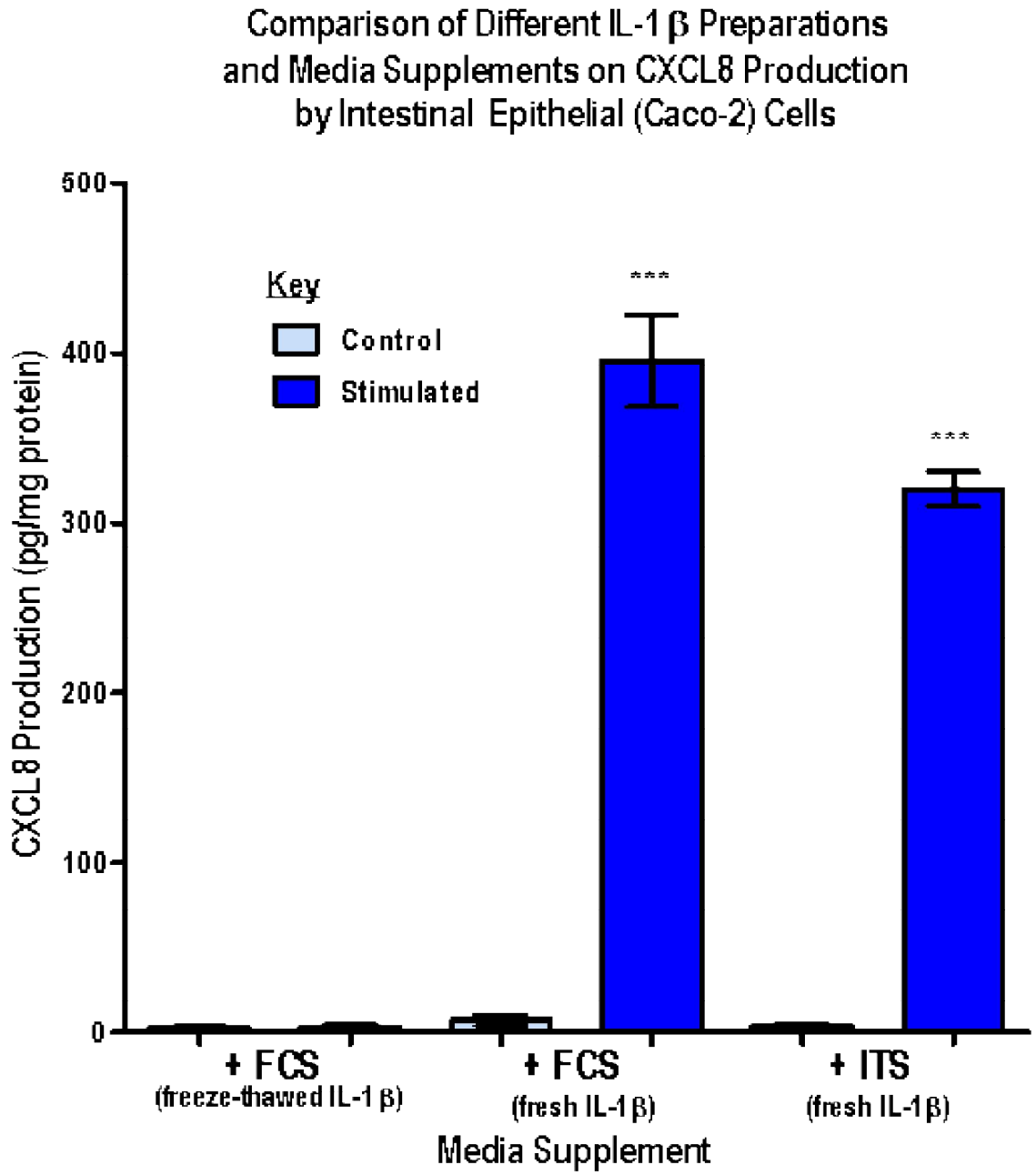

Figure 4-14 Comparison of Different IL -1β Preparations and Media Supplements on CXCL8 Production by Intestinal Epithelial (Caco-2) Cells

Caco-2 cells were stimulated with 1 ng/ml IL-1β for 24 hours, diluted in +FCS media or +ITS media (as described in 3.1.1). CXCL8 production was measured by ELISA and normalized to cellular protein content (measured by BCA protein assay). Bars represent mean ± SEM, n = 2. Statistical analysis was performed using the Student's *t*-test. *** signifies P<0.001.

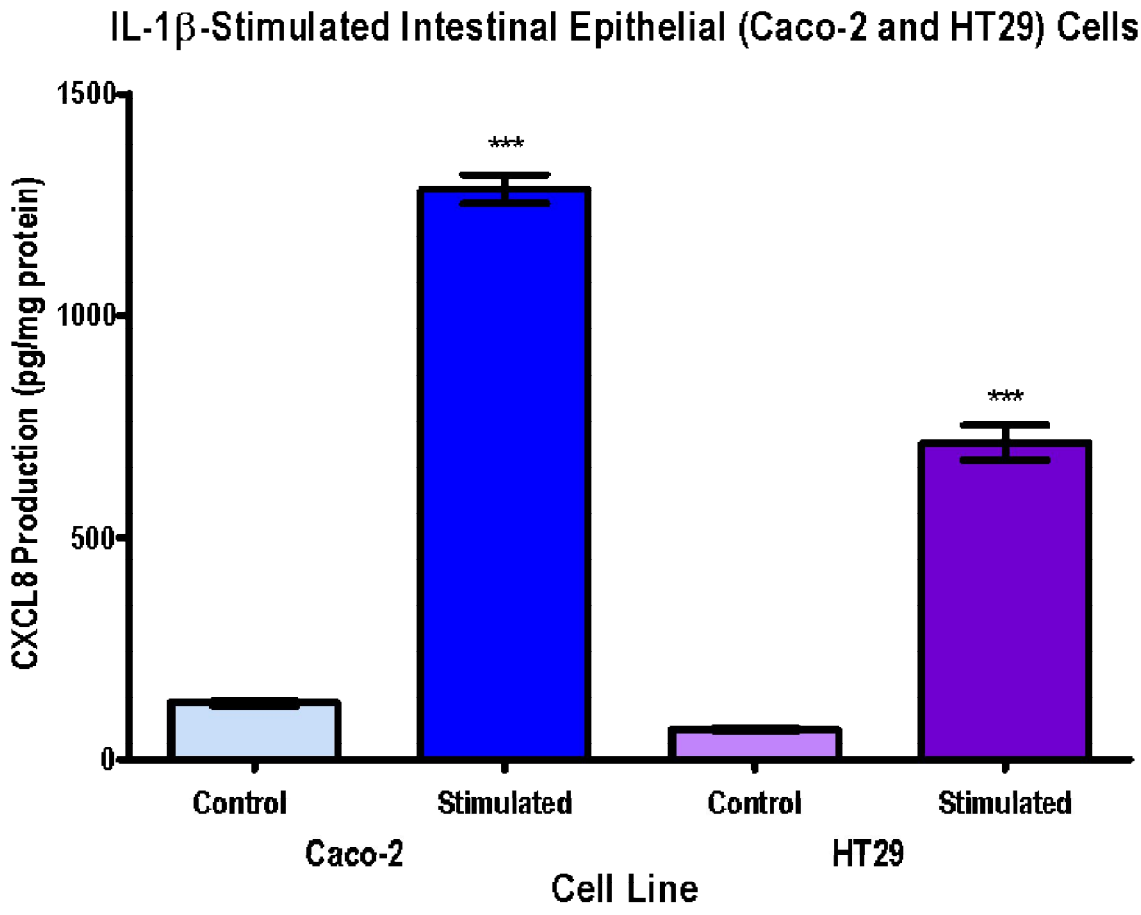

Figure 4-15 IL-1β-Stimulated Intestinal Epithelial (Caco-2 and HT29) Cells

Caco-2 and HT29 cells were stimulated with 1 ng/ml IL-1β for 24 hours. CXCL8 production was measured by ELISA and normalized to cellular protein content (measured by BCA protein assay). Bars represent mean ± SEM, n = 1. Statistical analysis was performed using the Student's *t*-test. *** signifies P<0.001.

Tolerance was established by stimulating one set of Caco-2 cells with 1 ng/ml IL-1β for 24 hours, and pre-stimulating another set of cells twice with 1 ng/ml IL-1β for 24 hours followed by another stimulation with 1 ng/ml IL-1β for 24 hours (as described in Figure 3-2). The conditioned media was collected and the amount of CXCL8 produced measured by ELISA. This was normalized to the total cellular protein content, as measured by BCA protein assay. As mentioned previously, the CXCL8 production results were converted into a percentage of the mean IL-1β-stimulated CXCL8 production (Figure 4-16), in order to combine multiple experiments. Caco-2 cells stimulated once by IL-1β express the greatest production of CXCL8 whilst the tolerized cells express a reduced production of CXCL8, ~50% of the stimulated expression level. The reduction in CXCL8 production by tolerized cells compared to stimulated cells was statistically significant ($P<0.001$), as calculated by Student's *t* test. Therefore, tolerance induction is a statistically significant and reproducible effect.

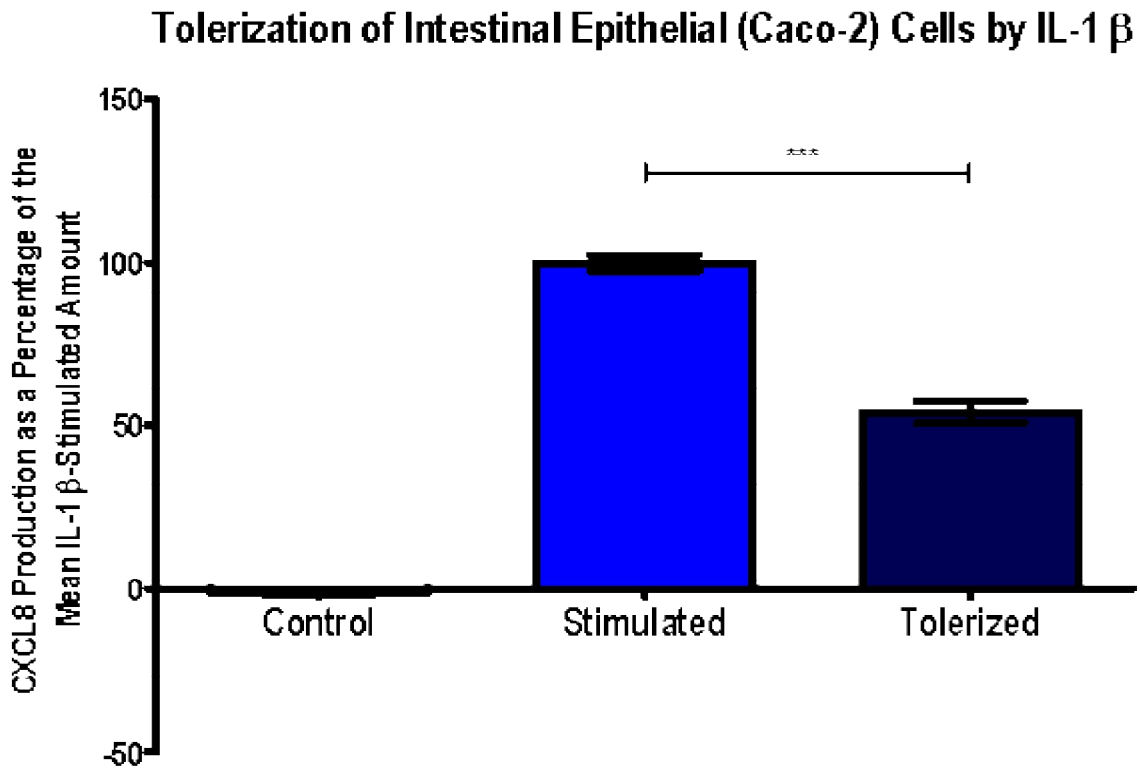

Figure 4-16 Tolerization of Intestinal Epithelial (Caco-2) Cells by IL-1β

Caco-2 cells were stimulated with 1 ng/ml IL-1β for 24 hours and tolerized by a prior stimulation of 1 ng/ml IL-1β 24 hours earlier, as described in Figure 3-2. CXCL8 production was measured by ELISA and normalized to cellular protein content (measured by BCA protein assay). Multiple experiments were combined by calculating CXCL8 production as a percentage of the mean CXCL8 production per single stimulation of IL-1β. Bars represent mean ± SEM, n = 8. Statistical analysis was performed using the Student's *t*-test. *** signifies P<0.001.

To address criticism that CXCL8 mRNA may still be present from IL-1β-pre-stimulation when the second stimulation was given, another condition was added to the tolerization experiments, that of pre-stimulated only cells. Pre-stimulated cells were stimulated with 1 ng/ml IL-1β for 24 hours 48 hours prior to sample collection (as described in Figure 3-3). The conditioned media was washed out with PBS to remove all traces of IL-1β and fresh unstimulated media was added to the cells for the final 24 hours before sample collection. Stimulated and tolerized cells were stimulated as previously described in Figure 3-2. The conditioned media was collected and the amount of CXCL8 produced measured by ELISA. This was normalized to the total cellular protein content, as measured by BCA protein assay. Figure 4-17 displays the production of CXCL8 in two forms, as the normalized values in pg/mg protein (top graph) and as percentages of the mean stimulated amount (bottom graph). The production of CXCL8 in stimulated and tolerized cells was similar in both Figure 4-16 and Figure 4-17, both figures showing a statistically signficant ~50% reduction in CXCL8 expression in tolerized cells as compared to stimulated cells ($P<0.001$). As shown in Figure 4-17, the amount of CXCL8 expressed by pre-stimulated cells was extremely low and though greater than in control cells, this was not statistically significant. Therefore the changes induced by pre-stimulating the cells were not due to CXCL8 still being produced by the first IL-1β-stimulation.

A comparison of the top and bottom graphs of Figure 4-17 shows that expressing the values as percentages does not alter the trend of CXCL8 production. The range and variance of the values in each condition is reduced, as illustrated by the smaller error bars in the bottom graph of Figure 4-17. As the production of CXCL8 in pre-stimulated cells is not statistically greater than that of the control cells, it indicates that CXCL8 production has ceased by the time that the tolerized cells receive their second IL-1β-stimulation. Tolerance is therefore a true effect and the reduction in CXCL8 production is not the tail-end of the original stimulation.

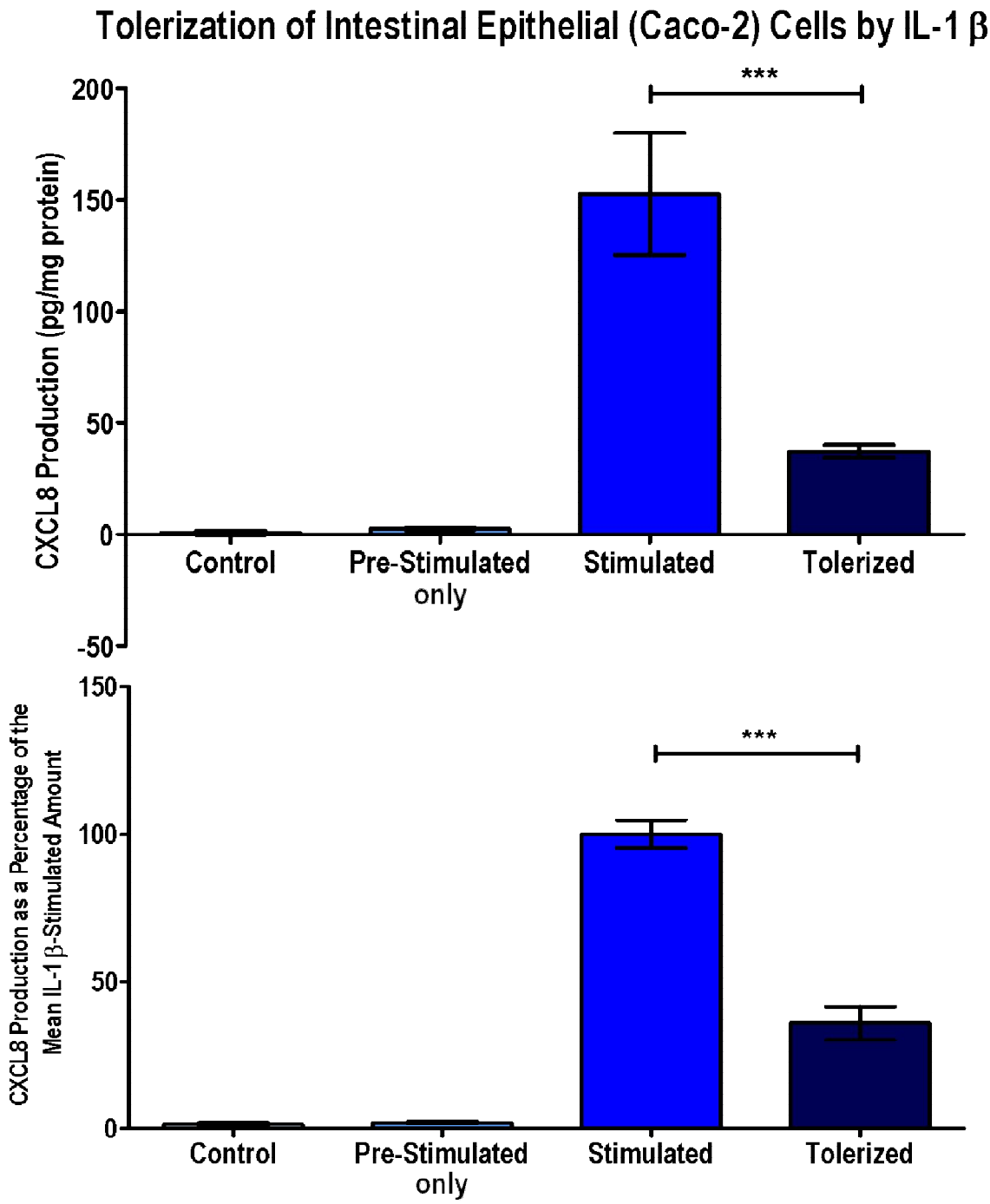

Figure 4-17 Tolerization of Intestinal Epithelial (Caco-2) Cells by IL-1β

Caco-2 cells were pre-stimulated with 1 ng/ml IL-1β for 24 hours before the cells were washed with PBS and the conditioned media replaced with fresh media. Caco-2 cells were stimulated with 1 ng/ml IL-1β for 24 hours and tolerized by a prior stimulation of 1 ng/ml IL-1β 24 hours earlier, as described in Figure 3-3. CXCL8 production was measured by ELISA and normalized to cellular protein content (measured by BCA protein assay). The top graph is of the normalized CXCL8 values in pg/mg protein whilst the bottom graph represents the values as percentages. Multiple experiments were combined by calculating CXCL8 production as a percentage of the mean CXCL8 production per single stimulation of IL-1β. Bars represent mean ± SEM, n = 4. Statistical analysis was performed using the Student's *t*-test. *** signifies P<0.001.

Tolerance was also established at transcription by stimulating Caco-2 cells with 1 ng/ml IL-1β for 24 hours followed by a second stimulation by IL-1β for 2 hours before extracting total RNA and measuring CXCL8 and β-Actin mRNA production by RT-PCR (Figure 3-5). CXCL8 mRNA was produced by Caco-2 cells with both single and double stimulations of IL-1β. However, although production of CXCL8 appears to be lower in the double IL-1β-stimulated cells (Figure 4-18), the exact difference was not possible to determine as RT-PCR is a qualitative technique. Thus, the production of CXCL8 cannot be proven to be statistically different between single and double stimulations of IL-1β.

Quantitative PCR (qPCR) produces quantitative numerical results that can be statistically analysed and hence verify that repeated stimulation of Caco-2 cells with IL-1β induces tolerization of CXCL8 at the level of mRNA as well as protein, but because we had quantitative protein assays that showed statistical differences, we did not undertake the qPCR experiments.

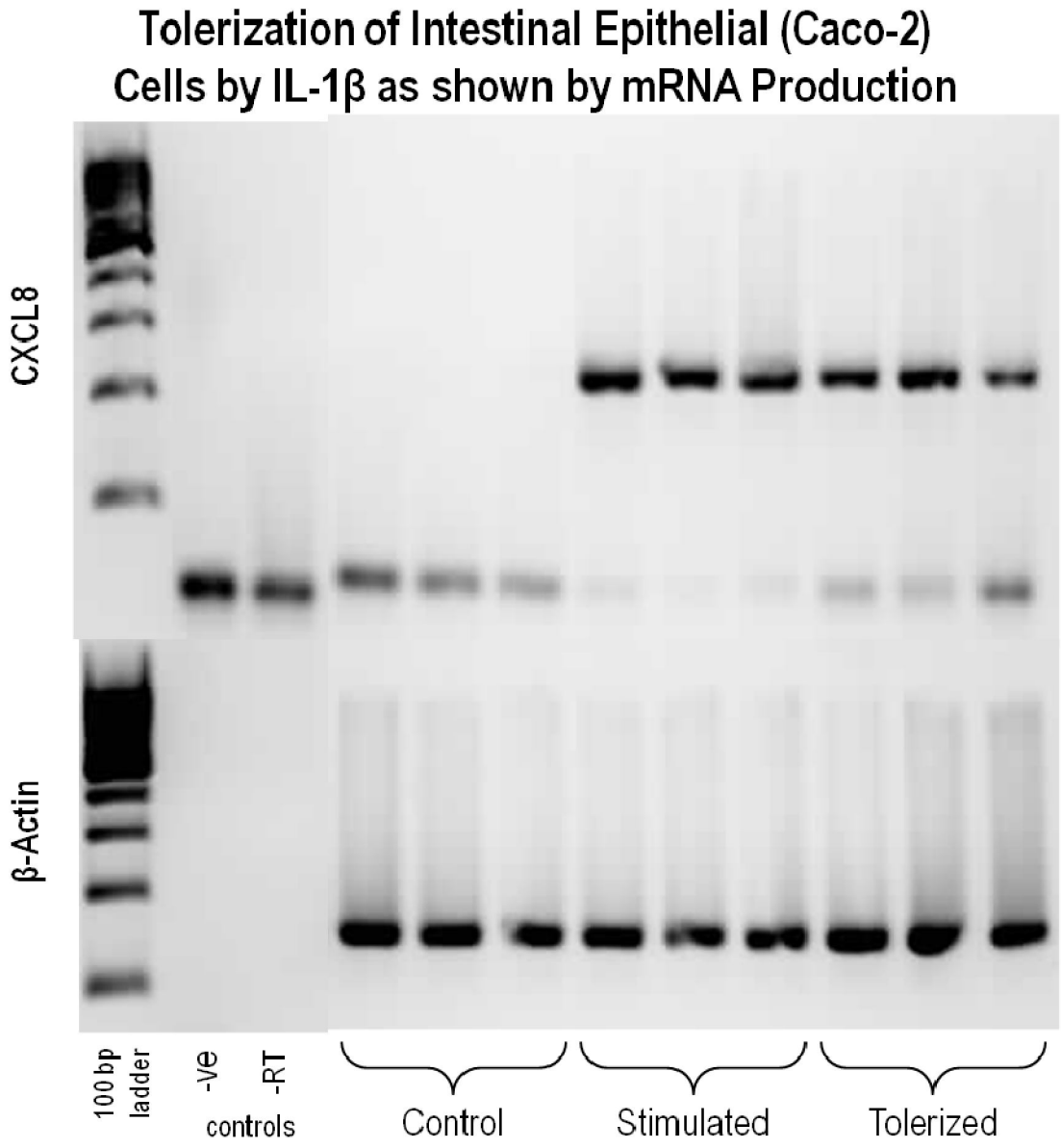

Figure 4-18 Tolerization of Intestinal Epithelial (Caco-2) Cells by IL-1β as shown by mRNA Production

Caco-2 cells were stimulated with 1 ng/ml IL-1β for 2 hours (stimulated) and tolerized by a prior stimulation of IL-1β, 24 hours earlier, as described in Figure 3-5. CXCL8 mRNA production was measured by RT-PCR with β-Actin as the loading control. –ve and –RT signify negative and "no Reverse Transcriptase" controls, respectively.

To further address a criticism that the effects of a pre-stimulation of intestinal epithelial cells are not finished by the second stimulation and is therefore responsible for the reduction in CXCL8 expression in tolerized cells; the expression of several inflammatory and intestine-specific genes was monitored over 48 hours by qPCR. Total RNA was extracted from IL-1β-stimulated Caco-2 cells using TRIzol®, incubated with DNase I to remove any residual DNA and cDNA synthesized. The amount of cDNA present in each sample was measured using qPCR and the primers described in Table 3-7. Each target was normalized to β-Actin and again to the mean 0 hour value for each respective gene. As shown in Figure 4-19, the expression profiles of IL-6, CXCL8, IL-10, CCL2 (or MCP-1, monocyte chemoattractant protein 1), DEFB4A (or BD-2, human β-defensin 2) and TNF are plotted as fold changes in expression over the 48 hours of IL-1β-stimulation. IL-6 and CXCL8 both show maximal expression at 2 – 4 hours after IL-1β-stimulation, with a subsequent decrease back to levels similar to that at 0 hours by 24 hours, which is before the second stimulation is given. There is a second peak in expression of CXCL8 2 – 4 hours after the second IL-1β-stimulation (26 – 28 hours), though this is smaller than the first stimulation, in agreement with the tolerizing effect of the first stimulation observed in the experiments measuring protein expression (Figure 4-17). Expression decreases back to background levels again 24 hours after the stimulus is applied. These results are consistent with the protein data shown in Figure 4-16 and Figure 4-17. TNF shows similar activity to IL-6 and CXCL8, though the peaks in expression are of similar magnitude. The amounts of TNF cDNA measured were often below the detection limit with only one value being obtained for the 1 and 2 hour time points and none at all for 0 hours. TNF fold changes are therefore normalized to the mean 24 hour value. IL-10 expression shows a small increase at 1 hour, followed by a decrease to almost background levels and a subsequent increase again at 8 hours. A decrease back to background levels occurs again with a smaller peak at 28 hours. As IL-10 is an anti-inflammatory cytokine, it is not unexpected that it shows a different expression profile to the pro-inflammatory cytokines IL-8, CXCL8 and

TNF. Neither CCL2 nor DEFB4A show signs of being tolerized, as the second IL-1β-stimulation causes a peak in expression that is larger than the peak after the first stimulation.

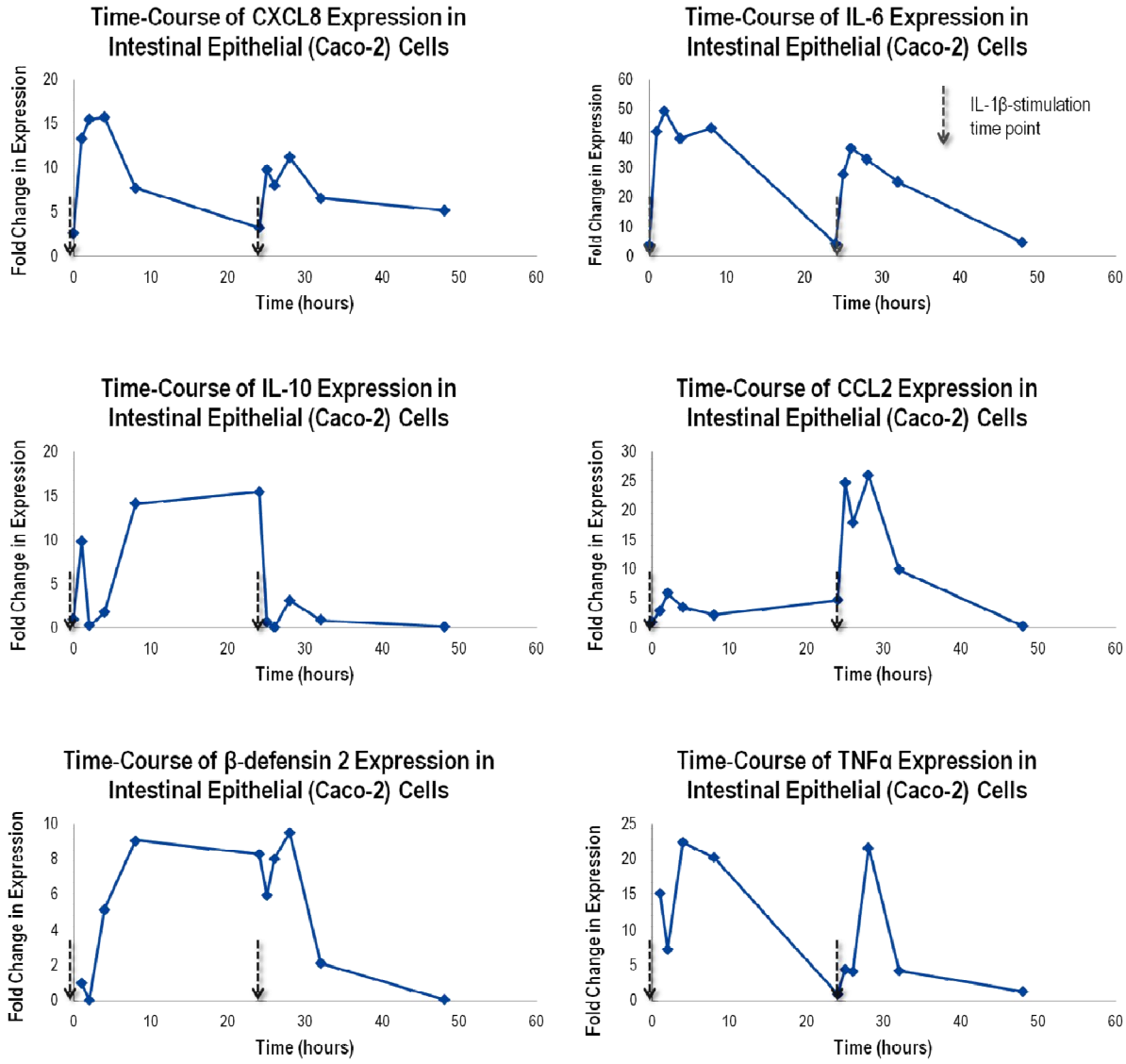

Figure 4-19 Time-Course of Tolerizable and Non-Tolerizable Gene Expression in Intesinal Epithelial (Caco-2) Cells

Caco-2 cells were stimulated twice with 1 ng/ml IL-1β for 24 hours each, as described in Figure 3-6, and illustrated with dashed grey arrows. Cell samples were collected at 0, 1, 2, 4, 8, 24, 25, 26, 28, 32 and 48 hours using TRIzol®. Total RNA was extracted, cDNA synthesized and measured by qPCR. The amounts of IL-6, CXCL8, IL-10, CCL2, DEFB4A and TNF were normalized to ACTB and analysed using the $\Delta\Delta C_T$ method. The expression levels of each gene were plotted as fold changes normalized to the fold change value at 0 hours against time. Error bars are omitted for clarity. n = 4

4.2 Establishment of Cross-Tolerance

We have demonstrated that intestinal epithelial cells can be tolerized to the TLR2 agonist P3CK and to the pro-inflammatory cytokine IL-1β. P3CK is representative of a physiological stimulant (lipoprotein component of the microbiotal or pathogenic bacterial cell wall) and IL-1β is a cytokine overexpressed during inflammation in general, and in IBD patients in particular. As both stimulants are present in the inflamed intestinal lumen we decided to investigate the effect on CXCL8 expression of pre-stimulating the intestinal epithelial cells with a different agent to the second stimulation. In particular, we wished to ascertain if constant stimulation by a bacterial product reduced the effect of IL-1β stimulation. This represents a reductionist model of the luminal bacteria on the response of the epithelium to inflammatory stimuli. Caco-2 cells were pre-stimulated with P3CK rather than IL-1β as commensal bacteria are constantly present in the intestine from shortly after birth, whereas IL-1β expression is dependent upon the circumstances e.g. pathogens, injury, disease state etc. The microbiota, which contains products such as bacterial lipoprotein, is required for the correct development of tolerance. This has been shown by the susceptibility to IBD of germ-free mice. Additionally, these mice exhibit intestinal immunological defects and immunomodulatory deficiencies e.g. altered T cell development particularly of Treg cells (179), a lack of bacterially-generated ATP resulting in a lack of anti-inflammatory IL-17 (180), a lack of commensal bacterial DNA which cannot induce protective signalling through TLR9 (181). Therefore, as bacteria are required for the correct development of tolerance, we used P3CK to pre-stimulate the Caco-2 cells, simulating the microbiota's ability to tolerize the epithelium. We recognize that other mechanisms are possible in a multi-cell intestine.

The experimental method for inducing tolerance described in Figure 3-2 in Caco-2 cells was modified to investigate whether epithelial cells can be cross-tolerized to different pro-inflammatory

stimuli. This modification was to pre-stimulate the Caco-2 cells with P3CK before the stimulation with IL-1β (Figure 3-2). This model is a simple representation of the microbiota tolerizing the intestinal epithelial cells to subsequent stimulations by pro-inflammatory cytokines e.g. IL-1β. 48 hours prior to sample collection, the tolerized and cross-tolerized cells were pre-stimulated with 1 ng/ml IL-1β and 25 μg/ml P3CK, respectively for 24 hours. 24 hours prior to sample collection, both tolerized and cross-tolerized cells, in addition to the stimulated cells, were further stimulated with 1 ng/ml IL-1β for another 24 hours. All CXCL8 production values were converted to a percentage of the mean IL-1β-stimulated production of CXCL8.

The production of CXCL8 was greatest by the cells that were stimulated once by IL-1β and was decreased to 50% by the IL-1β-only-tolerized cells (Figure 4-20). The cross-tolerized cells (cells pre-stimulated with P3CK) expressed a statistically significant increase in CXCL8 production than the cells tolerized with IL-1β alone ($P<0.001$), but less than the cells that were only stimulated once with IL-1β (78%) (Figure 4-20). This was a statistically significant reduction, as calculated by Student's *t*-test ($P<0.001$), thus bacterial products can cause intestinal epithelial cells to be hyporesponsive to IL-1β stimulation.

The CXCL8 values normalized to the total protein content are plotted in Figure 4-21. CXCL8 production is greatest in stimulated cells, reduced to approximately half the amount in tolerized cells and reduced in cross-tolerized cells, but to about three-quarters of the amount of stimulated cells. This is the same effect seen in Figure 4-20, but the range of values is larger, as shown by the larger error bars and the reduction in statistical significance between tolerized and cross-tolerized cells from $P<0.001$ to $P<0.01$.

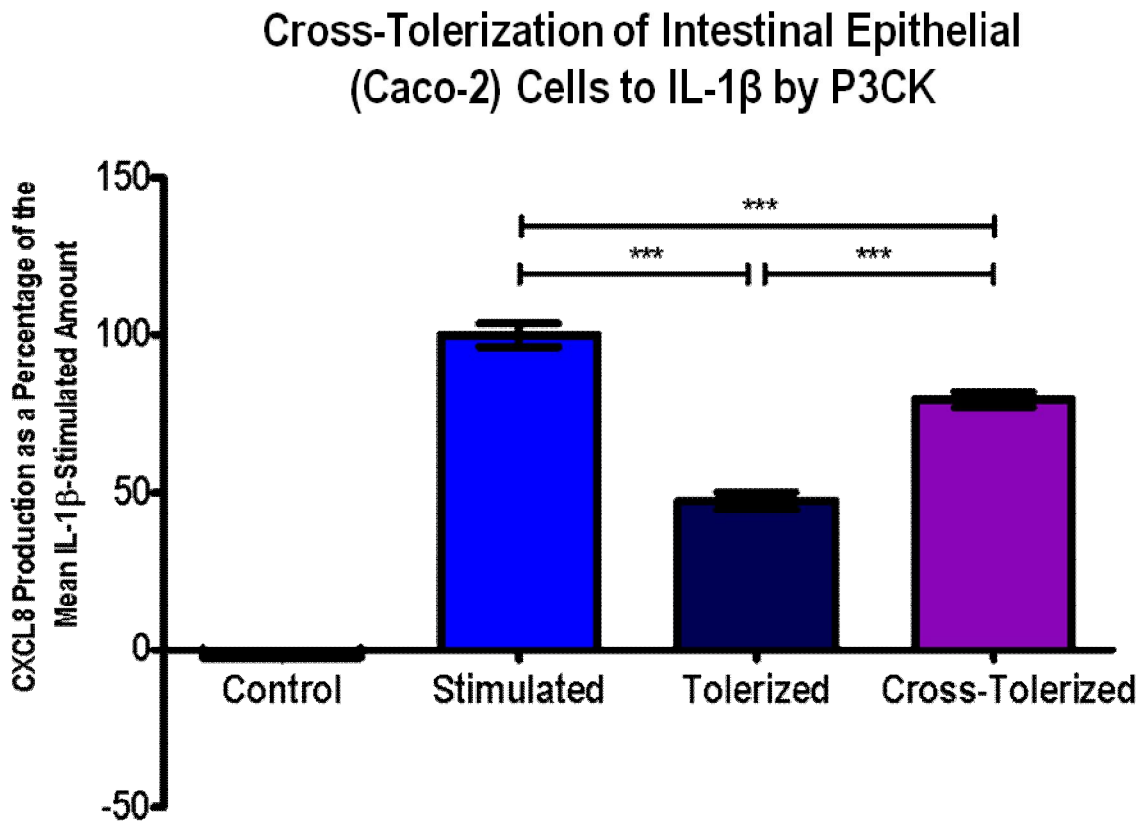

Figure 4-20 Cross-Tolerization of Intestinal Epithelial (Caco-2) Cells to IL-1β by P3CK

Caco-2 cells were stimulated with 1 ng/ml IL-1β for 24 hours and tolerized by a prior stimulation of 1 ng/ml IL-1β 24 hours earlier, as described in Figure 3-2. Cross-tolerance was established by pre-stimulating Caco-2 cells with 25 µg/ml P3CK for 24 hours before stimulating them with 1 ng/ml IL-1β for another 24 hours. CXCL8 production was measured by ELISA and normalized to cellular protein content (measured by BCA protein assay). Multiple experiments were combined by calculating CXCL8 production as a percentage of the mean CXCL8 production per single stimulation of IL-1β. Bars represent mean ± SEM, n = 5. Statistical analysis was performed using the Student's *t*-test. *** signifies P<0.001.

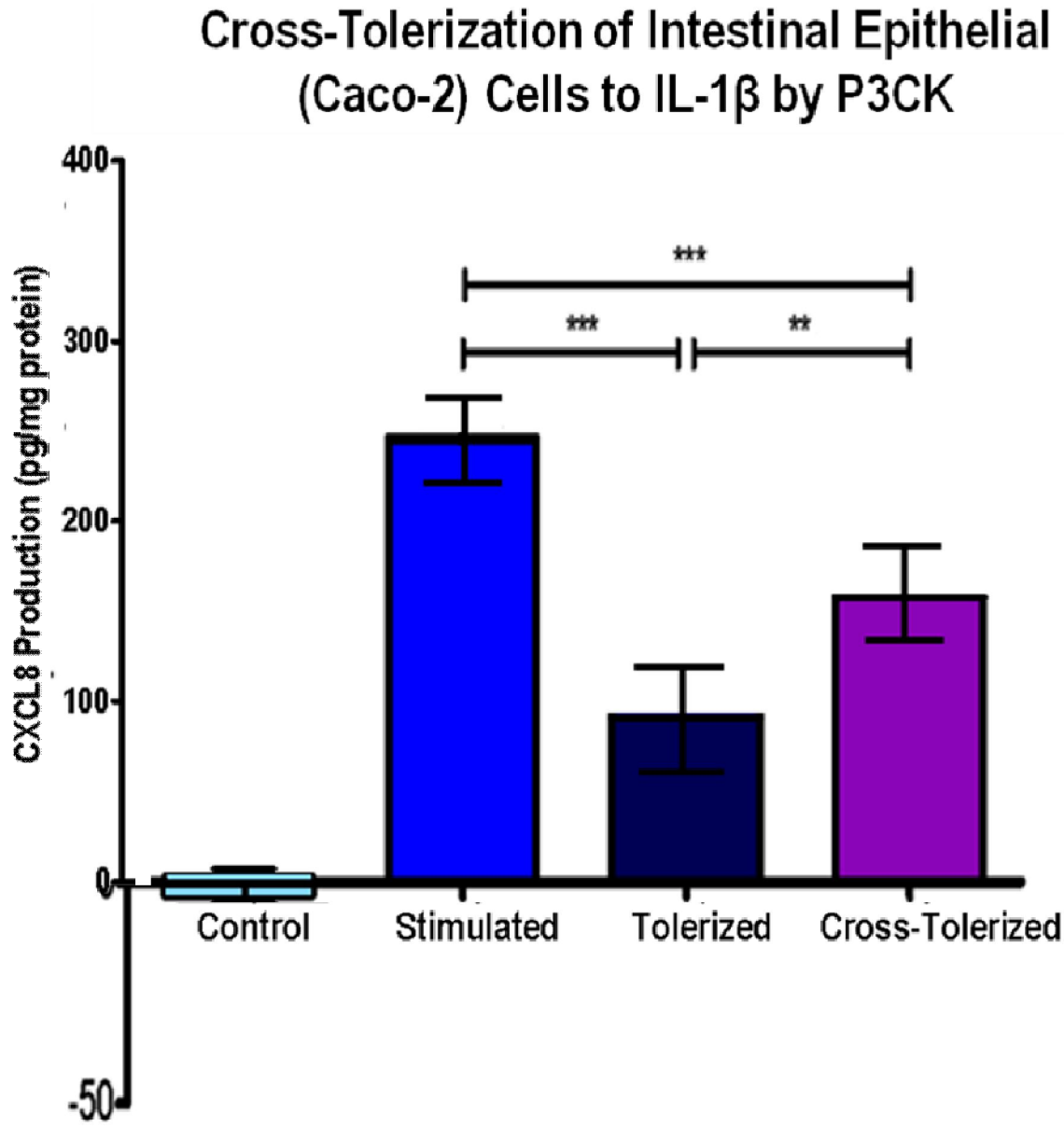

Figure 4-21 Cross-Tolerization of Intestinal Epithelial (Caco-2) Cells to IL-1β by P3CK

Caco-2 cells were stimulated with 1 ng/ml IL-1β for 24 hours and tolerized by a prior stimulation of 1 ng/ml IL-1β 24 hours earlier, as described in Figure 3-2. Cross-tolerance was established by pre-stimulating Caco-2 cells with 25 µg/ml P3CK for 24 hours before stimulating them with 1 ng/ml IL-1β for another 24 hours. CXCL8 production was measured by ELISA and normalized to cellular protein content (measured by BCA protein assay). Bars represent mean ± SEM, n = 5. Statistical analysis was performed using the Student's *t*-test. ** and *** signifies $P<0.01$ and <0.001, respectively.

4.3 Conclusions

In conclusion, both P3CK and IL-1β stimulate and tolerize Caco-2 cells. NCM460 cells are tolerized by P3CK, but are unresponsive to stimulation by IL-1β. Tolerance is therefore a true and reproducible effect in intestinal epithelial cells. Tolerance to P3CK in NCM460 cells demonstrates that tolerance is not a phenomenon seen only in malignant cells. Due to the greater stimulation of Caco-2 cells by IL-1β than NCM460 cells by P3CK, all further experiments examining the underlying mechanisms of tolerance regulation were designed using Caco-2 cells and IL-1β. This is because the greater the CXCL8 production, the easier it is to induce tolerance and achieve a statistically significant difference. It was also more economical to use IL-1β than P3CK as it is a more potent agonist (1 ng/ml IL-1β produces more CXCL8 than 25 µg/ml P3CK). The ability of P3CK to cross-tolerize Caco-2 cells to IL-1β represents an ability of the microbiota to tolerize the epithelium to a pro-inflammatory stimulus.

The combination of ELISA data from pre-stimulated only Caco-2 cells and the qPCR data show that the induction of CXCL8 is finished before the second IL-1β-stimulation and therefore the reduction in CXCL8 expression seen in tolerized cells is due to tolerance and not the end of a previous stimulation.

5 Histone Methylation and its Effect on Tolerance in Intestinal Epithelial Cells

Epigenetic involvement in tolerance in macrophages has been proposed by several groups (81, 87), but has not been investigated in epithelial cells. This can be examined by modifying the existing epigenetic features and measuring their effect on tolerance. For example, a histone lysine methyltransferase inhibitor will decrease the level of methylation present at a particular epigenetic locus. If this then causes a change in the level of CXCL8 produced when the cells are stimulated the second time with IL-1β, as compared to when the inhibitor is not present, epigenetics has an involvement in tolerance

The effect of epigenetic modifying enzyme inhibitors, in this work, was focussed on three specific epigenetic markers: H3K4me3, H3K9me3 and H3K27me3. Tri-methylated residues rather than mono- or di-methylated residues are most likely to be affected by epigenetic inhibitors, as they have the greatest number of methyl groups. A methyltransferase inhibitor should prevent the formation of tri-methylated residues as a residue needs to be mono- and then di-methylated first before it can be tri-methylated. Conversely, demethylase inhibitors will prevent the conversion of tri-methylated residues to di-methylated residues. However, inhibition of the other demethylases should increase the substrates available for the tri-methyl-methyltransferases thus promoting the formation of tri-methylated residues. If a study of epigenetic inhibition were to focus on mono- or di-methylated residues, it is possible that no change would be seen as an increase in di-methylation would act as a substrate for di-methyl-demethylases and tri-methyl-methyltransferases.

H3K4me3, H3K9me3 and H3K27me3 affect transcription and are therefore likely to be involved in regulation of tolerance that is based on gene regulation. In most cell-types under the majority of circumstances, H3K4me3 is associated with transcriptional activation whilst both H3K9me3 and H3K27me3 are associated with transcriptional repression (122). Although other epigenetic markers may be involved in tolerance and the inhibitors chosen may affect multiple markers, it is the most efficient use of time and resources to concentrate on these three, as they were used to examine the principle that histone methylation might affect tolerance. It was not our aim to examine every aspect of the molecular mechanisms underlying tolerance, but to establish the principle that histone methylation is an integral part of the regulatory system.

5.1 Inhibition of Histone Methyltransferases

Evidence for the involvement of epigenetics can be determined by altering the activity of epigenetic enzymes using small molecule inhibitors. A range of histone methyltransferase and histone demethylase inhibitors was used to alter the methylation level of particular Histone H3 lysine residues. Table 5-1 lists the epigenetic inhibitors used for this research with the enzyme specificity and the predicted effect on particular Histone H3 lysine residues. As inhibitor specificity is determined *in vitro* using purified enzymes and synthetic histone proteins, it is possible that the expected effect on relative histone methylation amounts will not be produced *in vivo* in intestinal epithelial cells.

Two inhibitors were chosen for activity against histone methyltransferases and histone demethylases. One of the inhibitors for each class of enzymes had a broad range of activity, whilst the other inhibitor had specific activity against one enzyme or range of enzymes for one

particular histone H3 residue. Though SAH, for example, was predicted to affect many histone methyltransferases, its main effect was predicted to be on Histone H3K27me3. Chaetocin, as a specific inhibitor of SU(VAR)3-9, which is a K9-specific histone methyltransferase, is predicted to effect the methylation level of H3K9me3 most. Both demethylase inhibitors, 2,4-PDCA and pargyline hydrochloride, are predicted to affect the levels of H3K4me3, though pargyline hydrochloride should also alter the level of H3K9me3.

Inhibitor	Enzyme	Enzyme Specificity	Potential Histone Residue Affected
S-adenosyl-L-homocysteine (SAH)	Methyltransferase	Broad	H3K27me3 ↓, (H3K9me3 ↓, H3K4me3 ↓)
Chaetocin	Methyltransferase	H3K9-specific	H3K9me3 ↓
Pargyline hydrochloride	Demethylase	Monoamine oxidase-specific, broad demethylase range	H3K4me3 ↑, H3K9me3 ↑
2,4-pyridinedicarboxylic acid (2,4-PDCA)	Demethylase	H3K4-specific	H3K4me3 ↑

Table 5-1 Table of Epigenetic Inhibitors and Their Predicted Effect on Histone H3 Lysine Residues

A table listing the small molecule inhibitors of histone methyltransferases and histone demethylases used in this research with their enzyme specificity and predicted effect on Histone H3 lysine residues from a variety of cell lines.

5.1.1 S-adenosyl-L-homocysteine (SAH)

A literature search was performed to find existing histone methyltransferase inhibitors. This was achieved by performing a web-search for commercially available inhibitors, as well as searching PubMed for published data on histone methyltransferases. Non-specific inhibitors were prioritised as the particular enzymes, as well as the specific histone methylation marks themselves, are unknown. *S*-adenosyl-L-homocysteine (SAH) (Figure 5-1) was chosen as it is a non-specific inhibitor of multiple histone methyltransferases. It is also the product of *S*-adenosyl-methionine (SAM)-dependent methylation of DNA, RNA and proteins and therefore acts as a natural competitor and competitive inhibitor of methyltransferases (182).

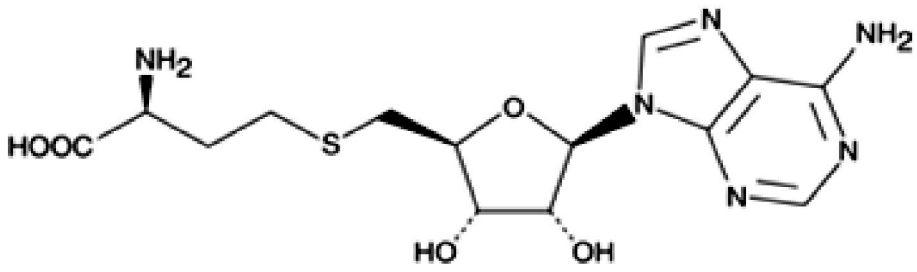

Figure 5-1 Structure of *S*-adenosyl-L-homocysteine (SAH)

The 3D chemical structure of *S*-adenosyl-L-homocysteine (taken as a screenshot from the Cayman Chemical website (182)).

Intestinal epithelial cells were incubated with 0, 1 or 100 μM SAH for 72 hours and the histones extracted for Western Blot analysis of methylation levels. As shown in Figure 5-2, both H3K9me3 and H3K27me3 increased in methylation levels as the concentration of SAH increases. H3K9me3 increased by 2.2 fold and H3K27me3 by 1.6 fold. This was contrary to expectation as SAH is a histone methyltransferase inhibitor so it would be expected that as the level of SAH increases, the amount of histone methylation decreases. Whilst this was surprising, it was reproducible (Figure 5-3) and we have a possible explanation: SAH may degrade *in vivo* to adenosine and

homocysteine and increase the SAM/SAH ratio. SAM acts as a substrate for histone methyltransferases and promotes histone methylation (183) therefore the amount of histone methylation would increase as the concentration of SAH increases, thus explaining the effect seen once in Figure 5-2 and reproducibly in Figure 5-3.

The fold changes in methylation resulting from SAH were plotted as shown in Figure 5-3. H3K9me3 (shown in purple) did not significantly vary as the concentration of SAH increased. Whilst both H3K4me3 (blue) and H3K27me3 (brown) showed a ~1.5-fold increase in methylation at 1 μM, only the increase in H3K27me3 showed a statistically significant increase ($P<0.05$). However, in parallel with previous experiments that investigated the effect of SAH on histone methylation levels (184) all further experiments with SAH used 100 μM to test its effect on modifying tolerance.

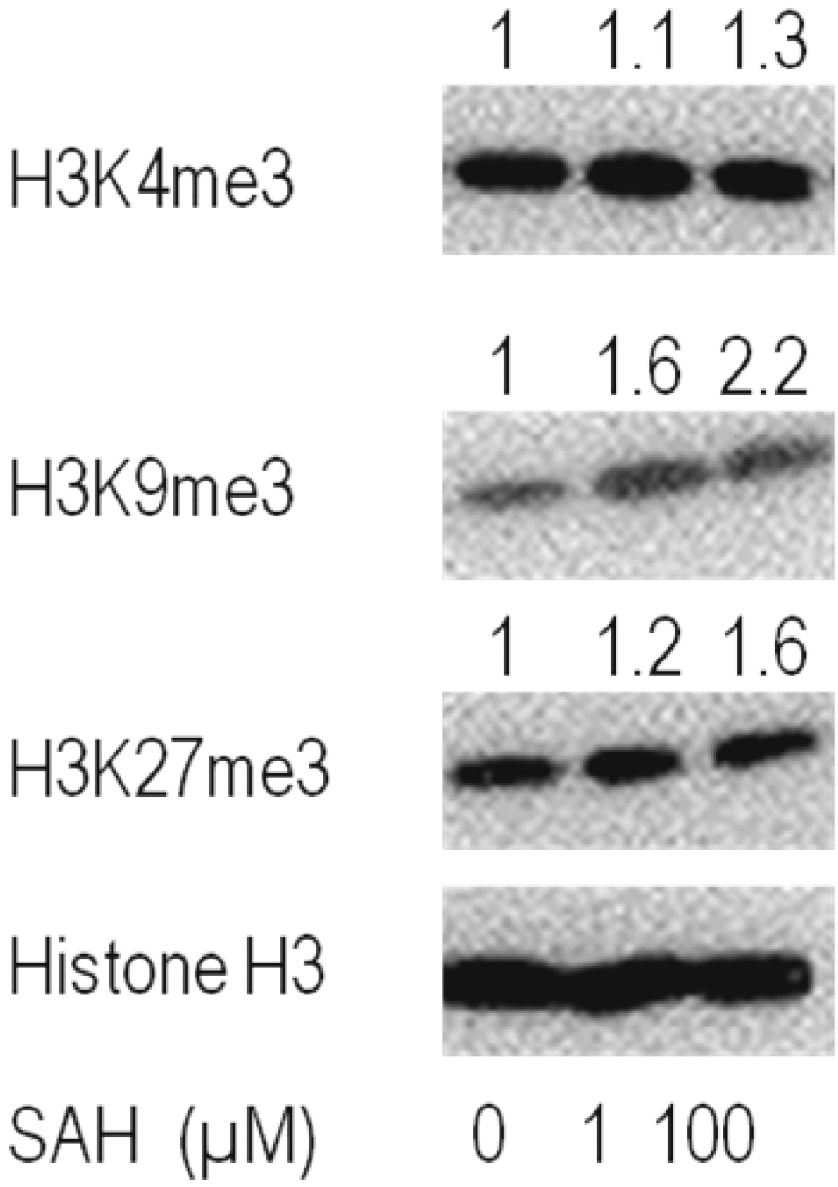

Figure 5-2 Dose-Response Effect of SAH on Histone Methylation

Caco-2 cells were incubated with 0, 1 or 100 µM SAH for 72 hours. Histones were extracted according to the Histone Acid Extraction Protocol from Abcam and the amount measured by BCA assay. Equal amounts of histone protein were loaded onto 12% agarose gels and separated by gel electrophoresis before being transferred to PVDF membranes. Membranes were blocked in 5% milk in 0.1% TBST, incubated with the primary antibody (Histone H3, H3K4me3, H3K9me3 or H3K27me3) at 4 °C overnight and detected with an anti-rabbit secondary antibody. Bands were visualised using ECL detection reagent and hyperfilm developer. ImageJ software was used to normalise the histone H3 bands to each other and calculate the adjusted density values for each histone methylation marker. Representative of n=5 experiments – see Figure 5-3.

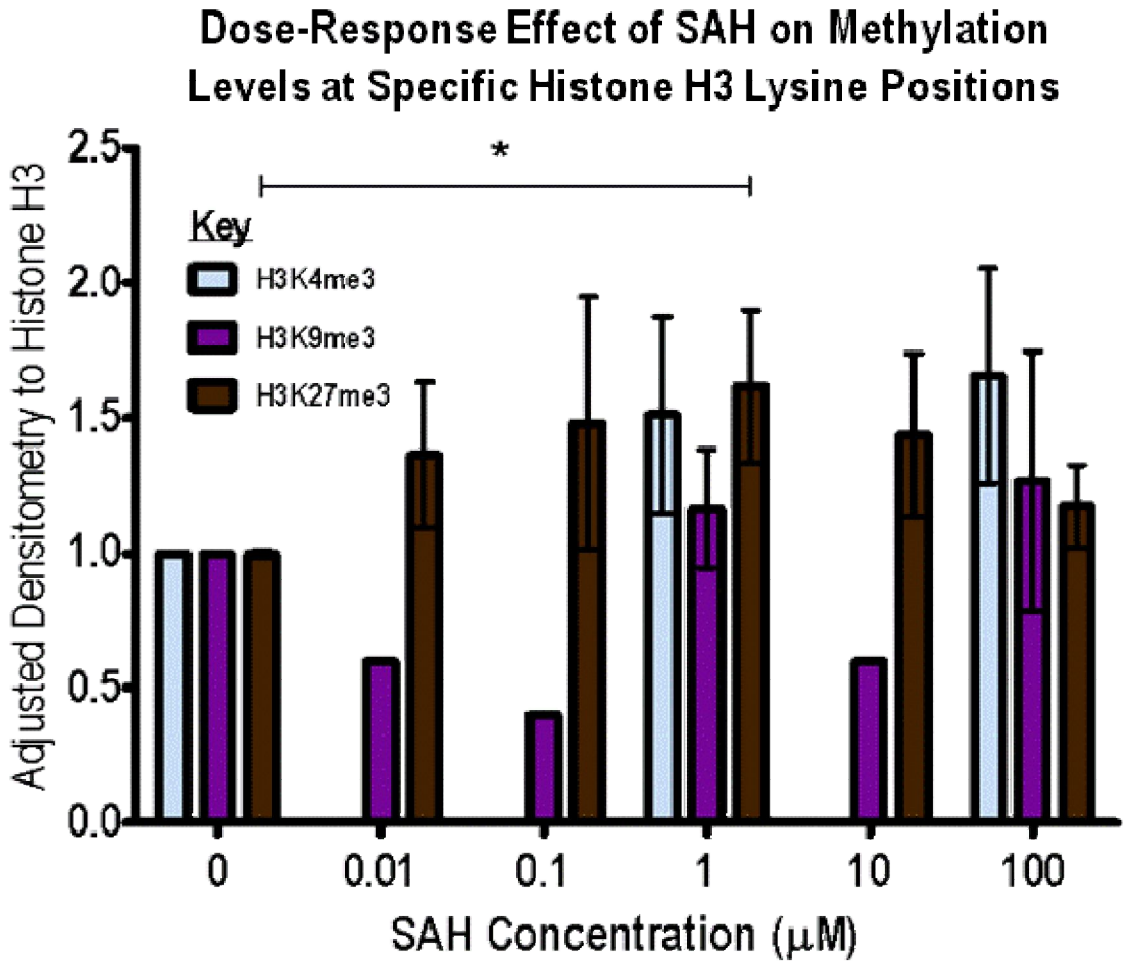

Figure 5-3 Dose-Response Effect of SAH on Methylation Levels at Specific Histone H3 Lysine Positions

Western blots were performed on histone samples extracted from Caco-2 cells incubated with a ten-fold serial dilution of SAH ranging from 100 μM to 0.01 μM for 24 hours. ImageJ software was used to normalise the histone H3 bands to each other and calculate the adjusted density values for each histone methylation marker. The fold-changes in adjusted density of all SAH Western Blots were compiled and the adjusted densitometry plotted against the concentration of SAH used for each of the three epigenetic marks H3K4me3, H3K9me3 and H3K27me3. Statistical analysis was performed using the Student's *t*-test. n = 5. * represents $P<0.05$.

Western blotting produces qualitative results, which can be analysed statistically. However, a technique which produces quantitative results enables statistical analysis to be performed. Therefore, histone samples that were extracted from Caco-2 cells that had been incubated with 0 and 100 µM SAH were interrogated using the Histone H3 PTM Multiplex assay from Active Motif (Methods 3.8). This technique uses a smaller amount of protein than Western blotting to measure the level of methylation present at multiple histone H3 lysine residues. The sample binds to the PTM antibody-conjugated magnetic bead and forms a sandwich complex with a biotinylated histone H3 antibody. This histone-antibody sandwich binds proportionally to streptavidin-phycoerythrin, according to the amount of PTM histone present. The fluorescence emitted by the streptavidin-phycoerythrin is measured using Luminex technology and converted into quantitative median fluorescence intensity (MFI) value. This is normalised to the total histone H3 protein present.

Figure 5-4 represents the MFI of H3K4me3, H3K9me3 and H3K27me3 in Caco-2 cells incubated with 100 µM SAH as a percentage of the methylation level of each residue in Caco-2 cells that have not been incubated with SAH. H3K4me3 and H3K9me3 levels were unaltered by SAH, comparable to the Western blotting results. However, H3K27me3 levels were shown to decrease, by a statistically significant amount ($P<0.01$), when Caco-2 cells are incubated with 100 µM SAH (Figure 5-4). This is the opposite effect to what is seen in Western blotting, though the expected effect of a histone methyltransferase inhibitor. This could be due to the increased sensitivity of the multiplex assay in comparison to Western blotting or interactions between the multiple antibodies preventing the H3K27me3 antibody in the multiplex solution from binding to its epitope resulting in an artificial decrease in H3K27me3 levels.

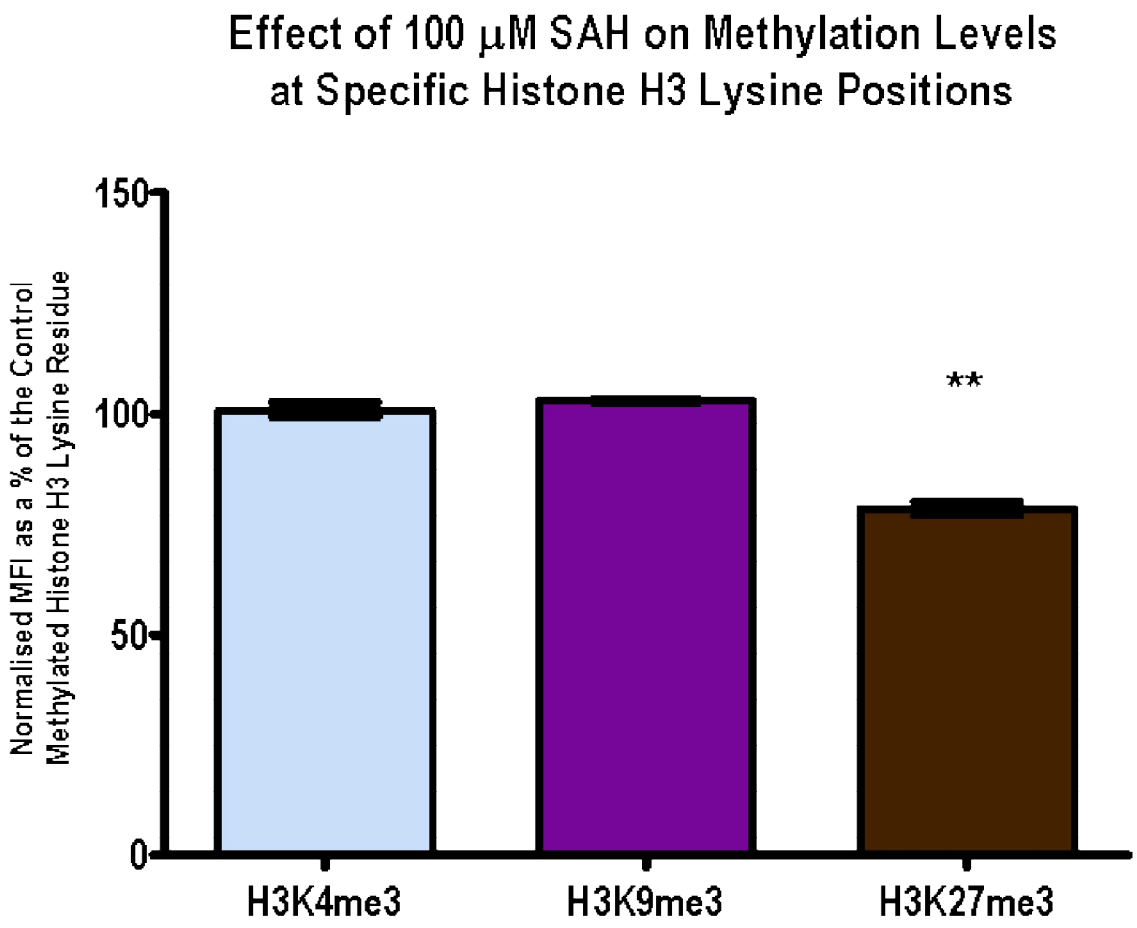

Figure 5-4 Effect of 100 µM SAH on Methylation Levels at Specific Histone H3 Lysine Positions

Caco-2 cells were incubated with 0 and 100 µM SAH for 24 hours. Histones were extracted according to the Histone Acid Extraction Protocol from Abcam and the amount measured by BCA assay. Equal amounts of histone protein were analysed for methylation levels of H3K4me3, H3K9me3 and H3K27me3 using the Histone H3 PTM Multiplex kit from Active Motif. Histone proteins were incubated with H3K4me3, H3K9me3 and H3K27me3 antibody conjugated magnetic beads. Biotinylated Histone H3 antibody and streptavidin-phycoerythrin were added and the resulting fluorescent complex was read by a MAGPIX™ instrument with xPONENT® software. The amount of fluorescence (MFI) for each methylated residue was normalized to total Histone H3. Multiple experiments were combined by plotting the MFI of each methylated residue at 100 µM SAH as a percentage of the MFI of each methylated residue at 0 µM SAH (control). Statistical analysis was performed using the Student's *t*-test. n = 3. ** represents $P<0.01$.

5.1.2 Chaetocin

Though SAH is a non-specific histone methyltransferase inhibitor, it has been demonstrated here by Western Blotting and use of multiplexed antibodies on Luminex beads that SAH only significantly affects H3K27me3 levels. Therefore, an alternative methyltransferase inhibitor was chosen with specific activity against a different histone lysine residue. Chaetocin is a 3,6-epidithio-diketopiperazine (ETP) metabolite from the fungus *Chaetomium minutum*. It is a *cis* fused dimer of two five-membered rings, as shown in Figure 5-5. Inhibition studies by Cherblanc *et al* have shown that only the unique ETP core of Chaetocin is required for inhibition of histone methyltransferases by forming a covalent bond between Chaetocin and the enzyme (185). As well as being a specific inhibitor of the histone lysine methyltransferase SUV39H1 (IC_{50} = 0.8 μM) (186), Chaetocin has also been shown to have antimicrobial (187), antitumour (188) and cytotoxic (189) activity. SUV39H1 is responsible for methylating lysine9 on Histone H3, a repressive epigenetic marker. Therefore, inhibiting H3K9 methylation with Chaetocin will determine whether epigenetic repression is involved in the regulation of immune tolerance in intestinal epithelial cells.

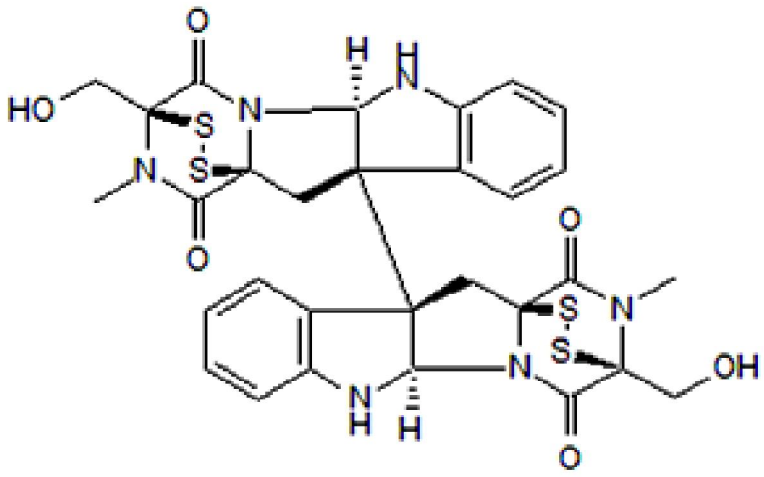

Figure 5-5 Structure of Chaetocin

The 3D chemical structure of Chaetocin (taken as a screenshot from the Tocris website (190)).

Caco-2 cells were incubated with a 10-fold serially diluted range of Chaetocin concentrations beginning at 5000 nM for 18 hours. Based on the data in Tran *et al.* (191), and the IC_{50} data, 5000 nM was chosen as the maximum concentration for the dose-response curve. It is almost 10-fold more concentrated than required to inhibit the enzyme activity to 50%. 100 – 200 nM Chaetocin reduced the level of methylation at H3K9. The histones were extracted using the acid extraction protocol from Abcam and the methylation status investigated by Western Blotting. As shown in Figure 5-6, although the methylation status of the three lysine residues tested varied across the range of Chaetocin concentrations used, only H3K9me3 showed a two-fold increase in methylation in cells incubated with 500 nM Chaetocin compared to cells incubated without Chaetocin. Chaetocin is an inhibitor of a methyltransferase and as such the degree of methylation would be expected to decrease as the concentration of Chaetocin increases. The data (Figure 5-6) showed the opposite effect to that which was predicted. Though the results with a Chaetocin concentration of 5000 nM are included, the Caco-2 cells showed significant toxicity to Chaetocin at this concentration.

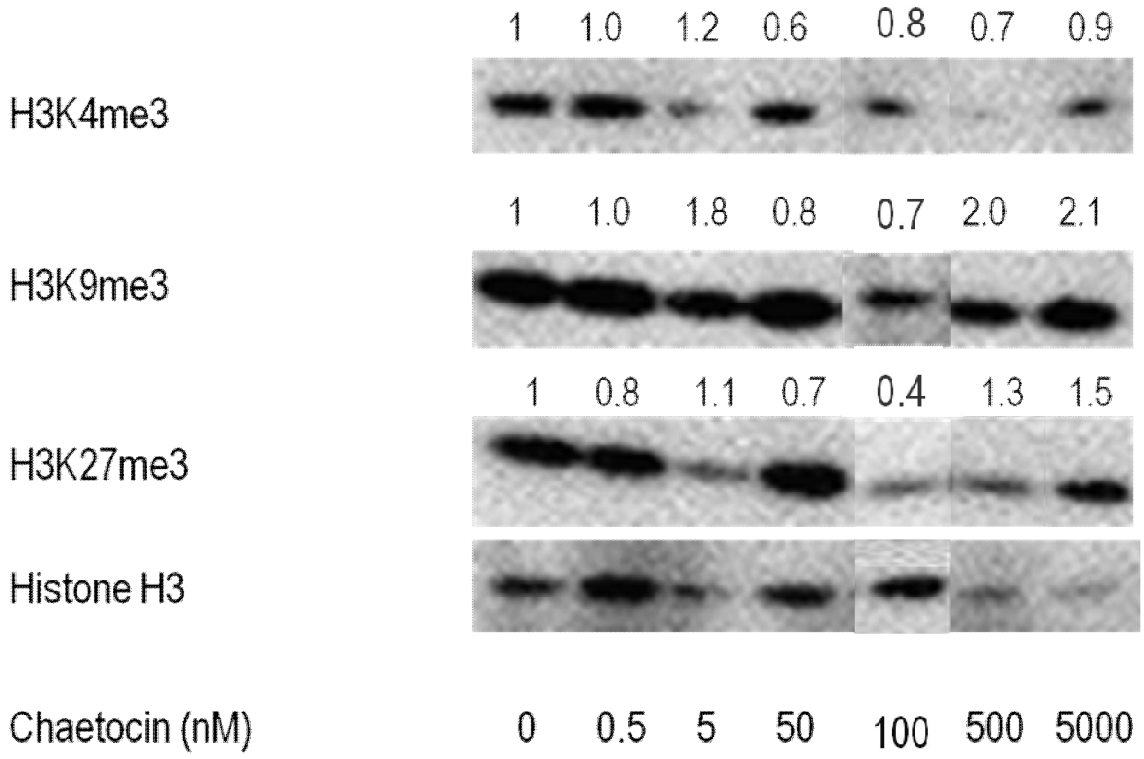

Figure 5-6 Dose-Response Effect of Chaetocin on Histone Methylation

Caco-2 cells were incubated with a ten-fold serial dilution of Chaetocin starting at 5000 nM for 18 hours, with an additional condition at 100 nM. Histones were extracted according to the Histone Acid Extraction Protocol from Abcam and the amount measured by BCA assay. Equal amounts of histone protein were loaded onto 12% agarose gels and separated by gel electrophoresis before being transferred to PVDF membranes. Membranes were blocked in 5% milk in 0.1% TBST, incubated with the primary antibody (Histone H3, H3K4me3, H3K9me3 or H3K27me3) at 4 °C overnight and detected with an anti-rabbit secondary antibody. Bands were visualised using ECL detection reagent and hyperfilm developer. ImageJ software was used to normalise the histone H3 bands to each other and calculate the adjusted density values for each histone methylation marker. Representative of n=5 experiments – see Figure 5-7.

The fold changes in methylation resulting from Chaetocin were plotted as shown in Figure 5-7. The amount of H3K4me3 was reduced by ~0.5-fold at both 100 nM and 500 nM Chaetocin ($P<0.05$). H3K27me3 levels were reduced by ~0.6-fold and ~0.4-fold at 50 nM and 100 nM Chaetocin, respectively ($P<0.05$). When multiple experiments were combined, H3K9me3 levels were reduced by ~0.7-fold at both 50 nM and 100 nM Chaetocin ($P<0.05$). 500 nM and 5000 nM Chaetocin produced an increase in the amount of H3K9me3 and H3K27me3, which was contrary to expectation. This was likely due to the high amount of cell death present at these higher concentrations and therefore 100 nM Chaetocin was used for all further experiments.

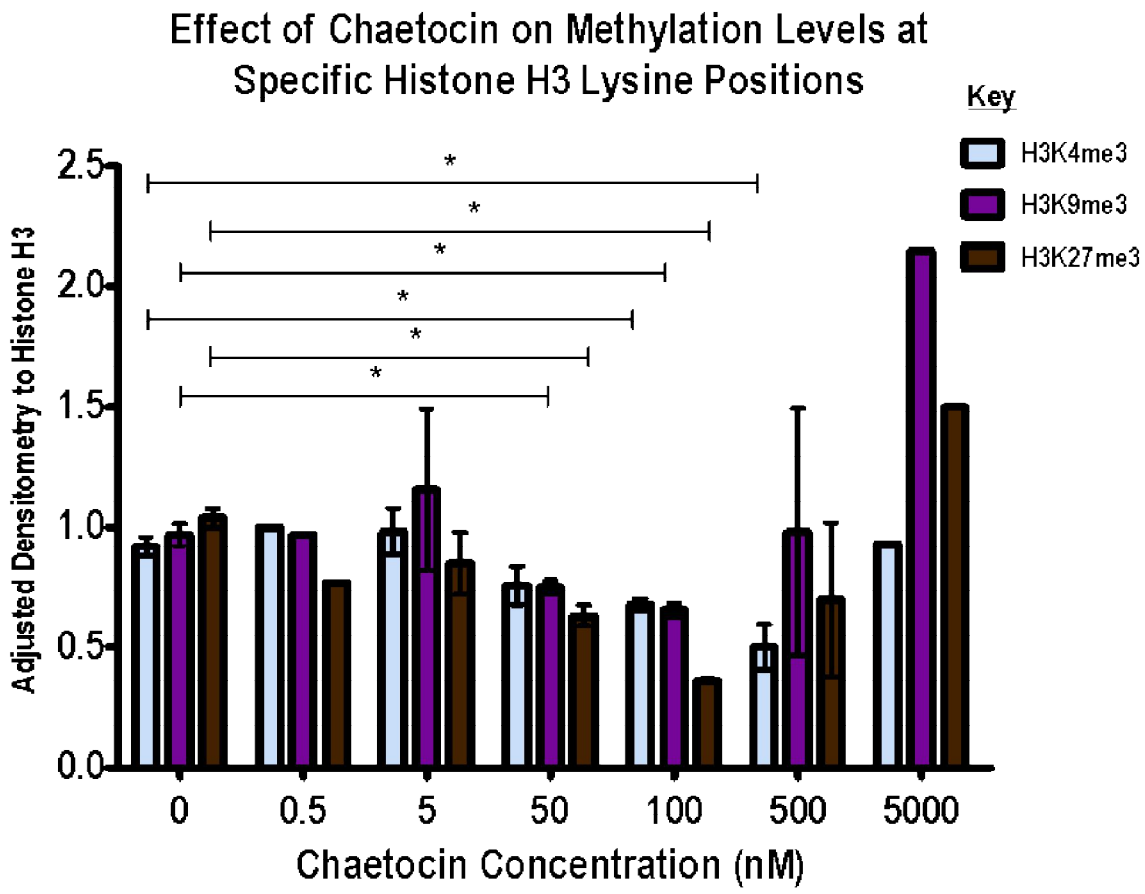

Figure 5-7 Effect of Chaetocin on Methylation Levels at Specific Histone H3 Lysine Positions

Western blots were performed on histone samples extracted from Caco-2 cells incubated with ten-fold serial dilutions of Chaetocin ranging from 5000 nM to 0.5 nM for 18 hours. ImageJ software was used to normalise the histone H3 bands to each other and calculate the adjusted density values for each histone methylation marker. The fold-changes in adjusted density of all Chaetocin Western Blots were compiled and the adjusted densitometry plotted against the concentration of Chaetocin used for each of the three epigenetic marks H3K4me3, H3K9me3 and H3K27me3. Statistical analysis was performed using the Student's *t*-test. n = 5. * represents $P<0.05$.

5.2 Effect of Histone Methyltransferase Inhibition on Immune Tolerance in Intestinal Epithelial Cells

5.2.1 *S*-adenosyl-L-homocysteine (SAH)

We examined if altering histone methylation affected CXCL8 production and therefore had an impact on tolerance. This was established by comparing the CXCL8 production of cells that were stimulated with 1 ng/ml IL-1β for 24 hours and cells that were stimulated with 1 ng/ml IL-1β twice for 24 hours each with cells that had been incubated with different concentrations of SAH as well as being tolerized by 1 ng/ml IL-1β (Figure 3-7). Conditioned media were collected and the amount of CXCL8 produced measured by ELISA and normalized to the cellular protein content, as measured by BCA assay.

As shown in Figure 5-8, the production of CXCL8 is greatest in the cells that have only been stimulated once with IL-1β and is decreased, but still greater than the unstimulated control cells, in the cells that have been tolerized, as described in Chapter 4, Figure 4-16. This decrease is a statistically significant difference ($P<0.001$), as calculated by Student's *t* test. The addition of SAH to the tolerized cells did not significantly alter CXCL8 production compared to CXCL8 produced by tolerized cells alone, except when SAH is at 100 μM. The addition of 100 μM SAH to Caco-2 cells tolerized with IL-1β resulted in an increase in CXCL8 production that was statistically significantly greater than that of tolerized cells alone but is less than that of stimulated cells ($P<0.05$, in each case). The results of the statistical tests ($P<0.05$) showing a significant difference between each of the 50 – 90 μM SAH concentrations and stimulated cells are omitted for clarity. Therefore, 72 hours incubation with 100 μM SAH causes cells that have been stimulated twice with IL-1β to break tolerance.

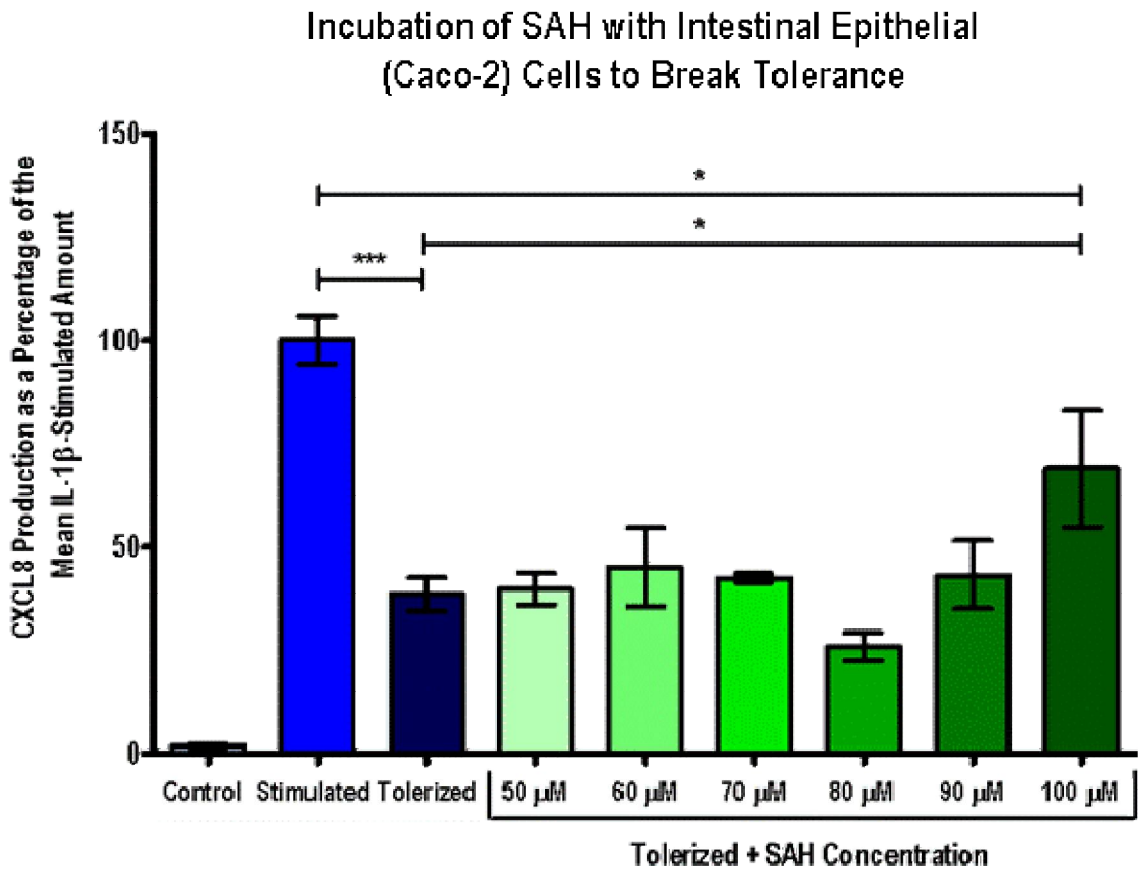

Figure 5-8 Incubation of SAH with Intestinal Epithelial (Caco-2) Cells to Break Tolerance

Caco-2 cells were stimulated with 1 ng/ml IL-1β for 24 hours and tolerized by a prior stimulation of 1 ng/ml IL-1β 24 hours earlier, as described in Figure 3-7. SAH was diluted to the required concentrations (50-100 µM) and incubated with Caco-2 cells for 72 hours in total, as described for 100 µM SAH in Figure 3-7. Caco-2 cells were tolerized by a prior stimulation with 1 ng/ml IL-1β for 24 hours followed by stimulation with 1 ng/ml IL-1β for 24 hours, as well as being incubated with fresh preparations of SAH (if required). CXCL8 production was measured by ELISA and normalized to cellular protein content (measured by BCA protein assay). Multiple experiments were combined by calculating CXCL8 production as a percentage of the mean CXCL8 production per single stimulation of IL-1β. Bars represent mean ± SEM, n = 3. Statistical analysis was performed using the Student's *t*-test and Mann-Whitney U test. n = 5. * and *** represent $P<0.05$ and <0.001, respectively.

After confirming that SAH had an effect on tolerance, the time period necessary to cause that effect was investigated. Tolerized cells were incubated with 100 μM SAH at different time points and for different periods of time: 24 (prior to IL-1β stimulation, with the first IL-1β stimulation and with the second IL-1β stimulation), 48 (not including the second IL-1β stimulation and not including the 24 hours before IL-1β stimulation) and 72 hours. Only 72 hours incubation with 100 μM SAH resulted in a statistically significantly increased production of CXCL8 (Figure 5-9). All of the tolerized + SAH conditions produced a statistically significant reduction of CXCL8 compared to stimulated cells, though the results of the statistical tests ($P<0.05$) are omitted from Figure 5-9 for clarity. Figure 5-9 emphasises the importance of inhibitor incubation time on the ability to break tolerance.

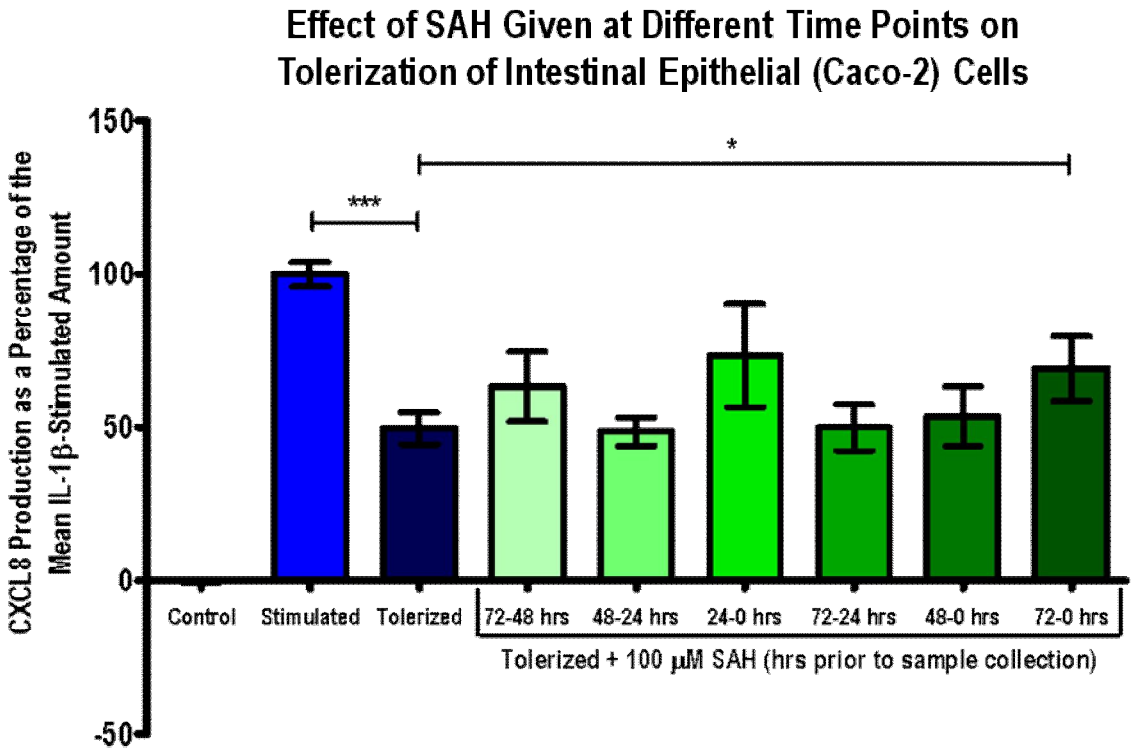

Figure 5-9 Effect of SAH Given at Different Time Points on Tolerization of Intestinal Epithelial (Caco-2) Cells

Caco-2 cells were stimulated with 1 ng/ml IL-1β for 24 hours and tolerized by a prior stimulation of 1 ng/ml IL-1β 24 hours earlier, as described in Figure 3-2. SAH was diluted to 100 μM and incubated with Caco-2 cells for 24, 48 or 72 hours prior to sample collection. Fresh preparations of SAH (if required) and two stimulations of 1 ng/ml IL-1β 24 hours apart were added to the cells. CXCL8 production was measured by ELISA and normalized to cellular protein content (measured by BCA protein assay). Multiple experiments were combined by calculating CXCL8 production as a percentage of the mean CXCL8 production per single stimulation of IL-1β. Bars represent mean ± SEM, n = 3. Statistical analysis was performed using the Student's *t*-test and Mann-Whitney U test. n = 4. * and *** represent $P<0.05$ and <0.001, respectively.

The effect of SAH on tolerized cells was confirmed. The effect on unstimulated and stimulated cells was also tested for by incubating Caco-2 cells with 100 μM SAH for 72 hours and IL-1β if required. Though the sample variation is greater in the cells treated with SAH than in the cells not treated with SAH, it is not a statistically significant difference. It is only for tolerized cells that treatment with SAH affects the production of CXCL8 to a statistically significant level ($p<0.05$) (Figure 5-10). Therefore, SAH breaks tolerance, thus showing that using an agent capable of modifying histone methylation has an effect on tolerance.

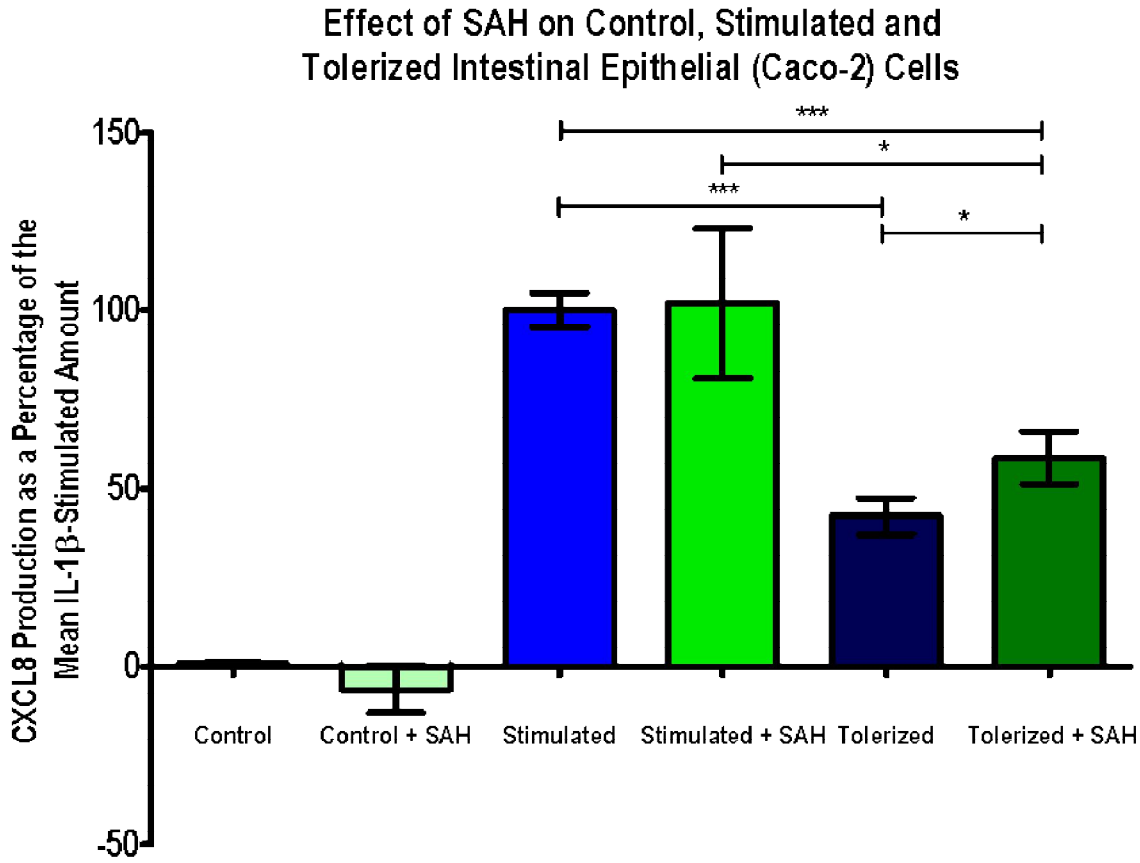

Figure 5-10 Effect of SAH on Control, Stimulated and Tolerized Intestinal Epithelial (Caco-2) Cells

Caco-2 cells were stimulated with 1 ng/ml IL-1β for 24 hours and tolerized by a prior stimulation of 1 ng/ml IL-1β 24 hours earlier, as described in Figure 3-7. SAH was diluted to 100 µM and incubated with control, stimulated and tolerized Caco-2 cells for 72 hours (48 hours for stimulated cells) prior to sample collection. Fresh preparations of SAH (if no IL-1β was required) and two stimulations of 1 ng/ml IL-1β 24 hours apart were added to the cells. CXCL8 production was measured by ELISA and normalized to cellular protein content (measured by BCA protein assay). Multiple experiments were combined by calculating CXCL8 production as a percentage of the mean CXCL8 production per single stimulation of IL-1β. Bars represent mean ± SEM, n = 3. Statistical analysis was performed using the Student's *t*-test and Mann-Whitney U test. n = 4. * and *** represent $P<0.05$ and <0.001, respectively.

The effect of SAH on tolerized cells is also shown in Figure 5-11, but the normalized CXCL8 values in pg/mg protein are plotted instead of percentages of the mean stimulated amount. Like the same conditions in Figure 5-10, Figure 5-11 shows that the tolerized cells express ~50% the amount of CXCL8 as stimulated cells ($P<0.001$). The tolerized cells that are incubated with 100 μM SAH express a statistically significant greater amount of CXCL8 than tolerized cells alone do ($P<0.05$). However, even though it is a statistically significant difference, it is only a small increase in CXCL8 production. Plotting the original normalized values highlights the range of values produced each time the experiment is repeated. Though the effect is the same for each repetition, the actual values vary. By representing the values as a percentage of the mean stimulated amount the values are brought closer together as shown by the tighter error bars in Figure 5-10.

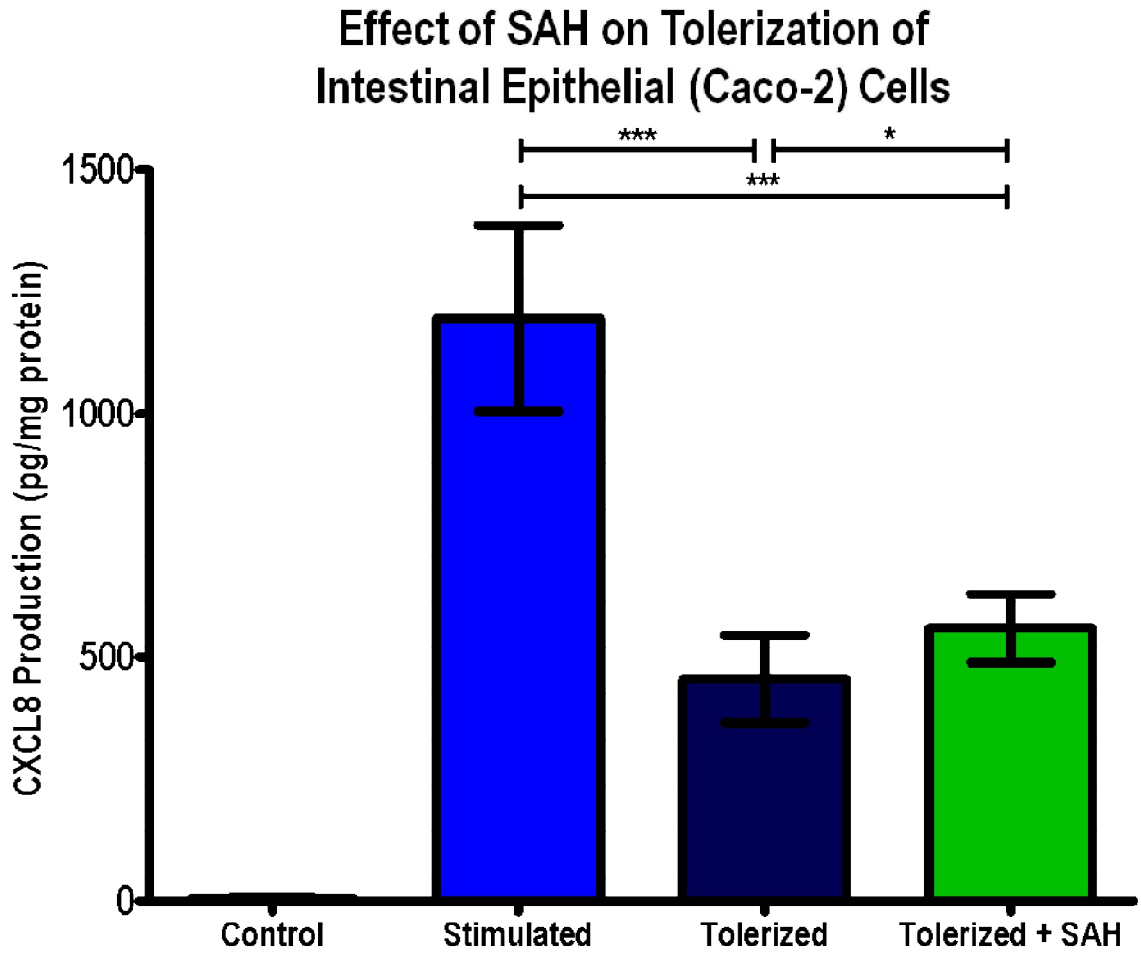

Figure 5-11 Effect of SAH on Tolerization of Intestinal Epithelial (Caco-2) Cells

Caco-2 cells were stimulated with 1 ng/ml IL-1β for 24 hours and tolerized by a prior stimulation of 1 ng/ml IL-1β 24 hours earlier, as described in Figure 3-7. SAH was diluted to 100 µM and incubated with tolerized Caco-2 cells for 72 hours prior to sample collection. Fresh preparations of SAH and two stimulations of 1 ng/ml IL-1β 24 hours apart were added to the cells. CXCL8 production was measured by ELISA and normalized to cellular protein content (measured by BCA protein assay). Bars represent mean ± SEM, n = 4. Statistical analysis was performed using the Mann-Whitney U test. * and *** represent $P<0.05$ and <0.001, respectively.

5.2.2 Chaetocin

Chaetocin was also investigated for its effect on tolerance in intestinal epithelial cells. SAH is a broad spectrum histone methyltransferase inhibitor, so a more specific inhibitor with an effect on a different epigenetic marker was investigated to see if the same effect on tolerance was seen. As determined by Western blotting of a range of Chaetocin concentrations, 100 nM Chaetocin was incubated with Caco-2 cells for 1 hour prior to stimulation by IL-1β (or at that time point in the unstimulated cells) and was added directly into the media for 8 or 18 hours prior to sample collection. In data not shown, cells incubated with 100 nM Chaetocin for greater than 12 hours died (data not shown). One hour incubation was not enough to alter the methylation level of epigenetic markers but if incubated for too long the cells did not survive, so the incubation period was separated into two periods of short duration, as described in Figure 3-7.

Unstimulated Caco-2 cells incubated with Chaetocin had a small increase in CXCL8 production ($P<0.05$). Stimulated (1+8 hrs) cells showed no difference in CXCL8 production but stimulated (1+18 hrs) showed a large increase in the production of CXCL8 ($P<0.001$) (Figure 5-12). The variation is much larger in all of the Chaetocin incubated samples compared to the non-Chaetocin counterparts, due to cell death creating artificially increased values thus enhancing the p value.

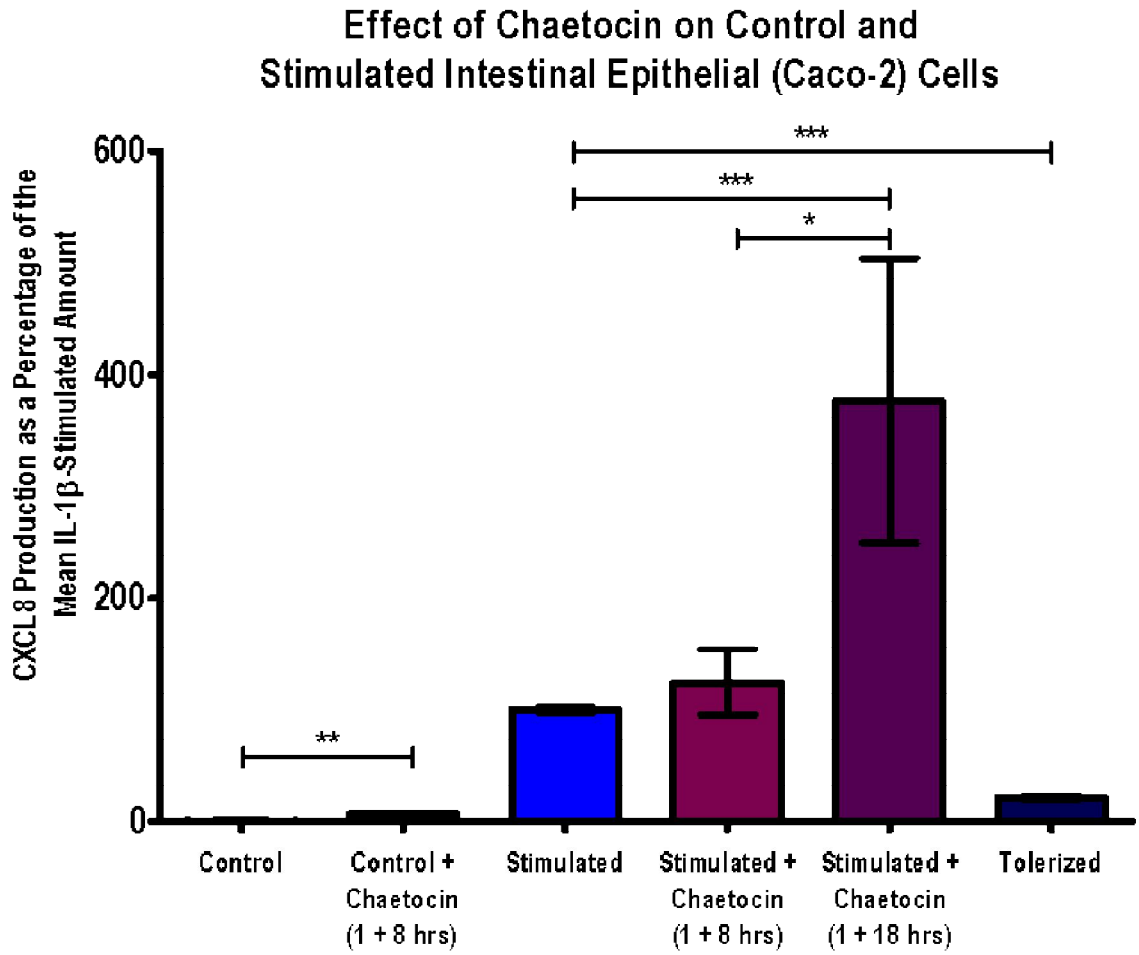

Figure 5-12 Effect of Chaetocin on Control and Stimulated Intestinal Epithelial (Caco-2) Cells

Caco-2 cells were stimulated with 1 ng/ml IL-1β for 24 hours and tolerized by a prior stimulation of 1 ng/ml IL-1β 24 hours earlier, as described in Figure 3-2. Chaetocin was diluted to 100 nM and incubated with control and stimulated Caco-2 cells for 1 hour followed by fresh media/ 1ng/ml IL-1β for 18 hours then 100 nM Chaetocin added directly to the cells for 8 hours. CXCL8 production was measured by ELISA and normalized to cellular protein content (measured by BCA protein assay). Multiple experiments were combined by calculating CXCL8 production as a percentage of the mean CXCL8 production per single stimulation of IL-1β. Bars represent mean ± SEM, n = 3. Statistical analysis was performed using the Student's *t*-test and Mann-Whitney U test. *, ** and *** represent P<0.05, <0.01 and <0.001, respectively.

The effect of Chaetocin on tolerance was investigated by incubating Caco-2 cells with 100 nM Chaetocin for one hour prior to the second IL-1β stimulation and again 8 or 18 hours before sample collection (Figure 3-7). As seen in Figure 5-13, both incubation times result in an increased level of CXCL8 production compared to tolerized only cells ($P<0.001$) showing that incubation with Chaetocin breaks tolerance. CXCL8 produced by 1 + 8 hours incubation is statistically significantly lower than stimulated cells ($P<0.001$) but there is no statistical difference between tolerized + 100 nM Chaetocin (1 + 18 hours) cells and stimulated only cells ($P>0.05$). Although 1 + 8 hours incubation is sufficient to break tolerance, an increase in the incubation length of the epigenetic inhibitor Chaetocin is associated with an increase in CXCL8 production.

In summary, whilst both SAH and Chaetocin increase histone methylation levels at H3K9 and H3K27, as measured by Western blotting, SAH causes a decrease in H3K27me3 levels when measured using the Histone H3 PTM Multiplex Luminex technology. Tolerance is broken following incubation with either inhibitor, thereby proving that tolerance is regulated, at least in part, by epigenetics.

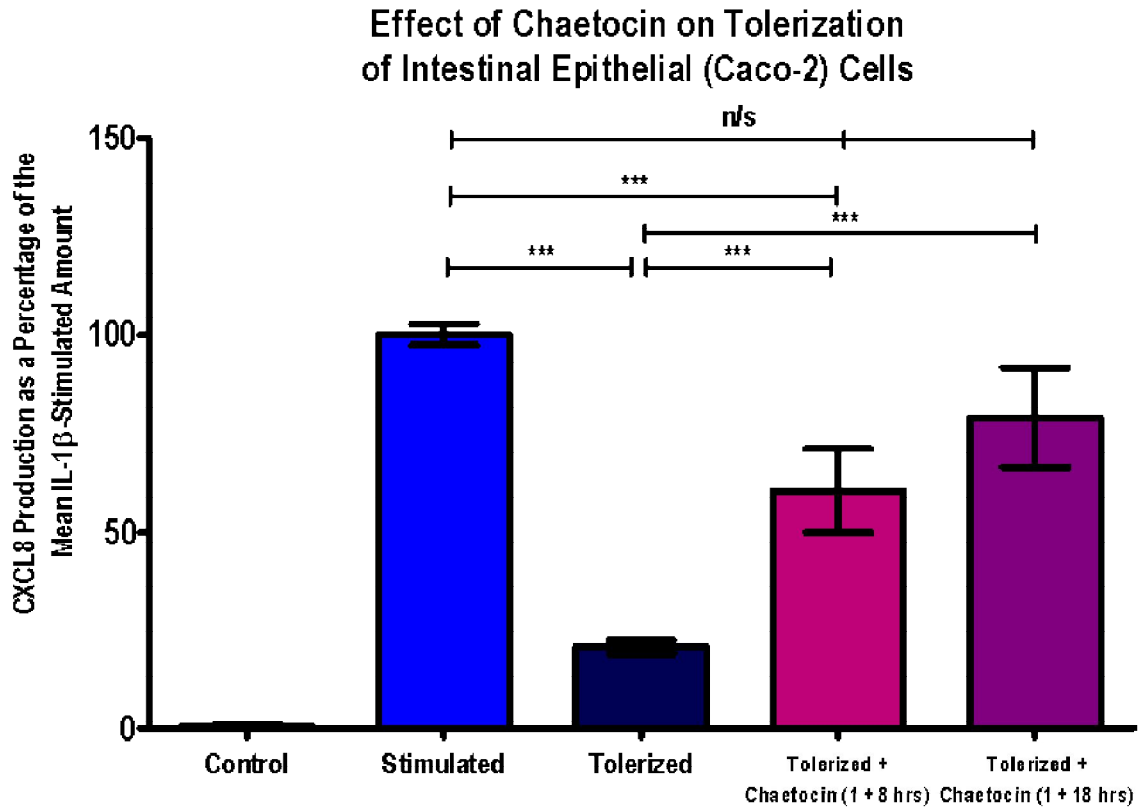

Figure 5-13 Effect of Chaetocin on Tolerization of Intestinal Epithelial (Caco-2) Cells

Caco-2 cells were stimulated with 1 ng/ml IL-1β for 24 hours and tolerized by a prior stimulation of 1 ng/ml IL-1β 24 hours earlier, as described in Figure 3-7. Chaetocin was added directly to pre-stimulated Caco-2 cells at a concentration of 100 nM for 1 hour. The second stimulation with IL-1β was followed by another incubation with 100 nM Chaetocin for 8 or 18 hours prior to sample collection, as described in Figure 3-7. CXCL8 production was measured by ELISA and normalized to cellular protein content (measured by BCA protein assay). Multiple experiments were combined by calculating CXCL8 production as a percentage of the mean CXCL8 production per single stimulation of IL-1β. Bars represent mean ± SEM, n = 5. Statistical analysis was performed using the Student's *t*-test and Mann-Whitney U test. *** represents P<0.001.

The effect of Chaetocin on tolerized cells is also shown in Figure 5-14, but the normalized CXCL8 values in pg/mg protein are plotted instead of percentages of the mean stimulated amount. Like the same conditions in Figure 5-13, Figure 5-14 shows that the tolerized cells express ~25% of the amount of CXCL8 as stimulated cells ($P<0.001$). The tolerized cells that are incubated with 100 nM Chaetocin express a statistically significant greater amount of CXCL8 than tolerized cells alone do ($P<0.01$ for 1 + 8 hours and $P<0.001$ for 1 + 18 hours). Due to the greater range of values in each condition, the statistical significance of some tests in Figure 5-13 and Figure 5-14 are different. Though in Figure 5-13 tolerized + Chaetocin for 1 + 18 hours cells do not produce a statistically significant reduction in CXCL8 in comparison to stimulated cells, the original normalized values in Figure 5-14 show that there is a reduction. Incubating tolerized cells with Chaetocin for 1 + 8 hours produces a statistically significant increase in CXCL8 compared to tolerized cells only. This has a P value of <0.01 in Figure 5-14 but <0.001 in Figure 5-13. This is due to the smaller spread of the values in Figure 5-13 compared to Figure 5-14.

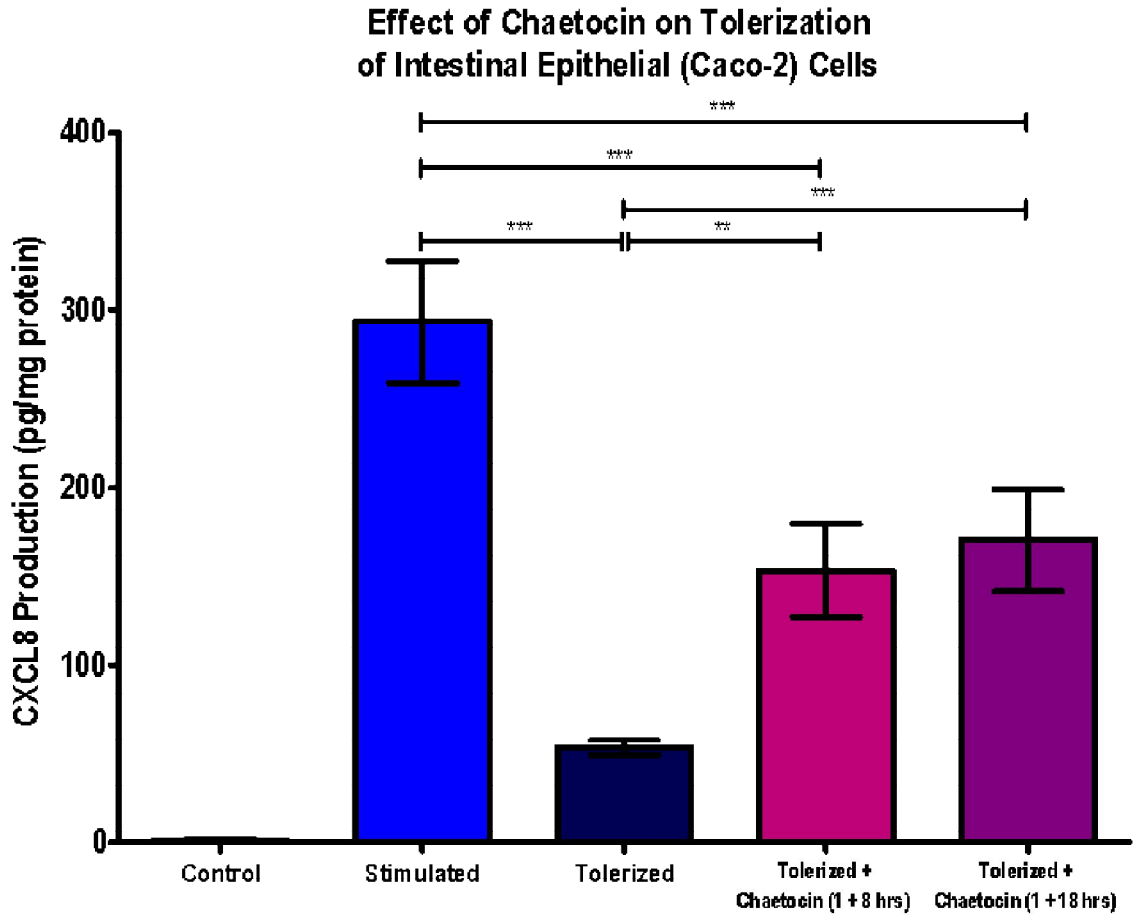

Figure 5-14 Effect of Chaetocin on Tolerization of Intestinal Epithelial (Caco-2) Cells

Caco-2 cells were stimulated with 1 ng/ml IL-1β for 24 hours and tolerized by a prior stimulation of 1 ng/ml IL-1β 24 hours earlier, as described in Figure 3-7. Chaetocin was added directly to pre-stimulated Caco-2 cells at a concentration of 100 nM for 1 hour. The second stimulation with IL-1β was followed by another incubation with 100 nM Chaetocin for 8 or 18 hours prior to sample collection, as described in Figure 3-7. CXCL8 production was measured by ELISA and normalized to cellular protein content (measured by BCA protein assay). Bars represent mean ± SEM, n = 5. Statistical analysis was performed using the Student's *t*-test and Mann-Whitney U test. ** and *** represent P<0.01 and <0.001, respectively.

5.3 Inhibition of Histone Demethylases

Histone lysine demethylases have the opposite function to histone methyltransferases as they catalyse the removal of a methyl group from the lysine residue in histone proteins, rather than catalyse methylation. Histone lysine demethylases were not discovered until 2004 (192) thereby proving that histone methylation is not an irreversible process as previously thought (193).

5.3.1 Pargyline

Pargyline was first developed as a non-selective monoamine oxidase inhibitor with antihypertensive and antidepressive properties (194). It was marketed under the name Eutonyl until its discontinuation in 2007 due to its interaction with other non-prescribed compounds (195). Pargyline and other monoamine oxidase inhibitors prevent the metabolism of tyramine, commonly found in certain foods and drinks including anchovies, sherry, salami, bananas, soy sauce etc, resulting in severe headaches and cerebral haemorrhages, hence the discontinuation of pargyline as a therapeutic drug. Pargyline inhibits monoamine oxidases by covalently binding to the FAD cofactor in the enzyme's active site, as shown by the crystal structure produced by Binda *et al* (196). The alkyne moiety in the pargyline structure (Figure 5-15) reacts with the flavin-dependent enzyme cofactor, creating a covalent adduct and inhibiting FAD-dependent enzymes.

The structural similarity of monoamine oxidases to other FAD-dependent enzymes, including LSD1 (lysine specific demethylase 1), implies that pargyline will bind to and inhibit histone demethylases as well (197). LSD1 catalyses the demethylation of mono- and di-methylated

lysines 4 and 9 in Histone H3 (H3K4 and H3K9). As the concentration of pargyline increases, the relative amount of H3K4me2 also increases (198).

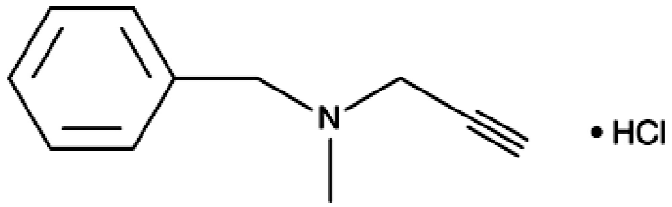

Figure 5-15 Chemical Structure of Pargyline Hydrochloride

Chemical structure of Pargyline hydrochloride taken as a screenshot from the Cayman Chemical website (199).

Caco-2 cells were incubated for 1 hour with a range of pargyline concentrations starting at 3 mM and diluted ten-fold each time until 0.3 μM was reached. As pargyline is an inhibitor of histone demethylases, the amount of methylation should increase as the concentration of pargyline increases. As shown in Figure 5-16, the amount of H3K4me3 and H3K9me3 increases as the concentration of pargyline increases. H3K4me3 increases 1.6-fold whilst a much smaller effect is had on H3K9me3. Figure 5-16 is representative of n=5 experiments, which are combined in Figure 5-17. LSD1 is an H3K4me2 and H3K9me2 specific demethylase. Therefore as the concentration of pargyline increases, the amount of H3K4me2/H3K9me2 increases thus increasing the amount of substrate for the H3K4me3/H3K9me3 methyltransferase resulting in an increased amount of H3K4me3/H3K9me3. H3K9me2 is only a specific substrate for LSD1 when it is coupled to the androgen receptor, therefore its inhibition by pargyline will have a greater effect on H3K4me3 than H3K9me3, as shown in Figure 5-16.

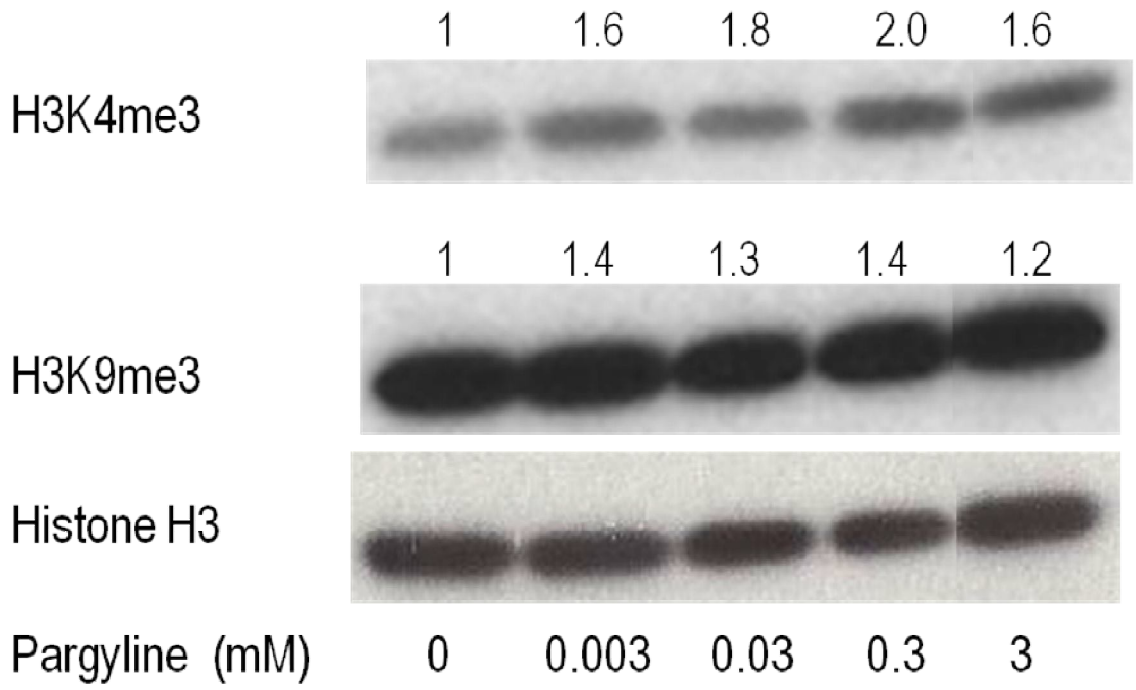

Figure 5-16 Dose-Response Effect of Pargyline on Histone Methylation

Caco-2 cells were incubated with a ten-fold serial dilution of Pargyline hydrochloride starting at 3 mM for 1 hour. Histones were extracted according to the Histone Acid Extraction Protocol from Abcam and the amount measured by BCA assay. Equal amounts of histone protein were loaded onto 12% agarose gels and separated by gel electrophoresis before being transferred to PVDF membranes. Membranes were blocked in 5% milk in 0.1% TBST, incubated with the primary antibody (Histone H3, H3K4me3, H3K9me3 or H3K27me3) at 4 °C overnight and detected with an anti-rabbit secondary antibody. Bands were visualised using ECL detection reagent and hyperfilm developer. ImageJ software was used to normalise the histone H3 bands to each other and calculate the adjusted density values for each histone methylation marker. Representative of n=5 experiments – see Figure 5-17.

The fold changes in methylation resulting from pargyline were plotted as shown in Figure 5-17. H3K27me3 (shown in brown) does not significantly vary as the concentration of pargyline increases. This is as expected as pargyline is not known to have activity against any H3K27 specific demethylases. A subtle, but statistically significant (ANOVA $P=0.0163$) increase in the amount of H3K9me3 (shown in purple) across all concentrations of pargyline was found, though the only concentrations to produce a statistically significant increase were 0.003 and 0.3 mM. Pargyline mainly affects the level of H3K4me3, as shown in blue in Figure 5-17. A statistically significant increase in the amount of H3K4me3 across all concentrations was found (ANOVA $P=0.0012$). Each concentration of pargyline between 3 mM and 0.003 mM causes a maximal two-fold increase in the amount of H3K4me3 ($P<0.05$). 3 mM pargyline hydrochloride was used for all subsequent experiments to ensure maximal inhibition.

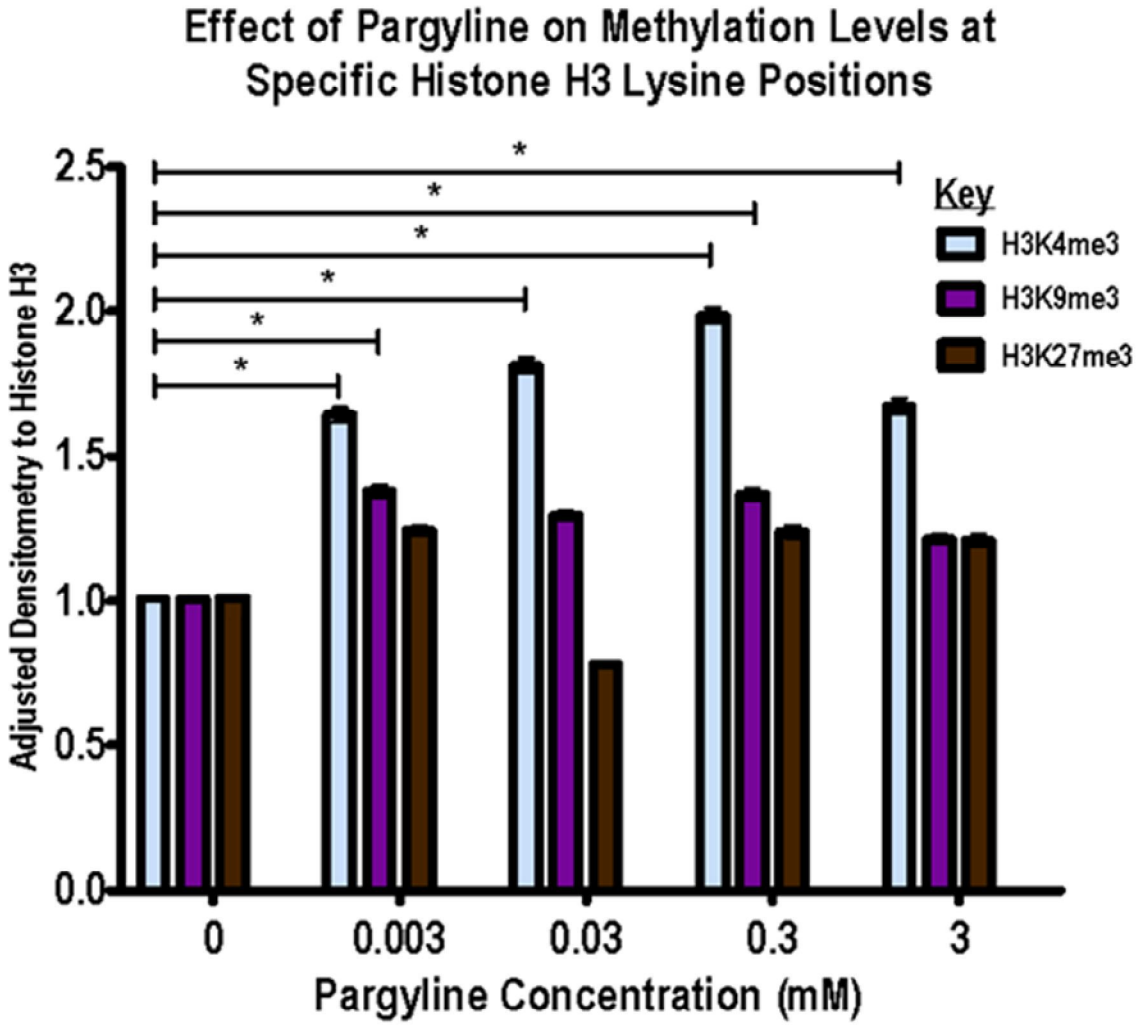

Figure 5-17 Effect of Pargyline on Methylation Levels at Specific Histone H3 Lysine Positions

Western blots were performed on histone samples extracted from Caco-2 cells incubated with a ten-fold serial dilution of pargyline hydrochloride ranging from 3 mM to 3 μM for 24 hours. ImageJ software was used to normalise the histone H3 bands to each other and calculate the adjusted density values for each histone methylation marker. The fold-changes in adjusted density of all pargyline Western blots were compiled and the adjusted densitometry plotted against the concentration of pargyline used for each of the three epigenetic marks H3K4me3, H3K9me3 and H3K27me3. Statistical analysis was performed using the Student's *t*-test. n = 5. * represents $P<0.05$.

In experiments on macrophages undertaken by Foster *et al*, pargyline was incubated with the cells for 1 hour only. In our experiments, the effect of incubation length on histone methylation levels was investigated by incubating the intestinal epithelial cells with 3 mM pargyline hydrochloride for 1, 2, 3, 6 and 24 hours. All of the fold-changes were accumulated and plotted against incubation time (Figure 5-18). An ANOVA performed on each histone methylation mark showed that only H3K4me3 showed a statistically significant increase in the amount of methylation over time ($P<0.0001$). At least 6 hours of incubation is required to produce a statistically significant increase in H3K4me3 ($P<0.05$ for both 6 and 24 hours incubation).

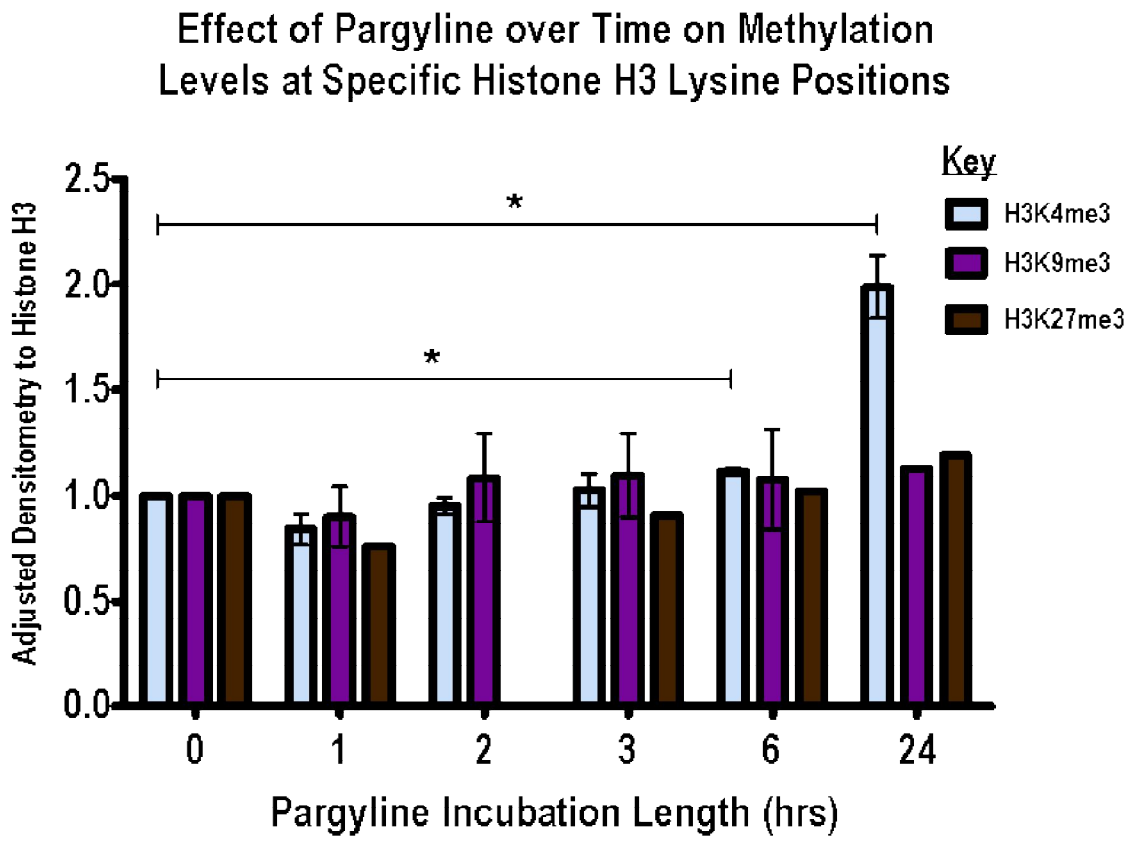

Figure 5-18 Effect of Pargyline over Time on Methylation Levels at Specific Histone H3 Lysine Positions

Western blots were performed on histone samples extracted from Caco-2 cells incubated with 3 mM Pargyline hydrochloride for a range of time periods from 1 hour to 24 hours. ImageJ software was used to normalise the histone H3 bands to each other and calculate the adjusted density values for each histone methylation marker. The fold-changes in adjusted density of all pargyline Western blots were compiled and the adjusted densitometry plotted against the concentration of pargyline used for each of the three epigenetic marks H3K4me3, H3K9me3 and H3K27me3. Statistical analysis was performed using the Student's *t*-test. n = 5. * represents $P<0.05$.

5.3.2 2,4-Pyridinedicarboxylic Acid (2,4-PDCA)

As with histone lysine methyltransferases, two separate histone demethylase inhibitors were used to investigate the effect of histone methylation on immune tolerance in intestinal epithelial cells. 2,4-Pyridinedicarboxylic acid (2,4-PDCA) is a 2-oxogluturate mimic (as illustrated in Figure 5-19) that chelates zinc, thus explaining its ability to inhibit a range of enzymes, including histone lysine demethylases at low micromolar concentrations (200). The carboxylic groups in 2,4-PDCA form interactions with the amino acid side chains in the histone demethylase binding sites. The different enzymes conserve the active site structure, but there are some variations in the amino acids used. These alterations could explain the change in potency that 2,4-PDCA has in different enzymes e.g. the change from lysine in the enzyme KDM4A to glycine in the enzyme KDM6A reduces the strength of the interaction with 2,4-PDCA and accounts for the reduction in inhibitor potency (200).

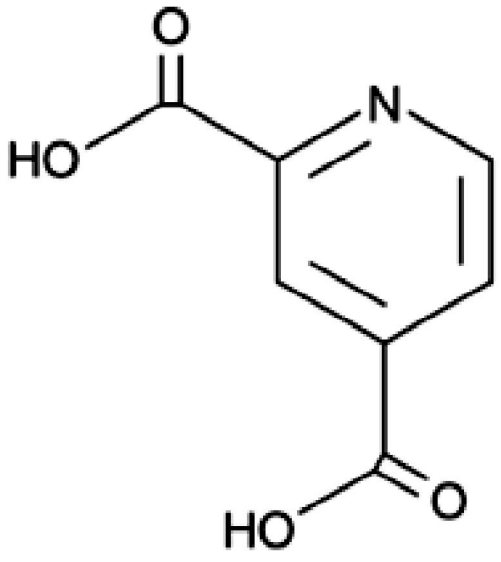

Figure 5-19 Chemical Structure of 2,4-Pyridinedicarboxylic Acid (2,4-PDCA)

Chemical structure of 2,4-PDCA taken as a screenshot from Cayman Chemical (www.caymanchem.com/app/template/Product.vm/catalog/11138).

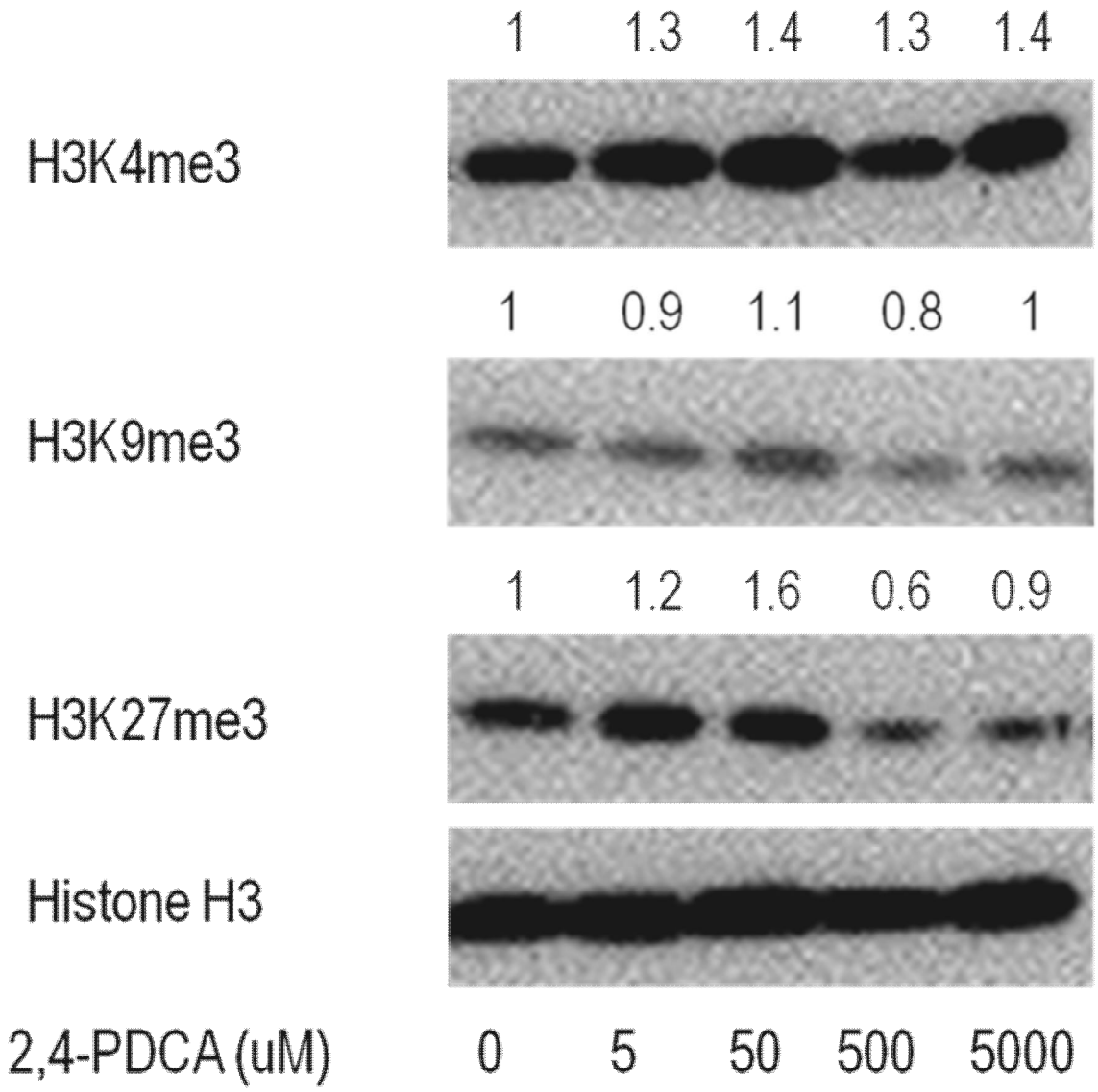

Figure 5-20 Dose-Response Effect of 2,4-PDCA on Histone Methylation

Caco-2 cells were incubated with a ten-fold serial dilution of 2,4-PDCA starting at 5000 µM for 72 hours. Histones were extracted according to the Histone Acid Extraction Protocol from Abcam and the amount measured by BCA assay. Equal amounts of histone protein were loaded onto 12% agarose gels and separated by gel electrophoresis before being transferred to PVDF membranes. Membranes were blocked in 5% milk in 0.1% TBST, incubated with the primary antibody (Histone H3, H3K4me3, H3K9me3 or H3K27me3) at 4 °C overnight and detected with an anti-rabbit secondary antibody. Bands were visualised using ECL detection reagent and hyperfilm developer. ImageJ software was used to normalise the histone H3 bands to each other and calculate the adjusted density values for each histone methylation marker. Representative of n=6 experiments – see Figure 5-21.

Caco-2 cells were incubated with a range of concentrations of 2,4-PDCA, serially diluted ten-fold from 5 mM to 5 μM, for 72 hours. As expected, as the concentration of 2,4-PDCA increases, so does the amount of histone tri-methylation on lysine 4 (Figure 5-20). The level of H3K9me3 does not differ over the range of 2,4-PDCA concentrations tested. H3K27me3 levels vary over the range of concentrations tested but they do not change in a consistent manner (Figure 5-20). 2,4-PDCA can only be said to have a consistent effect on H3K4me3.

The fold changes in methylation resulting from 2,4-PDCA were plotted as shown in Figure 5-21. H3K27me3 (shown in brown) does not significantly vary as the concentration of 2,4-PDCA increases. This is as expected as 2,4-PDCA is not known to have activity against any H3K27 specific demethylases. Whilst both H3K4me3 and H3K9me3 show a ~2.5-fold increase in methylation levels when incubated with 5000 μM 2,4-PDCA, only H3K4me3 is a statistically significant increase ($P<0.05$). The increase in H3K4me3 only being significant was unexpected as the increase in H3K9me3 was as large. However, previous studies on the crystal structure of histone demethylases bound to 2,4-PDCA show that 2,4-PDCA is more potent in H3K4-specific demethylases (200). Therefore, all further experiments with 2,4-PDCA will use 5000 μM.

Figure 5-22 represents the MFI (median fluorescence intensity) of H3K4me3, H3K9me3 and H3K27me3 in Caco-2 cells incubated with 5 mM 2,4-PDCA as a percentage of the methylation level of each residue in Caco-2 cells that have not been incubated with 2,4-PDCA. H3K27me3 levels were unaltered by 2,4-PDCA, comparable to the Western blotting results. Both H3K4me3 and H3K9me3 levels were shown to increase, by a statistically significant amount ($P<0.001$ and $P<0.01$, respectively) when Caco-2 cells are incubated with 5 mM 2,4-PDCA (Figure 5-22). Only H3K4me3 levels were shown to increase in the presence of 2,4-PDCA in Western blotting, probably due to the increased sensitivity of the multiplex assay.

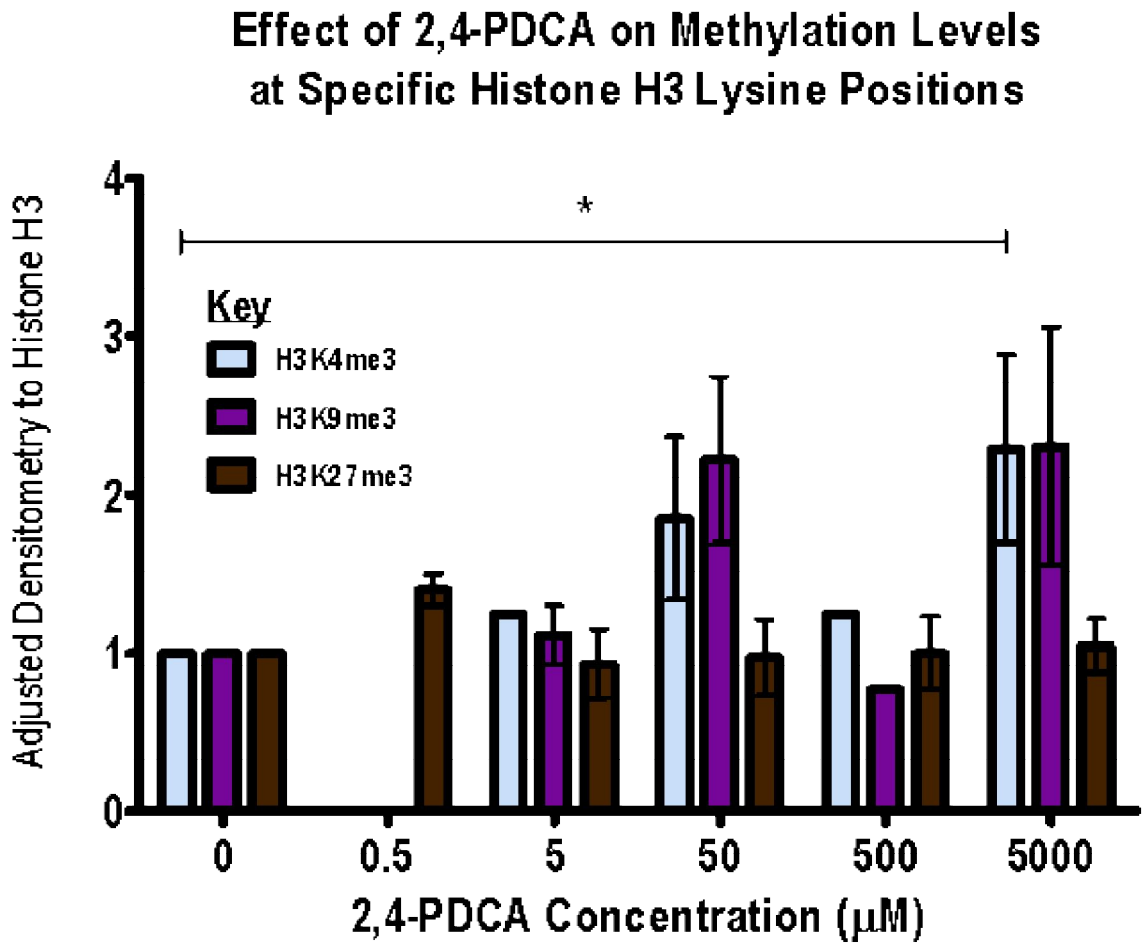

Figure 5-21 Effect of 2,4-PDCA on Methylation Levels at Specific Histone H3 Lysine Positions

For each western blot, Caco-2 cells were incubated with a ten-fold serial dilution of 2,4-PDCA ranging from 5 mM to 0.5 μM for 24 hours. Histones were extracted according to the Histone Acid Extraction Protocol from Abcam and the amount measured by BCA assay. Equal amounts of histone protein were loaded onto 12% agarose gels and separated by gel electrophoresis before being transferred to PVDF membranes. Membranes were blocked in 5% milk in 0.1% TBST, incubated with the primary antibody (Histone H3, H3K4me3, H3K9me3 or H3K27me3) at 4 °C overnight and detected with an anti-rabbit secondary antibody. Bands were visualised using ECL detection reagent and hyperfilm developer. ImageJ software was used to normalise the histone H3 bands to each other and calculate the adjusted density values for each histone methylation marker. The fold changes in adjusted density for each methylation marker were plotted in a bar chart and statistical analysis was performed using the Student's *t*-test. n = 6. * represents $P<0.05$.

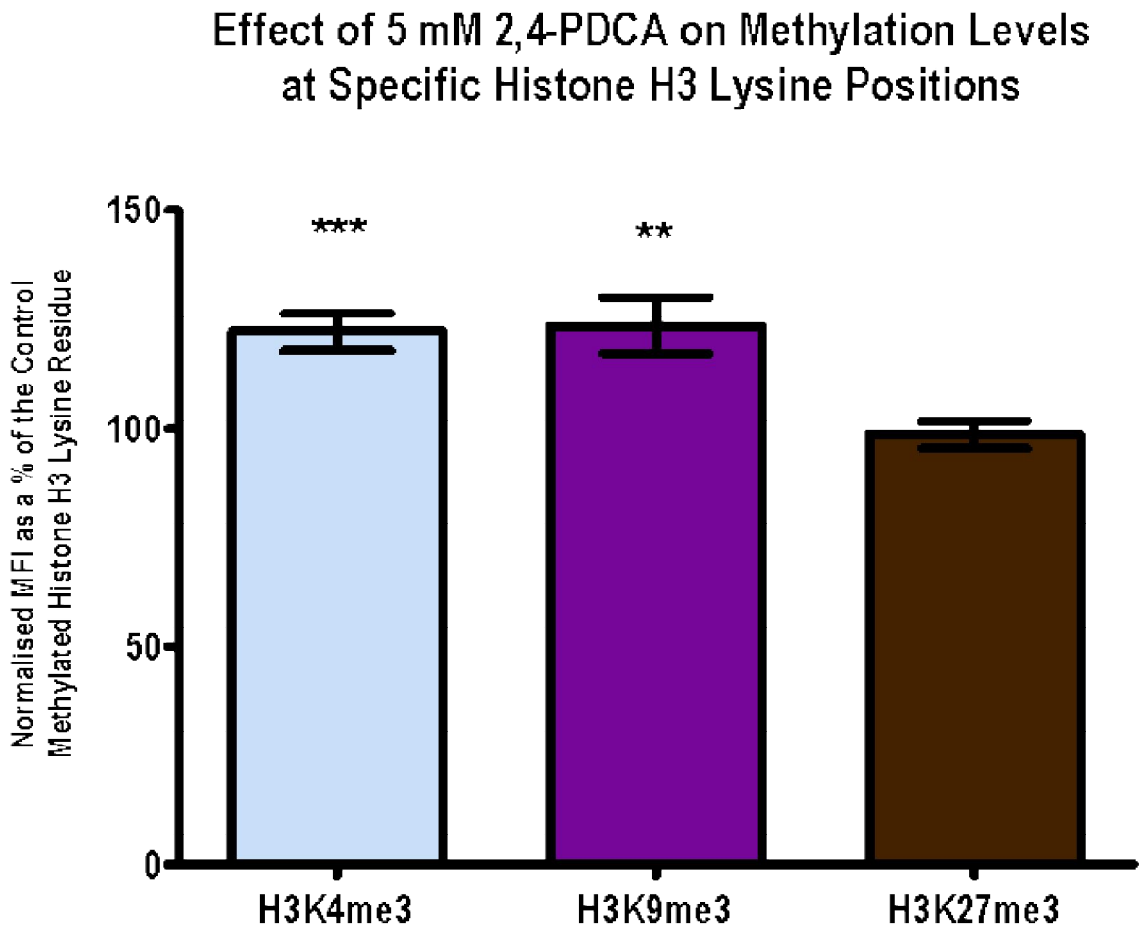

Figure 5-22 Effect of 5 mM 2,4-PDCA on Methylation Levels at Specific Histone H3 Lysine Positions

Caco-2 cells were incubated with 0 and 5 mM 2,4-PDCA for 24 hours. Histones were extracted according to the Histone Acid Extraction Protocol from Abcam and the amount measured by BCA assay. Equal amounts of histone protein were analysed for methylation levels of H3K4me3, H3K9me3 and H3K27me3 using the Histone H3 PTM Multiplex kit from Active Motif. Histone proteins were incubated with H3K4me3, H3K9me3 and H3K27me3 antibody conjugated magnetic beads. Biotinylated Histone H3 antibody and streptavidin-phycoerythrin were added and the resulting fluorescent complex was read by a MAGPIX™ instrument with xPONENT® software. The amount of fluorescence (MFI) for each methylated residue was normalized to total Histone H3. Multiple experiments were combined by plotting the MFI of each methylated residue at 5 mM 2,4-PDCA as a percentage of the MFI of each methylated residue at 0 mM 2,4-PDCA (control). Statistical analysis was performed using the Student's *t*-test. n=3. ** and *** represent $P<0.01$ and $P<0.001$, respectively.

5.4 Effect of Histone Demethylase Inhibition on Immune Tolerance in Intestinal Epithelial Cells

5.4.1 Pargyline hydrochloride

As described in Foster *et al*., pargyline is a known epigenetic modifier that alters tolerance. 3 mM pargyline hydrochloride was incubated with control, stimulated and tolerized Caco-2 cells for 1 hour 25 hours before sample collection and again for 12 hours before sample collection. As shown in Figure 5-23, pargyline causes the production of CXCL8 to increase dramatically in stimulated and unstimulated (control) cells ($P<0.001$ and <0.01, respectively). It breaks tolerance by increasing the CXCL8 production of tolerized cells ($P<0.001$) though the amount is less than stimulated only cells ($P<0.001$). The production of CXCL8 by tolerized + pargyline cells is still much less than the amount produced by stimulated + pargyline cells, as expected. The important difference is the change in CXCL8 expression between tolerized cells and tolerized + epigenetically inhibited cells.

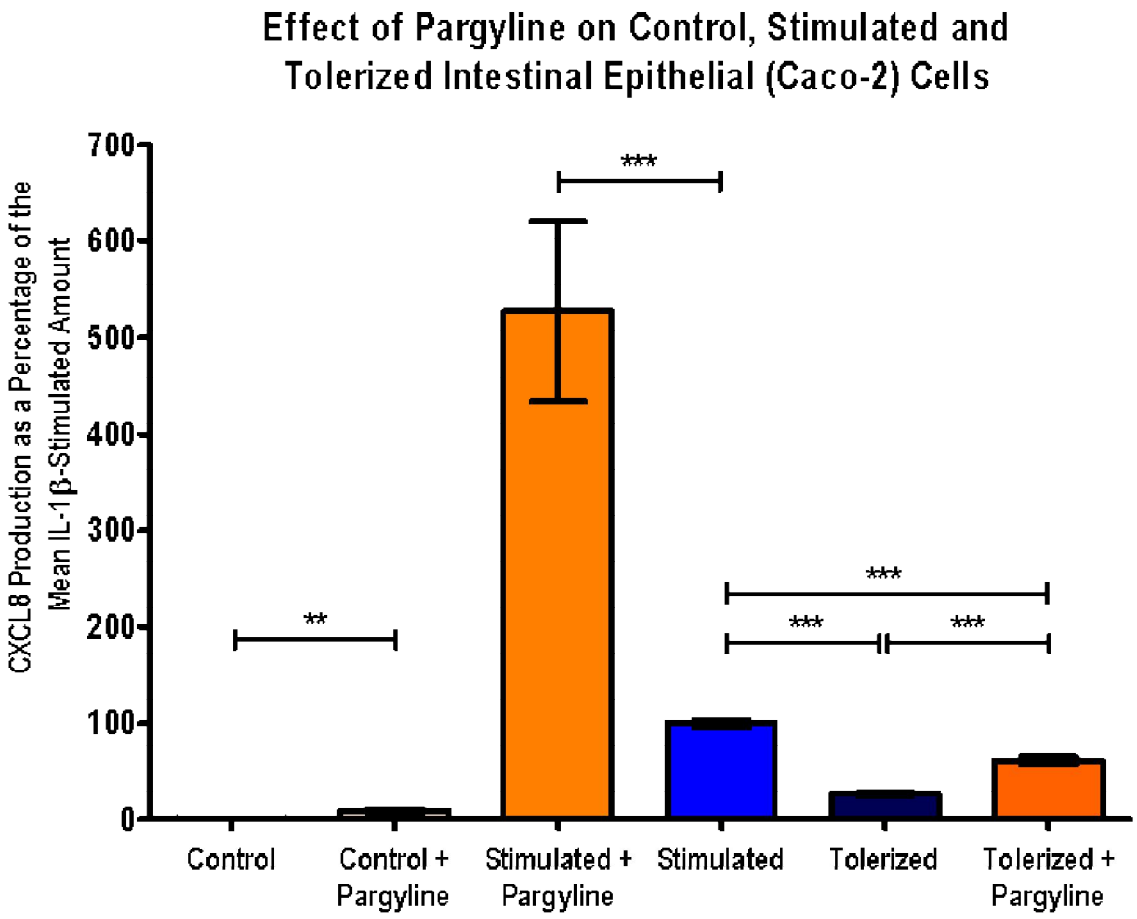

Figure 5-23 Effect of Pargyline on Control, Stimulated and Tolerized Intestinal Epithelial (Caco-2) Cells

Caco-2 cells were stimulated with 1 ng/ml IL-1β for 24 hours and tolerized by a prior stimulation of 1 ng/ml IL-1β 24 hours earlier, as described in Figure 3-2. Pargyline was added directly to the cells at a concentration of 3 mM for 1 hour prior to the second IL-1β-stimulation and again 12 hours prior to sample collection, as described in Figure 5-24. CXCL8 production was measured by ELISA and normalized to cellular protein content (measured by BCA protein assay). Multiple experiments were combined by calculating CXCL8 production as a percentage of the mean CXCL8 production per single stimulation of IL-1β. Bars represent mean ± SEM, n = 5. Statistical analysis was performed using the Student's *t*-test and Mann-Whitney U test. ** and *** represent $P<0.01$ and <0.001, respectively.

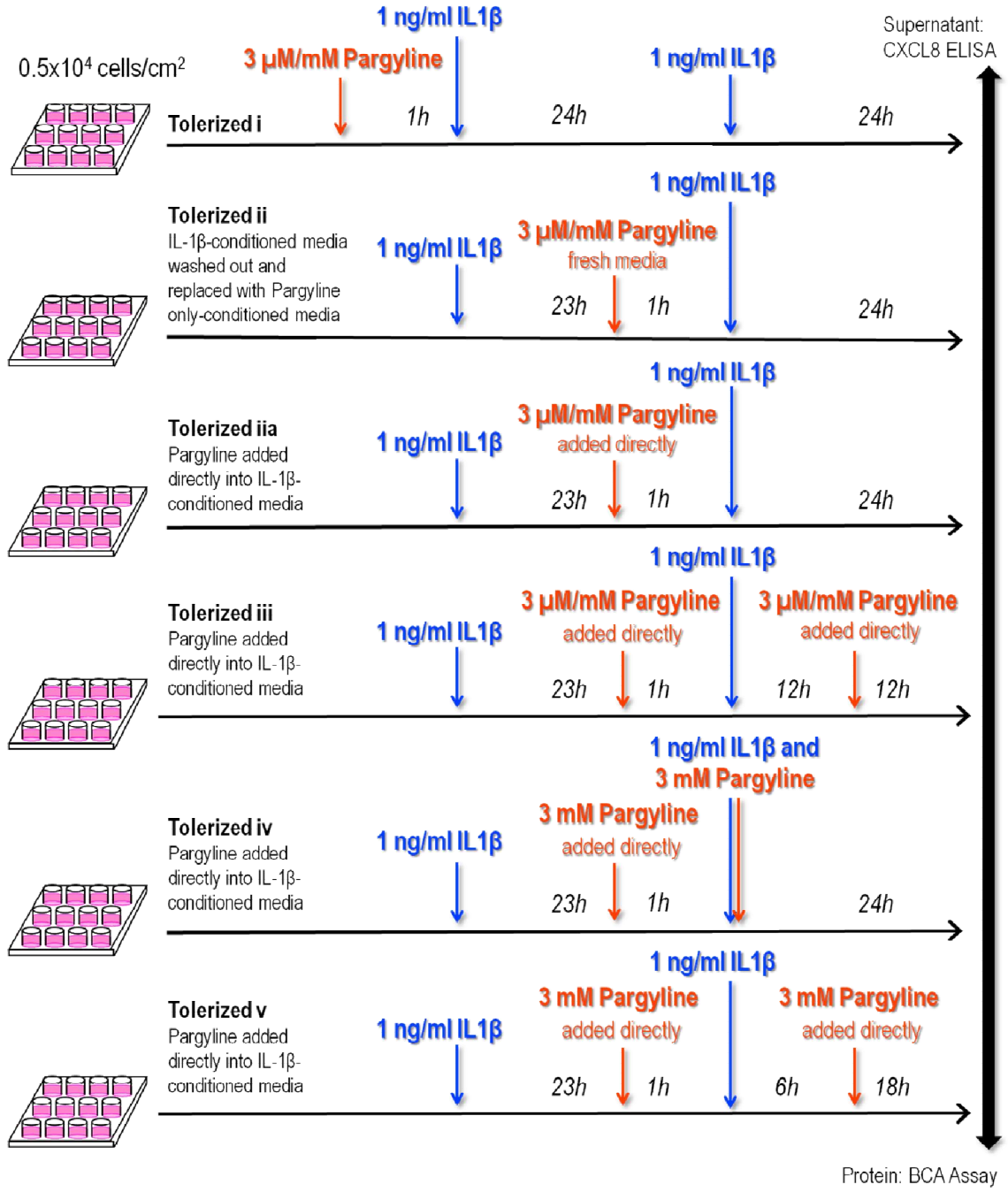

Figure 5-24 Schematic Diagram of the Different Pargyline Incubation Time Points in Tolerized Cells

A schematic diagram highlighting the different time points for pargyline incubation in tolerized cell experiments. In the first version, tolerized i, Caco-2 cells were incubated with 3 µM or 3 mM pargyline hydrochloride for 1 hour prior to the first stimulation with 1 ng/ml IL-1β. For both tolerized ii and tolerized iia, 3 µM or 3 mM pargyline hydrochloride was incubated with the cells for 1 hour prior to the second stimulation with IL-1β. Pargyline was added directly to the cells in tolerized iia whilst the IL-1β-conditioned media was washed out of the cells before the pargyline was added in tolerized iia. In tolerized iii, Caco-2 cells were incubated twice with 3 µM or 3 mM pargyline hydrochloride, the first for 1 hour prior to the second IL-1β-stimulation and the second was added directly to the cells 12 hours before sample collection. Tolerized iv and tolerized v were incubated with 3 mM pargyline hydrochloride for 1 hour prior to the second stimulation with IL-1β and again for 24 hours and 18 hours, respectively, before sample collection. Media supernatants are measured for CXCL8 by ELISA and normalized to total protein, as determined by BCA Assay.

A number of different time points were investigated to find the optimum condition required for Pargyline to break tolerance, as described in Figure 5-24. A single one hour stimulation of 3 μM pargyline hydrochloride was added to the Caco-2 cells as described in Foster *et al* before the first IL-1β stimulation (i), before the second IL-1β stimulation where the media containing the IL-1β from the first stimulation is washed out and fresh 3 μM pargyline containing media is added (ii), added directly into the media before the second IL-1β stimulation (iia) and before the second IL-1β stimulation and again added directly into the media 12 hours before sample collection (iii). As shown in Figure 5-25, incubation of tolerized cells with 3 μM pargyline hydrochloride did not produce an increase in CXCL8 production. Though 3 μM pargyline hydrochloride demonstrated inhibition of H3K4me3 and H3K9me3 demethylases by Western blotting (Figure 5-17), Figure 5-25 shows that it was not able to break tolerance.

3 μM Pargyline hydrochloride, has been demonstrated by Foster *et al* to break tolerance in macrophages (87), but as was demonstrated in Figure 5-25, it was not able to break tolerance in intestinal epithelial cells. 3 mM Pargyline hydrochloride was used under the same time conditions apart from condition tolerized + pargyline iv (Figure 5-24) where the second pargyline incubation was for 24 hours. CXCL8 production was only increased when the second pargyline incubation was for 24 hours ($P<0.001$) (Figure 5-26). From observation, a large proportion of cells died during condition tolerization + pargyline iv. As CXCL8 was normalized to total protein content, this should be corrected for. However, it is possible that the smaller protein amount in condition tolerized + pargyline iv could result in artificially increased CXCL8 expression if the amount of protein at the end of the assay does not represent the amount of protein (i.e. viable cells) throughout the experiment. The experiment was redesigned to account for this.

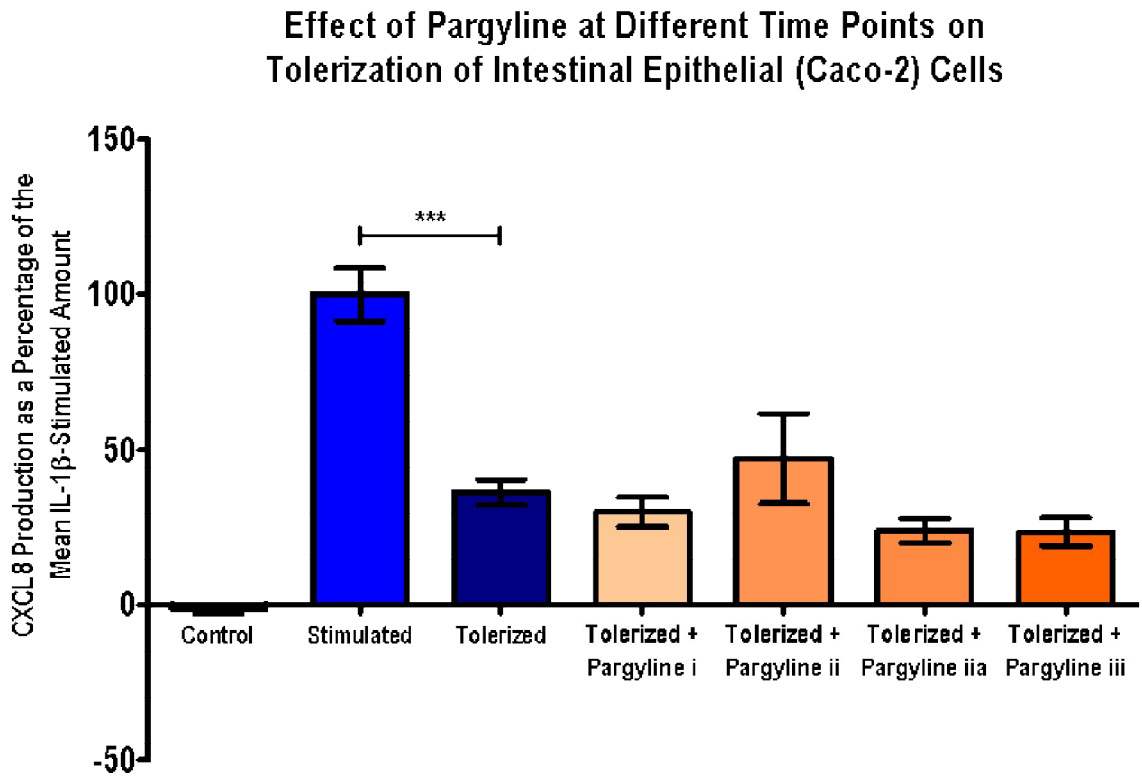

Figure 5-25 Effect of Pargyline at Different Time Points on Tolerization of Intestinal Epithelial (Caco-2) Cells

Caco-2 cells were stimulated with 1 ng/ml IL-1β for 24 hours and tolerized by a prior stimulation of 1 ng/ml IL-1β 24 hours earlier, as described in Figure 3-2. 3 µM Pargyline hydrochloride was added to the pre-stimulated Caco-2 cells at different time points according to Figure 5-24. CXCL8 production was measured by ELISA and normalized to cellular protein content (measured by BCA protein assay). Multiple experiments were combined by calculating CXCL8 production as a percentage of the mean CXCL8 production per single stimulation of IL-1β. Bars represent mean ± SEM, n = 3. Statistical analysis was performed using the Student's *t*-test and Mann-Whitney U test. *** represents $P<0.001$.

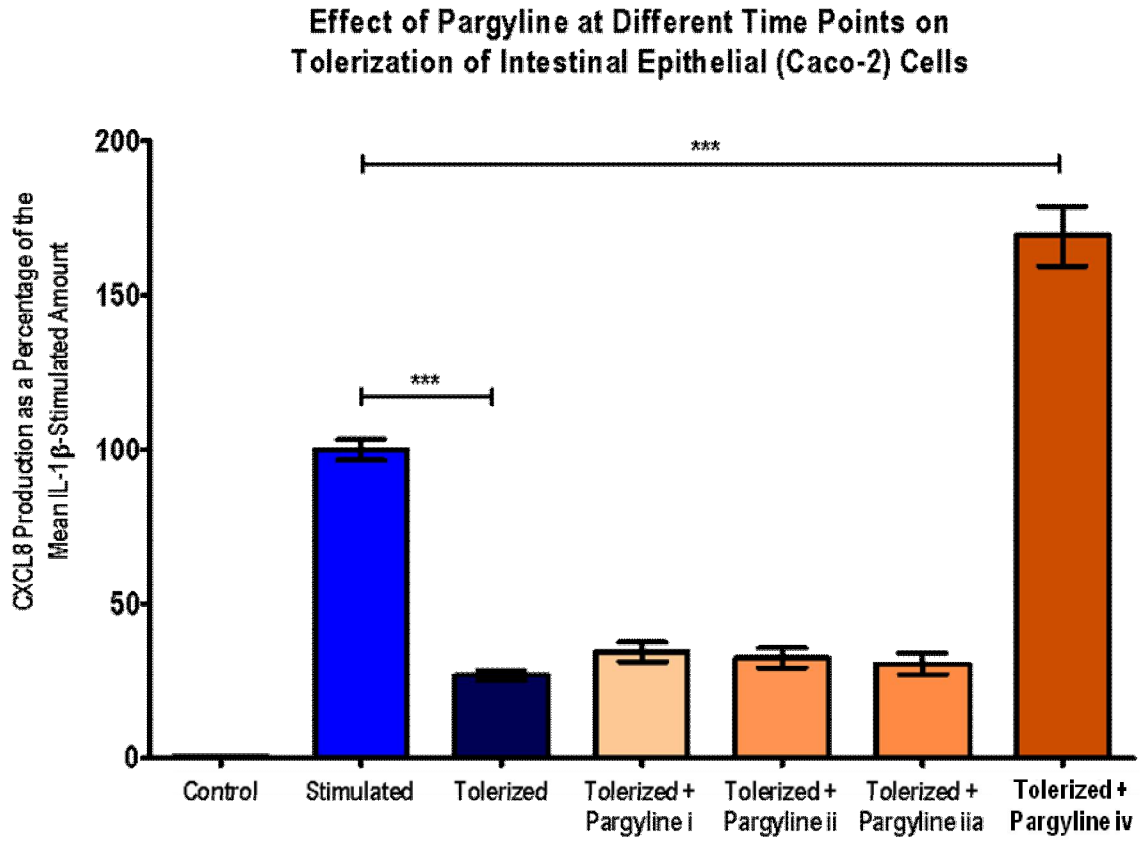

Figure 5-26 Effect of Pargyline at Different Time Points on Tolerization of Intestinal Epithelial (Caco-2) Cells

Caco-2 cells were stimulated with 1 ng/ml IL-1β for 24 hours and tolerized by a prior stimulation of 1 ng/ml IL-1β 24 hours earlier, as described in Figure 3-2. 3 mM Pargyline hydrochloride was added to the pre-stimulated Caco-2 cells at different time points according to Figure 5-24. CXCL8 production was measured by ELISA and normalized to cellular protein content (measured by BCA protein assay). Multiple experiments were combined by calculating CXCL8 production as a percentage of the mean CXCL8 production per single stimulation of IL-1β. Bars represent mean ± SEM, n = 3. Statistical analysis was performed using the Student's *t*-test and Mann-Whitney U test. *** represents $P<0.001$.

Due to 24 hours being too long an incubation period for cell viability, another range of time periods for the second pargyline incubation were tested: 12 and 18 hours. Incubation for both 12 and 18 hours breaks tolerance by increasing CXCL8 production to greater than that of tolerized only cells, though both are lower than stimulated only cells ($P<0.001$) (Figure 5-27).

There is no statistically significant difference between the amounts of CXCL8 produced when the cells are incubated with 3 mM pargyline hydrochloride for 12 hours (iii) or 18 hours (v). Therefore, the results from incubation for 12 and 18 hours were pooled for clarity (Figure 5-28). Figure 5-28 shows that two incubations of 3 mM pargyline hydrochloride for one hour then at least 12 hours is sufficient to break tolerance and that tolerance is broken by an epigenetic factor.

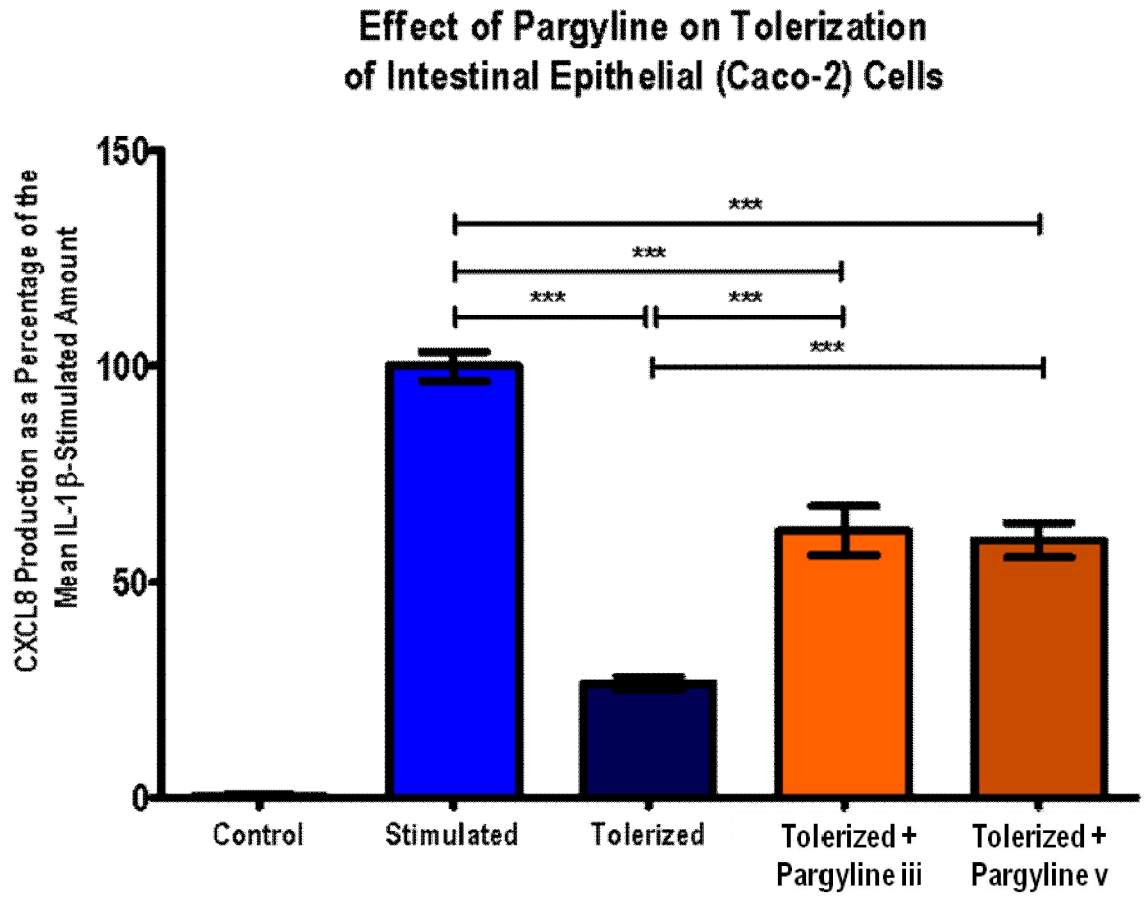

Figure 5-27 Effect of Pargyline on Tolerization of Intestinal Epithelial (Caco-2) Cells

Caco-2 cells were stimulated with 1 ng/ml IL-1β for 24 hours and tolerized by a prior stimulation of 1 ng/ml IL-1β 24 hours earlier, as described in Figure 3-7. 3 mM Pargyline hydrochloride was added directly to pre-stimulated Caco-2 cells according to Figure 5-24. CXCL8 production was measured by ELISA and normalized to cellular protein content (measured by BCA protein assay). Multiple experiments were combined by calculating CXCL8 production as a percentage of the mean CXCL8 production per single stimulation of IL-1β. Bars represent mean ± SEM, n = 4. Statistical analysis was performed using the Student's *t*-test and Mann-Whitney U test. *** represents P<0.001.

.

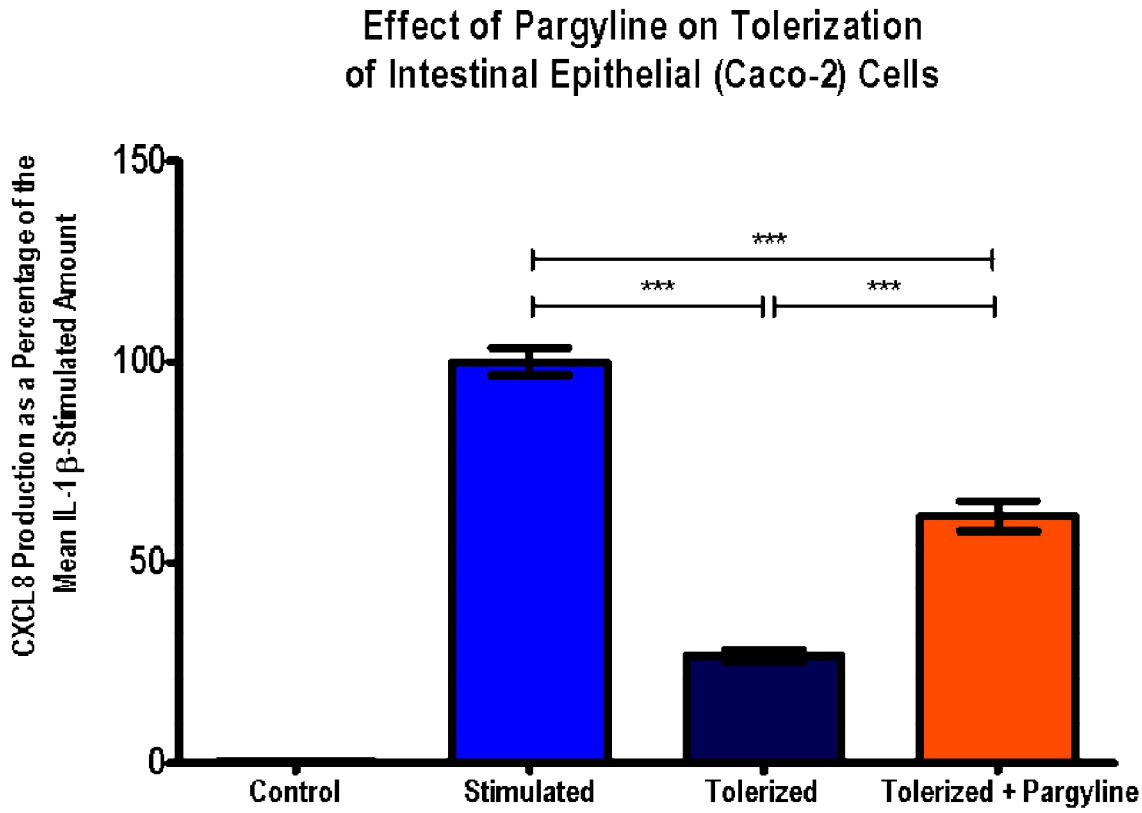

Figure 5-28 Effect of Pargyline on Tolerization of Intestinal Epithelial (Caco-2) Cells

Caco-2 cells were stimulated with 1 ng/ml IL-1β for 24 hours and tolerized by a prior stimulation of 1 ng/ml IL-1β 24 hours earlier, as described in Figure 3-7. Pargyline hydrochloride was incubated with cells as described in tolerized + pargyline iii and tolerized + pargyline v in Figure 5-24. CXCL8 production was measured by ELISA and normalized to cellular protein content (measured by BCA protein assay). Multiple experiments were combined by calculating CXCL8 production as a percentage of the mean CXCL8 production per single stimulation of IL-1β. The results from tolerized + pargyline iii and tolerized + pargyline v were pooled together and represented as one samples, as indicated in Figure 5-27. Bars represent mean ± SEM, n = 8. Statistical analysis was performed using the Student's *t*-test and Mann-Whitney U test. *** represents P<0.001.

The effect of pargyline on tolerized cells is also shown in Figure 5-29, but the original normalized CXCL8 values in pg/mg protein are plotted instead of percentages of the mean stimulated amount. Like the same conditions in Figure 5-28, Figure 5-29 shows that the tolerized cells express about a third of the amount of CXCL8 as stimulated cells ($P<0.001$). The tolerized cells that are incubated with 3 mM pargyline hydrochloride express a statistically significant greater amount of CXCL8 than tolerized cells alone do ($P<0.001$) (Figure 5-29). Due to the greater range of values in each condition, the amount of CXCL8 produced by tolerized + pargyline cells is shown as being statistically significantly greater than in stimulated cells ($P<0.05$) (Figure 5-29) whereas in Figure 5-28 tolerized + pargyline cells express a statistically significant reduction in CXCL8 compared to stimulated cells ($P<0.001$). The error bars in Figure 5-29 are much larger than in Figure 5-28, thereby contributing to the change in relationship between stimulated and tolerized + pargyline cells. Both show that pargyline breaks tolerance, as there is an associated increase in the expression of CXCL8.

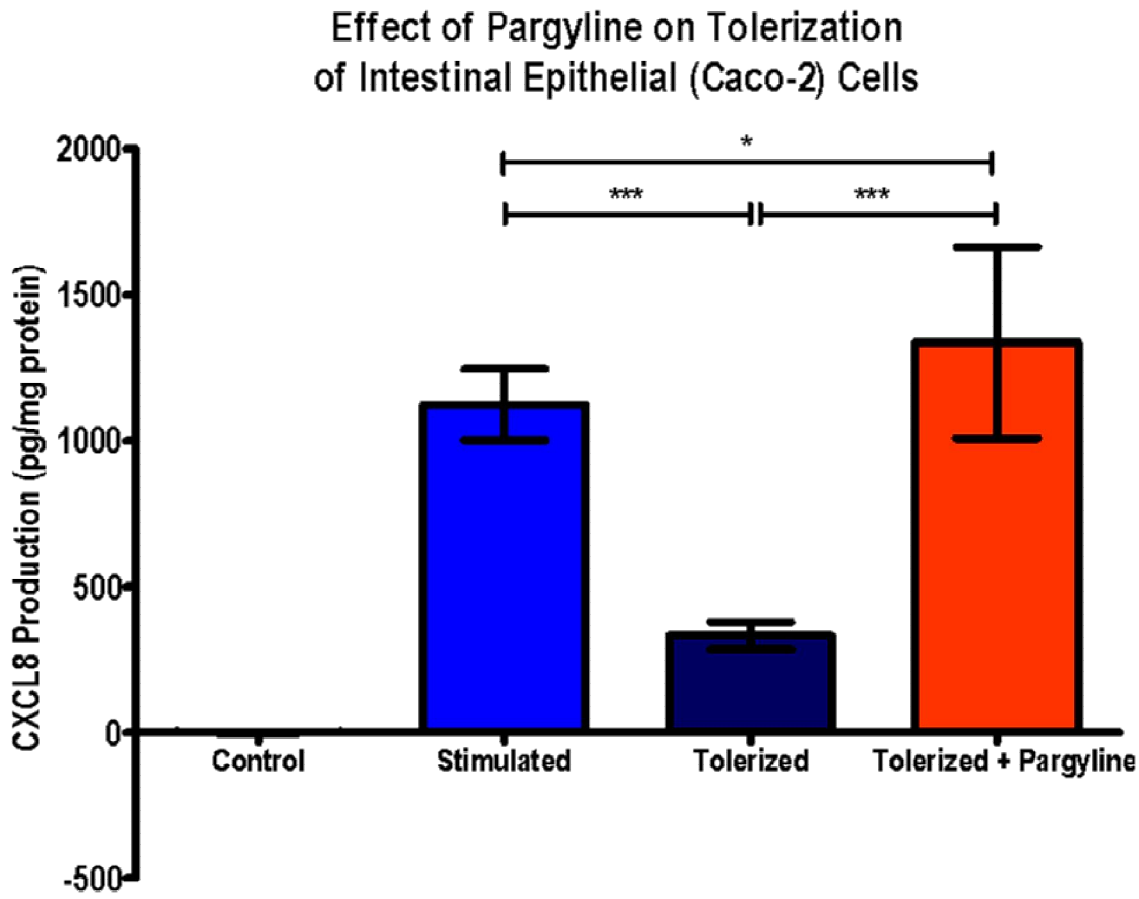

Figure 5-29 Effect of Pargyline on Tolerization of Intestinal Epithelial (Caco-2) Cells

Caco-2 cells were stimulated with 1 ng/ml IL-1β for 24 hours and tolerized by a prior stimulation of 1 ng/ml IL-1β 24 hours earlier, as described in Figure 3-7. Pargyline hydrochloride was incubated with cells as described in tolerized + pargyline iii and tolerized + pargyline v in Figure 5-24. CXCL8 production was measured by ELISA and normalized to cellular protein content (measured by BCA protein assay). The results from tolerized + pargyline iii and tolerized + pargyline v were pooled together and represented as one sample, as indicated in Figure 5-27. Bars represent mean ± SEM, n = 8. Statistical analysis was performed using the Student's *t*-test and Mann-Whitney U test. * and *** represent $P<0.01$ and <0.001, respectively.

5.4.2 2,4-Pyridinedicarboxylic Acid (2,4-PDCA)

2,4-PDCA is an alternative histone demethylase inhibitor to pargyline. A 10-fold serial dilution of 2,4-PDCA was prepared starting at 5 mM. Each 2,4-PDCA concentration was incubated with Caco-2 cells for 72 hours, beginning 24 hours before the first IL-1β stimulation (Figure 3-7). The samples were collected, CXCL8 measured by ELISA and normalised to the total protein content as measured by BCA assay. Only the highest concentration of 5 mM significantly altered the CXCL8 amount ($P<0.001$). In contrast to all other inhibition of epigenetic modifying enzymes experiments so far, CXCL8 production in tolerized cells incubated with 2,4-PDCA was lowered compared to tolerized only cells (Figure 5-30). Tolerance is not broken as CXCL8 production is reduced but epigenetic modification via 2,4-PDCA have an increased effect on tolerance.

In case the reason for the reduction in CXCL8 production was due to 2,4-PDCA causing a global reduction in gene expression, 2,4-PDCA was incubated for 48 hours with Caco-2 cells that were only stimulated once with IL-1β. This resulted in a small but statistically significant reduction in CXCL8 expression ($P<0.01$) (Figure 5-31). 5 mM 2,4-PDCA causes a reduction in CXCL8 production for both stimulated and tolerized cells ($P<0.01$ and <0.001, respectively).

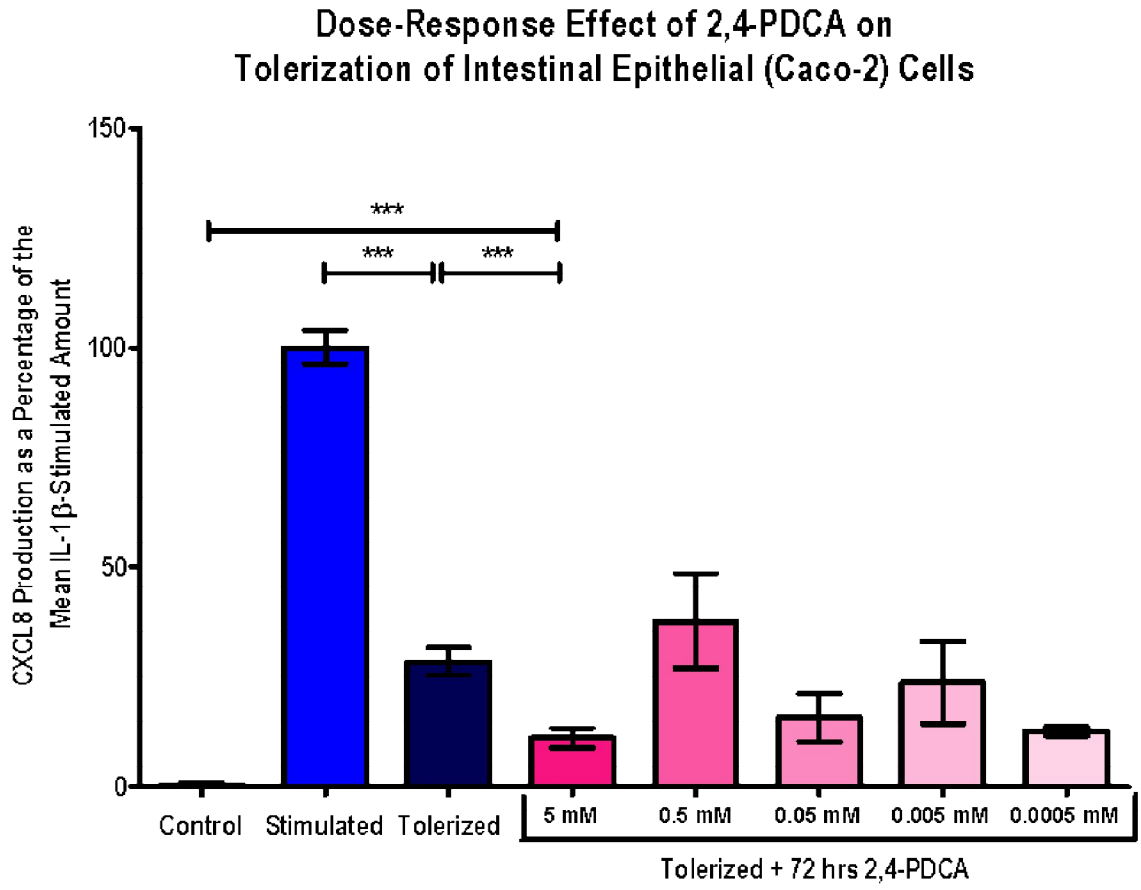

Figure 5-30 Dose-Response Effect of 2,4-PDCA on Tolerization of Intestinal Epithelial (Caco-2) Cells

Caco-2 cells were stimulated with 1 ng/ml IL-1β for 24 hours and tolerized by a prior stimulation of 1 ng/ml IL-1β 24 hours earlier, as described in Figure 3-2. 2,4-PDCA was diluted to the required concentrations (5-0.0005 mM) and incubated with Caco-2 cells for 72 hours in total. Fresh preparations of 2,4-PDCA (if required) and two stimulations of 1 ng/ml IL-1β 24 hours apart were added to the cells. CXCL8 production was measured by ELISA and normalized to cellular protein content (measured by BCA protein assay). Multiple experiments were combined by calculating CXCL8 production as a percentage of the mean CXCL8 production per single stimulation of IL-1β. Bars represent mean ± SEM, n = 5. Statistical analysis was performed using the Student's *t*-test and Mann-Whitney U test. *** represents P<0.001.

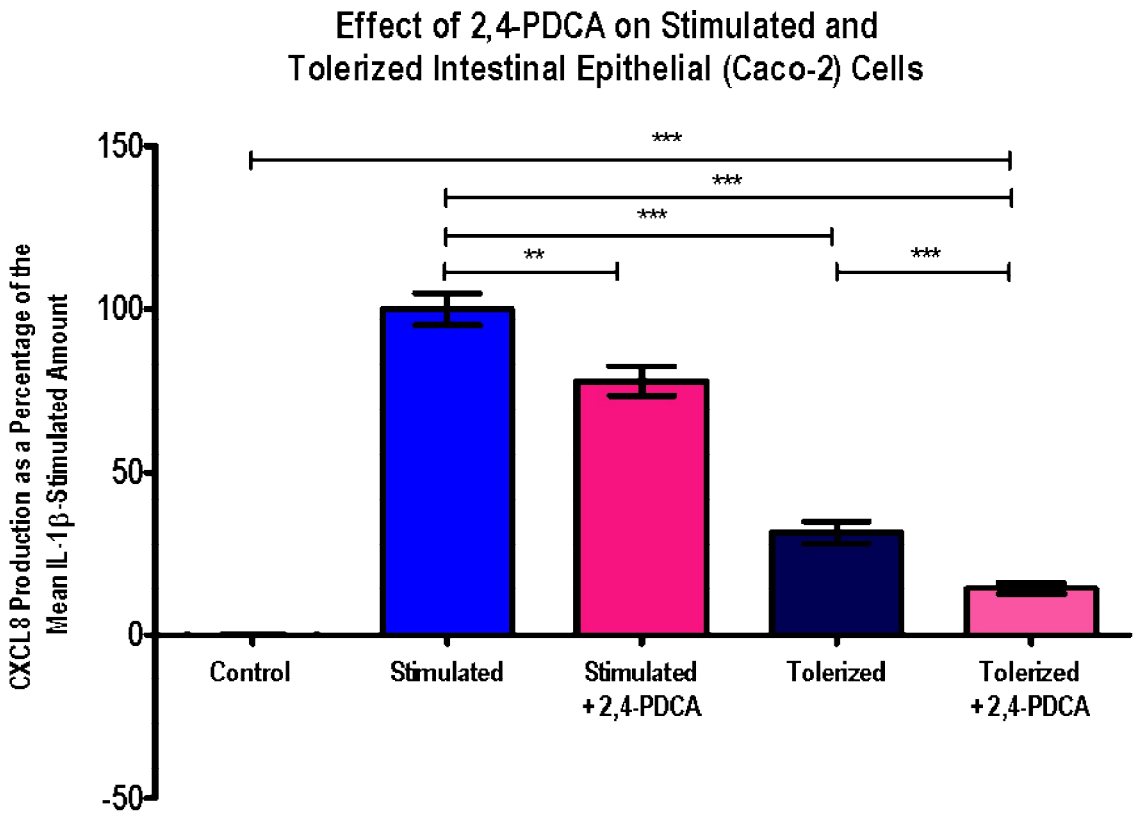

Figure 5-31 Effect of 2,4-PDCA on Stimulated and Tolerized Intestinal Epithelial (Caco-2) Cells

Caco-2 cells were stimulated with 1 ng/ml IL-1β for 24 hours and tolerized by a prior stimulation of 1 ng/ml IL-1β 24 hours earlier, as described in Figure 3-2. 2,4-PDCA was diluted to 5 mM and incubated with stimulated and tolerized Caco-2 cells for 72 hours (48 hours for stimulated cells) prior to sample collection, as described in Figure 3-7. Fresh preparations of 2,4-PDCA (if no IL-1β was required) and two stimulations of 1 ng/ml IL-1β 24 hours apart were added to the cells. CXCL8 production was measured by ELISA and normalized to cellular protein content (measured by BCA protein assay). Multiple experiments were combined by calculating CXCL8 production as a percentage of the mean CXCL8 production per single stimulation of IL-1β. Bars represent mean ± SEM, n = 6. Statistical analysis was performed using the Student's *t*-test and Mann-Whitney U test. ** and *** represent $P<0.01$ and <0.001, respectively.

The effect of 2,4-PDCA on tolerized cells is also shown in Figure 5-32, but the original normalized CXCL8 values in pg/mg protein are plotted instead of percentages of the mean stimulated amount. Like the same conditions in Figure 5-31, Figure 5-32 shows that the tolerized cells express about a third of the amount of CXCL8 as stimulated cells ($P<0.001$). The tolerized cells that are incubated with 5 mM 2,4-PDCA express a statistically significant decreased amount of CXCL8 than tolerized cells alone do ($P<0.01$) (Figure 5-32). Due to the greater range of values in each condition, the amount of CXCL8 produced by tolerized + 2,4-PDCA cells is shown as being statistically significantly decreased than in tolerized cells ($P<0.01$) (Figure 5-32) whereas in Figure 5-31 this is more statistically significant ($P<0.001$). The error bars in Figure 5-32 are slightly larger than in Figure 5-31, thereby contributing to the change in statistical significance.

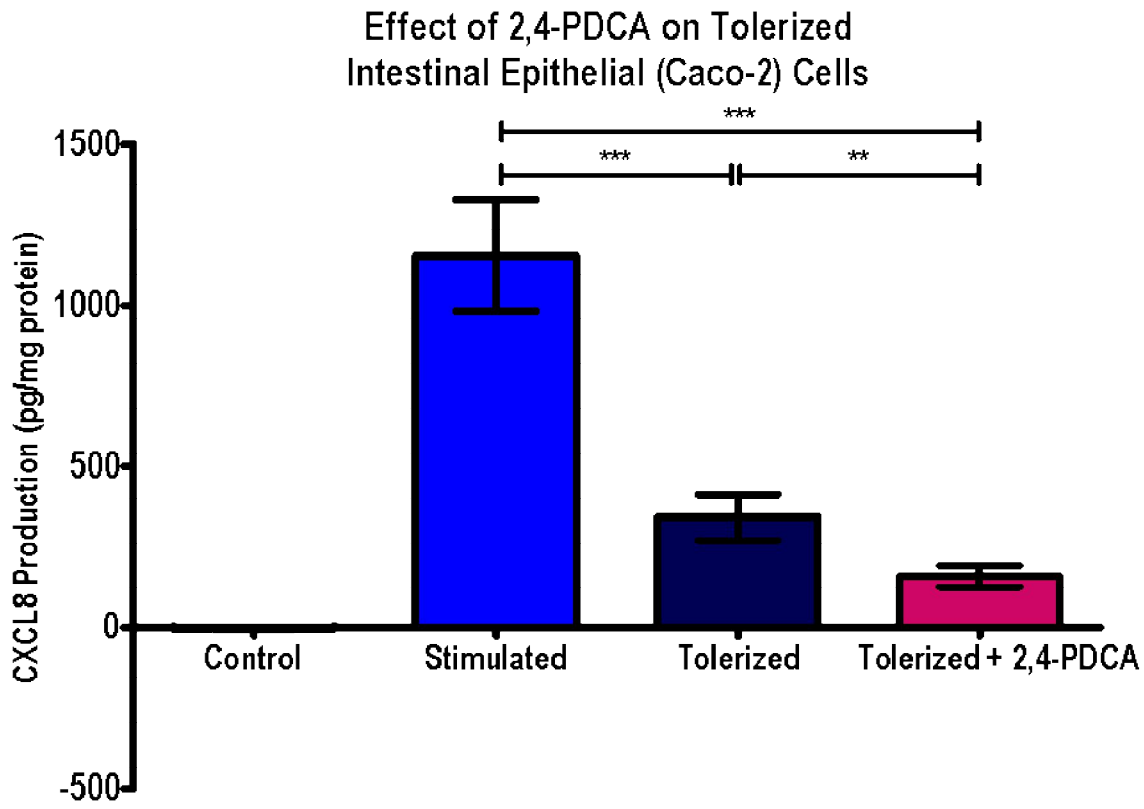

Figure 5-32 Effect of 2,4-PDCA on Tolerized Intestinal Epithelial (Caco-2) Cells

Caco-2 cells were stimulated with 1 ng/ml IL-1β for 24 hours and tolerized by a prior stimulation of 1 ng/ml IL-1β 24 hours earlier, as described in Figure 3-2. 2,4-PDCA was diluted to 5 mM and incubated with tolerized Caco-2 cells for 72 hours prior to sample collection, as described in Figure 3-7. Fresh preparations of 2,4-PDCA and two stimulations of 1 ng/ml IL-1β 24 hours apart were added to the cells. CXCL8 production was measured by ELISA and normalized to cellular protein content (measured by BCA protein assay). Bars represent mean ± SEM, n = 6. Statistical analysis was performed using the Mann-Whitney U test. ** and *** represent $P<0.01$ and <0.001, respectively.

The effect of 2,4-PDCA on stimulated cells was investigated further. Stimulated Caco-2 cells were incubated with 5 mM 2,4-PDCA for 24 (prior to or with IL-1β stimulation) or 48 hours. Neither incubation for 24 hours showed a difference in CXCL8 production compared to stimulated only cells (Figure 5-33). Only stimulated cells incubated with 2,4-PDCA for 48 hours resulted in a decrease in CXCL8 production ($P<0.01$).

The important time points required for 2,4-PDCA to have an effect on tolerance were investigated by incubating Caco-2 cells with 5 mM 2,4-PDCA for 24 (prior to IL-1β stimulation, with the first IL-1β stimulation and with the second IL-1β stimulation), 48 (not including the second IL-1β stimulation and not including the 24 hours before IL-1β stimulation) and 72 hours. 24 hours incubation did not result in a statistically different production of CXCL8 (Figure 5-34). Both versions of 48 hours incubation caused a change in CXCL8 production. Cells incubated for 72-24 hours resulted in a slightly increased production of CXCL8 compared to tolerized only cells ($P<0.001$) as well as cells incubated for 72 hours ($P<0.001$). Cells incubated with 2,4-PDCA for 48-0 hours expressed significantly lower CXCL8 than tolerized only cells ($P<0.001$), cells incubated for 72-24 hours ($P<0.01$) and cells incubated for 72 hours ($P<0.05$).

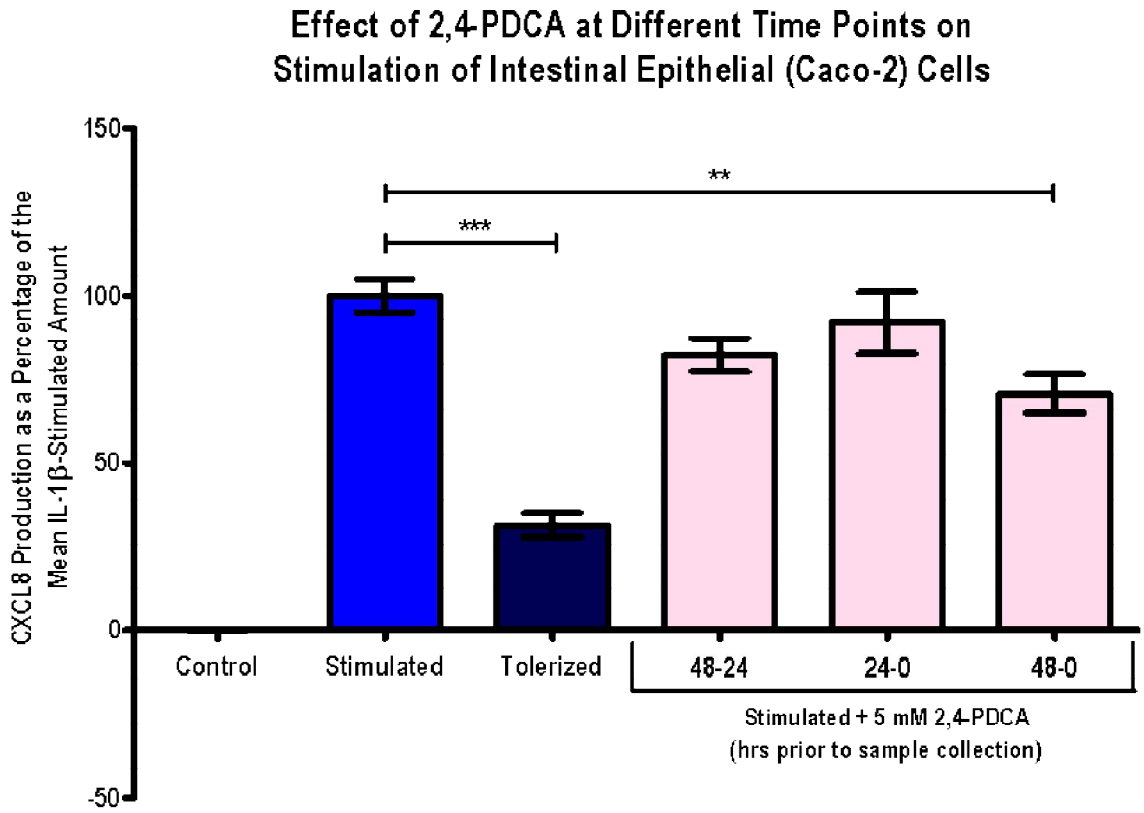

Figure 5-33 Effect of 2,4-PDCA at Different Time Points on Stimulation of Intestinal Epithelial (Caco-2) Cells

Caco-2 cells were stimulated with 1 ng/ml IL-1β for 24 hours and tolerized by a prior stimulation of 1 ng/ml IL-1β 24 hours earlier, as described in Figure 3-2. 2,4-PDCA was added directly to IL-1β-stimulated Caco-2 cells at a concentration of 5 mM for 24 or 48 hours prior to sample collection. CXCL8 production was measured by ELISA and normalized to cellular protein content (measured by BCA protein assay). Multiple experiments were combined by calculating CXCL8 production as a percentage of the mean CXCL8 production per single stimulation of IL-1β. Bars represent mean ± SEM, n = 3. Statistical analysis was performed using the Student's *t*-test and Mann-Whitney U test. ** and *** represent P<0.01 and <0.001, respectively.

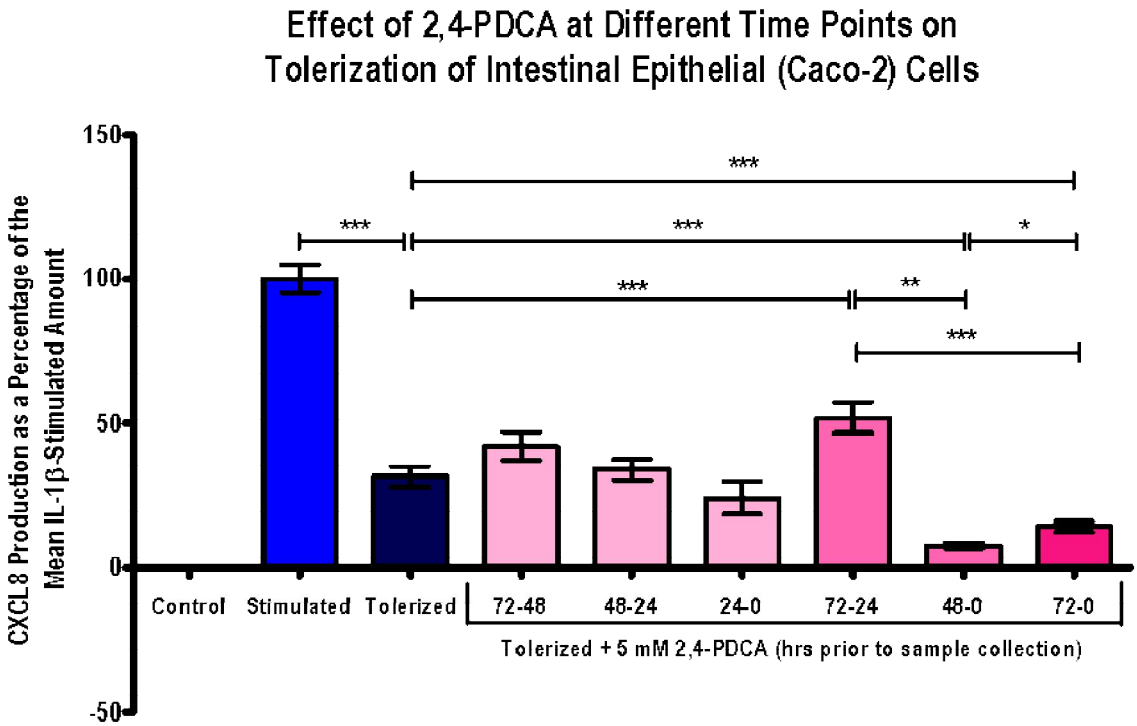

Figure 5-34 Effect of 2,4-PDCA at Different Time Points on Tolerization of Intestinal Epithelial (Caco-2) Cells

Caco-2 cells were stimulated with 1 ng/ml IL-1β for 24 hours and tolerized by a prior stimulation of 1 ng/ml IL-1β 24 hours earlier, as described in Figure 3-2. 2,4-PDCA was diluted to 5 mM and incubated with Caco-2 cells for 24, 48 or 72 hours prior to sample collection. Fresh preparations of 2,4-PDCA (if required) and two stimulations of 1 ng/ml IL-1β 24 hours apart were added to the cells. CXCL8 production was measured by ELISA and normalized to cellular protein content (measured by BCA protein assay). Multiple experiments were combined by calculating CXCL8 production as a percentage of the mean CXCL8 production per single stimulation of IL-1β. Bars represent mean ± SEM, n = 5. Statistical analysis was performed using the Student's *t*-test and Mann-Whitney U test. *, ** and *** represent $P<0.05$, <0.01 and <0.001, respectively.

5.5 Conclusions

A number of small molecule epigenetic inhibitors were tested for their effect on global histone H3 lysine methylation levels in intestinal epithelial (Caco-2) cells. The empirically determined effects of SAH, Chaetocin, pargyline and 2,4-PDCA on histone H3 lysine tri-methylation levels and tolerance are summarised in Table 5-2. Though some of the effects are easily explained and conform to previously published data, others are contradictory and cannot be fully explained by the results obtained here. Whilst bearing in mind that there are severe limitations on the conclusions that can be drawn from this data, some general effects can be seen.

The SU(VAR)3-9-specific histone methyltransferase inhibitor Chaetocin caused a statistically significant decrease in the relative amount of H3K9me3 and a non-significant reduction in H3K27me3 levels. These two epigenetic marks are associated with repression of gene transcription (122). The reduction in H3K9me3 and H3K27me3 releases genes from their repressed state so that they are able to be transcribed. As shown in Figure 5-13, transcription of CXCL8 was increased when tolerized Caco-2 cells were incubated with Chaetocin. Therefore, inhibition of a H3K9-specific histone methyltransferase results in a reduction in H3K9me3 levels and an increase in gene expression, to a statistically significant amount to break tolerance.

Incubation of tolerized Caco-2 cells with pargyline also resulted in a statistically significant increase in the production of CXCL8 (Figure 5-28). Pargyline caused a statistically significant increase in the relative amounts of both H3K4me3 and H3K9me3, though the increase in H3K4me3 levels was larger than the increase in H3K9me3 levels. H3K4me3 is associated with activation of gene transcription (122) therefore an increase in an activatory mark should result in a further increase in gene transcription. The increase in H3K4me3 levels appears to have had the

dominant effect, as expression of CXCL8 was increased by a statistically significant amount, thus breaking tolerance.

The effects of SAH and 2,4-PDCA are less straightforward to explain. Contrary to expectation, increasing concentrations of the histone methyltransferase inhibitor SAH caused the global levels of H3K27me3 to increase rather than decrease, according to measurements made by Western blotting. The opposite effect was seen with the Histone PTM Multiplex Luminex assay. A possible explanation for this is that the Luminex assay measures multiple histone marks in multiplex so an interaction between the antibodies could prevent the H3K27me3 antibody from binding to its epitope resulting in an artificially reduced amount of H3K27me3. In light of this, we took the Western blotting result as the true effect for all of the other epigenetic inhibitors.

Not only did SAH have the opposite effect on H3K27me3 levels to that expected, CXCL8 expression was also increased despite an increase in a repressive epigenetic marker. The increase in CXCL8 production was sufficient to break tolerance, even though it was only just statistically significant ($P<0.05$) (Figure 5-10). It is not known which genes the increase in H3K27me3 relative levels affects and further research is required to fully explain how SAH causes tolerance to break.

2,4-PDCA, like pargyline, caused a statistically significant increase in the relative amount of H3K4me3, as measured by both Western blotting and the Histone PTM Multiplex Luminex assay. However, unlike pargyline, tolerized Caco-2 cells incubated with 2,4-PDCA produced a statistically significant reduction of CXCL8 (Figure 5-31) and tolerance is not broken. This was an unexpected result as one would predict an increase in gene transcription with cells that have an increased amount of H3K4me3. However, Western blotting and Luminex multiplex assays

measure the global change in histone methylation levels, not the amount of histone methylation at specific genes. It is unknown which genes pargyline and 2,4-PDCA have their effects upon and it is possible that they affect different genes resulting in the contradictory effects on CXCL production and tolerance.

As shown in Figure 5-13, when the incubation length of Chaetocin was increased from 8 hours to 18 hours, the production of CXCL8 also increased, by a non-statistically significant amount. This shows that the production of CXCL8 is regulated epigenetically. None of the inhibitors caused the production of CXCL8 to increase to the same level as stimulated Caco-2 cells. Whilst this could imply that the epigenetic inhibitors were not incubated with the cells for long enough or at a high enough concentration to completely break tolerance, it is more likely that the other pathways involved in the regulation of tolerance are still effective. Tolerance is regulated by a number of redundant pathways, many of which are effective even under epigenetic manipulation, thereby preventing the production of CXCL8 from reaching the same amount as stimulated Caco-2 cells. This is the first instance of tolerance regulation in intestinal epithelial cells being shown to have an epigenetic component. At no point does this research attempt to fully explain the regulation the tolerance, nor integrate the effects of epigenetics with the other methods previously described.

Inhibitor	Effect on Relative Amount of Histone H3 Lysine Methylation			Effect on Tolerance
	H3K4me3	H3K9me3	H3K27me3	
Chaetocin	---	↓*	↓	Broken
Pargyline hydrochloride	↑*	↑*	---	Broken
S-adenosyl-L-homocysteine (SAH)	---	---	↑*	Broken
2,4-pyridinedicarboxylic acid (2,4-PDCA)	↑*	---	---	Maintained

Table 5-2 Summary of the Effect Epigenetic Inhibitors had on the Relative Amount of Histone H3 Lysine Methylation and Consequently Tolerance

A table summarising the small molecule epigenetic inhibitors of histone methyltransferases and histone demethylases used in this research with their effect on Histone H3 lysine residues. ↑ represents a fold-change increase in the amount of methylation at that particular Histone H3 lysine residue whilst ↓ represents a fold-change decrease in the amount of methylation. The size of the arrow represents the relative effect size i.e. pargyline hydrochloride has a larger effect on H3K4me3 levels than H3K9me3. Statistically significant fold-changes are indicated by a *, where * represents $P<0.05$. Statistical analysis was performed using the Student's *t*-test.

6 Specific Changes in Histone Methylation Marks at the CXCL8 Locus in Tolerized Intestinal Epithelial Cells

6.1 Histone Methylation Marks at the CXCL8 Locus

The ENCODE (Encyclopedia of DNA Elements) project is a follow-up project to the Human Genome Project, whose aim is to understand the remaining unknown parts of the genome. It investigates the role of non-protein coding or junk DNA and its role in human disease. For example, all DNase I hypersensitivity sites have been mapped in a number of cell types and disease conditions (201). DNase I hypersensitivity is an indication of open chromatin i.e. chromatin that is transcriptionally active as the RNA polymerase has access to the DNA (202). This tool was used to identify regions of the CXCL8 locus to investigate with ChIP and investigate which specific histone methylation marks were associated with the regulation of tolerance. Three regions around the CXCL8 locus were chosen for investigation: upstream of the CXCL8 promoter, the CXCL8 promoter and the gene body of CXCL8.

The region 5' upstream of the promoter was chosen (Figure 6-1) as it has been shown to be enriched in H3K9me3 as well as a small H3K4me1 and H3K4me3 enrichment, which indicates a possible enhancer region (203).

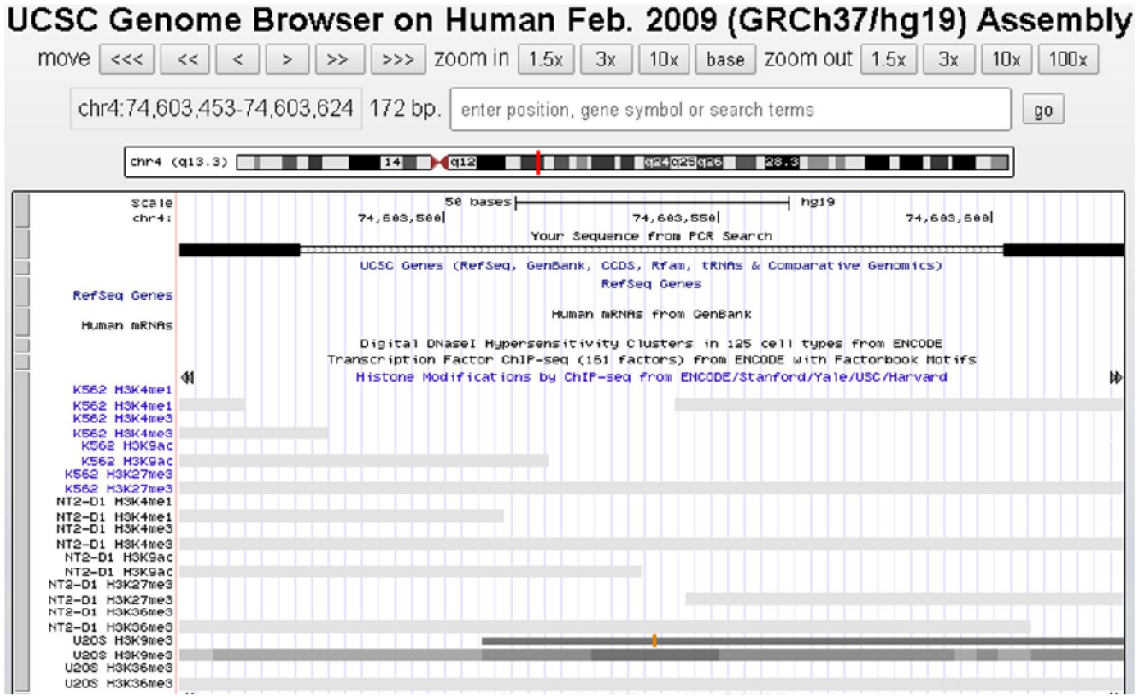

Figure 6-1 Chromosomal Location of the qPCR Product for ChIP Analysis of the Locus 5' Upstream of the CXCL8 Promoter

ENCODE data was used to identify the epigenetic signatures present 5' upstream of the CXCL8 promoter region. The PCR function in the UCSC genome browser was used to illustrate the location of the primer pair and PCR product.

The promoter region is an important region of the CXCL8 gene to investigate for histone methylation marks. Primers were designed around an area of DNase I hypersensitivity, which indicates the presence of regulatory elements (see Figure 6-2) such as H3K4me1, HeK4me3 and H3K27ac, all of which are associated with active transcription (203). This region also includes the NF-κB binding site, which as described in Figure 1-2, is necessary for the induction of CXCL8 expression. Therefore, analysing the epigenetic signature associated with its binding may offer insights into the regulation of CXCL8 expression.

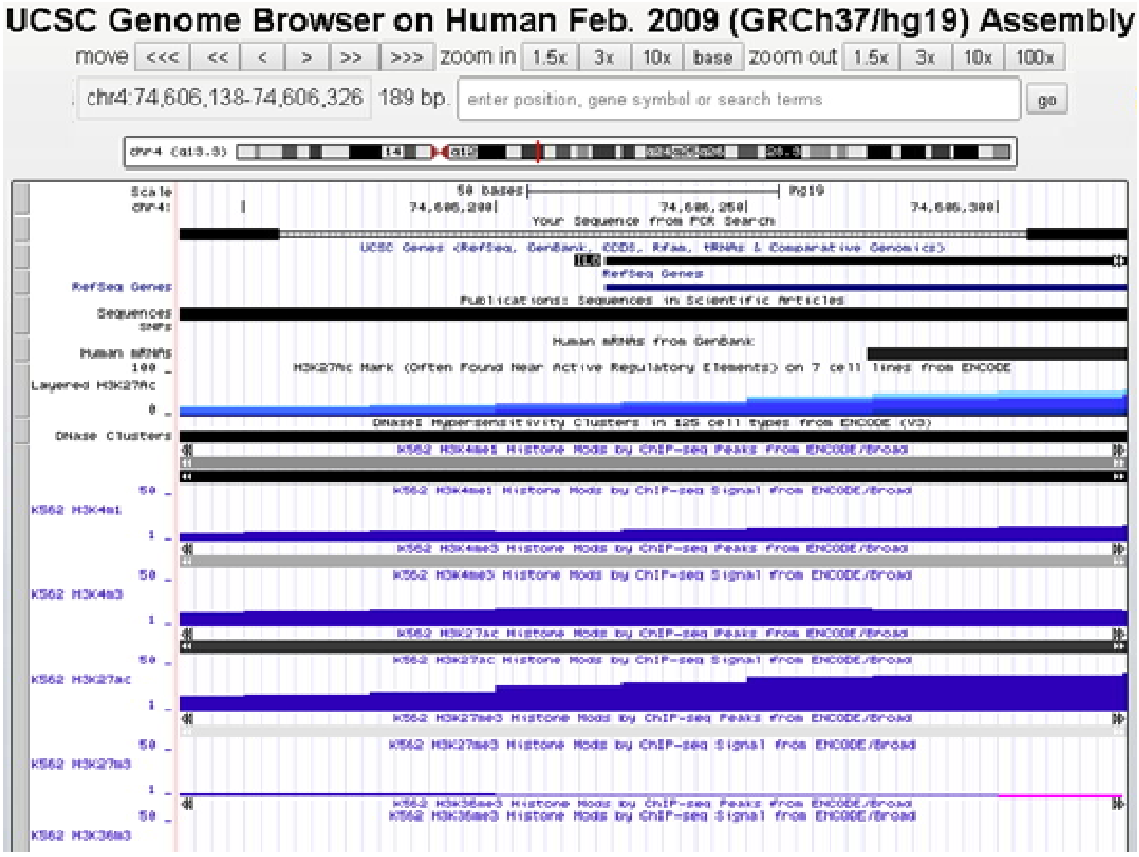

Figure 6-2 Chromosomal Location of the qPCR Product for ChIP Analysis of the CXCL8 Promoter

ENCODE data was used to identify the epigenetic signatures present at the CXCL8 promoter region. The In-Silico PCR function in the UCSC genome browser was used to illustrate the location of the primer pair and PCR product.

Lastly, the CXCL8 gene itself was chosen as it is a DNase I hypersensitivity area (indicating the presence of a regulatory element and that the chromatin is open) but the exact nature of these regulatory elements is unknown (see Figure 6-3).

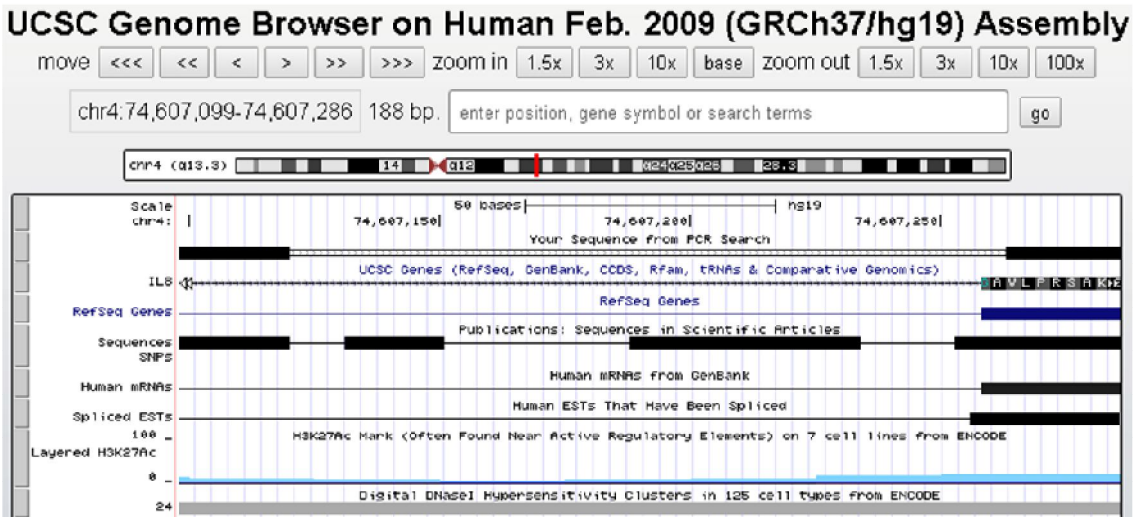

Figure 6-3 Chromosomal Location of the qPCR Product for ChIP Analysis of the CXCL8 Gene Body

ENCODE data was used to identify the epigenetic signatures present in the gene body of the CXCL8 gene. The PCR function in the UCSC genome browser was used to illustrate the location of the primer pair and PCR product.

6.2 Histone Methylation Marks at the CXCL8 Locus in Intestinal Epithelial Cells

The previous chapter investigated the effect of epigenetic inhibitors on global histone methylation levels and CXCL8 expression. Demonstrating that there is a definitive correlation between a change in the epigenetic signature and the regulation of tolerance requires the investigation of specific histone methylation changes at the CXCL8 locus. This can be achieved by using ChIP to investigate the epigenetic signature present at different loci around the CXCL8 gene under different conditions and stimulations of intestinal epithelial (Caco-2) cells i.e. stimulated vs tolerized Caco-2 cells and tolerized vs. epigenetically inhibited intestinal epithelial cells. The three histone methylation marks that were examined in the previous chapter were analysed using ChIP at the CXCL8 gene.

Caco-2 cells were stimulated, tolerized and epigenetically inhibited as described in Figure 3-7. An aliquot of conditioned media was removed for analysis by CXCL8 ELISA in order to confirm that the Caco-2 cells were tolerized. The cells were then fixed with formaldehyde, the chromatin was extracted, sonicated and incubated with Histone H3, H3K4me3, H3K9me3 and H3K27me3 antibodies and magnetic beads; and the immunoprecipitated chromatin purified and eluted to be analysed by qPCR. Three areas of the CXCL8 gene locus were analysed as pictured in Figure 6-1, Figure 6-2 and Figure 6-3; 5' upstream of the promoter region, the promoter region and the middle of the gene body itself. The fold changes for each immunoprecipitation are normalised to the input chromatin and then again to Histone H3, which confirms the presence of the nucleosome.

Figure 6-4 illustrates the H3K4me3, H3K9me3 and H3K27me3 fold changes present upstream of the CXCL8 promoter. As the values for H3K4me3 and H3K27me3 are small in comparison to the

values for H3K9me3, Figure 6-4b highlights just these values. H3K4me3 is greatest in control and tolerized + pargyline cells and is decreased in stimulated and tolerized cells (Figure 6-4**b**). Tolerized + chaeotcin cells show a small fold change increase in H3K4me3, but it does not reach the same level as in control cells. H3K9me3 fold change levels are relatively consistent across the five cell treatment conditions with an increase in tolerized cells (Figure 6-4**a**). H3K27me3 fold changes show a similar pattern to H3K4me3 (Figure 6-4**b**) where the levels decrease in stimulated cells and decrease further in tolerized cells, compared to control cells but show an increase in both epigenetically inhibited and tolerized cells.

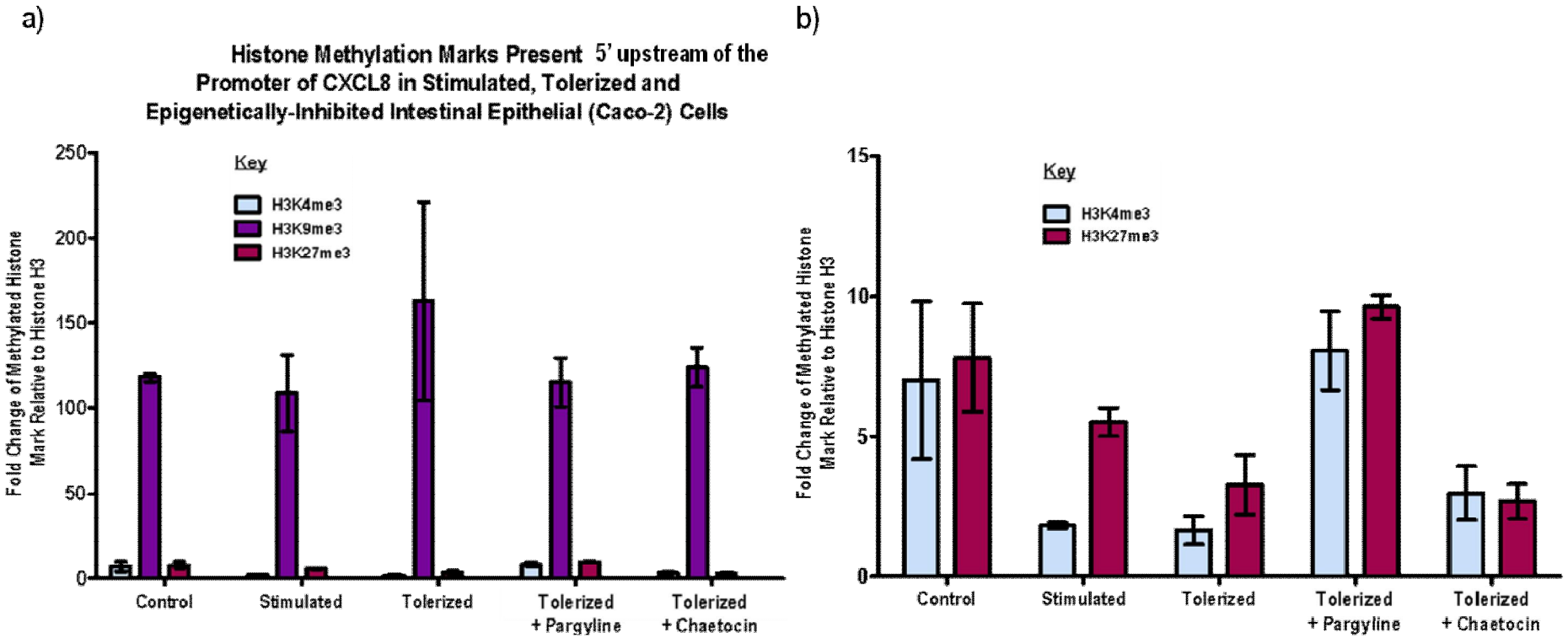

Figure 6-4 Histone Methylation Marks Present 5' upstream of the Promoter of CXCL8 in Stimulated, Tolerized and Epigenetically-Inhibited Intestinal Epithelial (Caco-2) Cells

Caco-2 cells were stimulated with 1 ng/ml IL-1β for 24 hours and tolerized by a prior stimulation of 1 ng/ml IL-1β 24 hours earlier, as described in Figure 3-2. Pargyline hydrochloride and Chaetocin were added directly to pre-stimulated Caco-2 cells at concentrations of 3 mM and 100 nM, respectively, for 1 hour prior to the second stimulation with IL-1β. The second IL-1β-stimulation was followed by another incubation with 3mM or 100 nM Chaetocin for 18 hours prior to sample collection, as described in Figure 3-7. CXCL8 production was measured by ELISA. DNA was extracted and sonicated and histone methylation was measured by ChIP using antibodies against Histone H3, H3K4me3, H3K9me3 and H3K27me3 at three different CXCL8 loci. The level of histone methylation 5' upstream of the CXCL8 promoter was calculated as a proportion of the input DNA and normalized to Histone H3. **a)** Represents H3K4me3, H3K9me3 and H3K27me3 fold changes and **b)** illustrates the fold changes of H3K4me3 and H3K27me3 at a magnified scale. Bars represent mean ± SEM, n =2.

As the fold changes for each immunoprecipitated histone methylation mark vary in size compared to each other as well as across the range of cell conditions, the fold changes were represented as a percentage of the mean stimulated amount, as the ELISA results in chapter 4 Immune Tolerance in Intestinal Epithelial Cells and chapter 5 Histone Methylation and its Effect on Tolerance in Intestinal Epithelial Cells were. The ChIP results present 5' upstream of the promoter, represented as percentage of the mean stimulated fold change are illustrated in Figure 6-5. This method highlights the change in fold change relative to the stimulated level. As in Figure 6-4, H3K4me3 levels are decreased in stimulated cells relative to control cells, and slightly decreased again in tolerized cells. There is a large increase in H3K4me3 in tolerized + pargyline cells with a smaller increase in tolerized + chaetocin cells. H3K9me3 levels are consistent in control, stimulated and tolerized cells with a small increase in tolerized + pargyline cells and a larger increase in tolerized + chaetocin cells (Figure 6-5). The small differences in H3K9me3 fold changes pictured in Figure 6-4**a** appear larger as percentages in Figure 6-5 which makes it easier to see how the relationships between the different cell conditions change. H3K27me3, as shown in Figure 6-5, decrease slightly from control to stimulated and from stimulated to tolerized, with a large increase in tolerized + pargyline greater than in control cells and a smaller increase in tolerized + chaetocin cells compared to tolerized only cells.

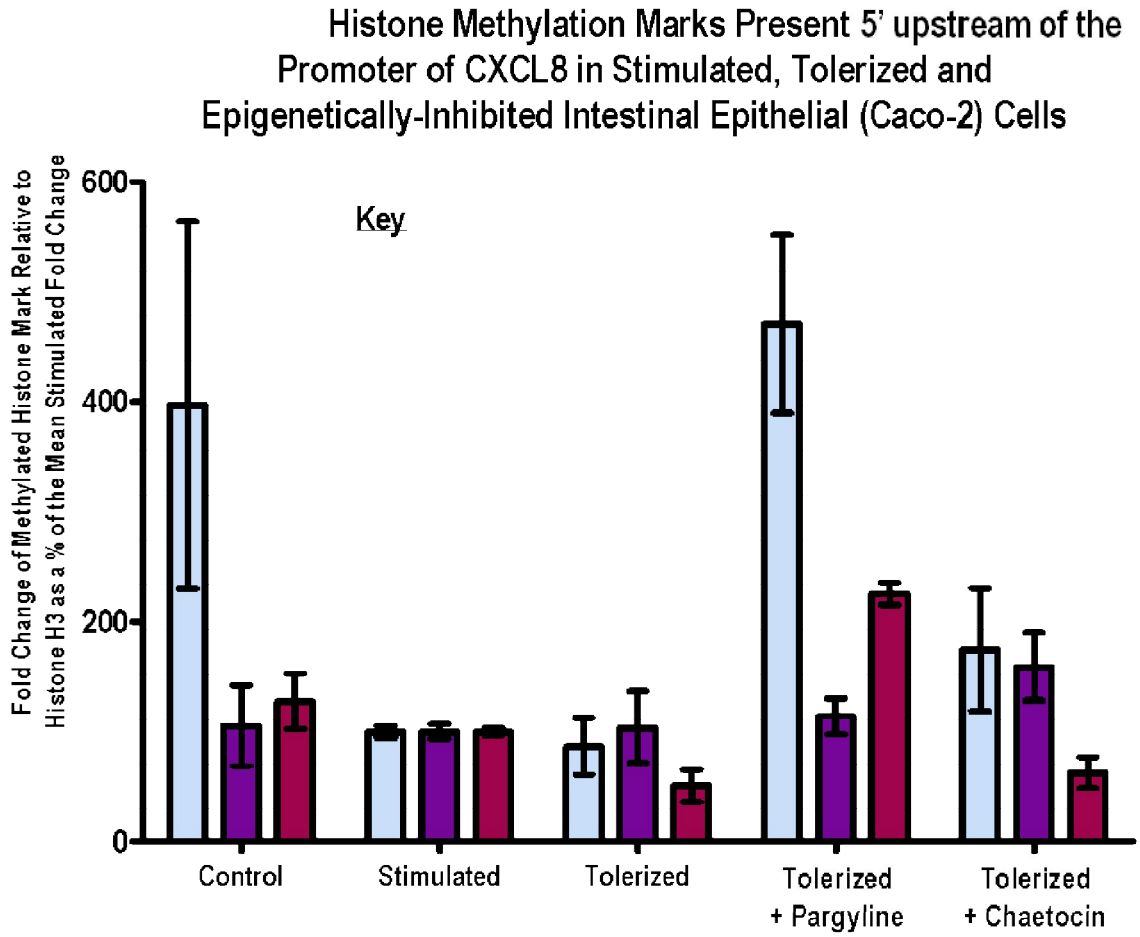

Figure 6-5 Histone Methylation Marks Present 5' upstream of the Promoter of CXCL8 in Stimulated, Tolerized and Epigenetically-Inhibited Intestinal Epithelial (Caco-2) Cells (represented as a % of the mean stimulated amount)

Caco-2 cells were stimulated with 1 ng/ml IL-1β for 24 hours and tolerized by a prior stimulation of 1 ng/ml IL-1β 24 hours earlier, as described in Figure 3-2. Pargyline hydrochloride and Chaetocin were added directly to pre-stimulated Caco-2 cells at concentrations of 3 mM and 100 nM, respectively, for 1 hour prior to the second stimulation with IL-1β. The second IL-1β-stimulation was followed by another incubation with 3mM or 100 nM Chaetocin for 18 hours prior to sample collection, as described in Figure 3-7. CXCL8 production was measured by ELISA. DNA was extracted and sonicated and histone methylation was measured by ChIP using antibodies against Histone H3, H3K4me3, H3K9me3 and H3K27me3 at three different CXCL8 loci. The level of histone methylation 5' upstream of the CXCL8 promoter was calculated as a proportion of the input DNA and normalized to Histone H3. Each fold change is represented as a percentage of the mean stimulated fold change. Bars represent mean ± SEM, n =2.

Figure 6-6 shows the fold changes for the histone methylation marks H3K4me3, H3K9me3 and H3K27me3 present at the promoter of the CXCL8 gene. Like in the region 5' upstream of the promoter, the fold change values for H3K4me3 and H3K27me3 were much smaller than the fold change values for H3K9me3, thus Figure 6-6**b** replots H3K4me3 and H3K27me3 at a more suitable scale. H3K4me3 fold changes vary only subtly across the different cell conditions. Control cells have a slightly greater H3K4me3 level than stimulated cells, which are consistent with the level for tolerized + chaetocin cells, which in turn are only slightly greater than the levels for tolerized and tolerized + pargyline. H3K9me3 fold changes are greatest in tolerized + chaetocin cells with decreasing levels in each of control, stimulated, tolerized and tolerized + pargyline cells, though stimulated and tolerized cells have very similar levels (Figure 6-6**a**). Figure 6-6**b** shows the levels of H3K27me3, which are greatest in control cells, decreasing in stimulated cells and again in tolerized cells. In epigenetically inhibited cells, H3K27me3 levels rise above that of stimulated cells, but not as high as in control cells (Figure 6-6**b**).

As for the 5' upstream of the promoter region, the histone methylation mark fold changes for the promoter were represented as percentages of the mean stimulated fold change amount (Figure 6-7). The patterns of histone methylation change for H3K4me3 and H3K27me3 when plotted as percentages in Figure 6-7, are the same as the fold changes in Figure 6-6**b**. H3K9me3 fold changes, shown as percentages, are decreased in stimulated cells with a small increase in tolerized vs stimulated cells (Figure 6-7). Tolerized + pargyline cells show a further increase with tolerized + chaetocin cells showing the largest increase in H3K9me3, relative to stimulated cells.

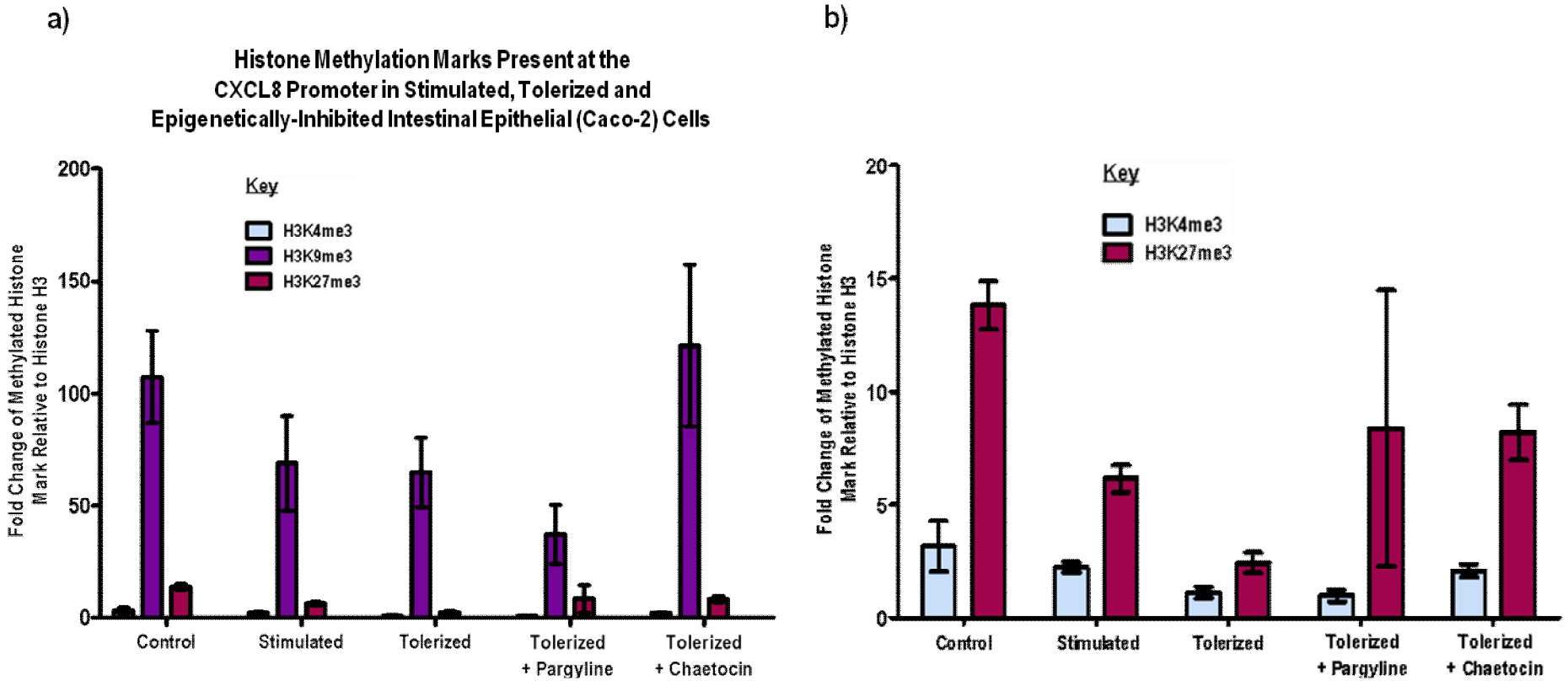

Figure 6-6 Histone Methylation Marks Present at the CXCL8 Promoter in Stimulated, Tolerized and Epigenetically-Inhibited Intestinal Epithelial (Caco-2) Cells

Caco-2 cells were stimulated with 1 ng/ml IL-1β for 24 hours and tolerized by a prior stimulation of 1 ng/ml IL-1β 24 hours earlier, as described in Figure 3-2. Pargyline hydrochloride and Chaetocin were added directly to pre-stimulated Caco-2 cells at concentrations of 3 mM and 100 nM, respectively, for 1 hour prior to the second stimulation with IL-1β. The second IL-1β-stimulation was followed by another incubation with 3mM or 100 nM Chaetocin for 18 hours prior to sample collection, as described in Figure 3-7. CXCL8 production was measured by ELISA. DNA was extracted and sonicated and histone methylation was measured by ChIP using antibodies against Histone H3, H3K4me3, H3K9me3 and H3K27me3 at three different CXCL8 loci. The level of histone methylation at the CXCL8 promoter was calculated as a proportion of the input DNA and normalized to Histone H3. **a)** Represents H3K4me3, H3K9me3 and H3K27me3 fold changes and **b)** illustrates the fold changes of H3K4me3 and H3K27me3 at a magnified scale. Bars represent mean ± SEM, n =2.

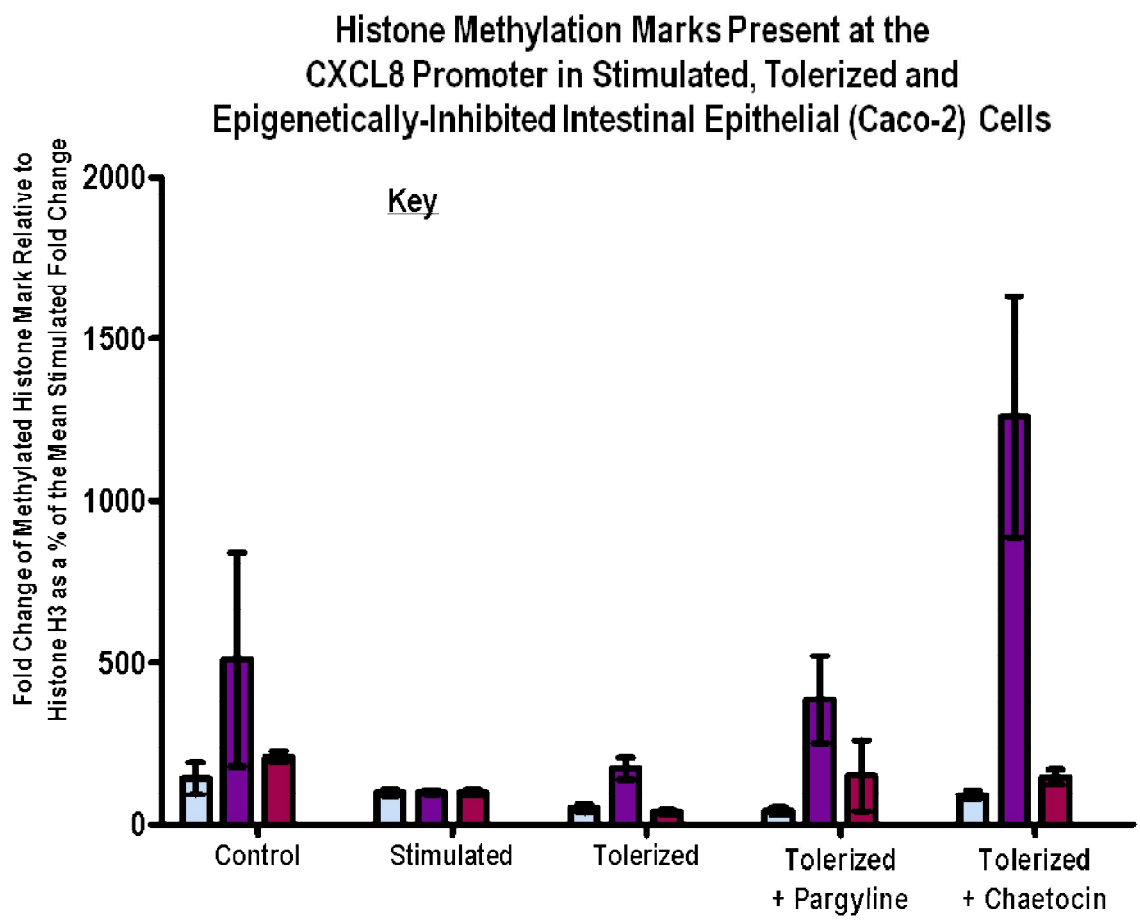

Figure 6-7 Histone Methylation Marks Present at the CXCL8 Promoter in Stimulated, Tolerized and Epigenetically-Inhibited Intestinal Epithelial (Caco-2) Cells (represented as a % of the mean stimulated amount)

Caco-2 cells were stimulated with 1 ng/ml IL-1β for 24 hours and tolerized by a prior stimulation of 1 ng/ml IL-1β 24 hours earlier, as described in Figure 3-2. Pargyline hydrochloride and Chaetocin were added directly to pre-stimulated Caco-2 cells at concentrations of 3 mM and 100 nM, respectively, for 1 hour prior to the second stimulation with IL-1β. The second IL-1β-stimulation was followed by another incubation with 3mM or 100 nM Chaetocin for 18 hours prior to sample collection, as described in Figure 3-7. CXCL8 production was measured by ELISA. DNA was extracted and sonicated and histone methylation was measured by ChIP using antibodies against Histone H3, H3K4me3, H3K9me3 and H3K27me3 at three different CXCL8 loci. The level of histone methylation at the CXCL8 promoter was calculated as a proportion of the input DNA and normalized to Histone H3. Each fold change is represented as a percentage of the mean stimulated fold change. Bars represent mean ± SEM, n =2.

Finally, the histone methylation fold changes for H3K4me3, H3K9me3 and H3K27me3 in the gene body of CXCL8 were measured (Figure 6-8). H3K4me3 fold changes are very small and vary only slightly across the five different cell stimulations and conditions. Control, tolerized and tolerized + chaetocin conditions have a slightly larger H3K4me3 fold change in comparison to stimulated and tolerized + pargyline cells, as shown in Figure 6-8. The fold changes of H3K9me3 are much greater than for H3K4me3 (Figure 6-8). In control and tolerized cells the amount of H3K9me3 is approximately the same, with an increase in stimulated cells. There is a small decrease in tolerized + pargyline cells and a much larger decrease in tolerized + chaetocin cells (Figure 6-8). H3K27me3 fold change amounts vary greatly across the different conditions. Stimulated cells show an increase in comparison to control cells whilst tolerized cells have a reduction in H3K27me3 almost to nothing (Figure 6-8). Tolerized + pargyline cells also have next to no H3K27me3 (Figure 6-8) whilst tolerized + chaetocin cells have a large increase to above the level of control cells (Figure 6-8).

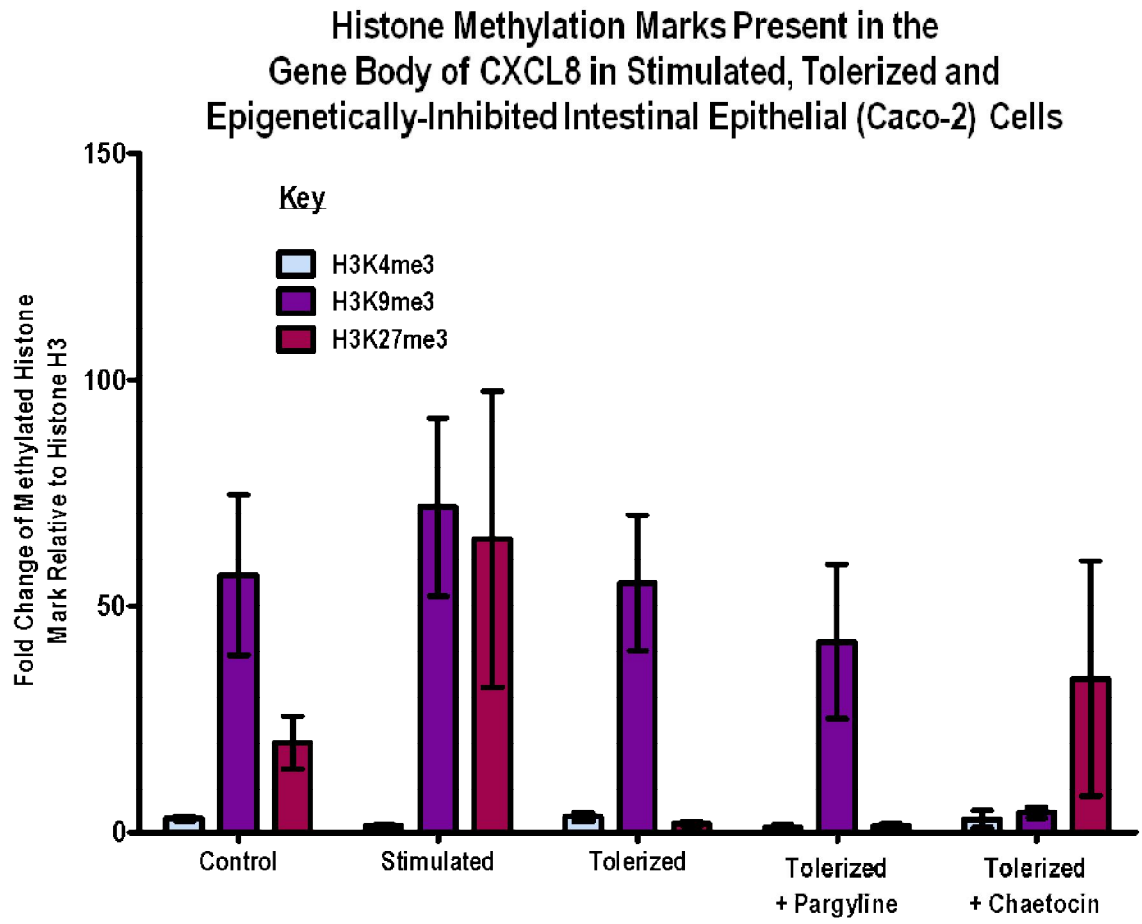

Figure 6-8 Histone Methylation Marks Present in the Gene Body of CXCL8 in Stimulated, Tolerized and Epigenetically-Inhibited Intestinal Epithelial (Caco-2) Cells

Caco-2 cells were stimulated with 1 ng/ml IL-1β for 24 hours and tolerized by a prior stimulation of 1 ng/ml IL-1β 24 hours earlier, as described in Figure 3-2. Pargyline hydrochloride and Chaetocin were added directly to pre-stimulated Caco-2 cells at concentrations of 3 mM and 100 nM, respectively, for 1 hour prior to the second stimulation with IL-1β. The second IL-1β-stimulation was followed by another incubation with 3mM or 100 nM Chaetocin for 18 hours prior to sample collection, as described in Figure 3-7. CXCL8 production was measured by ELISA. DNA was extracted and sonicated and histone methylation was measured by ChIP using antibodies against Histone H3, H3K4me3, H3K9me3 and H3K27me3 at three different CXCL8 loci. The level of histone methylation in the gene body of the CXCL8 gene was calculated as a proportion of the input DNA and normalized to Histone H3. Bars represent mean ± SEM, n =2.

As for the other two CXCL8 loci, the histone methylation marks in the CXCL8 gene body are also plotted as percentages of the mean stimulated amount (Figure 6-9). Showing fold changes, H3K4me3 in particular, as percentages makes the relative differences easier to see. Stimulated and tolerized + pargyline cells have a similar amount of H3K4me3, whilst control, tolerized and tolerized + chaetocin cells have 2 – 3 times as much H3K4me3 (Figure 6-9). The amount of H3K9me3 is decreased in control and tolerized cells relative to stimulated cells, though the amount of H3K9me3 in tolerized cells is slightly higher than in control cells (Figure 6-9). The amount of H3K9me3 is almost doubled in tolerized + pargyline cells relative to stimulated cells, whereas in tolerized + chaetocin cells it is reduced to approximately a quarter of that of stimulated cells (Figure 6-9). H3K27me3 levels are increased in control cells relative to stimulated cells and greatly decreased in all tolerized cell conditions (Figure 6-9). Tolerized and tolerized + chaetocin cells have a similar low proportion of H3K27me3 whilst the proportion of H3K27me3 in tolerized + pargyline cells is next to nothing (Figure 6-9).

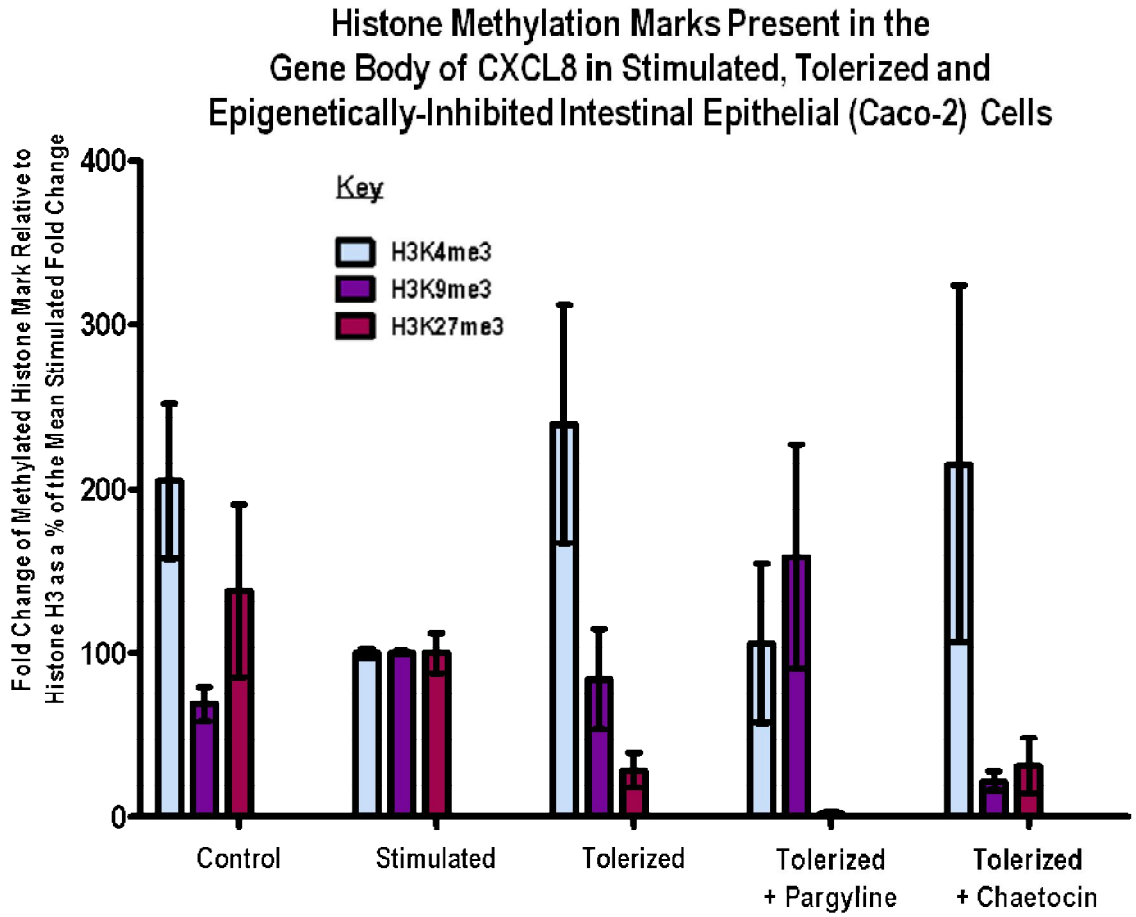

Figure 6-9 Histone Methylation Marks Present in the Gene Body of CXCL8 in Stimulated, Tolerized and Epigenetically-Inhibited Intestinal Epithelial (Caco-2) Cells (represented as a % of the mean stimulated amount)

Caco-2 cells were stimulated with 1 ng/ml IL-1β for 24 hours and tolerized by a prior stimulation of 1 ng/ml IL-1β 24 hours earlier, as described in Figure 3-2. Pargyline hydrochloride and Chaetocin were added directly to pre-stimulated Caco-2 cells at concentrations of 3 mM and 100 nM, respectively, for 1 hour prior to the second stimulation with IL-1β. The second IL-1β-stimulation was followed by another incubation with 3mM or 100 nM Chaetocin for 18 hours prior to sample collection, as described in Figure 3-7. CXCL8 production was measured by ELISA. DNA was extracted and sonicated and histone methylation was measured by ChIP using antibodies against Histone H3, H3K4me3, H3K9me3 and H3K27me3 at three different CXCL8 loci. The level of histone methylation at the gene body of the CXCL8 gene was calculated as a proportion of the input DNA and normalized to Histone H3. Each fold change is represented as a percentage of the mean stimulated fold change. Bars represent mean ± SEM, n =2.

6.3 Conclusions

In conclusion, histone methylation marks around the CXCL8 gene are dynamic and vary according to both locus and cell stimulation conditions. Three loci around the CXCL8 gene were chosen for their likelihood of being enriched for regulatory elements, thus maximising the possibility of detecting a change in histone methylation between stimulated, tolerized and epigenetically-inhibited tolerized intestinal epithelial cells. The first locus was 5' upstream of the promoter, but proximal enough to still be associated with the CXCL8 gene. According to ENCODE data, it was enriched for H3K9me3 and had a peak for DNase I hypersensitivity, indicating that it is a potential enhancer site. According to Figure 6-4**a**, this area was enriched for H3K9me3, above that of H3K4me3 and H3K27me3, though this mark did not vary across conditions as much as H3K4me3 did (Figure 6-5). Table 6-1 summarises the changes seen in Figure 6-4 and Figure 6-5. H3K4me3 is associated with gene transcription and the changes seen in the potential enhancer region of CXCL8 reflect this, apart from in control cells which have a large amount of H3K4me3 even though transcription is low. The decrease in tolerized cells reflects the decrease in CXCL8 production whilst the increase in both epigenetically inhibited tolerized cells is associated with the increase in CXCL8 production seen when tolerance is broken. H3K9me3 is increased in all tolerized cells, despite the conflicting actions seen in CXCL8 transcription. H3K27me3 is increased in both control and tolerized + pargyline cells, which is expected for control cells as H3K27me3 is an inhibitory mark. However, it is unexpected for tolerized + pargyline cells as CXCL8 production is much higher than in control cells. It is decreased in comparison to stimulated cells so could be acting in conjunction with the increase in H3K9me3. H3K27me3 is decreased in tolerized and tolerized + chaetocin cells which indicates a release of inhibition in comparison to stimulated cells. However, neither of these cell conditions produce more CXCL8 than stimulated cells.

Cell Conditions	Histone H3 Lysine Methylation Changes in Comparison to Stimulated Caco-2 Cells		
	H3K4me3	H3K9me3	H3K27me3
Control	↑	---	↑
Tolerized	↓	↑	↓
Tolerized + 3 mM Pargyline hydrochloride	↑	↑	↑
Tolerized + 100 nM Chaetocin	↑	↑	↓

Table 6-1 Histone Methylation Changes 5' Upstream of the CXCL8 Promoter

The changes to histone tri-methylation at lysine positions 4, 9 and 27 5' upstream of the CXCL8 promoter are summarised in the table above. ↑ indicates that the amount of methylation is greater than the amount of methylation in the stimulated cells whilst ↓ indicates that the amount of methylation is less than the amount of methylation in stimulated cells. --- indicates that the amount of methylation is approximately the same as the amount of methylation in stimulated cells. The cell conditions refer to the experimental protocols described in Figure 3-7.

The promoter region, which contains the NF-κB binding site necessary for induction of CXCL8 expression, as well as the binding site for RNA polymerase, is enriched for transcriptionally active epigenetic marks (Figure 6-2). Figure 6-6 showed that the promoter was predominately enriched with H3K9me3, though Figure 6-7 shows how H3K4me3 varies in a large degree in comparison to the level in stimulated cells, as well as the large changes in H3K9me3 between the different conditions. Table 6-2 summarises the changes in histone methylation seen in Figure 6-6 and Figure 6-7. H3K4me3 is shown to be increased in control cells relative to stimulated cells, which does not correspond with the lack of CXCL8 production. However, the decrease in H3K4me3 in tolerized and tolerized + pargyline cells relative to stimulated cells corresponds to the reduction in CXCL8 production. The relatively similar levels of H3K4me3 in stimulated and tolerized + chaetocin cells corresponds to the high production of CXCL8 in chaetocin-inhibited cells, which approaches the same levels as stimulated cells. The increase in H3K9me3 in all cell conditions

relative to stimulated cells reflects an inhibitory effect on transcription. Control and all tolerized cells express decreased, to different degrees, amounts of CXCL8 in comparison to the production of CXCL8 by stimulated cells. The same effect can be seen with H3K27me3, although tolerized only cells showed a decrease in H3K27me3 relative to stimulated cells, which is opposite to expected as a decrease in CXCL8 production would expect to be associated with an increase in an epigenetic inhibitory mark.

Cell Conditions	Histone H3 Lysine Methylation Changes in Comparison to Stimulated Caco-2 Cells		
	H3K4me3	H3K9me3	H3K27me3
Control	↑	↑	↑
Tolerized	↓	↑	↓
Tolerized + 3 mM Pargyline hydrochloride	↓	↑	↑
Tolerized + 100 nM Chaetocin	---	↑	↑

Table 6-2 Histone Methylation Changes at the CXCL8 Promoter

The changes to histone tri-methylation at lysine positions 4, 9 and 27 at the CXCL8 promoter are summarised in the table above. ↑ indicates that the amount of methylation is greater than the amount of methylation in the stimulated cells whilst ↓ indicates that the amount of methylation is less than the amount of methylation in stimulated cells. --- indicates that the amount of methylation is approximately the same as the amount of methylation in stimulated cells. The cell conditions refer to the experimental protocols described in Figure 3-7.

The gene body itself, though demonstrating a peak in DNase I hypersensitivity according to ENCODE (Figure 6-3), did not have existing data on what those regulatory features were. Figure 6-8 shows that there is an enrichment of H3K9me3 and H3K27me3, though according to Figure 6-9 H3K4me3 shows the greatest change between cell conditions. Table 6-3 summarises the changes in histone methylation seen in Figure 6-8 and Figure 6-9. The increase in H3K4me3 in

all cell conditions relative to stimulated cells, except for tolerized + pargyline cells where it is approximately the same, is contrary to expectation as although all of these conditions produce CXCL8 at differing amounts, they do not express more CXCL8 than stimulated cells. H3K9me3 changes show the inverse effect of H3K4me3 with tolerized + pargyline showing an increase in H3K9me3. The decrease in an inhibitory mark is associated with an increase in expression although the amount of CXCL8 expressed is decreased in comparison to stimulated cells. H3K27me3 was shown to be increased in control cells, which reflects the lack of CXCL8 expression in control cells compared to stimualted cells. H3K27me3 is decreased in all tolerized cells, which, like H3K9me3, would be expected to be associated with an increase in gene transcription as the amount of an inhibitory epigenetic mark has decreased. However, the expression of CXCL8 is decreased in all tolerized cells compared to stimulated cells.

Cell Conditions	**Histone H3 Lysine Methylation Changes in Comparison to Stimulated Caco-2 Cells**		
	H3K4me3	**H3K9me3**	**H3K27me3**
Control	↑	↓	↑
Tolerized	↑	↓	↓
Tolerized + 3 mM Pargyline hydrochloride	**---**	↑	↓
Tolerized + 100 nM Chaetocin	↑	↓	↓

Table 6-3 Histone Methylation Changes in the CXCL8 Gene Locus

The changes to histone tri-methylation at lysine positions 4, 9 and 27 in the CXCL8 gene locus are summarised in the table above. ↑ indicates that the amount of methylation is greater than the amount of methylation in the stimulated cells whilst ↓ indicates that the amount of methylation is less than the amount of methylation in stimulated cells. --- indicates that the amount of methylation is approximately the same as the amount of methylation in stimulated cells. The cell conditions refer to the experimental protocols described in Figure 3-7.

In conclusion, the epigenetic signature at the promoter of a gene is the one that is most closely associated with the transcriptional outcome. The signature present in the gene body does not conform to published epigenetic research, possibly because the transcriptional machinery binding to the chromatin is not affected by modified chromatin located downstream of the promoter. Enhancer regions play a part, though not as much as the promoter. This is the first demonstration of a detailed analysis of the histone methylation marks around the CXCL8 locus in a number of different cell conditions, namely how the epigenetic signature changes between stimulated, tolerized and epigenetically-inhibited intestinal epithelial cells.

7 Discussion

7.1 Relevance of the Research

This form of tolerance is primarily due to a reduction in expression of inflammatory and immunological genes by intestinal epithelial cells. Therefore, in order to understand tolerance, we need to examine the mechanisms of regulating gene transcription in the healthy intestine. Only then can its relevance to the dysregulation of inflammation and the immune system be properly understood and applied to clinical conditions e.g. IBD and NEC.

Regulation is required to prevent deleterious injury from dysregulated inflammation. Though inflammation is beneficial when the body is injured or infected, long lasting and severe inflammation can cause tissue damage. Therefore, tight control of the induction and maintenance of inflammation is required. Many of the proteins that are pro-inflammatory mediators are also able to downregulate their own activity e.g. NF-κB. NF-κB is a transcription factor for several pro-inflammatory cytokines, including IL-1β, IL-6 and CXCL8. Induction of inflammation also induces the transcription of several genes whose function is to either inhibit the activation of NF-κB or down-regulate the inflammatory pathway. These mediators include A20 (A20 or TNFAIP3 is a zinc finger protein with both ubiquitin ligase and deubiquitinase activity that prevents TNF-induced activation of NF-κB (204)), IκB (a kinase complex which prevents NF-κB translocation to the nucleus and thus controls its activation state (205)) and SIGIRR (a receptor which negatively regulates TLR and IL-1R signalling via interaction with TRAF6 (206) to downregulate immune expression in the intestinal epithelium (207)), all of which control NF-κB activity.

There are a number of mechanisms whereby the intestine is inhibited from reacting to the microbial content of the intestinal lumen. These include barriers of mucus and the integrity of the epithelial cell monolayer prevents unrestricted access to immune cells in the lamina propria, and hyporesponsiveness of these immune cells to microbial products. This thesis has concentrated on the epithelial cells themselves. They are capable of secreting cytokines but do so only in limited amounts *in vivo*.

The production of inflammation is also downregulated by the concurrent induction of anti-inflammatory cytokines e.g. IL-10, TGF-β, IL-1RA and lipoxins. Anti-inflammatory cytokines act by either promoting the differentiation of effector immune cells into regulatory or suppressive cells (TGF-β) or downregulating pro-inflammatory cytokine expression (IL-10 and IL-1RA). Other mediators promote the resolution of inflammation by stimulating the conversion of M1 (inflammatory) macrophages to the M2 type, which decrease inflammation and promote tissue repair (208).

.

These mediators function to limit the aggressiveness of inflammation and terminate its effect by downregulating pro-inflammatory cytokine expression, causing the conversion of effector T cells into regulatory T cells which suppress inflammation, and promoting the resolution of inflammation by macrophage phagocytosis of apoptosed inflamed cells.

As described by Foster *et al*, tolerance regulation is both gene-specific and epigenetic (87). It has long been known that changes to the epigenetic signature are associated with differences in gene expression. Epigenetics is only one area of gene transcription regulation and as described above there are many other factors that have been proven to have a role in the regulation of inflammation and tolerance, e.g. feedback loops and pro-inflammatory mediators with short half-

lives. Regulation of tolerance is a redundant system. If one component fails, the whole system is protected by the other mechanisms, under the majority of circumstances. Initiation of the inflammatory signalling pathway specific to the failed gene results in inflammation, often the only method of determining the gene's function.

The role of genes demonstrated to have a role in the regulation of tolerance is most clearly shown by knock-out mice. Mice with a homozygous knock-out of NF-κB are not substantially affected. Despite having an increased number of leukocytes, increased circulating levels of free fatty acids and alkaline phosphatase, decreased circulating levels of sodium and amylase and a decreased body mass, NF-κB knockout mice are relatively healthy (209). Knocking-out IL-10 results in mice susceptible to inflammation with spontaneously developing colitis (210). Although these mice have dysregulated inflammation and are not healthy, the loss of IL-10 is not embryonically lethal and the mice reach adulthood relatively healthily. A20, being a major regulator, causes susceptibility to a large number of diseases including SLE and IBD. None of these diseases are conclusively caused by a deficiency in A20; therefore A20 is not the sole regulator of inflammation and tolerance (211).

Regulation of tolerance is complicated and involves many mediators; many of the examples described above involve genes whose regulation is driven by its promoter and transcription factors. The role of epigenetics is relatively unknown and requires further research. That is not to say that the other methods of self-limiting the induction of inflammation are not active in this model of tolerance, just that this research project aims to show that epigenetics plays a part. A recent paper by Bhatt and Ghosh describes how histone modifications contribute to the priming of NF-κB so that inflammatory genes can be rapidly expressed under necessary conditions (212).

7.2 Overview of Results

This research has conclusively shown that intestinal epithelial cells can be tolerized in response to repeated stimulation by microbial products or pro-inflammatory agents. This was demonstrated in Figure 4-4, where Caco-2 cells induced the transcription of CXCL8 in response to P3CK stimulation. TLR2 is a PRR recognising lipoteichoic acid, a known microbial PAMP. P3CK is a synthetic version of lipoteichoic acid and a TLR2 agonist. Its stimulation of CXCL8 expression represents a physiological response of the intestinal epithelium to the presence of bacteria. 25 μg/ml P3CK is a high concentration of stimulant to produce a response. lL-1β produces a stronger response with a lower concentration of 1 ng/ml (Figure 4-2) hence its use for the subsequent experiments designed to understand the epigenetic inhibition in tolerized cells experiments.

Repeated stimulation of both P3CK and IL-1β, individually (tolerized) and together (cross-tolerized), caused a hyporesponsive state and reduced CXCL8 expression, as shown in Figure 4-4, Figure 4-16, Figure 4-17 and Figure 4-20. This is a reproducible, consistent, statistically significant effect. As shown by Figure 4-17, the reduction in CXCL8 production in cells that have been pre-stimulated and stimulated (tolerized) is an identifiable and characteristic feature. Pre-stimulated only cells, in conjunction with the qPCR data shown in Figure 4-19 where CXCL8 mRNA expression returns to background levels before the second IL-1β-stimulation is administered, show that the reduction in CXCL8 production seen in tolerized cells is due to a change in expression and is not a diminishing continuation of the initial stimulation.

Non-malignant intestinal epithelial cells, NCM460, are also tolerized by P3CK to a statistically significant level (Figure 4-5). This demonstrates that tolerance is not a feature of malignancy and

is a characteristic of intestinal epithelial cells. As Caco-2 cells give the greatest response to IL-1β-stimulation, IL-1β and Caco-2 cells were used to understand the mechanism of epigenetic inhibition of tolerance.

Examination of histone methylation by immunoblotting showed only showed a small fold-change in the level of methylation. As shown in Figure 5-3, Figure 5-7, Figure 5-17 and Figure 5-21, when the fold-changes from each Western blot are combined, the statistical power increases and even though the fold-change is small, it is statistically significant. SAH, though a histone methyltransferase inhibitor, caused an increase in the amount of methylation at H3K27me3. This increase in the amount of H3K27me3 methylation, though small, was sufficient to break tolerance. A decrease in the amount of H3K27me3 in Caco-2 cells incubated with 100 μM SAH compared to the control condition was seen when methylation levels were measured by Histone PTM Multiplex Luminex assay (Figure 5-4), which is the expected effect of SAH. A possible explanation for this is that the Luminex assay measures multiple histone marks in multiplex so an interaction between the antibodies could prevent the H3K27me3 antibody from binding to its epitope resulting in an artificially reduced amount of H3K27me3. In light of this, we took the Western blotting result as the true effect for all of the other epigenetic inhibitors. Chaetocin, another histone methyltransferase inhibitor, had its predominant effect on H3K9me3 rather than H3K27me3 but caused a decrease in the amount of methylation. As with SAH, Chaetocin also broke tolerance due to loss of a repressive epigenetic mark allowing an increase in gene transcription.

Pargyline, though a specific inhibitor of monoamine oxidases, also inhibits histone demethylases. It reduced the relative amounts of both H3K4me3 and H3K9me3, but predominantly H3K4me3. As expected, inhibition of a histone demethylase caused an increase in methylation levels. An

increase in an activatory epigenetic mark, as expected caused an increase in gene transcription. Pargyline, like SAH and Chaetocin, reversed tolerance even with a small fold-change in the amount of histone methylation. 2,4-PDCA, though a histone demethylase inhibitor like pargyline which caused an increase in the amount of H3K4me3 by both Western blotting (Figure 5-20 and Figure 5-21) and Multiplex Luminex assay (Figure 5-22), had the converse effect on gene transcription and did not break tolerance. The production of CXCL8 by tolerized cells incubated with 2,4-PDCA was reduced. This appears to be a further reduction as stimulated cells incubated with 2,4-PDCA produce a similar level of CXCL8 as stimulated only cells (Figure 5-31). Why two different inhibitors targeting the same epigenetic marker and having the same effect on that marker result in opposing effects on tolerance is not known, especially as one might expect to see a concomitant increase in gene transcription with an increase in the amount of H3K4me3.

The effects of two of the inhibitors, Chaetocin and pargyline, can be easily explained and conform to previously published data. The increase in gene transcription resulting in the breaking of tolerance is as expected according to the epigenetic changes seen. Loss of a repressive marker (H3K9me3 with Chaetocin) and increase of an activatory mark (H3K4me3 with pargyline) both explain the increase in gene transcription. The effects of the other two inhibitors SAH and 2,4-PDCA are more difficult to fully explain, and may also act on other methyl sites of which we are unaware.

The concomitant increase of H3K27me3 levels and gene transcription when incubated with SAH is a contradictory result, as H3K27me3 has been shown to be associated with repression of gene transcription not activation. Whilst there is a possible explanation for the increase rather than decrease in H3K27me3 relative amounts, the results produced here cannot fully explain why this is also associated with an increase in gene expression. SAH, *in vivo*, can be hydrolysed to

adenosine and homocysteine, where homocysteine is converted into methionine, which, when it is attached to adenosyl, is a methyltransferase substrate (183). Experimentally increasing the concentration of SAH is often associated with an increase in SAM (213). In order to confirm that an increase in the SAM/SAH ratio is responsible for the surprising effect of SAH on histone methylation, the concentration of SAM in the tolerized Caco-2 cells before and after incubation with SAH would need to be measured. Though SAH, under the conditions investigated in this project, only has a statistically significant effect on H3K27me3, it is possible that SAH alters the relative amounts of methylation at other residues that were not tested and further investigation would be required to provide a complete explanation.

Despite pargyline and 2,4-PDCA both causing an increase in the relative amount of H3K4me3, they had opposing effects on gene transcription and only pargyline broke tolerance. There is insufficient data to fully explain these contradictory effects, though we can demonstrate that they are reproducible and statistically significant. Investigation of other epigenetic marks is required to completely describe the epigenetic signature present when tolerized intestinal epithelial cells are incubated with each inhibitor resulting in the change in gene transcription. This project highlights that epigenetic signatures are complex and combinatorial, in conjunction with current research (214), and that current research still has much further to go before the association between epigenetics and gene expression is completely understood. Nevertheless, this is the first demonstration of tolerance regulation in intestinal epithelial cells having an epigenetic component.

ChIP analysis of the histone post-translational modifications around the CXCL8 gene confirm that epigenetic signatures are varied and dynamic. Loci upstream of the promoter and transcriptional start site (Table 6-1 and Table 6-2) have epigenetic signatures that conform most closely to

published data. Though the levels of H3K4me3 were relatively low compared to the levels of H3K9me3, their relative levels in the different cell conditions is important in the regions 5' upstream of the transcriptional start site as well as the promoter, as shown in current research (215). The extremely low levels of H3K4me3 present in the gene body are expected, as shown in previous research (123). The epigenetic signature found around the promoter of the CXCL8 gene is most closely associated with the transcriptional outcome. The epigenetic marks found at enhancer regions are also associated with transcription, but H3K4me1, acetylation of H3K27 and transcription factor occupancy needs to be measured to confirm that the locus is a true enhancer (216). This research contributes to current knowledge as a detailed analysis of H3K4me3, H3K9me3 and H3K27me3 levels around the CXCL8 gene and how they change in intestinal epithelial cells under inflammatory stimulation, tolerization and epigenetically-inhibited cells.

7.3 Conclusions with Regard to the Hypothesis

The results of this research project support the hypothesis that epigenetics play a role in the regulation of tolerance. First, intestinal epithelial cells are tolerized by different immune stimulants, P3CK and IL-1β. Both of these pro-inflammatory agents are found in the human intestine at elevated concentrations, particularly in patients with an inflammatory disease e.g. IBD. Therefore, these results can be considered as a physiological model. It is interesting that tolerance has been shown in epithelial cells as the majority of existing published research has been performed in immune cells e.g. macrophages. Intestinal macrophages are not adjacent to the intestinal lumen so they are not the first cells that the microbiota (represented here by P3CK) interacts with. However, they still require mechanisms to limit inflammation and the subsequent damage (217). As epithelial cells line the intestinal lumen, the microbiota and other proteins, such as pro-inflammatory cytokines, interact with them first. Therefore, epithelial cells are an important cell type to exhibit tolerance. Otherwise, the epithelial cells would be in a continuously activated and stimulated state signalling to the immune system that inflammation is required.

The involvement of epigenetics in the regulation of tolerance was demonstrated by incubating epigenetic inhibitors with tolerized Caco-2 cells, resulting in increased production of CXCL8. Tolerance was broken by the change to the epigenetic signature causing an increase in gene expression. CXCL8 production by epigenetically inhibited cells did not reach the same level as CXCL8 produced by stimulated cells. This could be due to the small fold-changes in histone methylation level seen by using these inhibitors or perhaps other regulatory mediators need to be enhanced in order to overcome a latent tolerized effect. ChIP was used to monitor the specific epigenetic changes around the CXCL8 gene and how these change when intestinal epithelial cells are stimulated with IL-1β and incubated with epigentic inhibitors. Epigenetics provides

another layer to the regulatory mechanisms that ensures the continued maintenance, safety and protection of the epithelium (218) and immune system to microbiota, infectious agents and deleterious inflammation.

7.4 Limitations of the Experiments

In the Foster *et al* paper (87), the effect of tolerance on multiple genes was investigated. I have demonstrated that small molecule epigenetic inhibitors are able to break tolerance, but I have only shown that effect on CXCL8. To confirm that tolerance is truly regulated by epigenetics, the effect of epigenetic inhibitors on other tolerizable genes should be investigated. In particular, the pro-inflammatory genes were identified by Foster *et al* as being transiently silenced while the anti-microbial genes were primed by repeated pro-inflammatory stimulation.

An unexpected finding was the failure of IL-1β to properly stimulate CXCL8 production in NCM460 cells above background levels and the subsequent failure to induce tolerance. However, the NCM460 cell-line fully responded to stimulation and was tolerized by P3CK which demonstrated that tolerance was not a consequence of malignancy. As P3CK induces the expression of CXCL8, it can be assumed that the signalling pathway downstream from at least the TRAF6-phosphorylated-IRAK1(2) complex, shown in Figure 1-2, is functioning in NCM460 cells, as that is the convergence point for the signalling pathways from both the TLR and IL-1β receptor. Though the individual CXCL8 values expressed as chemokine per unit weight of epithelial cell protein are larger in NCM460 cells than in Caco-2 cells, the pattern of production as shown by the dose-response curves in Figure 4-2 and Figure 4-3, implies that the signalling process is similar in both cell-lines and thus likely to be regulated in a similar manner.

NCM460 cells presumably do not express any or very few IL-1β receptors and so are unable to induce expression of CXCL8 in response to IL-1β stimulation. In support of the notion that this cell line expresses few IL-1β receptors, a paper by Kim *et al* shows that there is only a small induction of PGE_2 expression following IL-1β stimulation (219). This could be corrobated by using an

antibody to IL-1R to confirm or deny the presence of IL-1β receptors. However, there is very little published research using IL-1β-stimulated NCM460 cells so a future experiment using FACS (Fluorescence Activated Cell Sorting) or immunostaining would be required to confirm or deny the existence of IL-1β receptors on the NCM460 cell surface.

.

7.5 Strengths and Weaknesses

The use of cell-lines rather than primary cells or clinical samples is both a strength and a weakness of this research. Whilst the Caco-2 cell-line has been used extensively as a good model of the intestinal epithelium, it acquired potentially problematical characteristics during its immortalisation as an adenocarcinoma (159). In contrast the NCM460 cell-line is derived from the normal colonic mucosa of a 68-year-old Hispanic male (220). These cells have not been transfected with any genetic material and are non-tumourigenic. They express cytokeratins, villin and other epithelial cell antigens and some cells synthesise mucin, making them as close to physiologically normal as possible whilst also being immortal. As shown in Figure 4-5, tolerance is not a phenomenon seen only in malignant cells, as the same effect is seen in NCM460 cells as in Caco-2 cells. Therefore, tolerance is something that is intrinsic to normal healthy epithelial cells. The cell-line data are representative of the physiological situation.

The use of P3CK is also both an advantage and a disadvantage. P3CK is a synthetic lipoprotein that is a mimic of the acylated amino terminal of bacterial lipoproteins (Figure 4-1). It acts as an agonist for TLR2 thus activating NF-κB and initiating an inflammatory response (221). Its advantage as a pro-inflammatory stimulant is that it is a physiological activator of an inflammatory response. IL-1β is also physiological, but it is not the initiating point. However, P3CK is a synthetic mimic rather than an actual bacterial lipoprotein or whole bacteria, neither pathogenic nor symbiotic. This is a small difference as P3CK has a long proven record of successfully stimulating an immune response via TLR2. This research has shown that tolerance is induced at two different starting points which converge in the activation of NF-κB.

A further strength of using P3CK is that it mimics, very simply, the presence of the microbiota and their interaction with intestinal epithelial cells. There is much research into the effect of the microbiota on the development of diseases, in particular IBD (222), and how different bacterial species can have an effect on both eitology and cure. It is well established that the presence of microbiota is required for development of a healthy intestine which responds correctly to inflammatory stimuli in later life (222). This research has shown that P3CK, a synthetic bacterial lipoprotein can down-regulate the intestinal epithelial cell response to inflammatory stimuli (Figure 4-20).

The main weakness of this research is the small fold-changes in histone methylation demonstrated in response to the range of epigenetic inhibitors. SAH and 2,4-PDCA were chosen for their lack of specificity. They both have a broad range of epigenetic modifying enzyme targets and were chosen for that reason as the specific enzymes that are required to modify H3K27me3 and H3K4me3, respectively, with regards to tolerance are not already known. Chaetocin and pargyline, in contrast, are inhibitors with specificity for H3K9me3 and H3K4me3, respectively.

Data provided by suppliers and previously published experiments gave IC_{50} values and suggested experimental parameters. However, even at concentrations several-fold higher than the published IC_{50} values the effect on histone methylation was small. There are many explanations for this, the most likely being that the experiments to determine the IC_{50} values were performed on purified enzymes with synthetic substrates whilst this research used whole cells. It is probable that the total amount of inhibitor is not fully transported into the cells so the concentration interacting with the enzymes is likely to be much lower than the concentration in the medium.

The inhibitors have an effect on multiple enzymes, so they may alter the methylation levels of multiple marks. Histone methyltransferase and histone demethylase activity is in equilibrium. Inhibiting histone methyltransferase activity results in an increase in the amount of substrate, which shifts the balance of equilibrium towards the corresponding demethylase reaction (Figure 7-1). Similarly, inhibiting the demethylase reactions causes the amount of methylated histone to increase. This is the substrate for the next methyltransferase reaction thus decreasing the amount of histone with the required number of methyl groups. Focussing on tri-methylated residues should have avoided the complications provided by the connected equations in equilibrium with the one of interest as the tri-methylated histone residue is the end point of the system.

Histone methyltransferase inhibition should result in a reduction of tri-methylated histone as the methyltransferase reaction producing it is being inhibited and there is not a demethylase reaction that produces tri-methylated residues. Conversely, inhibition of histone demethylase activity should result in an increase of the amount of tri-methylated histone as the demethylase reaction has been inhibited and there is not a methyltransferase reaction using tri-methylated histone as a substrate. Therefore, these are the residues that are most likely to show the effect of the small molecule inhibitors. They are also the epigenetic marks that are associated with a change in gene transcription and thus the ones most likely to affect the regulation of tolerance.

The sometimes conflicting results described in chapters 5 and 6 indicate that there are limits to the conclusions that can be drawn. The effects of some of the epigenetic inhibitors on the global levels of histone methylation were sometimes opposite to expected. However, the results have been shown to be consistent and reproducible and possible explanations have been provided. It is not possible to know how every inhibitor will behave in all conditions in all cell types. Cells have

also been shown to adapt to a modified epigenetic signature (223) and adjust transcription accordingly, which could be playing a part here. The results taken from the ChIP data for the loci 5' upstream of the promoter and at the promoter are particularly interesting as they fit into existing understanding of how histone modifications, epigenetic inhibitors and transcriptional expression work. Current research into the combinatorial nature of epigenetics shows how important it is not study any one modification in isolation, or even one type of epigenetic modification as has been done here. Cheng and Blumenthal describe how histone and DNA methylation are linked with several modifications being dependent on each other for their activation (224).

$$\text{Histone Lysine} + \text{X-CH}_3 \underset{b}{\overset{a}{\rightleftharpoons}} \text{Mono-methylated Histone lysine} + \text{X}$$

$$\text{Mono-methylated Histone Lysine} + \text{X-CH}_3 \underset{d}{\overset{c}{\rightleftharpoons}} \text{Di-methylated Histone lysine} + \text{X}$$

$$\text{Di-methylated Histone Lysine} + \text{X-CH}_3 \underset{f}{\overset{e}{\rightleftharpoons}} \text{Tri-methylated Histone Lysine} + \text{X}$$

Figure 7-1 Histone Lysine Methylation Equations

The equations representing the cumulative methylation of individual histone lysine residues are illustrated here with X representing a methyl-donor; a, c and e represent histone lysine methyltransferases; b, d and f represent histone lysine demethylases.

A major strength of this research is that the results are quantitative, reproducible and can be statistically validated. ELISAs produce quantitative results and different samples can be compared across plates. This is important as the results can be analysed by statistical tests thereby proving that the result is true within strict confidence limits and not subject to chance. qPCR was used to measure the expression of inflammatory cytokines (IL6, CXCL8 and TNF) over a 48 hour time period including two 24 hour stimulations with IL-1β. The down-regulation of mRNA expression to background levels before the second IL-1β-stimulation was applied proves

that tolerance is a true characteristic. The reduction in expression seen after the second stimulation is a result of the pre-stimulation and not just the down-regulation of transcription. This also applies to the use of ChIP when investigating the specific histone modifications present at individual loci. Though the results from chapter 5 are useful, the epigenetic inhibitors are having a non-specific global effect. Chapter 6 looks specifically and quantitatively at the effects of those inhibitors in discrete loci.

The CXCL8 values in individual experiments, particularly by tolerized cells, vary from experiment to experiment, as shown by the range of CXCL8 produced by each IL-1β concentration in Figure 4-6. In order to compensate for this variation across experiments, the CXCL8 values are represented as a percentage of the stimulated amount. The advantage of presenting the data in this format is that the *n* number sample size for each experiment is increased thus increasing the power of the statistical tests.

A relatively small concentration of IL-1β (1 ng/ml IL-1β compared to 25 μg/ml P3CK) produces a strong and reproducible inflammatory response. This is a reliable effect producing similar amounts of CXCL8 every time. Multiple experiments can be combined for increased statistical verification by representing the expression of CXCL8 produced by the tolerized cells as a proportion of the amount produced by the stimulated cells. There is a clear and statistically significant difference in the expression of CXCL8 produced by stimulated and tolerized cells even using such a small concentration of IL-1β making the results reliable and yet the IL-1β not having a deleterious effect on cells. The amount we used in the experiments is physiologically relevant, as demonstrated by the measurements of IL-1β produced by lamina propria mononuclear cells taken from the mucosa of patients with involved and non-involved CD and UC by Reinecker *et al* (225). In all disease cases, the concentration of IL-1β produced was statistically significantly

greater than the concentration of IL-1β produced by normal mucosal cells. This ranged from 44 pg/ml in normal mucosa to 100 pg/ml and 108 pg/ml in non-involved CD and UC, respectively (disease vs. normal $P<0.001$) and up to 305 pg/ml and 356 pg/ml in involved CD and UC, respectively ($P<0.0001$ involved vs. non-involved mucosa) (225). Therefore, even though 1 ng/ml IL-1β is a higher concentration than that measured in IBD samples, it is not an unlikely physiological concentration, especially as local concentration will be greater than Reinecker's measurements.

7.6 Future Work

The work here can be expanded by examining the effect of SAH, Chaetocin, Pargyline and 2,4-PDCA on P3CK-induced tolerance in both Caco-2 and NCM460 cells. The work in this thesis has shown that SAH, Chaetocin and Pargyline break IL-1β-induced tolerance. However, their effect on P3CK-induced tolerance is unknown. I predict that the results will be comparable, as both IL-1β- and P3CK-stimulated signalling converges on the activation of NF-κB and the subsequent induction of inflammatory gene expression. It is worth investigating the inhibitors' effect in both cell types as the size of the CXCL8 response was higher in the NCM460 cell-line than the Caco-2 cell-line.

As all of the experiments in this project were performed in cell-lines, further research should be performed on human samples taken from patients with inflammatory intestinal diseases e.g. IBD or NEC, as there is a plentiful supply of biopsy samples from patients with both diseases. Different regions of the biopsy sample should correspond to the different experimental conditions used. For example, the stimulated experimental condition should reflect the gene expression levels of the inflamed biopsy region whilst the tolerized condition should be similar to the non-inflamed and healthy surrounding tissue in the biopsy. Experiments performed on human IBD/NEC biopsy samples are necessary to confirm the relevance and applicability of the research in this project to patients with real inflammatory diseases, and not just as a theoretical exercise.

However, the difficulties of studying the epithelium in isolation are great. Biopsies taken from the intestine are a mixture of different cell types, as epithelial cells do not grow in isolation. Performing similar experiments as in this project on biopsy samples will produce a range of responses from the different cell types making it difficult to distinguish the epithelial cell response

from the Goblet cells, Paneth cells and intestinal immune cells etc. Epithelial cells can be isolated using EDTA or proteolytic enzymes such as trypsin or collegenase but remain viable for only very short time periods (226). Even if viable epithelial cells can be completely isolated, each cell will behave differently making the sample behave as a multi-cell sample. Published research by Jenke *et al.*, describes the difficulty of analysing epigenetic differences in biopsy samples. Though epithelial cells were successfully isolated from small bowel biopsies using both the EDTA and enzymatic methods, analysis of DNA methylation indicated variations between the differently isolated and non-isolated samples (227). Therefore, the method of cell isolation must be carefully considered so as not to mask cell-type specific results.

Epigenetic signatures are difficult to examine without the added complications of a range of cell types and behaviours. Large cell numbers per sample are also required which can be difficult to achieve from epithelial cells isolated from a biopsy when the majority of cells in the biopsy will be discarded. However, there has been some progress in studying epigenetics in single cells (228). This paper by Bintu *et al.* studied the dynamics of epigenetic regulation, but there is no reason why the technique cannot be adapted in order to the study of epigenetic signatures in individual cells. The epigenetic signature at the CXCL8 locus in both the inflamed and surrounding non-inflamed tissue would then be compared to the epigenetic signatures in the control, stimulated and tolerized cell-line samples. I predict that the inflamed tissue signature will resemble the stimulated samples whilst the non-inflamed tissue will resemble the tolerized cell-line samples. Non-inflamed tissue from IBD and NEC patients is not a true representation of healthy intestinal epithelium. It would be better to compare inflamed and non-inflamed diseased tissue against biopsies taken from healthy individuals.

This research hypothesised that epigenetics would play a role in the regulation of tolerance and the use of inhibitors is good evidence to support this. However, a more extensive investigation into the different epigenetic markers could be performed including H3K4me1, H3K36, H3K79 and non-methylation modifications. This would generate a more complete description of the epigenetic signature required to regulate tolerance. The specific enzymes that modify the epigenetic markers in the regulatory signature could also be identified in order to determine which markers are essential for regulating tolerance. This might be achieved by knocking out individual epigenetic modifying enzymes using shRNA or similar and measuring the effect on CXCL8 production after stimulation and tolerization with IL-1β and/or P3CK.

Because of the ability of P3CK to induce tolerance, we can infer that the presence of microbiota is important for the establishment of tolerance. The effect of the microbiota on tolerance has not previously been investigated in epithelial cells, though specific bacterial elements have been used. There is considerable research into the role of microbiota in disease and the changes in microbiota composition associated with specific diseases. It would be interesting to investigate whether a change in microbiota species can cause a change in tolerance. Villena *et al.* have shown how intestinal inflammation is modulated factors expressed by the microbiota (229). Is it possible for a particular species to either induce or break tolerance? This could be tested by incubating epithelial cells with a variety of different bacteria species identified in the literature as having a role in disease. It should be taken into account, however, that the microbiome continually adjusts to its environment and that there is a level of functional redundancy present whereby two microbiomes with different compositions behave in a similar fashion (230).

This research project used four commercially available inhibitors of epigenetic modifying enzymes. Chaetocin is an antifungal metabolite and SAH is a methylation metabolite whilst

Pargyline and 2,4-PDCA have been chemically synthesised. Future research could be conducted into whether there are any other naturally occurring inhibitors, in particular whether there are any inhibitors to be found as nutritional metabolites. If such inhibitors exist, is it possible for them to be ingested to a sufficient concentration such that they have a beneficial effect on the epigenetic signature? If so, they could be developed as a potential drug therapy or a dietary supplement for patients with inflammatory disorders.

Finally, this research project used one cell type in isolation for all experiments. A more realistic model of the intestinal epithelium would be a 3D model of the epithelium surrounding a lumen and intestinal immune cells to interact with the epithelial cells. Caco-2 and NCM460 cells in a monolayer is representative of the luminal lining, but in reality the epithelium is not in isolation and is in contact with the lamina propria, Goblet and Paneth cells and intestinal T cells, among others. A 3D model would also allow the interaction between epithelium and microbiota to be studied in a physiological manner. Nevertheless, my work shows for the first time that epigenetics plays an important role in the regulation of immune tolerance in intestinal epithelial cells. Though it is not the only factor involved, altering the epigenetic signature causes a change in CXCL8 or immune transcription and therefore an altered physiological response.

8 References

1. Nathan C. Points of control in inflammation. Nature. 2002;420(6917):846-52. Epub 2002/12/20. doi: 10.1038/nature01320 nature01320 [pii]. PubMed PMID: 12490957.

2. Medzhitov R. Origin and physiological roles of inflammation. Nature. 2008;454(7203):428-35. Epub 2008/07/25. doi: 10.1038/nature07201 nature07201 [pii]. PubMed PMID: 18650913.

3. Neth OW, Bajaj-Elliott M, Turner MW, Klein NJ. Susceptibility to infection in patients with neutropenia: the role of the innate immune system. Br J Haematol. 2005;129(6):713-22. Epub 2005/06/15. doi: BJH5462 [pii] 10.1111/j.1365-2141.2005.05462.x. PubMed PMID: 15952996.

4. Bradley DT, Bourke TW, Fairley DJ, Borrow R, Shields MD, Young IS, et al. Genetic susceptibility to invasive meningococcal disease: MBL2 structural polymorphisms revisited in a large case-control study and a systematic review. Int J Immunogenet. 2012;39(4):328-37. doi: 10.1111/j.1744-313X.2012.01095.x. PubMed PMID: 22296677.

5. Walport MJ, Davies KA, Morley BJ, Botto M. Complement deficiency and autoimmunity. Ann N Y Acad Sci. 1997;815:267-81. Epub 1997/04/05. PubMed PMID: 9186664.

6. Ferrero-Miliani L, Nielsen OH, Andersen PS, Girardin SE. Chronic inflammation: importance of NOD2 and NALP3 in interleukin-1beta generation. Clin Exp Immunol. 2007;147(2):227-35. doi: 10.1111/j.1365-2249.2006.03261.x. PubMed PMID: 17223962; PubMed Central PMCID: PMCPMC1810472.

7. NHS. Sepsis 2013. Available from: www.nhs.uk/conditions/Blood-poisoning/Pages/Introduction.aspx.

8. NHS. Diabetes 2013. Available from: www.nhs.uk/conditions/Diabetes-type1/Pages/Introduction.aspx.

9. NHS. Rheumatoid Arthritis 2013. Available from: www.nhs.uk/conditions/Rheumatoid-arthritis/Pages/Introduction.aspx.

10. NHS. Inflammatory Bowel Disease 2013. Available from: www.nhs.uk/conditions/Inflammatory-bowel-disease/Pages/Introduction.aspx.

11. Schmid-Schonbein GW. Analysis of inflammation. Annu Rev Biomed Eng. 2006;8:93-131. Epub 2006/07/13. doi: 10.1146/annurev.bioeng.8.061505.095708. PubMed PMID: 16834553.

12. Cotran RS, Kumar V, Collins T, Robbins SLPbod. Robbins pathologic basis of disease. 6th ed. / Ramzi S. Cotran, Vinay Kumar, Tucker Collins. ed. Philadelphia ; London: Saunders; 1999.

13. Balk RA. Systemic inflammatory response syndrome (SIRS): where did it come from and is it still relevant today? Virulence. 2014;5(1):20-6. Epub 2013/11/28. doi: 10.4161/viru.27135 27135 [pii]. PubMed PMID: 24280933; PubMed Central PMCID: PMC3916374.

14. Porth C. Essentials of pathophysiology : concepts of altered health states. 3rd ed. Philadelphia: Wolters Kluwer/Lippincott Williams & Wilkins; 2011. xxiv, 1256 p. p.

15. Gregor MF, Hotamisligil GS. Inflammatory mechanisms in obesity. Annu Rev Immunol. 2011;29:415-45. Epub 2011/01/12. doi: 10.1146/annurev-immunol-031210-101322. PubMed PMID: 21219177.

16. Rostami Nejad M, Ishaq S, Al Dulaimi D, Zali MR, Rostami K. The role of infectious mediators and gut microbiome in the pathogenesis of celiac disease. Arch Iran Med. 2015;18(4):244-9. Epub 2015/04/07. doi: 015184/AIM.0010 0010 [pii]. PubMed PMID: 25841946.

17. Fujimoto Y, Tanaka K, Shimoyama A, Fukase K. Self and nonself recognition with bacterial and animal glycans, surveys by synthetic chemistry. Methods Enzymol. 2010;478:323-42. doi: 10.1016/s0076-6879(10)78016-2. PubMed PMID: 20816488.

18. Kawai T, Akira S. The role of pattern-recognition receptors in innate immunity: update on Toll-like receptors. Nat Immunol. 2010;11(5):373-84. Epub 2010/04/21. doi: 10.1038/ni.1863 ni.1863 [pii]. PubMed PMID: 20404851.

19. Ozinsky A, Underhill DM, Fontenot JD, Hajjar AM, Smith KD, Wilson CB, et al. The repertoire for pattern recognition of pathogens by the innate immune system is defined by cooperation between toll-like receptors. Proc Natl Acad Sci U S A. 2000;97(25):13766-71. doi: 10.1073/pnas.250476497. PubMed PMID: 11095740; PubMed Central PMCID: PMCPMC17650.

20. Guan Y, Ranoa DR, Jiang S, Mutha SK, Li X, Baudry J, et al. Human TLRs 10 and 1 share common mechanisms of innate immune sensing but not signaling. J Immunol. 2010;184(9):5094-103. doi: 10.4049/jimmunol.0901888. PubMed PMID: 20348427.

21. Mizel SB, Honko AN, Moors MA, Smith PS, West AP. Induction of macrophage nitric oxide production by Gram-negative flagellin involves signaling via heteromeric Toll-like receptor 5/Toll-like receptor 4 complexes. J Immunol. 2003;170(12):6217-23. PubMed PMID: 12794153.

22. Re F, Strominger JL. Monomeric recombinant MD-2 binds toll-like receptor 4 tightly and confers lipopolysaccharide responsiveness. J Biol Chem. 2002;277(26):23427-32. doi: 10.1074/jbc.M202554200. PubMed PMID: 11976338.

23. Israël A. The IKK complex, a central regulator of NF-kappaB activation. Cold Spring Harb Perspect Biol. 2010;2(3):a000158. doi: 10.1101/cshperspect.a000158. PubMed PMID: 20300203; PubMed Central PMCID: PMCPMC2829958.

24. Beg AA, Ruben SM, Scheinman RI, Haskill S, Rosen CA, Baldwin AS. I kappa B interacts with the nuclear localization sequences of the subunits of NF-kappa B: a mechanism for cytoplasmic retention. Genes Dev. 1992;6(10):1899-913. PubMed PMID: 1340770.

25. Cargnello M, Roux PP. Activation and function of the MAPKs and their substrates, the MAPK-activated protein kinases. Microbiol Mol Biol Rev. 2011;75(1):50-83. doi:

10.1128/mmbr.00031-10. PubMed PMID: 21372320; PubMed Central PMCID: PMCPMC3063353.

26. Sharma M, Mohapatra J, Acharya A, Deshpande SS, Chatterjee A, Jain MR. Blockade of tumor necrosis factor-α converting enzyme (TACE) enhances IL-1β and IFN-γ via caspase-1 activation: a probable cause for loss of efficacy of TACE inhibitors in humans? Eur J Pharmacol. 2013;701(1-3):106-13. doi: 10.1016/j.ejphar.2012.12.002. PubMed PMID: 23266381.

27. Westbrook AM, Wei B, Hacke K, Xia M, Braun J, Schiestl RH. The role of tumour necrosis factor-α and tumour necrosis factor receptor signalling in inflammation-associated systemic genotoxicity. Mutagenesis. 2012;27(1):77-86. doi: 10.1093/mutage/ger063. PubMed PMID: 21980144; PubMed Central PMCID: PMCPMC3241942.

28. Oltmanns U, Issa R, Sukkar MB, John M, Chung KF. Role of c-jun N-terminal kinase in the induced release of GM-CSF, RANTES and IL-8 from human airway smooth muscle cells. Br J Pharmacol. 2003;139(6):1228-34. Epub 2003/07/23. doi: 10.1038/sj.bjp.0705345. PubMed PMID: 12871843; PubMed Central PMCID: PMC1573939.

29. Brynskov J, Foegh P, Pedersen G, Ellervik C, Kirkegaard T, Bingham A, et al. Tumour necrosis factor alpha converting enzyme (TACE) activity in the colonic mucosa of patients with inflammatory bowel disease. Gut. 2002;51(1):37-43. Epub 2002/06/22. PubMed PMID: 12077089; PubMed Central PMCID: PMC1773288.

30. Stidham RW, Lee TC, Higgins PD, Deshpande AR, Sussman DA, Singal AG, et al. Systematic review with network meta-analysis: the efficacy of anti-TNF agents for the treatment of Crohn's disease. Aliment Pharmacol Ther. 2014;39(12):1349-62. Epub 2014/04/23. doi: 10.1111/apt.12749. PubMed PMID: 24749763.

31. Stidham RW, Lee TC, Higgins PD, Deshpande AR, Sussman DA, Singal AG, et al. Systematic review with network meta-analysis: the efficacy of anti-tumour necrosis factor-alpha

agents for the treatment of ulcerative colitis. Aliment Pharmacol Ther. 2014;39(7):660-71. Epub 2014/02/11. doi: 10.1111/apt.12644. PubMed PMID: 24506179.

32. Edye ME, Lopez-Castejon G, Allan SM, Brough D. Acidosis drives damage-associated molecular pattern (DAMP)-induced interleukin-1 secretion via a caspase-1-independent pathway. J Biol Chem. 2013;288(42):30485-94. doi: 10.1074/jbc.M113.478941. PubMed PMID: 24022484; PubMed Central PMCID: PMCPMC3798512.

33. Dinarello CA. The interleukin-1 family: 10 years of discovery. FASEB J. 1994;8(15):1314-25. Epub 1994/12/01. PubMed PMID: 8001745.

34. O'Neill LA. The interleukin-1 receptor/Toll-like receptor superfamily: 10 years of progress. Immunol Rev. 2008;226:10-8. Epub 2009/01/24. doi: 10.1111/j.1600-065X.2008.00701.x IMR701 [pii]. PubMed PMID: 19161412.

35. Martinon F. Detection of immune danger signals by NALP3. J Leukoc Biol. 2008;83(3):507-11. doi: 10.1189/jlb.0607362. PubMed PMID: 17982111.

36. Banks WA, Kastin AJ, Gutierrez EG. Penetration of interleukin-6 across the murine blood-brain barrier. Neurosci Lett. 1994;179(1-2):53-6. Epub 1994/09/26. doi: 0304-3940(94)90933-4 [pii]. PubMed PMID: 7845624.

37. Parikh AA, Salzman AL, Kane CD, Fischer JE, Hasselgren PO. IL-6 production in human intestinal epithelial cells following stimulation with IL-1 beta is associated with activation of the transcription factor NF-kappa B. J Surg Res. 1997;69(1):139-44. doi: 10.1006/jsre.1997.5061. PubMed PMID: 9202660.

38. Tesoriere L, Attanzio A, Allegra M, Gentile C, Livrea MA. Indicaxanthin inhibits NADPH oxidase (NOX)-1 activation and NF-κB-dependent release of inflammatory mediators and prevents the increase of epithelial permeability in IL-1β-exposed Caco-2 cells. Br J Nutr. 2014;111(3):415-23. doi: 10.1017/s0007114513002663. PubMed PMID: 23931157.

39. Dyer DP, Thomson JM, Hermant A, Jowitt TA, Handel TM, Proudfoot AE, et al. TSG-6 inhibits neutrophil migration via direct interaction with the chemokine CXCL8. J Immunol. 2014;192(5):2177-85. doi: 10.4049/jimmunol.1300194. PubMed PMID: 24501198; PubMed Central PMCID: PMCPMC3988464.

40. Yu H, Huang X, Ma Y, Gao M, Wang O, Gao T, et al. Interleukin-8 regulates endothelial permeability by down-regulation of tight junction but not dependent on integrins induced focal adhesions. Int J Biol Sci. 2013;9(9):966-79. Epub 2013/10/25. doi: 10.7150/ijbs.6996 ijbsv09p0966 [pii]. PubMed PMID: 24155670; PubMed Central PMCID: PMC3805902.

41. Van Damme J, Rampart M, Conings R, Decock B, Van Osselaer N, Willems J, et al. The neutrophil-activating proteins interleukin 8 and beta-thromboglobulin: in vitro and in vivo comparison of NH2-terminally processed forms. Eur J Immunol. 1990;20(9):2113-8. doi: 10.1002/eji.1830200933. PubMed PMID: 2145175.

42. Schutyser E, Struyf S, Proost P, Opdenakker G, Laureys G, Verhasselt B, et al. Identification of biologically active chemokine isoforms from ascitic fluid and elevated levels of CCL18/pulmonary and activation-regulated chemokine in ovarian carcinoma. J Biol Chem. 2002;277(27):24584-93. doi: 10.1074/jbc.M112275200. PubMed PMID: 11978786.

43. Van den Steen PE, Proost P, Wuyts A, Van Damme J, Opdenakker G. Neutrophil gelatinase B potentiates interleukin-8 tenfold by aminoterminal processing, whereas it degrades CTAP-III, PF-4, and GRO-alpha and leaves RANTES and MCP-2 intact. Blood. 2000;96(8):2673-81. PubMed PMID: 11023497.

44. Loos T, Opdenakker G, Van Damme J, Proost P. Citrullination of CXCL8 increases this chemokine's ability to mobilize neutrophils into the blood circulation. Haematologica. 2009;94(10):1346-53. Epub 2009/07/18. doi: 10.3324/haematol.2009.006973 haematol.2009.006973 [pii]. PubMed PMID: 19608678; PubMed Central PMCID: PMC2754949.

45. Proost P, Loos T, Mortier A, Schutyser E, Gouwy M, Noppen S, et al. Citrullination of CXCL8 by peptidylarginine deiminase alters receptor usage, prevents proteolysis, and dampens tissue inflammation. J Exp Med. 2008;205(9):2085-97. Epub 2008/08/20. doi: 10.1084/jem.20080305
jem.20080305 [pii]. PubMed PMID: 18710930; PubMed Central PMCID: PMC2526203.

46. Kuilman T, Michaloglou C, Vredeveld LC, Douma S, van Doorn R, Desmet CJ, et al. Oncogene-induced senescence relayed by an interleukin-dependent inflammatory network. Cell. 2008;133(6):1019-31. Epub 2008/06/17. doi: 10.1016/j.cell.2008.03.039
S0092-8674(08)00620-X [pii]. PubMed PMID: 18555778.

47. Ivison SM, Wang C, Himmel ME, Sheridan J, Delano J, Mayer ML, et al. Oxidative stress enhances IL-8 and inhibits CCL20 production from intestinal epithelial cells in response to bacterial flagellin. Am J Physiol Gastrointest Liver Physiol. 2010;299(3):G733-41. doi: 10.1152/ajpgi.00089.2010. PubMed PMID: 20595617.

48. Sunil Y, Ramadori G, Raddatzc D. Influence of NFkappaB inhibitors on IL-1beta-induced chemokine CXCL8 and -10 expression levels in intestinal epithelial cell lines: glucocorticoid ineffectiveness and paradoxical effect of PDTC. Int J Colorectal Dis. 2010;25(3):323-33. doi: 10.1007/s00384-009-0847-3. PubMed PMID: 19921217; PubMed Central PMCID: PMCPMC2814033.

49. Jeon MK, Klaus C, Kaemmerer E, Gassler N. Intestinal barrier: Molecular pathways and modifiers. World J Gastrointest Pathophysiol. 2013;4(4):94-9. doi: 10.4291/wjgp.v4.i4.94. PubMed PMID: 24244877; PubMed Central PMCID: PMCPMC3829455.

50. Moran GW, Leslie FC, Levison SE, Worthington J, McLaughlin JT. Enteroendocrine cells: neglected players in gastrointestinal disorders? Therap Adv Gastroenterol. 2008;1(1):51-60. Epub 2008/07/01. doi: 10.1177/1756283X08093943. PubMed PMID: 21180514; PubMed Central PMCID: PMC3002486.

51. Medema JP, Vermeulen L. Microenvironmental regulation of stem cells in intestinal homeostasis and cancer. Nature. 2011;474(7351):318-26. Epub 2011/06/17. doi: 10.1038/nature10212
nature10212 [pii]. PubMed PMID: 21677748.

52. Burkitt HG, Young B, Heath JW. *Wheater's Functional Histology* 3rd edition ed1993.

53. Jung C, Hugot JP, Barreau F. Peyer's Patches: The Immune Sensors of the Intestine. Int J Inflam. 2010;2010:823710. doi: 10.4061/2010/823710. PubMed PMID: 21188221; PubMed Central PMCID: PMCPMC3004000.

54. Agace WW, Roberts AI, Wu L, Greineder C, Ebert EC, Parker CM. Human intestinal lamina propria and intraepithelial lymphocytes express receptors specific for chemokines induced by inflammation. Eur J Immunol. 2000;30(3):819-26. doi: 10.1002/1521-4141(200003)30:3<819::AID-IMMU819>3.0.CO;2-Y. PubMed PMID: 10741397.

55. Niess JH, Brand S, Gu X, Landsman L, Jung S, McCormick BA, et al. CX3CR1-mediated dendritic cell access to the intestinal lumen and bacterial clearance. Science. 2005;307(5707):254-8. doi: 10.1126/science.1102901. PubMed PMID: 15653504.

56. Braunstein J, Qiao L, Autschbach F, Schürmann G, Meuer S. T cells of the human intestinal lamina propria are high producers of interleukin-10. Gut. 1997;41(2):215-20. PubMed PMID: 9301501; PubMed Central PMCID: PMCPMC1891463.

57. Hendrickson BA, Gokhale R, Cho JH. Clinical aspects and pathophysiology of inflammatory bowel disease. Clin Microbiol Rev. 2002;15(1):79-94. PubMed PMID: 11781268; PubMed Central PMCID: PMCPMC118061.

58. McAlindon ME, Gray T, Galvin A, Sewell HF, Podolsky DK, Mahida YR. Differential lamina propria cell migration via basement membrane pores of inflammatory bowel disease mucosa. Gastroenterology. 1998;115(4):841-8. PubMed PMID: 9753486.

59. Fuller R, Perdigo\n G. Gut flora, nutrition, immunity and health. Oxford: Blackwell; 2003.

60. Petri WA, Miller M, Binder HJ, Levine MM, Dillingham R, Guerrant RL. Enteric infections, diarrhea, and their impact on function and development. J Clin Invest. 2008;118(4):1277-90. doi: 10.1172/JCI34005. PubMed PMID: 18382740; PubMed Central PMCID: PMCPMC2276781.

61. Ley RE, Peterson DA, Gordon JI. Ecological and evolutionary forces shaping microbial diversity in the human intestine. Cell. 2006;124(4):837-48. doi: 10.1016/j.cell.2006.02.017. PubMed PMID: 16497592.

62. Ben-Neriah Y, Schmidt-Supprian M. Epithelial NF-kappaB maintains host gut microflora homeostasis. Nat Immunol. 2007;8(5):479-81. doi: 10.1038/ni0507-479. PubMed PMID: 17440457.

63. Pastorelli L, De Salvo C, Mercado JR, Vecchi M, Pizarro TT. Central role of the gut epithelial barrier in the pathogenesis of chronic intestinal inflammation: lessons learned from animal models and human genetics. Front Immunol. 2013;4:280. doi: 10.3389/fimmu.2013.00280. PubMed PMID: 24062746; PubMed Central PMCID: PMCPMC3775315.

64. Koch S, Nusrat A. The life and death of epithelia during inflammation: lessons learned from the gut. Annu Rev Pathol. 2012;7:35-60. doi: 10.1146/annurev-pathol-011811-120905. PubMed PMID: 21838548.

65. Goto Y, Ivanov II. Intestinal epithelial cells as mediators of the commensal-host immune crosstalk. Immunol Cell Biol. 2013;91(3):204-14. doi: 10.1038/icb.2012.80. PubMed PMID: 23318659; PubMed Central PMCID: PMCPMC3969236.

66. Bianconi E, Piovesan A, Facchin F, Beraudi A, Casadei R, Frabetti F, et al. An estimation of the number of cells in the human body. Ann Hum Biol. 2013;40(6):463-71. doi: 10.3109/03014460.2013.807878. PubMed PMID: 23829164.

67. Backhed F, Ley RE, Sonnenburg JL, Peterson DA, Gordon JI. Host-bacterial mutualism in the human intestine. Science. 2005;307(5717):1915-20. Epub 2005/03/26. doi: 307/5717/1915 [pii]

10.1126/science.1104816. PubMed PMID: 15790844.

68. Mazmanian SK, Round JL, Kasper DL. A microbial symbiosis factor prevents intestinal inflammatory disease. Nature. 2008;453(7195):620-5. Epub 2008/05/30. doi: 10.1038/nature07008

nature07008 [pii]. PubMed PMID: 18509436.

69. Favier CF, Vaughan EE, De Vos WM, Akkermans AD. Molecular monitoring of succession of bacterial communities in human neonates. Appl Environ Microbiol. 2002;68(1):219-26. Epub 2002/01/05. PubMed PMID: 11772630; PubMed Central PMCID: PMC126580.

70. Round JL, Lee SM, Li J, Tran G, Jabri B, Chatila TA, et al. The Toll-like receptor 2 pathway establishes colonization by a commensal of the human microbiota. Science. 2011;332(6032):974-7. Epub 2011/04/23. doi: 10.1126/science.1206095

science.1206095 [pii]. PubMed PMID: 21512004; PubMed Central PMCID: PMC3164325.

71. Abt MC, Artis D. The dynamic influence of commensal bacteria on the immune response to pathogens. Curr Opin Microbiol. 2013;16(1):4-9. doi: 10.1016/j.mib.2012.12.002. PubMed PMID: 23332724; PubMed Central PMCID: PMCPMC3622187.

72. Sartor RB. Therapeutic manipulation of the enteric microflora in inflammatory bowel diseases: antibiotics, probiotics, and prebiotics. Gastroenterology. 2004;126(6):1620-33. Epub 2004/05/29. doi: S0016508504004561 [pii]. PubMed PMID: 15168372.

73. Abraham C, Medzhitov R. Interactions between the host innate immune system and microbes in inflammatory bowel disease. Gastroenterology. 2011;140(6):1729-37. doi: 10.1053/j.gastro.2011.02.012. PubMed PMID: 21530739; PubMed Central PMCID: PMCPMC4007055.

74. Viladomiu M, Hontecillas R, Yuan L, Lu P, Bassaganya-Riera J. Nutritional protective mechanisms against gut inflammation. J Nutr Biochem. 2013. Epub 2013/04/02. doi: S0955-2863(13)00030-2 [pii]

10.1016/j.jnutbio.2013.01.006. PubMed PMID: 23541470.

75. Clarke JO, Mullin GE. A review of complementary and alternative approaches to immunomodulation. Nutr Clin Pract. 2008;23(1):49-62. Epub 2008/01/22. doi: 23/1/49 [pii]. PubMed PMID: 18203964.

76. Borody T, Torres M, Campbell J, Leis S, Nowak A. Reversal of Inflammatory Bowel Disease (IBD) with Recurrent Faecal Microbiota Transplants (FMT). American Journal of Gastroenterology. 2011;106:S366-S. PubMed PMID: ISI:000299772001542.

77. Colman RJ, Rubin DT. Fecal microbiota transplantation as therapy for inflammatory bowel disease: a systematic review and meta-analysis. J Crohns Colitis. 2014;8(12):1569-81. doi: 10.1016/j.crohns.2014.08.006. PubMed PMID: 25223604; PubMed Central PMCID: PMCPMC4296742.

78. Bakken JS, Borody T, Brandt LJ, Brill JV, Demarco DC, Franzos MA, et al. Treating Clostridium difficile infection with fecal microbiota transplantation. Clin Gastroenterol Hepatol. 2011;9(12):1044-9. Epub 2011/08/30. doi: 10.1016/j.cgh.2011.08.014 S1542-3565(11)00891-3 [pii]. PubMed PMID: 21871249; PubMed Central PMCID: PMC3223289.

79. Gerding DN, Meyer T, Lee C, Cohen SH, Murthy UK, Poirier A, et al. Administration of spores of nontoxigenic Clostridium difficile strain M3 for prevention of recurrent C. difficile infection: a randomized clinical trial. JAMA. 2015;313(17):1719-27. doi: 10.1001/jama.2015.3725. PubMed PMID: 25942722.

80. Beeson PB. Tolerance to Bacterial Pyrogens : I. Factors Influencing Its Development. J Exp Med. 1947;86(1):29-38. Epub 1947/06/30. PubMed PMID: 19871652; PubMed Central PMCID: PMC2135744.

81. West MA, Heagy W. Endotoxin tolerance: A review. Crit Care Med. 2002;30(1 Supp):S64-S73. Epub 2002/03/14. PubMed PMID: 11891406.

82. West MA, Heagy W. Endotoxin tolerance: a review. Crit Care Med. 2002;30(1 Suppl):S64-73. Epub 2002/01/10. PubMed PMID: 11782563.

83. Savidge TC, Newman PG, Pan WH, Weng MQ, Shi HN, McCormick BA, et al. Lipopolysaccharide-induced human enterocyte tolerance to cytokine-mediated interleukin-8 production may occur independently of TLR-4/MD-2 signaling. Pediatr Res. 2006;59(1):89-95. doi: 10.1203/01.pdr.0000195101.74184.e3. PubMed PMID: 16326999; PubMed Central PMCID: PMCPMC4465784.

84. Biswas SK, Lopez-Collazo E. Endotoxin tolerance: new mechanisms, molecules and clinical significance. Trends Immunol. 2009;30(10):475-87. doi: 10.1016/j.it.2009.07.009. PubMed PMID: 19781994.

85. Lotz M, Gütle D, Walther S, Ménard S, Bogdan C, Hornef MW. Postnatal acquisition of endotoxin tolerance in intestinal epithelial cells. J Exp Med. 2006;203(4):973-84. doi: 10.1084/jem.20050625. PubMed PMID: 16606665; PubMed Central PMCID: PMCPMC2118301.

86. Cavaillon JM, Adib-Conquy M. Bench-to-bedside review: endotoxin tolerance as a model of leukocyte reprogramming in sepsis. Crit Care. 2006;10(5):233. doi: 10.1186/cc5055. PubMed PMID: 17044947; PubMed Central PMCID: PMCPMC1751079.

87. Foster SL, Hargreaves DC, Medzhitov R. Gene-specific control of inflammation by TLR-induced chromatin modifications. Nature. 2007;447(7147):972-8. Epub 2007/06/01. doi: nature05836 [pii]
10.1038/nature05836. PubMed PMID: 17538624.

88. Liu C, Yu Y, Liu F, Wei X, Wrobel JA, Gunawardena HP, et al. A chromatin activity-based chemoproteomic approach reveals a transcriptional repressome for gene-specific silencing. Nat Commun. 2014;5:5733. doi: 10.1038/ncomms6733. PubMed PMID: 25502336; PubMed Central PMCID: PMCPMC4360912.

89. Pahl HL. Activators and target genes of Rel/NF-kappa B transcription factors. Oncogene. 1999;18(49):6853-66. doi: DOI 10.1038/sj.onc.1203239. PubMed PMID: ISI:000083896500003.

90. Dinarello CA. Interleukin-1 in the pathogenesis and treatment of inflammatory diseases. Blood. 2011;117(14):3720-32. doi: DOI 10.1182/blood-2010-07-273417. PubMed PMID: ISI:000289265500007.

91. Re F, Mengozzi M, Muzio M, Dinarello CA, Mantovani A, Colotta F. Expression of Interleukin-1 Receptor Antagonist (Il-1ra) by Human Circulating Polymorphonuclear Cells. Eur J Immunol. 1993;23(2):570-3. doi: DOI 10.1002/eji.1830230242. PubMed PMID: ISI:A1993KM03300041.

92. Mosser DM, Zhang X. Interleukin-10: new perspectives on an old cytokine. Immunol Rev. 2008;226:205-18. Epub 2009/01/24. doi: 10.1111/j.1600-065X.2008.00706.x IMR706 [pii]. PubMed PMID: 19161426; PubMed Central PMCID: PMC2724982.

93. Kuhn R, Lohler J, Rennick D, Rajewsky K, Muller W. Interleukin-10-Deficient Mice Develop Chronic Enterocolitis. Cell. 1993;75(2):263-74. doi: Doi 10.1016/0092-8674(93)80068-P. PubMed PMID: ISI:A1993MD88500008.

94. Braat H, Rottiers P, Hommes DW, Huyghebaert N, Remaut E, Remon JP, et al. A phase I trial with Transgenic bacteria expressing interleukin-10 in Crohn's disease. Clin Gastroenterol H. 2006;4(6):754-9. doi: DOI 10.1016/j.cgh.2006.03.028. PubMed PMID: ISI:000238350500015.

95. Ohtsuka Y, Sanderson IR. Transforming growth factor-beta: an important cytokine in the mucosal immune response. Curr Opin Gastroen. 2000;16(6):541-5. doi: Doi 10.1097/00001574-200011000-00014. PubMed PMID: ISI:000089969900014.

96. Hahm KB, Im YH, Parks TW, Park SH, Markowitz S, Jung HY, et al. Loss of transforming growth factor beta signalling in the intestine contributes to tissue injury in inflammatory bowel disease. Gut. 2001;49(2):190-8. doi: Doi 10.1136/Gut.49.2.190. PubMed PMID: ISI:000169965000009.

97. Del Zotto B, Mumolo G, Pronio AM, Montesani C, Tersigni R, Boirivant M. TGF-beta 1 production in inflammatory bowel disease: differing production patterns in Crohn's disease and ulcerative colitis. Clinical and Experimental Immunology. 2003;134(1):120-6. doi: DOI 10.1046/j.1365-2249.2003.02250.x. PubMed PMID: ISI:000185345200019.

98. Neagos J, Standiford TJ, Newstead MW, Zeng X, Huang SK, Ballinger MN. Epigenetic Regulation of Tolerance to Toll-Like Receptor Ligands in Alveolar Epithelial Cells. Am J Respir Cell Mol Biol. 2015;53(6):872-81. doi: 10.1165/rcmb.2015-0057OC. PubMed PMID: 25965198; PubMed Central PMCID: PMCPMC4742943.

99. Macdonald TT, Monteleone G. Immunity, inflammation, and allergy in the gut. Science. 2005;307(5717):1920-5. Epub 2005/03/26. doi: 307/5717/1920 [pii] 10.1126/science.1106442. PubMed PMID: 15790845.

100. Prager M, Buettner J, Buening C. Genes involved in the regulation of intestinal permeability and their role in ulcerative colitis. J Dig Dis. 2015;16(12):713-22. doi: 10.1111/1751-2980.12296. PubMed PMID: 26512799.

101. Molodecky NA, Soon IS, Rabi DM, Ghali WA, Ferris M, Chernoff G, et al. Increasing Incidence and Prevalence of the Inflammatory Bowel Diseases With Time, Based on Systematic Review. Gastroenterology. 2012;142(1):46-54. doi: DOI 10.1053/j.gastro.2011.10.001. PubMed PMID: ISI:000298250800028.

102. Magro F, Rodrigues A, Vieira AI, Portela F, Cremers I, Cotter J, et al. Review of the disease course among adult ulcerative colitis population-based longitudinal cohorts. Inflamm Bowel Dis. 2012;18(3):573-83. doi: 10.1002/ibd.21815. PubMed PMID: 21793126.

103. Marshall JK, Thabane M, Steinhart AH, Newman JR, Anand A, Irvine EJ. Rectal 5-aminosalicylic acid for induction of remission in ulcerative colitis. Cochrane Database Syst Rev. 2010(1):CD004115. doi: 10.1002/14651858.CD004115.pub2. PubMed PMID: 20091560.

104. Ford AC, Moayyedi P, Hanauer SB. Ulcerative colitis. Brit Med J. 2013;346. doi: ARTN f432
DOI 10.1136/bmj.f432. PubMed PMID: ISI:000314806700007.
105. Muraro D, Lauffenburger DA, Simmons A. Prioritisation and network analysis of Crohn's disease susceptibility genes. PLoS One. 2014;9(9):e108624. doi: 10.1371/journal.pone.0108624. PubMed PMID: 25268122; PubMed Central PMCID: PMCPMC4182533.
106. Fiocchi C. Inflammatory bowel disease: Etiology and pathogenesis. Gastroenterology. 1998;115(1):182-205. doi: Doi 10.1016/S0016-5085(98)70381-6. PubMed PMID: ISI:000074434500028.
107. Rampton DS. Regular review - Management of Crohn's disease. Brit Med J. 1999;319(7223):1480-5. PubMed PMID: ISI:000084129200025.
108. Gibson PR, Shepherd SJ. Personal view: food for thought--western lifestyle and susceptibility to Crohn's disease. The FODMAP hypothesis. Aliment Pharmacol Ther. 2005;21(12):1399-409. doi: 10.1111/j.1365-2036.2005.02506.x. PubMed PMID: 15948806.
109. Durchschein F, Petritsch W, Hammer HF. Diet therapy for inflammatory bowel diseases: The established and the new. World J Gastroenterol. 2016;22(7):2179-94. doi: 10.3748/wjg.v22.i7.2179. PubMed PMID: 26900283; PubMed Central PMCID: PMCPMC4734995.
110. Luger K, Mäder AW, Richmond RK, Sargent DF, Richmond TJ. Crystal structure of the nucleosome core particle at 2.8 A resolution. Nature. 1997;389(6648):251-60. doi: 10.1038/38444. PubMed PMID: 9305837.
111. Felsenfeld G, Groudine M. Controlling the double helix. Nature. 2003;421(6921):448-53. Epub 2003/01/24. doi: 10.1038/nature01411
nature01411 [pii]. PubMed PMID: 12540921.

112. Rogakou EP, Pilch DR, Orr AH, Ivanova VS, Bonner WM. DNA double-stranded breaks induce histone H2AX phosphorylation on serine 139. J Biol Chem. 1998;273(10):5858-68. PubMed PMID: 9488723.

113. Thoma F, Koller T, Klug A. Involvement of histone H1 in the organization of the nucleosome and of the salt-dependent superstructures of chromatin. J Cell Biol. 1979;83(2 Pt 1):403-27. PubMed PMID: 387806; PubMed Central PMCID: PMCPMC2111545.

114. Elgin SC. Heterochromatin and gene regulation in Drosophila. Curr Opin Genet Dev. 1996;6(2):193-202. PubMed PMID: 8722176.

115. Collas P. The current state of chromatin immunoprecipitation. Mol Biotechnol. 2010;45(1):87-100. Epub 2010/01/16. doi: 10.1007/s12033-009-9239-8. PubMed PMID: 20077036.

116. Tsankova N, Renthal W, Kumar A, Nestler EJ. Epigenetic regulation in psychiatric disorders. Nat Rev Neurosci. 2007;8(5):355-67. doi: 10.1038/nrn2132. PubMed PMID: 17453016.

117. Deaton AM, Bird A. CpG islands and the regulation of transcription. Genes Dev. 2011;25(10):1010-22. Epub 2011/05/18. doi: 10.1101/gad.2037511 25/10/1010 [pii]. PubMed PMID: 21576262; PubMed Central PMCID: PMC3093116.

118. Barakat TS, Gribnau J. X chromosome inactivation and embryonic stem cells. Adv Exp Med Biol. 2010;695:132-54. Epub 2011/01/12. doi: 10.1007/978-1-4419-7037-4_10. PubMed PMID: 21222204.

119. Issa JP. CpG-island methylation in aging and cancer. Curr Top Microbiol Immunol. 2000;249:101-18. Epub 2000/05/10. PubMed PMID: 10802941.

120. Allfrey VG, Faulkner R, Mirsky AE. Acetylation and Methylation of Histones and Their Possible Role in the Regulation of Rna Synthesis. Proc Natl Acad Sci U S A. 1964;51:786-94. Epub 1964/05/01. PubMed PMID: 14172992; PubMed Central PMCID: PMC300163.

121. Fusunyan RD, Quinn JJ, Fujimoto M, MacDermott RP, Sanderson IR. Butyrate switches the pattern of chemokine secretion by intestinal epithelial cells through histone acetylation. Mol Med. 1999;5(9):631-40. Epub 1999/11/07. doi: 0179 [pii]. PubMed PMID: 10551904; PubMed Central PMCID: PMC2230463.

122. Sims RJ, Nishioka K, Reinberg D. Histone lysine methylation: a signature for chromatin function. Trends Genet. 2003;19(11):629-39. doi: 10.1016/j.tig.2003.09.007. PubMed PMID: 14585615.

123. Hon GC, Hawkins RD, Ren B. Predictive chromatin signatures in the mammalian genome. Hum Mol Genet. 2009;18(R2):R195-201. doi: 10.1093/hmg/ddp409. PubMed PMID: 19808796; PubMed Central PMCID: PMCPMC2912651.

124. Noma K, Allis CD, Grewal SI. Transitions in distinct histone H3 methylation patterns at the heterochromatin domain boundaries. Science. 2001;293(5532):1150-5. Epub 2001/08/11. doi: 10.1126/science.1064150
293/5532/1150 [pii]. PubMed PMID: 11498594.

125. Nowak SJ, Corces VG. Phosphorylation of histone H3 correlates with transcriptionally active loci. Genes Dev. 2000;14(23):3003-13. Epub 2000/12/15. PubMed PMID: 11114889; PubMed Central PMCID: PMC317109.

126. Foster ER, Downs JA. Histone H2A phosphorylation in DNA double-strand break repair. FEBS J. 2005;272(13):3231-40. Epub 2005/06/28. doi: EJB4741 [pii]
10.1111/j.1742-4658.2005.04741.x. PubMed PMID: 15978030.

127. Briggs SD, Xiao T, Sun ZW, Caldwell JA, Shabanowitz J, Hunt DF, et al. Gene silencing: trans-histone regulatory pathway in chromatin. Nature. 2002;418(6897):498. Epub 2002/08/02. doi: 10.1038/nature00970
nature00970 [pii]. PubMed PMID: 12152067.

128. Shiio Y, Eisenman RN. Histone sumoylation is associated with transcriptional repression. Proc Natl Acad Sci U S A. 2003;100(23):13225-30. Epub 2003/10/28. doi: 10.1073/pnas.1735528100
1735528100 [pii]. PubMed PMID: 14578449; PubMed Central PMCID: PMC263760.

129. Kothapalli N, Camporeale G, Kueh A, Chew YC, Oommen AM, Griffin JB, et al. Biological functions of biotinylated histones. J Nutr Biochem. 2005;16(7):446-8. Epub 2005/07/05. doi: S0955-2863(05)00098-7 [pii]
10.1016/j.jnutbio.2005.03.025. PubMed PMID: 15992689; PubMed Central PMCID: PMC1226983.

130. Cosgrove MS, Boeke JD, Wolberger C. Regulated nucleosome mobility and the histone code. Nat Struct Mol Biol. 2004;11(11):1037-43. doi: 10.1038/nsmb851. PubMed PMID: 15523479.

131. Cooke J, Zhang H, Greger L, Silva AL, Massey D, Dawson C, et al. Mucosal genome-wide methylation changes in inflammatory bowel disease. Inflamm Bowel Dis. 2012;18(11):2128-37. Epub 2012/03/16. doi: 10.1002/ibd.22942. PubMed PMID: 22419656.

132. Maile T, Kwoczynski S, Katzenberger RJ, Wassarman DA, Sauer F. TAF1 activates transcription by phosphorylation of serine 33 in histone H2B. Science. 2004;304(5673):1010-4. doi: 10.1126/science.1095001. PubMed PMID: 15143281.

133. Ng HH, Xu RM, Zhang Y, Struhl K. Ubiquitination of histone H2B by Rad6 is required for efficient Dot1-mediated methylation of histone H3 lysine 79. J Biol Chem. 2002;277(38):34655-7. doi: 10.1074/jbc.C200433200. PubMed PMID: 12167634.

134. Technology CS. Histone Modifications 2010. Available from: www.cellsignal.com/reference/pathway/histone_modification.html.

135. Peterson CL, Laniel MA. Histones and histone modifications. Curr Biol. 2004;14(14):R546-51. Epub 2004/07/23. doi: 10.1016/j.cub.2004.07.007

S0960982204004853 [pii]. PubMed PMID: 15268870.

136. Cosgrove MS, Boeke JD, Wolberger C. Regulated nucleosome mobility and the histone code. Nat Struct Mol Biol. 2004;11(11):1037-43. Epub 2004/11/04. doi: nsmb851 [pii] 10.1038/nsmb851. PubMed PMID: 15523479.

137. Wade PA, Pruss D, Wolffe AP. Histone acetylation: chromatin in action. Trends Biochem Sci. 1997;22(4):128-32. Epub 1997/04/01. doi: S0968-0004(97)01016-5 [pii]. PubMed PMID: 9149532.

138. Saccani S, Natoli G. Dynamic changes in histone H3 Lys 9 methylation occurring at tightly regulated inducible inflammatory genes. Genes Dev. 2002;16(17):2219-24. Epub 2002/09/05. doi: 10.1101/gad.232502. PubMed PMID: 12208844; PubMed Central PMCID: PMC186673.

139. Janzer A, Lim S, Fronhoffs F, Niazy N, Buettner R, Kirfel J. Lysine-specific demethylase 1 (LSD1) and histone deacetylase 1 (HDAC1) synergistically repress proinflammatory cytokines and classical complement pathway components. Biochem Biophys Res Commun. 2012. Epub 2012/05/01. doi: S0006-291X(12)00723-1 [pii] 10.1016/j.bbrc.2012.04.057. PubMed PMID: 22542627.

140. Vastenhouw NL, Schier AF. Bivalent histone modifications in early embryogenesis. Curr Opin Cell Biol. 2012;24(3):374-86. Epub 2012/04/20. doi: 10.1016/j.ceb.2012.03.009 S0955-0674(12)00052-X [pii]. PubMed PMID: 22513113; PubMed Central PMCID: PMC3372573.

141. Janzen WP, Wigle TJ, Jin J, Frye SV. Epigenetics: Tools and Technologies. Drug Discov Today Technol. 2010;7(1):e59-e65. doi: 10.1016/j.ddtec.2010.07.004. PubMed PMID: 21243036; PubMed Central PMCID: PMCPMC3018755.

142. Shi YJ, Lan F, Matson C, Mulligan P, Whetstine JR, Cole PA, et al. Histone demethylation mediated by the nuclear arnine oxidase homolog LSD1. Cell. 2004;119(7):941-53. PubMed PMID: ISI:000226109700007.

143. Lohse B, Kristensen JL, Kristensen LH, Agger K, Helin K, Gajhede M, et al. Inhibitors of histone demethylases. Bioorg Med Chem. 2011;19(12):3625-36. Epub 2011/05/21. doi: 10.1016/j.bmc.2011.01.046
S0968-0896(11)00075-7 [pii]. PubMed PMID: 21596573.

144. Zagni C, Chiacchio U, Rescifina A. Histone methyltransferase inhibitors: novel epigenetic agents for cancer treatment. Curr Med Chem. 2013;20(2):167-85. Epub 2012/12/06. doi: CMC-EPUB-20121126-6 [pii]. PubMed PMID: 23210854.

145. Blanchard F, Chipoy C. Histone deacetylase inhibitors: new drugs for the treatment of inflammatory diseases? Drug Discov Today. 2005;10(3):197-204. Epub 2005/02/15. doi: S1359644604033094 [pii]
10.1016/S1359-6446(04)03309-4. PubMed PMID: 15708534.

146. Metzger E, Wissmann M, Yin N, Muller JM, Schneider R, Peters AHFM, et al. LSD1 demethylates repressive histone marks to promote androgen-receptor-dependent transcription. Nature. 2005;437(7057):436-9. doi: Doi 10.1038/Nature04020. PubMed PMID: ISI:000231849100059.

147. Jostins L, Ripke S, Weersma RK, Duerr RH, McGovern DP, Hui KY, et al. Host-microbe interactions have shaped the genetic architecture of inflammatory bowel disease. Nature. 2012;491(7422):119-24. doi: 10.1038/nature11582. PubMed PMID: 23128233; PubMed Central PMCID: PMCPMC3491803.

148. Petronis A, Petroniene R. Epigenetics of inflammatory bowel disease. Gut. 2000;47(2):302-6. Epub 2000/07/18. PubMed PMID: 10896927; PubMed Central PMCID: PMC1728011.

149. Barnes PJ. Anti-inflammatory actions of glucocorticoids: molecular mechanisms. Clin Sci (Lond). 1998;94(6):557-72. PubMed PMID: 9854452.

150. Karatzas PS, Gazouli M, Safioleas M, Mantzaris GJ. DNA methylation changes in inflammatory bowel disease. Ann Gastroenterol. 2014;27(2):125-32. PubMed PMID: 24733658; PubMed Central PMCID: PMCPMC3982627.

151. Frank DN, St Amand AL, Feldman RA, Boedeker EC, Harpaz N, Pace NR. Molecular-phylogenetic characterization of microbial community imbalances in human inflammatory bowel diseases. Proc Natl Acad Sci U S A. 2007;104(34):13780-5. doi: 10.1073/pnas.0706625104. PubMed PMID: 17699621; PubMed Central PMCID: PMCPMC1959459.

152. Scheppach W, Sommer H, Kirchner T, Paganelli GM, Bartram P, Christl S, et al. Effect of butyrate enemas on the colonic mucosa in distal ulcerative colitis. Gastroenterology. 1992;103(1):51-6. PubMed PMID: 1612357.

153. Akolkar PN, Gulwani-Akolkar B, Heresbach D, Lin XY, Fisher S, Katz S, et al. Differences in risk of Crohn's disease in offspring of mothers and fathers with inflammatory bowel disease. Am J Gastroenterol. 1997;92(12):2241-4. PubMed PMID: 9399762.

154. Hardy TM, Tollefsbol TO. Epigenetic diet: impact on the epigenome and cancer. Epigenomics-Uk. 2011;3(4):503-18. doi: 10.2217/epi.11.71. PubMed PMID: 22022340; PubMed Central PMCID: PMCPMC3197720.

155. Epstein J, Sanderson IR, Macdonald TT. Curcumin as a therapeutic agent: the evidence from in vitro, animal and human studies. Br J Nutr. 2010;103(11):1545-57. doi: 10.1017/s0007114509993667. PubMed PMID: 20100380.

156. Sanderson IR, Udeen S, Davies PS, Savage MO, Walker-Smith JA. Remission induced by an elemental diet in small bowel Crohn's disease. Arch Dis Child. 1987;62(2):123-7. PubMed PMID: 3548602; PubMed Central PMCID: PMCPMC1778272.

157. Epstein J, Docena G, MacDonald TT, Sanderson IR. Curcumin suppresses p38 mitogen-activated protein kinase activation, reduces IL-1beta and matrix metalloproteinase-3 and

enhances IL-10 in the mucosa of children and adults with inflammatory bowel disease. Br J Nutr. 2010;103(6):824-32. doi: 10.1017/s0007114509992510. PubMed PMID: 19878610.

158. Jenke AC, Zilbauer M. Epigenetics in inflammatory bowel disease. Curr Opin Gastroenterol. 2012;28(6):577-84. doi: 10.1097/MOG.0b013e328357336b. PubMed PMID: 23041674.

159. Briske-Anderson MJ, Finley JW, Newman SM. The influence of culture time and passage number on the morphological and physiological development of Caco-2 cells. Proc Soc Exp Biol Med. 1997;214(3):248-57. Epub 1997/03/01. PubMed PMID: 9083258.

160. Mahraoui L, Rousset M, Dussaulx E, Darmoul D, Zweibaum A, Brot-Laroche E. Expression and localization of GLUT-5 in Caco-2 cells, human small intestine, and colon. Am J Physiol. 1992;263(3 Pt 1):G312-8. Epub 1992/09/01. PubMed PMID: 1384349.

161. Gstraunthaler G. Alternatives to the use of fetal bovine serum: serum-free cell culture. ALTEX. 2003;20(4):275-81. Epub 2003/12/13. PubMed PMID: 14671707.

162. Auwerx J. The human leukemia cell line, THP-1: a multifacetted model for the study of monocyte-macrophage differentiation. Experientia. 1991;47(1):22-31. PubMed PMID: 1999239.

163. Berg JM, Tymoczko JL, Stryer L. Biochemistry. 6th Edition ed: Sara Tenney; 2007.

164. Sigma-Aldrich. CelLytic™ M 2013. Available from: www.sigmaaldrich.com/catalog/product/sigma/c2978?lang=en&region=GB.

165. Dydensborg AB, Herring E, Auclair J, Tremblay E, Beaulieu JF. Normalizing genes for quantitative RT-PCR in differentiating human intestinal epithelial cells and adenocarcinomas of the colon. Am J Physiol Gastrointest Liver Physiol. 2006;290(5):G1067-74. Epub 2006/01/10. doi: 00234.2005 [pii]
10.1152/ajpgi.00234.2005. PubMed PMID: 16399877.

166. Vandesompele J, De Preter K, Pattyn F, Poppe B, Van Roy N, De Paepe A, et al. Accurate normalization of real-time quantitative RT-PCR data by geometric averaging of multiple

internal control genes. Genome Biol. 2002;3(7):RESEARCH0034. Epub 2002/08/20. PubMed PMID: 12184808; PubMed Central PMCID: PMC126239.

167. Schmittgen TD, Livak KJ. Analyzing real-time PCR data by the comparative C(T) method. Nat Protoc. 2008;3(6):1101-8. PubMed PMID: 18546601.

168. Josephy PD, Eling T, Mason RP. The horseradish peroxidase-catalyzed oxidation of 3,5,3',5'-tetramethylbenzidine. Free radical and charge-transfer complex intermediates. J Biol Chem. 1982;257(7):3669-75. PubMed PMID: 6277943.

169. Haring M, Offermann S, Danker T, Horst I, Peterhansel C, Stam M. Chromatin immunoprecipitation: optimization, quantitative analysis and data normalization. Plant Methods. 2007;3:11. doi: 10.1186/1746-4811-3-11. PubMed PMID: 17892552; PubMed Central PMCID: PMCPMC2077865.

170. Cho YK, Shusta EV. Antibody library screens using detergent-solubilized mammalian cell lysates as antigen sources. Protein Eng Des Sel. 2010;23(7):567-77. doi: 10.1093/protein/gzq029. PubMed PMID: 20498037; PubMed Central PMCID: PMCPMC2920304.

171. Keshavarzian A, Fusunyan RD, Jacyno M, Winship D, MacDermott RP, Sanderson IR. Increased interleukin-8 (IL-8) in rectal dialysate from patients with ulcerative colitis: evidence for a biological role for IL-8 in inflammation of the colon. Am J Gastroenterol. 1999;94(3):704-12. doi: 10.1111/j.1572-0241.1999.00940.x. PubMed PMID: 10086655.

172. Ohtsuka Y, Lee J, Stamm DS, Sanderson IR. MIP-2 secreted by epithelial cells increases neutrophil and lymphocyte recruitment in the mouse intestine. Gut. 2001;49(4):526-33. PubMed PMID: 11559650; PubMed Central PMCID: PMCPMC1728474.

173. Invivogen. Structure of Pam3CysK4 2011-2015. Available from: www.invivogen.com/pam3csk4.

174. Nemetz A, Nosti-Escanilla MP, Molnár T, Köpe A, Kovács A, Fehér J, et al. IL1B gene polymorphisms influence the course and severity of inflammatory bowel disease. Immunogenetics. 1999;49(6):527-31. PubMed PMID: 10380697.

175. Naik S, Kelly EJ, Meijer L, Pettersson S, Sanderson IR. Absence of Toll-like receptor 4 explains endotoxin hyporesponsiveness in human intestinal epithelium. J Pediatr Gastroenterol Nutr. 2001;32(4):449-53. Epub 2001/06/09. PubMed PMID: 11396812.

176. Gibco. IL1B Recombinant Human Protein 2011. Available from: https://www.lifetechnologies.com/order/catalog/product/PHC0815.

177. Abcam. Human IL-1 beta. Available from: http://www.abcam.com/active-human-il1-beta-full-length-protein-ab9617.html.

178. Fusunyan RD, Quinn JJ, Ohno Y, MacDermott RP, Sanderson IR. Butyrate enhances interleukin (IL)-8 secretion by intestinal epithelial cells in response to IL-1beta and lipopolysaccharide. Pediatr Res. 1998;43(1):84-90. Epub 1998/02/12. PubMed PMID: 9432117.

179. Round JL, Mazmanian SK. The gut microbiota shapes intestinal immune responses during health and disease. Nat Rev Immunol. 2009;9(5):313-23. doi: 10.1038/nri2515. PubMed PMID: 19343057; PubMed Central PMCID: PMCPMC4095778.

180. Atarashi K, Nishimura J, Shima T, Umesaki Y, Yamamoto M, Onoue M, et al. ATP drives lamina propria T(H)17 cell differentiation. Nature. 2008;455(7214):808-12. doi: 10.1038/nature07240. PubMed PMID: 18716618.

181. Hall JA, Bouladoux N, Sun CM, Wohlfert EA, Blank RB, Zhu Q, et al. Commensal DNA limits regulatory T cell conversion and is a natural adjuvant of intestinal immune responses. Immunity. 2008;29(4):637-49. doi: 10.1016/j.immuni.2008.08.009. PubMed PMID: 18835196; PubMed Central PMCID: PMCPMC2712925.

182. Chemical C. S-adenosyl-L-homocysteine. Available from: http://www.caymanchem.com/app/template/Product.vm/catalog/13603.

183. Handy DE, Castro R, Loscalzo J. Epigenetic modifications: basic mechanisms and role in cardiovascular disease. Circulation. 2011;123(19):2145-56. doi: 10.1161/circulationaha.110.956839. PubMed PMID: 21576679; PubMed Central PMCID: PMCPMC3107542.

184. Ngo S, Li X, O'Neill R, Bhoothpur C, Gluckman P, Sheppard A. Elevated S-adenosylhomocysteine alters adipocyte functionality with corresponding changes in gene expression and associated epigenetic marks. Diabetes. 2014;63(7):2273-83. doi: 10.2337/db13-1640. PubMed PMID: 24574043.

185. Cherblanc FL, Chapman KL, Reid J, Borg AJ, Sundriyal S, Alcazar-Fuoli L, et al. On the histone lysine methyltransferase activity of fungal metabolite chaetocin. J Med Chem. 2013;56(21):8616-25. doi: 10.1021/jm401063r. PubMed PMID: 24099080.

186. Greiner D, Bonaldi T, Eskeland R, Roemer E, Imhof A. Identification of a specific inhibitor of the histone methyltransferase SU(VAR)3-9. Nat Chem Biol. 2005;1(3):143-5. doi: 10.1038/nchembio721. PubMed PMID: 16408017.

187. Weber HP. The molecular structure and absolute configuration of chaetocin. Acta Crystallographica. 1972;B28(10):2945-51. doi: doi:10.1107/S0567740872007265.

188. Isham CR, Tibodeau JD, Bossou AR, Merchan JR, Bible KC. The anticancer effects of chaetocin are independent of programmed cell death and hypoxia, and are associated with inhibition of endothelial cell proliferation. Br J Cancer. 2012;106(2):314-23. doi: 10.1038/bjc.2011.522. PubMed PMID: 22187030; PubMed Central PMCID: PMCPMC3261675.

189. Isham CR, Tibodeau JD, Jin W, Xu R, Timm MM, Bible KC. Chaetocin: a promising new antimyeloma agent with in vitro and in vivo activity mediated via imposition of oxidative stress. Blood. 2007;109(6):2579-88. doi: 10.1182/blood-2006-07-027326. PubMed PMID: 17090648; PubMed Central PMCID: PMCPMC1852204.

190. Tocris. Chaetocin. Available from: http://www.tocris.com/dispprod.php?ItemId=341068#.VK1tQyusWSo.

191. Tran HT, Kim HN, Lee IK, Nguyen-Pham TN, Ahn JS, Kim YK, et al. Improved therapeutic effect against leukemia by a combination of the histone methyltransferase inhibitor chaetocin and the histone deacetylase inhibitor trichostatin A. J Korean Med Sci. 2013;28(2):237-46. doi: 10.3346/jkms.2013.28.2.237. PubMed PMID: 23400519; PubMed Central PMCID: PMCPMC3565135.

192. Shi Y, Lan F, Matson C, Mulligan P, Whetstine JR, Cole PA, et al. Histone demethylation mediated by the nuclear amine oxidase homolog LSD1. Cell. 2004;119(7):941-53. doi: 10.1016/j.cell.2004.12.012. PubMed PMID: 15620353.

193. Pedersen MT, Helin K. Histone demethylases in development and disease. Trends Cell Biol. 2010;20(11):662-71. doi: 10.1016/j.tcb.2010.08.011. PubMed PMID: 20863703.

194. Drugs Co. New Drugs and Developments in Therapeutics Pargyline Hydrochloride (Eutonyl). The Journal of the American Medical Association. 1963;184(11). doi: doi:10.1001/jama.1963.03700240079013.

195. Steven Pray W. Interactions Between Nonprescription Products and Psychotropic Medications. US Pharmacist. 2007;32(11):12-5.

196. Binda C, Newton-Vinson P, Hubálek F, Edmondson DE, Mattevi A. Structure of human monoamine oxidase B, a drug target for the treatment of neurological disorders. Nat Struct Biol. 2002;9(1):22-6. doi: 10.1038/nsb732. PubMed PMID: 11753429.

197. Chen Y, Yang Y, Wang F, Wan K, Yamane K, Zhang Y, et al. Crystal structure of human histone lysine-specific demethylase 1 (LSD1). Proc Natl Acad Sci U S A. 2006;103(38):13956-61. doi: 10.1073/pnas.0606381103. PubMed PMID: 16956976; PubMed Central PMCID: PMCPMC1599895.

198. Huang Y, Vasilatos SN, Boric L, Shaw PG, Davidson NE. Inhibitors of histone demethylation and histone deacetylation cooperate in regulating gene expression and inhibiting growth in human breast cancer cells. Breast Cancer Res Treat. 2012;131(3):777-89. doi: 10.1007/s10549-011-1480-8. PubMed PMID: 21452019; PubMed Central PMCID: PMCPMC3624096.

199. Chemical C. Structure of Pargyline Hydrochloride 2015. Available from: http://www.caymanchem.com/app/template/Product.vm/catalog/10007852.

200. Kristensen LH, Nielsen AL, Helgstrand C, Lees M, Cloos P, Kastrup JS, et al. Studies of H3K4me3 demethylation by KDM5B/Jarid1B/PLU1 reveals strong substrate recognition in vitro and identifies 2,4-pyridine-dicarboxylic acid as an in vitro and in cell inhibitor. FEBS J. 2012;279(11):1905-14. doi: 10.1111/j.1742-4658.2012.08567.x. PubMed PMID: 22420752.

201. Crawford GE, Holt IE, Whittle J, Webb BD, Tai D, Davis S, et al. Genome-wide mapping of DNase hypersensitive sites using massively parallel signature sequencing (MPSS). Genome Res. 2006;16(1):123-31. doi: 10.1101/gr.4074106. PubMed PMID: 16344561; PubMed Central PMCID: PMCPMC1356136.

202. Wang YM, Zhou P, Wang LY, Li ZH, Zhang YN, Zhang YX. Correlation between DNase I hypersensitive site distribution and gene expression in HeLa S3 cells. PLoS One. 2012;7(8):e42414. doi: 10.1371/journal.pone.0042414. PubMed PMID: 22900019; PubMed Central PMCID: PMCPMC3416863.

203. Shlyueva D, Stampfel G, Stark A. Transcriptional enhancers: from properties to genome-wide predictions. Nat Rev Genet. 2014;15(4):272-86. doi: 10.1038/nrg3682. PubMed PMID: 24614317.

204. Wertz IE, O'Rourke KM, Zhou H, Eby M, Aravind L, Seshagiri S, et al. De-ubiquitination and ubiquitin ligase domains of A20 downregulate NF-kappaB signalling. Nature. 2004;430(7000):694-9. doi: 10.1038/nature02794. PubMed PMID: 15258597.

205. Karin M. How NF-kappaB is activated: the role of the IkappaB kinase (IKK) complex. Oncogene. 1999;18(49):6867-74. doi: 10.1038/sj.onc.1203219. PubMed PMID: 10602462.

206. Wald D, Qin J, Zhao Z, Qian Y, Naramura M, Tian L, et al. SIGIRR, a negative regulator of Toll-like receptor-interleukin 1 receptor signaling. Nat Immunol. 2003;4(9):920-7. doi: 10.1038/ni968. PubMed PMID: 12925853.

207. Xiao H, Gulen MF, Qin J, Yao J, Bulek K, Kish D, et al. The Toll-interleukin-1 receptor member SIGIRR regulates colonic epithelial homeostasis, inflammation, and tumorigenesis. Immunity. 2007;26(4):461-75. doi: 10.1016/j.immuni.2007.02.012. PubMed PMID: 17398123.

208. Mills CD. M1 and M2 Macrophages: Oracles of Health and Disease. Crit Rev Immunol. 2012;32(6):463-88. Epub 2013/02/23. doi: 03b91cfa635b86ee,7acd81f604dc8b0c [pii]. PubMed PMID: 23428224.

209. Consortium IMP. Knockout Mouse - Gene: Nfkb1 2015. Available from: http://www.mousephenotype.org/data/genes/MGI:97312.

210. Scheinin T, Butler DM, Salway F, Scallon B, Feldmann M. Validation of the interleukin-10 knockout mouse model of colitis: antitumour necrosis factor-antibodies suppress the progression of colitis. Clin Exp Immunol. 2003;133(1):38-43. Epub 2003/06/26. doi: 2193 [pii]. PubMed PMID: 12823276; PubMed Central PMCID: PMC1808754.

211. Consortium IMP. Knockout Mouse - Gene:Tnfaip3 2015. Available from: www.mousephenotype.org/data/genes/MGI:1196377.

212. Bhatt D, Ghosh S. Regulation of the NF-κB-Mediated Transcription of Inflammatory Genes. Front Immunol. 2014;5:71. doi: 10.3389/fimmu.2014.00071. PubMed PMID: 24611065; PubMed Central PMCID: PMCPMC3933792.

213. Sibani S, Melnyk S, Pogribny IP, Wang W, Hiou-Tim F, Deng L, et al. Studies of methionine cycle intermediates (SAM, SAH), DNA methylation and the impact of folate deficiency on tumor numbers in Min mice. Carcinogenesis. 2002;23(1):61-5. PubMed PMID: 11756224.

214. Shema E, Jones D, Shoresh N, Donohue L, Ram O, Bernstein BE. Single-molecule decoding of combinatorially modified nucleosomes. Science. 2016;352(6286):717-21. doi: 10.1126/science.aad7701. PubMed PMID: 27151869; PubMed Central PMCID: PMCPMC4904710.

215. Palma L, Amatori S, Cruz Chamorro I, Fanelli M, Magnani M. Promoter-specific relevance of histone modifications induced by dexamethasone during the regulation of pro-inflammatory mediators. Biochim Biophys Acta. 2014;1839(7):571-8. doi: 10.1016/j.bbagrm.2014.05.006. PubMed PMID: 24844181.

216. Dogan N, Wu W, Morrissey CS, Chen KB, Stonestrom A, Long M, et al. Occupancy by key transcription factors is a more accurate predictor of enhancer activity than histone modifications or chromatin accessibility. Epigenetics Chromatin. 2015;8:16. doi: 10.1186/s13072-015-0009-5. PubMed PMID: 25984238; PubMed Central PMCID: PMCPMC4432502.

217. Italiani P, Boraschi D. New Insights Into Tissue Macrophages: From Their Origin to the Development of Memory. Immune Netw. 2015;15(4):167-76. doi: 10.4110/in.2015.15.4.167. PubMed PMID: 26330802; PubMed Central PMCID: PMCPMC4553254.

218. Iglesias-Bartolome R, Callejas-Valera JL, Gutkind JS. Control of the epithelial stem cell epigenome: the shaping of epithelial stem cell identity. Curr Opin Cell Biol. 2013;25(2):162-9. doi: 10.1016/j.ceb.2013.01.009. PubMed PMID: 23434069.

219. Kim EC, Zhu Y, Andersen V, Sciaky D, Cao HJ, Meekins H, et al. Cytokine-mediated PGE2 expression in human colonic fibroblasts. Am J Physiol. 1998;275(4 Pt 1):C988-94. PubMed PMID: 9755052.

220. Moyer MP, Manzano LA, Merriman RL, Stauffer JS, Tanzer LR. NCM460, a normal human colon mucosal epithelial cell line. In Vitro Cell Dev Biol Anim. 1996;32(6):315-7. Epub 1996/06/01. PubMed PMID: 8842743.

221. Nakayama H, Kurokawa K, Lee BL. Lipoproteins in bacteria: structures and biosynthetic pathways. FEBS J. 2012;279(23):4247-68. doi: 10.1111/febs.12041. PubMed PMID: 23094979.

222. Becker C, Neurath MF, Wirtz S. The Intestinal Microbiota in Inflammatory Bowel Disease. ILAR J. 2015;56(2):192-204. doi: 10.1093/ilar/ilv030. PubMed PMID: 26323629.

223. Halsall JA, Turan N, Wiersma M, Turner BM. Cells adapt to the epigenomic disruption caused by histone deacetylase inhibitors through a coordinated, chromatin-mediated transcriptional response. Epigenetics Chromatin. 2015;8:29. doi: 10.1186/s13072-015-0021-9. PubMed PMID: 26380582; PubMed Central PMCID: PMCPMC4572612.

224. Cheng X, Blumenthal RM. Coordinated chromatin control: structural and functional linkage of DNA and histone methylation. Biochemistry. 2010;49(14):2999-3008. doi: 10.1021/bi100213t. PubMed PMID: 20210320; PubMed Central PMCID: PMCPMC2857722.

225. Reinecker HC, Steffen M, Witthoeft T, Pflueger I, Schreiber S, MacDermott RP, et al. Enhanced secretion of tumour necrosis factor-alpha, IL-6, and IL-1 beta by isolated lamina propria mononuclear cells from patients with ulcerative colitis and Crohn's disease. Clin Exp Immunol. 1993;94(1):174-81. PubMed PMID: 8403503; PubMed Central PMCID: PMCPMC1534387.

226. Chopra DP, Dombkowski AA, Stemmer PM, Parker GC. Intestinal epithelial cells in vitro. Stem Cells Dev. 2010;19(1):131-42. doi: 10.1089/scd.2009.0109. PubMed PMID: 19580443; PubMed Central PMCID: PMCPMC3136723.

227. Jenke AC, Postberg J, Raine T, Nayak KM, Molitor M, Wirth S, et al. DNA methylation analysis in the intestinal epithelium-effect of cell separation on gene expression and methylation profile. PLoS One. 2013;8(2):e55636. doi: 10.1371/journal.pone.0055636. PubMed PMID: 23409010; PubMed Central PMCID: PMCPMC3568120.

228. Bintu L, Yong J, Antebi YE, McCue K, Kazuki Y, Uno N, et al. Dynamics of epigenetic regulation at the single-cell level. Science. 2016;351(6274):720-4. doi: 10.1126/science.aab2956. PubMed PMID: 26912859.

229. Villena J, Kitazawa H. Modulation of Intestinal TLR4-Inflammatory Signaling Pathways by Probiotic Microorganisms: Lessons Learned from Lactobacillus jensenii TL2937. Front Immunol. 2014;4:512. doi: 10.3389/fimmu.2013.00512. PubMed PMID: 24459463; PubMed Central PMCID: PMCPMC3890654.

230. Moya A, Ferrer M. Functional Redundancy-Induced Stability of Gut Microbiota Subjected to Disturbance. Trends Microbiol. 2016;24(5):402-13. doi: 10.1016/j.tim.2016.02.002. PubMed PMID: 26996765.